Aus dem Institut für Prophylaxe und Epidemiologie der Kreislaufkrankheiten
der Ludwig-Maximilians-Universität München
Direktor: Prof. Dr. med. P. C. Weber

Signaling pathways regulating LIM-kinase-1 activation and cofilin phosphorylation in activated platelets

Dissertation
zum Erwerb des Doktorgrades der Humanbiologie
an der Medizinischen Fakultät der
Ludwig-Maximilians-Universität zu München

vorgelegt von

Dharmendra Pandey

aus

Ahmednagar, Indien

2007

Mit Genehmigung der Medizinischen Fakultät
der Universität München

1. Berichterstatter:	**Prof. Dr. Med. Wolfgang Siess**
2. Berichterstatter:	**Prof. Dr. M. Schleicher**
Mitberichterstatter:	**Prof. Dr. B. Walzog**
	Priv. Doz. Dr. M. Weis
Dekan:	**Prof. Dr. med. D. Reinhardt**
Tag der mündlichen Prüfung:	**05.11.2007**

Dedicated To My Grandparents

Jai Kisan, Jai Jawan, Jai Vigyan

Table of contents

Abbreviations and units

Abbreviations

ABP	Actin binding proteins
ADF	Actin depolymerization factor
ADP	Adenosin-5'-diphosphate
APS	Ammonium persulphate
ATP	Adenosin-5'-triphosphate
BAPTA-AM	1,2-*bis*(*o*-Aminophenoxy)ethane tetraacetic aid-acetoxymethyl ester
BSA	Bovine serum albumin
cDNA	Complementary DNA
Cc	Critical concentration
DMSO	Dimethylsulfoxide
DNA	Deoxyribonucleic acid
DTS	Dense tubular system
E. coli	*Escherichia coli*
EC	Endothelial cell
EDTA	Ethylenediaminetetraacetic acid
EGTA	Ethyleneglycoltetraacetic acid
F-actin	Filamentous actin
FSC	Forward scatter
G-actin	Globular actin
GDP	Guanosine diphosphate
GFP	Green fluorescence protein
GP	Glycoprotein
GTP	Guanosine triphosphate
IB	Immunoblotting

IEF   Isoelectric focusing

LB   Luria-Bertani

LIMKs   LIM-kinases

LPA   Lysophosphatidic acid

MLC   Myosin light chain

MYPT   Myosin phosphatase targeting subunit

OCS   Open canalicular system

O.D   Optical density at a wavelength of x nm

PAK   p21-activated kinase

PBS   Phosphate buffered saline

PCR   Polymerase chain reaction

PDZ   <u>P</u>SD-95, <u>d</u>isc large, <u>Z</u>O-1

PKC   protein kinase C

PI   Phosphoinositides

PP   Protein phosphatase

PPP   Platelet poor plasma

PRP   Platelet rich plasma

SDS-PAGE   sodium dodecyl sulfate - polyacrylamide gel electrophoresis

SSC   Side scatter

TBST   Tris buffered saline with tween-20

TxA$_2$ Thromboxane A$_2$

v/v   volume by volume

vWF   von Willebrand factor

w/v   weight by volume

UV   Ultraviolet

<u>Units</u>

Ǻ	Armstrong
cm	centimeter
°C	degree Celsius
µg	microgram
µl	microliter
µm	micrometer
µM	micromolar
g	gram (weight) respective gravity (for centrifugation)
kb	kilo base pairs
kDa	kilo Dalton
M	molar (= mol/l)
mA	milliampere
mg	milligram
ml	milliliter
mm	millimeter
mM	millimolar
ng	nanogram
nm	nanometer
pmol	picomole
rpm	revolutions per minute
U	units of enzymatic activity
V	Volts

1. Introduction

1.1. Overview

Damage to blood vessels and small capillaries occurs frequently after injuries or cuts, destroying the integrity of the vascular wall. To minimize and arrest the loss of blood, platelets are recruited to the injured vessels. The exposure of sub-endothelial matrix at the site of injury leads to the adhesion of circulating platelets to the damaged vessel wall during primary hemostasis. Platelet adhesion promotes different platelet responses such as shape change, secretion of granule contents and the formation of platelet aggregates. As a result, the platelet haemostatic plug heals the injured site. Apart from the healing process, platelets are involved in atherogenesis and thrombotic complications occurring in atherosclerosis. Rupture of atherosclerotic plaques exposes pro-thrombotic substances to the circulating platelets leading to intra-arterial thrombus formation and vascular occlusion, which can cause acute coronary syndrome and myocardial infarction.

Since long scientists are trying to understand the physiological and pathological activation of platelets using different in vitro, in vivo or ex vivo methods. One of the important aspects of these studies is to understand the dynamic regulation and rearrangement of the platelet cytoskeleton during activation. The morphological and functional changes of platelets require a drastic remodeling of the actin cytoskeleton. Actin remodeling involves the depolymerization of existing filaments, and polymerization, branching and bundling of new filaments. These processes are regulated by numerous actin-binding proteins and signaling molecules such as the family of Rho-GTPases. The small GTPase Rho can regulate several aspects of cellular function, predominantly through its downstream effector p160ROCK (Rho-kinase). One of the well established Rho-kinase-mediated signaling pathways is the phosphorylation of myosin light chain (MLC) and its counteracting MLC phosphatase. Rho-kinase regulates a second pathway that involves activation LIM-kinases (LIMKs) and subsequent phosphorylation and inactivation of cofilin, an actin dynamizing protein. This study is focused on the regulation of the Rho-kinase/LIMKs/cofilin phosphorylation pathway for different morphological and functional platelet responses. As platelet stimuli, the physiological agonist thrombin and the pathophysiological relevant agonist lysophosphatidic acid (LPA), which is the main platelet-activating lipid in atherosclerotic plaque, were studied.

1.2. Platelets

Blood platelets are produced from megakaryocytes in the bone marrow. Although historically one of the first observations was the apparent shedding of platelets by megakaryocytes, the exact mechanism by which platelets are produced remains unclear. Cultured megakaryocytes after

maturation are observed to produce platelet in two phases; firstly an extension of cytoplasm into multiple long structures called proplatelets and then platelet formation at the end of these proplatelets (Hartwig and Italiano 2003). In vivo, each megakaryocyte produces an average of 1000-3000 platelets (Chernoff et al. 1980), and it has been estimated that 35,000-40,000 platelets are produced per day per µl of blood (Ballem et al. 1992). The physiological life span of human platelets is usually 7-10 days with a daily renewal rate of 20% of the total platelet count. Platelets from all common mammalian species are broadly similar in appearance; they are anucleated, discoid in shape and the smallest corpuscular component of circulating blood having a diameter of 2-4µm and an average surface area of 8µm² in non-activated state.

1.2.1. <u>Morphology of platelets</u>

The ultrastructure of platelets can be divided into four morphological regions: the peripheral zone, the structural zone, the zone of the organelles, and the membrane system (Figure 1.1)
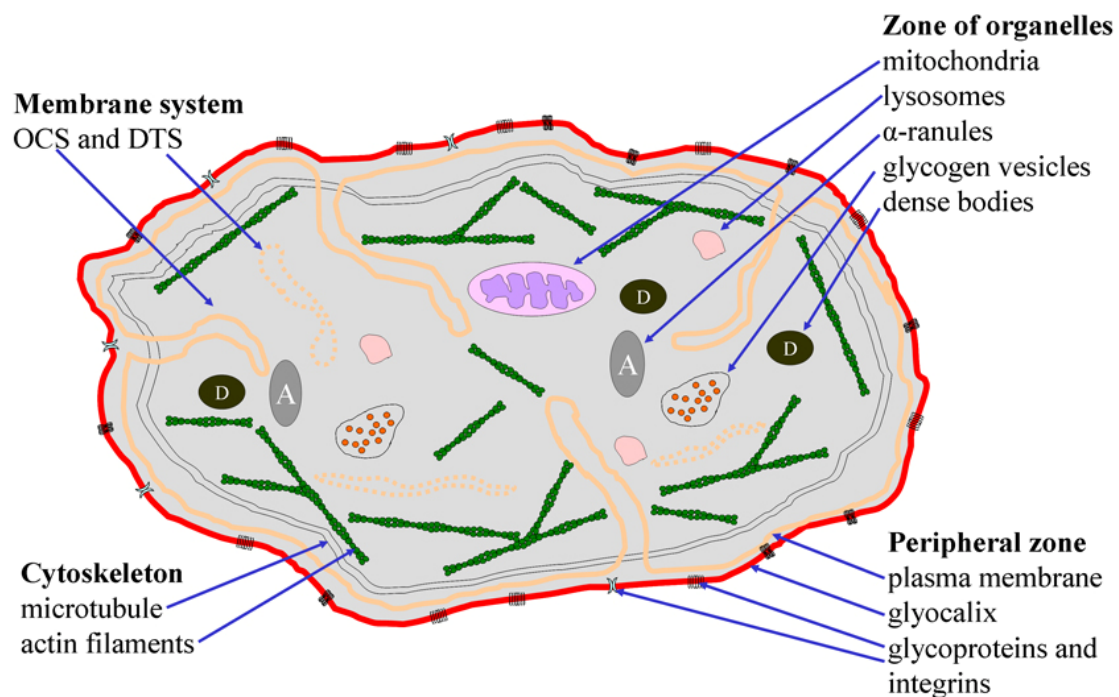
Figure 1.1 Schematic model of the platelet ultrastructure. Platelets structure is morphologically divided into four zones: 1) Peripheral zone, 2) Cytoskeleton, 3) Zone of organelles and 4) Membrane system. OCS, open canalicular system; DTS, dense tubular system.

The peripheral zone consists of the plasma membrane composed of a bilayer of phospholipids and embedded membrane proteins. The plasma membrane of platelets is covered on its extracellular side by a thin layer glycocalix (15-20nm), composed of various glycoproteins (GP), proteins, receptors and mucopolysaccharides. These glycoproteins embedded in the glycocalix satisfy important roles in the stickiness and adhesion of platelets (Nurden and Caen 1975). The phospholipids in the plasma membrane of platelets are asymmetrically organized; phosphotidylcholine and sphingomyelin are enriched in the outer monolayer, while

phosphatidylethanolamine and phosphatidylserine are more dominant in inner monolayer (Daniel 1981). Such kind of phospholipid arrangement in the plasma membrane is an important factor for platelet function (Gawaz 2001). Platelet membrane also contains cholesterol whose concentration depends on the plasma cholesterol concentration (Carvalho et al. 1974; Shattil et al. 1977).

The cytoskeleton also known as sol-gel zone contains microtubules and widely differing structural proteins. A single microtubule band goes around the circumference of platelets and is responsible for the discoid shape of non-activated platelets. The disassembly of the microtubule coil results in the loss of discoid shape (White and Rao 1982). Human platelets from heterozygous carriers of the Q43P point mutation in the microtubule subunit β1-tubulin (10% of normal population), which show normal levels of β1-tubulin expression, and platelets from β1-tubulin knock-out mice, which showed substantial reduction in the level of β1-tubulin expression, have been reported to be spherocytic (Schwer et al. 2001; Freson et al. 2005). The other main protein of the cytoskeleton is actin (15-20% of total platelet protein), which is regulated by numerous actin-binding proteins. Actin filaments within the cytoplasm organize into a space-filling network that gives form and strength to the cell. Filaments of actin together with myosin furnish a contractile complex involved in shape change, pseudopod extension, internal contraction, and secretion (White 1984). The actin cytoskeleton of platelets is described in detail in section 1.3.

Platelets contain several organelles in their cytosol such as mitochondria, glycogen vesicles, peroxisomes and three different forms of storage granules containing proteins and other substances essential for platelet function: dense bodies, α-granules, and lysosomes. The dense bodies (3-8 per platelet and mean diameter of 150 nm) are named after their characteristics inherent electron opacity; they contain high concentrations of ADP, ATP, Ca^{2+}, pyrophosphate and serotonin, which are prothrombotic and secreted to recruit other platelets (McNicol and Israels 1999). The α-granules represent the major granule population (50-80 in number) and are large organelles of 200-400 nm in diameter, enclosed by a membrane similar to the plasma membrane. They contain proteins that play a critical role in different biological functions such as platelet adhesion and aggregation, chemotaxis of leukocytes, proliferation of different vascular cells, inflammation and coagulation (Rendu and Brohard-Bohn 2001). The lysosomal bodies (175-200 nm in diameter) contain hydrolytic enzymes similar to the lysosomes of other cells. The components of all three granules are secreted during platelet activation, but lysosomal contents are more slowly and incompletely released than the contents of α-granules and dense bodies (Holmsen et al. 1982).

Two types of intracellular platelet membrane systems can be distinguished: the surface connected open canalicular system (OCS) and the dense tubular system (DTS). The OCS is an elaborate series of conduits that begin as an indentation of the plasma membrane, courses throughout the interior of the platelet, and return back to the plasma membrane. These conduits of OCS are

accessible from the extracellular space through pores. The OCS provides a potential route for transport of granule contents outside or for external elements to the interior of platelets. The OCS also serves as a storage site for the plasma membrane and plasma-membrane bound glycoproteins (Nurden et al. 1994). Upon activation, the platelet surface membrane increases due to exposure of the OCS. The DTS is a closed-channel network of residual endoplasmic reticulum from the megakaryocytes. The DTS is one of the main storage sites for free Ca^{2+}. Upon activation, Ca^{2+} is released from the DTS to the cytoplasm. The increase of cytosolic Ca^{2+} concentration plays a major role in the regulation of platelet metabolism and activation.

1.2.2. Platelet responses during hemostasis

Platelets are crucial at the site of vascular injury where they interact with the sub-endothelial matrix to form the hemostatic plug. The process of hemostatic plug formation is a complex multistep process that includes platelet tethering, adhesion, activation, spreading, aggregation, degranulation, procoagulant activation, and microparticle generation (Figure 1.2).
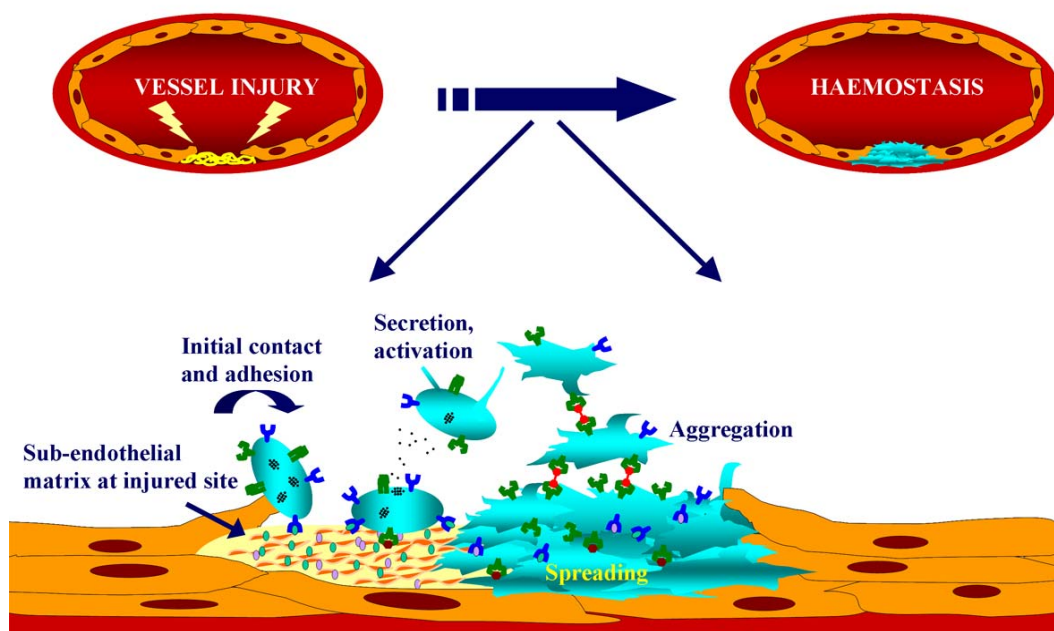
Figure 1.2 Response of platelets during hemostasis. Platelets tether, role and finally adhere to exposed sub-endothelial matrix at injured site. Platelets activation leads to shape change, secretion and recruitment of other platelets from circulation. Platelets aggregation and ultimate spreading result in closure of vessel wall.

Platelet adhesion and spreading need a supportive substratum, whereas the other platelet responses can also occur independently in suspension in order to support the formation of a stable hemostatic plug. The process of hemostatic plug formation starts with capturing of circulating platelets at the injury site. Platelet adhesion to the exposed subendothelium is a multistep process involving a diverse array of adhesive ligands (von Willebrand factor [vWF], collagen, fibronectin and laminin) and their receptors on the platelet surface (glycoproteins and integrins) (Chen and Lopez 2005). The high affinity interaction between GP-Ib-V-IX and vWF is required for the

initial platelet tether that slows down the velocity of circulating platelets, especially under high shear conditions. This interaction is not sufficient to hold platelets and is reversible, however the deceleration in platelet velocity allows other receptor-ligand interactions (for e.g., GP-VI with collagen, integrin $\alpha_{IIb}\beta_3$ with fibrinogen and vWF) to mediate a firm platelet adhesion (Jackson et al. 2003). These interactions upregulate signaling pathways that lead platelets into the activation phase. The platelets loose their discoid shape, extent pseudopods and protrude their surface membrane over the extracellular matrix. One important consequence is the activation of the integrin $\alpha_{IIb}\beta_3$ on the platelet surface. Integrin $\alpha_{IIb}\beta_3$ interaction with fibrinogen and vWF embedded in the subendothelial matrix help platelets to spread over the subendothelium. Platelet activation includes a rise in cytosolic Ca^{2+}, an enzymatic formation of thromboxane A_2 (TxA_2) from released arachidonic acid and the secretion of ADP from dense granules. TxA_2 and ADP release and their subsequent interaction with the respective G-protein coupled receptors reinforce platelet activation. The surface of activated platelets serves as an integral part of the prothrombinase complex for generation of thrombin (Dorsam et al. 2004). Locally accumulated thrombin and components released from granules, especially ADP, augment the adhesion process by autocrine mechanism. They also stimulate resting platelets in the circulation and recruit them to the site of injury for further consolidation of adhesion by paracrine mechanism. Recruitment of additional platelets to the adherent platelets causes them to interact with each other and to form aggregates, which are then eventually stabilized by a cross-linked fibrin clot to form a stable hemostatic plug. The process of aggregation requires an activation integrin $\alpha_{IIb}\beta_3$ by inside-out signaling and subsequent interaction between integrin $\alpha_{IIb}\beta_3$ on adjacent platelets through fibrinogen, which acts as a bridge between two platelets. Platelet aggregation in vitro can occurs in two phases; a primary reversible aggregation without secretion and a secondary irreversible aggregation usually associated with large secretion from granules.

A similar multistep process as described for hemostasis also underlies the pathological process of intravascular plug formation after rupture or erosion of atherosclerotic plaques. Platelet activation is initiated as they encounter matrix proteins and atherogenic substances exposed beneath ruptured or eroded atherosclerotic plaques (Ruggeri 2002), for example LPA (Siess et al. 1999; Rother et al. 2003), which induces platelet shape change, and platelet aggregation in synergism with ADP secreted from dense granules of platelets or released from erythrocytes (Haseruck et al. 2004).

1.2.3. <u>Signaling pathways for platelet activation</u>

Most of the physiological platelet stimuli like ADP, TxA_2, LPA, or thrombin act through seven transmembrane domain receptors that are coupled to heterotrimeric G proteins (α, β, and γ subunits). These G proteins are important mediators for intracellular signaling pathways in platelets. Receptor activation mediates a conformational change of G proteins leading to an exchange of GDP to GTP on their α-subunit, which then dissociates from their $\beta\gamma$ subunits. G

proteins are defined by the identity of their α-subunits and are grouped into four families, $G\alpha_s$, $G\alpha_i$, $G\alpha_q$, and $G\alpha_{12/13}$ (Offermanns 2000). Members of all four families are present in platelets. ADP through its receptors $P2Y_1$ and $P2Y_{12}$ activates G_q and G_i, respectively (Gachet 2001; Kunapuli et al. 2003), TxA_2 receptor is functionally coupled to G_q and $G_{12/13}$ proteins, LPA activates $G_{12/13}$ (Siess and Tigyi 2004), and protease-activated receptors (PARs) activated by thrombin are coupled to G_q, $G_{12/13}$, and G_i (Offermanns et al. 1994; Klages et al. 1999). While G_i, G_q, and $G_{12/13}$ transmit signals for platelet activation, G_s mediates platelet inhibition by coupling to the prostacyclin receptor and increasing intracellular cAMP levels. Studies on mouse platelets deficient in $G\alpha_q$, $G\alpha_{13}$, or G_{i2} proteins show that signaling through multiple G-protein pathways are necessary for secretion from dense granules and platelet aggregation. $G\alpha_q$-deficient platelets show shape change but fail to secrete and aggregate in response to thrombin or TxA_2, while ADP causes neither shape change nor aggregation (Offermanns et al. 1997). Platelets from mouse deficient in $G\alpha_{13}$ do not show a shape change response to low concentration of TxA_2 and thrombin and have impaired platelet aggregation and granule secretion responses after exposure to high concentrations of these agonists (Moers et al. 2003). $G\alpha_{i2}$-deficient platelets were irresponsive to ADP and showed a reduced aggregation in response to TxA_2 and thrombin, possibly due to the absence of additive stimulation induced by secreted ADP through the $P2Y_{12}$ receptor (Jantzen et al. 2001). Although the $G_{12/13}$-mediated signaling pathway mainly contributes to Ca^{2+}-independent platelet shape change, co-stimulation of $G_{12/13}$- and G_i-mediated signaling pathways in $G\alpha_q$-deficient platelets were sufficient to result in a small increase of intracellular Ca^{2+} and activate integrin $\alpha_{IIb}\beta_3$ leading to irreversible aggregation. Thus, G_q-mediated signaling alone or co-stimulation of $G_{12/13}$- and G_i-mediated signaling is needed for secretion and platelet aggregation (Dorsam et al. 2002; Nieswandt et al. 2002).

The α-subunit of G_q activates phospholipase C (PLC)-β, which in turn results in the formation of inositol 1,4,5 triphosphate (IP_3) and diacylglycerol leading to an elevation of free cytoplasmic Ca^{2+} and activation of protein kinase C (PKC), respectively (Offermanns et al. 1997). The activation of G_i leads to dissociation of its subunits, which results in inhibition of adenylyl cyclase and activation of PI3-kinase by α_i-subunit and released $\beta\gamma$ subunits, respectively (Offermanns 2000). Platelets from mice deficient in Akt, a downstream molecule of PI3-kinase, showed defects in secretion, aggregation and thrombus formation (Chen et al. 2004; Woulfe et al. 2004). An increase of intracellular Ca^{2+} and activation of PKC and PI3-kinase are involved in secretion, initial activation of the integrin $\alpha_{IIb}\beta_3$ by inside-out signaling and the subsequent stabilization of platelet aggregates (Shattil and Brass 1987).

Platelet shape change observed in $G\alpha_q$-deficient platelets suggested a role of $G_{12/13}$-mediated signaling for platelet shape change in a Ca^{2+}-independent manner (Offermanns et al. 1997). Furthermore, platelets of mice deficient in G_{13} and G_{12} alone showed that platelet shape change is due to activation of G_{13}, but not G_{12}. A significant reduction in platelet aggregation and the inability of G_{13}-deficient platelets to adhere on collagen matrix under high shear rates suggested

an important role of G_{13} in hemostasis and thrombosis (Moers et al. 2003). The signaling pathway induced by G_{13} involves Rho/Rho-kinase-mediated shape change of human platelets. Inactivation of Rho or inhibition of Rho-kinase blocked the Ca^{2+}-independent shape change in human platelets and G_q-deficient mice platelets (Bauer et al. 1999; Klages et al. 1999). The activation of Rho-kinase leads to phosphorylation of myosin light chain and thereby increases the actinomyosin contraction underlying platelet shape change. These studies indicate that G_q, G_i and G_{13} alone may still activate platelets, but signaling pathways via all three G proteins seem to be required for efficient platelet activation under physiological and pathological conditions (Figure 1.3).
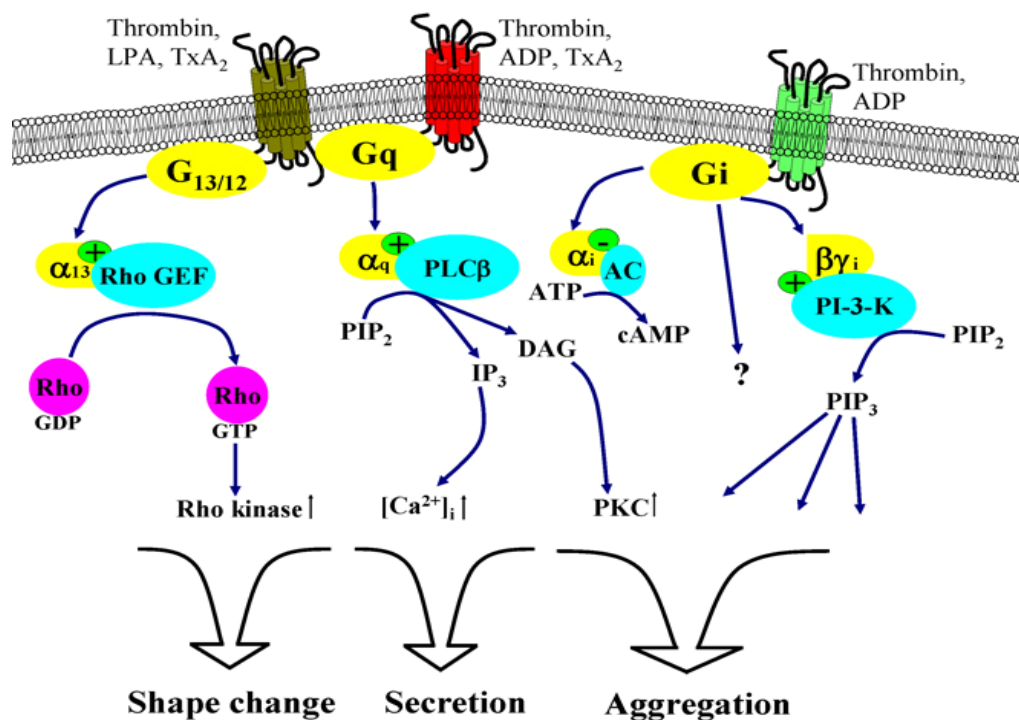
Figure 1.3 G-protein-mediated signaling pathways involved in platelet activation. Several agonists activate platelets through GPCRs coupled to G-proteins, which operate alone or in synergy with each other during platelet activation. Signaling pathways mediated by these G-proteins regulate shape change, secretion and aggregation.

1.3. <u>Regulation of platelet function by the cytoskeleton</u>

Changes in actin cytoskeleton of platelets play a central role in the different functional and morphological platelet responses induced by agonists. The cytoskeleton is rigid as well as dynamic. The rigid cytoskeleton keeps the unstimulated platelet in discoid shape, whereas its dynamic nature underlies the morphological and functional changes like shape change, secretion, aggregation and spreading after platelet activation. The dynamics in platelet cytoskeleton comprise the depolymerization, polymerization and crosslinking of cytoskeletal components such as actin and microtubules, and the interaction between myosin and actin filaments.

1.3.1. <u>The actin cytoskeleton in platelets</u>

The platelet actin cytoskeleton is a component of the structural zone. It is comprised of various elements that remain insoluble after lysis of platelets with Triton X-100. This insoluble fraction is further divided into two different forms depending on their structural organization and location: an actin network just beneath the plasma membrane (membrane skeleton) and a cytosolic actin network. The actin filaments of the membrane skeleton are shorter and require higher g-forces (100,000x g) to sediment than the longer filaments of the cytosolic network, which sediments at low g-forces (15,000x g).

Cytoskeleton proteins	Mol wt (kDa)	Properties
Actin	42	Building blocks of the actin filament, possesses ATPase activity; depolymerization and polymerization of actin filaments is involved in cytoskeleton based cell motility.
Gelsolin	91	Severs actin filaments; binds to barbed end of F-actin and facilitates nucleation
Cofilin	20	Binds with G-actin (1:1 ratio) and to the subunits of F-actin; accelerates depolymerization and treadmilling of the actin filaments
Arp2/3 complex	Complex of 7 proteins	Nucleates new actin filaments and accelerates actin polymerization; induces branching of filaments leading to dendritic actin network
Profilin	19	Forms 1:1 reversible complex with actin monomers; promotes exchange of ADP→ATP in actin monomers and enhances filament elongation
CapZ	36 and 32	Heterodimer; binds barbed end of actin filaments and inhibits actin polymerization
Thymosin β_4	5	Sequesters actin monomers and inhibits ADP→ATP exchange
WASP	62	Enhances Arp2/3 complex activity; binds profilin and signaling proteins
VASP	50	Exist as tetramer in vivo; binds profilin, vinculin and zyxin
α-Actinin	100 and 102	Dimer; binds actin at 1:10 stoichiometry; cross-links filaments and promotes actin polymerization
Filamin I	260	Binds actin protomers in filament with 1:14 ratio; cross-links actin filaments; binds cytoplasmic domains of gylcoproteins
Talin	235	Binds to other actin binding proteins like vinculin and α-actinin; binds integrin receptors
Spectrin	240 and 220	Dimer; forms a head to head associated tetramer; cross-links actin; interacts with integrin $\alpha_{IIb}\beta_3$; and possesses sites for calpain cleavage
Vinculin	130	Binds to talin; participates in actin to membrane proteins interaction at adhesion sites
Tropomyosin	28	Binds along the groove of actin filament helix in 1:7 ratio; plays a role in Ca^{2+}-mediated skeletal muscle contraction
Myosin II	480	Dimer of one heavy chain (200kDa) and two light chain (20kDa each); 2-5% of platelet protein; provides contractility to the actin filaments
Caldesmon	80	Binds actin, tropomyosin, myosin and calmodulin; may control actin filaments bundling
Fimbrin	68	Bundles actin filaments

Table 1.1 Proteins of the platelet cytoskeleton (Fox 1993; Hartwig et al. 1999; Fox 2001)

The short filaments of membrane skeleton associate with several proteins (e.g., spectrin) and glycoproteins (e.g., GP-Ib-V-IX and integrin $\alpha_{IIb}\beta_3$) known to cross-link actin filaments and regulate their interaction with the membrane, respectively. The distribution of membrane skeleton proteins and glycoproteins based on their differential sedimentation suggested that different components of membrane skeleton exist (Fox 2001). The longer filaments in the cytosol are cross-linked into a network that traverses throughout the body of the platelet. The filaments in cytosolic actin network are associated with another set of proteins such as α-actinin, tropomyosin, and cladesmon that regulate cross-linking of these filaments or the association with other proteins. Although, much of the information on the composition of the actin filament networks has come from studies on detergent-lysed platelets, a more intensive work towards knowledge of all proteins and their functions regulating actin cytoskeleton is needed. Some of the major components of the platelet contractile system are listed in table (Table 1.1). These elements are thought to contribute towards different platelet functions.

1.3.2. <u>Resting platelets</u>

In the unstimulated platelet, the actin cytoskeleton is thought to exist throughout the cytoplasm and in connection with the spectrin-based membrane skeleton that laminates the cytoplasmic side of the plasma membrane. The bipolar tetrameric strands of spectrin interconnect into a network using the ends of the filaments that are in proximity of the membrane. In this way the entire cytoskeleton functions together to support the plasma membrane and direct its contours. Compared to activated platelets, the actin filaments in unstimulated platelets are relatively stable and filament turnover is slow because the filamentous actins are capped on their barbed ends by the capping protein CapZ, whereas the monomeric actins are captured by the protein thymosin β_4, and thus, prevent the actin dynamics.

Actin filaments in unstimulated platelets are also fastened directly to the membrane glycoproteins. One important interaction is between the cytoplasmic tail of the GP-Ibα chain of the vWF receptor (vWFR) and the actin cross-linking and protein scaffolding protein, filamin1 (Okita et al. 1985). This interaction helps to align vWFRs into linear arrays, to stabilize the plasma membrane (Hartwig et al. 1999) and to regulate the function of vWFRs during platelet activation (Cunningham et al. 1996; Williamson et al. 2002). The importance of this interaction has been established in studies of platelets from patients with Bernard-Soulier syndrome, who possess qualitative and quantitative abnormalities in the GPIb/IX/V complex. These platelets are fragile, abnormally large in size and circulate poorly because of the absence of the GPIb-filamin linkage (Kanaji et al. 2002). Integrin $\alpha_{IIb}\beta_3$ associated with the membrane skeleton is supposed to be constrained in a quiescent low-affinity form by the actin cytoskeleton in unstimulated platelets. Evidences showing that disruption of actin cytoskeleton in either direction (stabilization or destabilization) affect the affinity of integrin $\alpha_{IIb}\beta_3$ for its ligand fibrinogen

suggested an important role of the actin cytoskeleton in regulating the integrin $\alpha_{IIb}\beta_3$ activation (Fox et al. 1996; Bennett et al. 1999).

1.3.3. <u>Stimulated platelets</u>

1.3.3.1. Shape change

Platelet shape change is the earliest response after activation. Platelets loose their normal discoid shape and transform into spiny spheres with long pseudopods. The microtubule ring responsible for maintaining platelet discoid shape disassembles rapidly during platelet activation. However, this process does not seem to be required for platelet shape change as it occurs even in the presence of microtubule destabilizing and stabilizing agents. An other established phenomenon observed during platelet shape change is the rapid reorganization of the actin filaments and increase in F-actin content (Nachmias 1980; Escolar et al. 1986). Several actin filament-severing and -depolymerizing proteins are activated depending on the type of stimulus, such as gelsolin (Lind et al. 1982), scinderin (Rodriguez Del Castillo et al. 1992) and cofilin (Davidson and Haslam 1994). Gelsolin, a Ca^{2+}-dependent actin severing protein, increases the number of short actin filaments after severing the existing filaments, and remains associated with the new barbed ends thereby substituting CapZ as the capping protein (Barkalow et al. 1996). Severing of actin filaments releases the constraints on the spectrin network and allows the incorporation of membranes from OCS into the plasma membrane in order to bring spherocytic change in platelet shape (but not to produce pseudopodia). The changes in actin cytoskeleton such as an increased F-actin content had been observed during Ca^{2+}-independent shape change (Bauer et al. 1999; Klages et al. 1999). However, the role of actin-binding proteins in reorganizing the actin cytoskeleton in the absence of Ca^{2+} is not clear.

The reorganization of the actin cytoskeleton is also accompanied by the activation of myosin via phosphorylation of one of its two light chains by Ca^{2+}-dependent MLC-kinase and Rho-kinase (Daniel and Adelstein 1976; Bauer et al. 1999), which contributes to the actomyosin contraction required for shape change and centralization of granules (Cohen 1979). The protrusive force for pseudopodial developments then comes from the subsequent actin polymerization onto newly severed and uncapped actin filaments. Gelsolin uncapping of actin filaments is accomplished by gelsolin binding to phosphoinositides (PIs), which are produced during platelet activation (Hartwig et al. 1995). Profilin that competes with thymosinβ_4 for G-actin binding facilitates actin polymerization by transferring monomeric actins from the pool of actin-thymosinβ_4 complex to the barbed ends of the actin filaments (Goldschmidt-Clermont et al. 1992). Furthermore, the activation of the Arp2/3 complex initiates de novo actin nucleation, and branching and polymerization of the actin filaments contributing to the platelet shape change (Li et al. 2002). Other proteins and signaling molecules implicated in platelet shape change with varied functions are the small GTPases (Rho, Rac, and Cdc42), WASP, VASP, vinculin, and zyxin (Fox 2001).

1.3.3.2. Secretion

The contractile mechanism involving actin and myosin is also thought to mediate granule secretion but the details remain obscure. Platelet activation leads to the granules coalesce in the center. Centralized granules then fuse with each other, with the OCS and with the plasma membrane in order to release the granule contents outside in the extracellular environment (Escolar and White 1991; Flaumenhaft 2003). Studies correlating the cytoskeletal rearrangement with granule secretion suggest that actomyosin contraction and the reorganization of actin cytoskeleton, but not the microtubule dynamics, might regulate secretion. The microtubule stabilizing agent taxol does not inhibit secretion (White and Rao 1983), whereas inhibitors of kinases involved in actin cytoskeleton dynamics such as the Rho-kinase inhibitor Y-27632 (Suzuki et al. 1999) and the MLC-kinase inhibitors, W-7 and ML-9 (Saitoh et al. 1986; Lokeshwar and Bourguignon 1992) inhibit secretion. However, cytochalasins, fungal metabolites that impair actin polymerization, have yielded conflicting results regarding the role of the actin cytoskeleton in secretion. One study showed an augmentation of collagen-induced secretion by cytochalasin-B, whereas another study demonstrated only little effect of cytochalasin-B on collagen-induced dense granule secretion (Haslam et al. 1975; Kirkpatrick et al. 1980). Studies using other agonists such as thrombin, phorbol esters, calcium ionophore, or ADP have also demonstrated either inhibition or augmentation of secretion by cytochalasins (Hashimoto et al. 1986; Cox 1988; Diaz-Ricart et al. 2002). Hence, it is not clear whether actin polymerization inhibits or facilitates secretion. A recent study suggested that the actin cytoskeleton differentially regulates platelet α-granule and dense granule secretion. Platelet exposures to low concentrations of actin-disrupting agents accelerated and augmented α-granule secretion, and decreased the agonist concentration required. In contrast, high concentrations of actin-disrupting agents inhibited α-granule secretion, but stimulated dense granule secretion (Flaumenhaft et al. 2005).

1.3.3.3. Aggregation

During aggregation of platelets, the bi-directional signaling through the integrin $\alpha_{IIb}\beta_3$ involves many proteins that regulate the dynamics of the actin cytoskeleton. It has been observed that inhibition of actin polymerization by cytochalasin-D or latrunculin-A can induce fibrinogen binding to the integrin $\alpha_{IIb}\beta_3$, whereas the actin-stabilizing agent jasplakinolide inhibited platelet aggregation. This study suggests a role of the actin cytoskeleton in integrin $\alpha_{IIb}\beta_3$-mediated platelet aggregation (Bennett et al. 1999). The different signaling pathways after platelet stimulation with agonists are supposed to converge at one point to transform the integrin $\alpha_{IIb}\beta_3$ from a low affinity to a high affinity state (inside-out signaling), which modulate the efficient fibrinogen binding to the receptors. An actin binding protein talin, which also binds to the cytoplasmic domain of the integrin β-subunit, is supposed to be the terminal point for integrin $\alpha_{IIb}\beta_3$ activation (Tadokoro et al. 2003). Another protein VASP has been suggested to keep integrin $\alpha_{IIb}\beta_3$ into the low-affinity state. Platelets from VASP knock-out mice showed an enhanced aggregation induced by different agonists (Aszodi et al. 1999; Hauser et al. 1999). The

binding of fibrinogen to the integrin $\alpha_{IIb}\beta_3$ mediates additional activation of signaling pathways (outside-in signaling) that are important for the stabilization of platelet aggregates, the release of procoagulant molecules, the further reorganization of the cytoskeleton, and later for fibrin clot retraction. The cytoskeleton reorganization by the activation of Ca^2-dependent calpain has been proposed to be important for clot retraction (Phillips and Jakabova 1977; Fox et al. 1993). This thiol protease cleaves several cytoskeleton proteins such as talin, spectrin, filamin, dystrophin-related protein, and protein 4.1 superfamily members, including several signaling proteins and the cytoplasmic tail of β_3-subunit of integrin itself (Schoenwaelder et al. 1997; Fox 1999).

1.4. Actin dynamics

Actin is an extremely conserved and an essential cytoskeletal component of eukaryotic cells. It is the most abundant protein of molecular mass of 43 kDa and exists in different isoforms throughout the eukaryotes. So far, six actin isoforms are known to be expressed as muscle specific (α- and γ-smooth muscle actins, α-skeleton actin and α-cardiac actin) and non-muscle specific (cytoplasmic β- and γ-actins) types and these are functionally specialized for the tissue in which they predominate (Khaitlina 2001; Chaponnier and Gabbiani 2004). The single actin molecule is a relatively flat (~67 x 40 x 37 Å), with four quasi-subdomains arranged to form a two-lobed molecule with two subdomains in each lobe and a central cleft between these two lobes (dos Remedios et al. 2003). The central cleft contains the binding sites for a nucleotide (ATP or ADP) and a divalent cation (Mg^{2+} or Ca^{2+}), which are essential cofactors of actin (De La Cruz and Pollard 1995; Kabsch and Holmes 1995). Actin monomers also known as globular actin (G-actin) are able to assemble spontaneously into polar helical filamentous actin (F-actin) under physiological salt conditions. The structure of F-actin is yet to determine but highly plausible models have been proposed based on the model of Holmes et al. (Holmes et al. 1990; dos Remedios et al. 2003).

1.4.1. Actin filament assembly and disassembly

The polymerization of G-actin to F-actin is an energy demanding process driven by actin's ATPase activity. Binding of ATP and Mg^{2+} to the cleft of monomeric actin (activation) is the initial step in this process, which is then followed by an oligomerization of actin molecules that act as nucleus for further elongation. This nucleation process is relatively slow due to the instability of these oligomers and contributes to the lag phase for actin polymerization and hence, described as the rate-limiting step. A rapid growth phase occurs as monomers are added bi-directionally to the actin nucleus causing filament elongation. The rate of filament elongation gradually reduces as the concentration of remaining free G-actin reaches a point where available monomers become exhausted. Since all these processes are reversible, an equilibrium is then established where the rate of subunit addition to the filament ends is exactly balanced by the rate

of subunit dissociation from the ends. The concentration of G-actin at this steady state is called critical concentration (Cc). Net polymerization occurs when the G-actin concentration is higher than Cc, and net depolymerization occurs when the G-actin concentration is lower than Cc (Pollard and Cooper 1986).

The chemical switch between polymerization and depolymerization of the actin filament is the hydrolysis of ATP. Each actin monomer carries a tightly bound ATP molecule, which gets hydrolyzed to a tightly bound ADP molecule soon after its assembly into the filament. Hydrolyses of ATP reduces the binding affinity of the subunit for its neighboring subunits and makes it more likely to dissociate from each ends of the filament. In rapidly assembling filaments, the hydrolysis lags behind the assembly, thus the hydrolysis of ATP is uncoupled from the fast growing assembly site (plus end), and the hydrolysis occurs at the rear ends of filaments, yielding first ADP-F-actin that leaves the filament from the slow growing disassembly site (minus end). At the steady state where rate of subunit addition at plus end is identical to the rate of subunit disassembly from minus end, the polymer maintains a constant length and this process is termed as treadmilling (Wegner 1976).

Due to the polar nature of each actin monomer, actin filaments created by the regular and parallel orientation of their subunits also have a unique polarity. This polarity can be detected by decorating actin filaments with fragments of myosin, which binds to the fast growing assembly site (plus end). Projections of myosin are tilted in one direction and appear as arrowheads. Thus, this end of the actin filaments is also called as the barbed end (plus end), whereas the slow growing is the pointed end (minus end) (Moore et al. 1970).

1.4.2. <u>Proteins regulating actin dynamics</u>

The process of treadmilling is thought to be responsible for protrusive motility in cells, however in vitro at steady state under physiological ion conditions this process is relatively slower than the cellular motility. In the steady state, growth at the barbed end is limited by dissociation from the pointed end resulting in effective growth rate of ~0.04 µm/min, which is 100-200 times slower than in cells (Pollard and Borisy 2003; Disanza et al. 2005). The higher rate of treadmilling in vivo is due to proteins that interact with actin filaments or monomers, known as actin-binding proteins (ABPs). A plethora of ABPs (approximately 162 distinct proteins) present in vivo regulates different aspects of the actin filaments like assembly, disassembly and organization of the filaments into functional higher order networks (dos Remedios et al. 2003). These proteins are classified into more than 60 different classes leaving behind many "orphan" proteins that do not fit into these classes. Following important ABP groups are distinguished based on their function to regulate actin dynamics. *1)* Monomer binders, proteins binding to ADP- or ATP-bound G-actin, sequestering them and preventing or facilitating actin polymerization (e.g., thymosin β4, profilin, and ADF/cofilin). *2)* Capping proteins, which bind to one of the two end

of the actin filament; they prevent the exchange of actin monomers at the pointed end (e.g., tropomodulin) or at the barbed end (e.g., CapZ and gelsolin). **3)** Severing and depolymerizing proteins, which shorten the average length of filaments by dissociating the subunits from either end or severing the filament at any place (e.g., ADF/cofilin, gelsolin, and scinderin). **4)** Cross-linking proteins, which contain at least two actin-binding sites; they facilitate the nucleation of new filaments, and induce bundling and branching of filaments into two- or three-dimensional networks (e.g., Arp2/3, formins, and α-actinin). **5)** Filament-stabilizing proteins that bind to the sides of the actin filaments and prevent their depolymerization (e.g., tropomyosin).

Some of these ABPs are not limited to one specific function, for e.g., gelsolin severs and caps the barbed end of the actin filaments, the Arp2/3 complex that consists of seven proteins nucleates and elongates the filaments and establishes branching points in actin networks, and ADF/cofilin not only severs and depolymerizes the actin filament, but also amplifies the local actin polymerization by acting synergistically with the Arp2/3 complex (DesMarais et al. 2005). Functional overlap of these ABPs makes their classification difficult; a more broadened picture of these ABPs is presented in Figure 1.4 and Table 1.1.
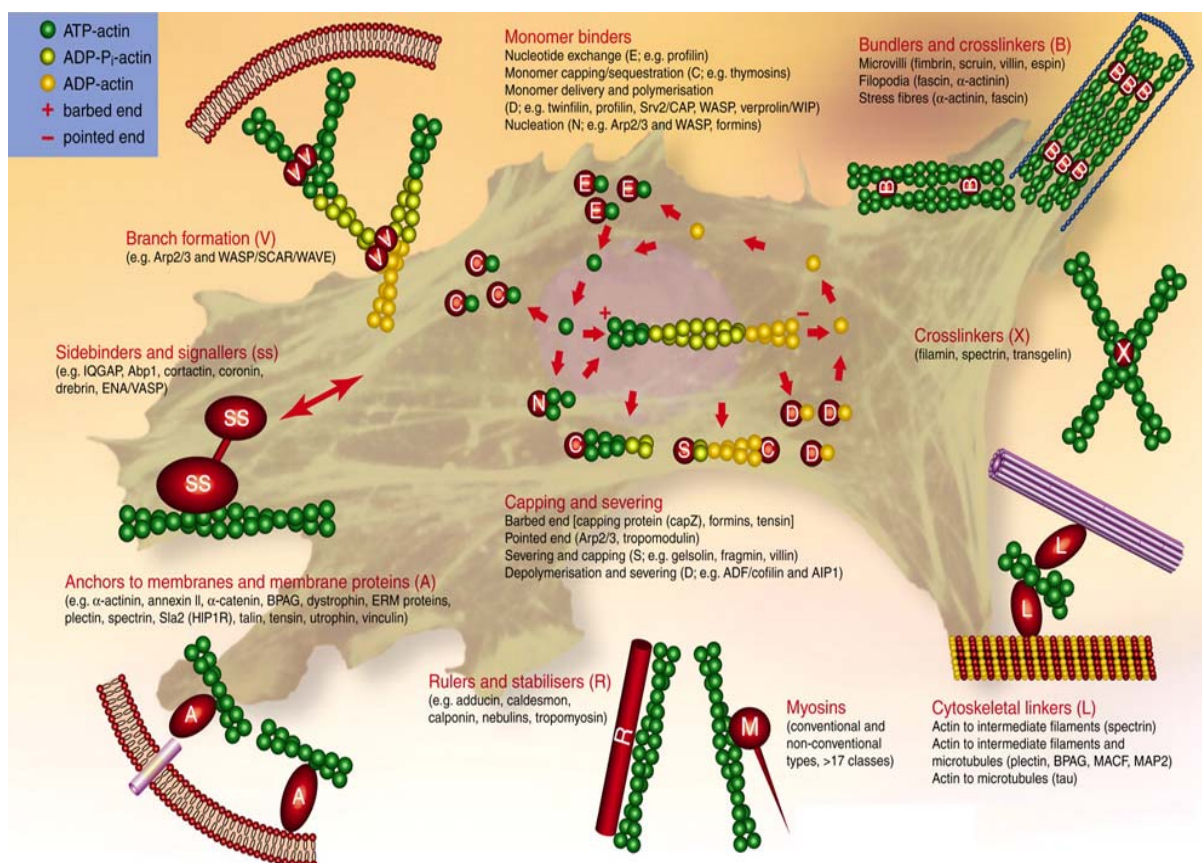
Figure 1.4 Actin-binding proteins and their function. Proteins involved in regulating the actin filament assembly and disassembly (center) are grouped into monomer binders and capping and severing proteins class. Proteins engaged in branch formation, cross-linking and bundling help the actin filaments to obtain higher-order structures. Proteins in classes like myosins, cytoskeletal linkers and membrane anchors contribute to the mechanical properties of the actin scaffold, (Winder and Ayscough 2005)**.**

1.4.3. <u>Signaling for actin dynamics</u>

The integration and coordination of the activities of all ABPs and the proteins affecting different steps of actin reorganization are needed to promote the cytoskeleton based cellular functions, which are 100-200 times faster than the in vitro actin dynamics under physiological ionic conditions. Actin regulatory proteins are also the targets for a number of signaling pathways, which transmit the signals in a temporally and spatially controlled fashion. Among the signaling proteins involved in actin dynamics, the Rho-GTPases family proteins of Ras superfamily GTPases have emerged as central players. Signaling through Rho-GTPases can be initiated by activation of different plasma membrane receptors such as tyrosine kinase receptors, G-protein-coupled receptors (see section 1.2.3), and integrins.

The family of Rho-GTPases consists of 25 members divided roughly into 6 subfamilies based on their primary sequence and known functions: Rho-like, Rac-like, Cdc42-like, Rnd, RhoBTB and Miro, except RhoD, Rif and TTF/RhoH, which do not obviously fall into any of these subfamilies (Wennerberg and Der 2004). Like all GTPases, Rho-GTPases cycle between active (GTP-bound) and inactive (GDP-bound) conformations regulated by guanine-nucleotide exchange factors (GEFs), and GTPase activating proteins (GAPs). In addition, Rho-GTPases are regulated further by guanine-nucleotide dissociation inhibitors (GDIs) that inhibits both the exchange of GTP and the hydrolysis of bound GTP (Van Aelst and D'Souza-Schorey 1997). Although, platelets lack a complete enlisting and characterization of its GTPases, Rac, Cdc42 and Rho are the three important Rho-GTPase subfamilies that regulate different signaling pathways underlying distinct actin dynamics based processes in platelets (see section 1.4.4). Although the presence of different isoforms of Rho (RhoA, RhoB, and RhoC) and Cdc42 proteins in platelets are yet to be characterized, RhoA expression seems to be dominant in platelets (Nemoto et al. 1992). Recently, it was found that Rac1 but neither Rac2 nor Rac3 isoforms is expressed in human and murine platelets (McCarty et al. 2005). Apart from the Rho-GTPases family proteins, some members of other GTPase families such as Ras (e.g., Rap1B, Rap2B) and Arf (Arf6) have been suggested to regulate cytoskeletal dynamics in activated platelets (Torti et al. 1999; Chrzanowska-Wodnicka et al. 2005; Choi et al. 2006).

1.4.4. <u>Effectors of Rho-, Rac- and Cdc42-like GTPases</u>

Members of the Rho family GTPase including Rho, Rac, and Cdc42 that are highly expressed in platelets regulate different dynamic actin structures underlying platelet activation. Rho is known for spheration and contractility (Klages et al. 1999), Rac1 regulates the formation of lamellipodia (McCarty et al. 2005), whereas Cdc42 controls the formation of filopodia during platelet activation (Chang et al. 2005). These Rho-GTPases regulates these distinct actin-related processes through specific downstream effector proteins. Rac and Cdc42 possess mainly common (Cotteret and Chernoff 2002) targets, whereas Rho effectors are specific albeit some of

them are influenced by Rac and Cdc42 also. Common targets for Rac and Cdc42 include serine-threonine kinases (e.g., p21 activated kinases, PAKs), lipid-kinases (e.g., PI3-kinase), and IQGAPs (Teo et al. 1995; Carpenter et al. 1997; Schmidt et al. 2003). Some of the Rac and Cdc42 effector proteins are different and specific however, the signaling pathways later converge onto a common target for regulating distinct functions. The best example of this intriguing complexity is the indirect activation of the Arp2/3 complex by both Rac and Cdc42, but through different effectors WAVEs and WASP that lead to morphologically distinct protrusions at the plasma membrane, lamellipodia and filopodia, respectively (Falet et al. 2002; Jaffe and Hall 2005).

The most prominent and common target of Rac and Cdc42 are PAKs. All PAKs identified to date share a similar 18-amino acid CRIB (Cdc42/Rac interactive binding) motif that mediates the interaction with Rac and Cdc42 (Bokoch 2003). Activation of PAK regulates several processes: an activation of LIMK-1 with the subsequent inactivation of cofilin (Arber et al. 1998; Dan et al. 2001); and an inhibition of MLC-kinase thereby inhibiting MLC phosphorylation and reducing the actomyosin structures (Sanders et al. 1999; van Leeuwen et al. 1999). So far, the characterization and specific role of PAK isoforms in platelets remain to be elucidated. Another common target of Rac and Cdc42 are IQGAPs that are able to bind to both Rac and Cdc42, and hence thereby facilitating the actin filament cross-linking activity of these proteins (Brill et al. 1996). The two homologous isoforms of IQGAPs (IQGAP1 and IQGAP2) are present in human platelets. IQGAP1 binds specifically to GTP-bound forms of Rac1 and Cdc42, whereas IQGAP2 can bind to both the inactive (GDP) and active (GTP) forms of Rac1/Cdc42; therefore they could mediate divergent actin-related responses (Schmidt et al. 2003).

Rho stimulates several signaling proteins such as the Rho-kinases (ROCKs), protein kinase novel (PKN), myosin binding subunit, kinectin, mDia and citron kinase (Van Aelst and D'Souza-Schorey 1997). Furthermore, Rho directly or indirectly stimulates lipid kinases (PIP5-kinase and PI3-kinase), which are also targets for Rac and Cdc42. The well elucidated Rho target in platelets is Rho-kinase (Ishizaki et al. 1996) and to some extent the lipid kinases that are observed to be activated through Rho, however direct interaction of these lipid kinases with Rho is still questionable (Zhang et al. 1993; Yang et al. 2004). The presence of other Rho targets and whether they could influence actin dynamics in activated platelets is not known. Rho interaction with mDia, a member of the formin family of proteins, stimulates actin polymerization by binding with the profilin/actin complex and delivering it to the barbed end of the filament (Li and Higgs 2003). Citron kinase, which like Rho-kinase stimulates MLC phosphorylation and enhances myosin activity, appears to function primarily during mitosis, specifically at the cleavage furrow in other cell types (Madaule et al. 1998).

1.4.5. <u>Rho-kinase</u>

Rho-kinases or ROCKs, a serine/threonine protein kinases, were the first effectors of Rho to be discovered, and were initially characterized for the formation of RhoA-induced stress fibers and focal adhesions (Leung et al. 1996). Two isoforms of Rho-kinases have been identified that are encoded by different genes; ROCKI (also known as ROKβ or p160 ROCK) and ROCKII (also known as ROKα). These two proteins share an overall sequence similarity at amino-acid level of 65% and in their kinase domains of 92% (Nakagawa et al. 1996). These kinases consist of an amino terminal kinase domain followed by a coiled-coil region and a Rho-binding domain, and a pleckstrin homology (PH) domain at C-terminal. Rho-kinase (p160ROCK; ROCKI) was firstly isolated from human platelets as a 160 kDa protein homologous to myotonic dystrophy kinase (Ishizaki et al. 1996). Since no attempt to identify ROCKII in platelets has been performed and Rho-kinase inhibitors cannot differentiate between these two isoforms, most of the studies in platelets use Rho-kinase as general term to indicate both isoforms.
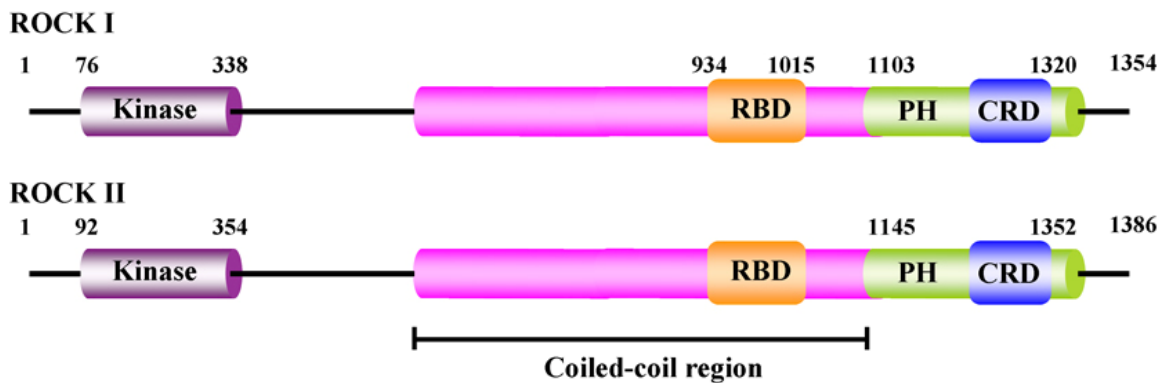
Figure 1.5 The structure of Rho-kinases. The kinase domain of Rho-kinases is situated in the N-terminus, and it possesses high homology between the two isoforms (92% identity). The sequence of the Rho-binding domain (RBD) of ROCKI (amino acids 934-1015) is highly homologous in ROCKII. In the C-terminus of Rho-kinases there is a pleckstrin homology (PH) domain with an internal cysteine-rich region/domain (CRD). The region between the kinase domain and the PH domain is predicted to form coiled-coil structure.

The kinase activity of Rho-kinases is enhanced after binding with Rho-GTP. ROCKI but not ROCKII, is also activated in vivo by caspase-3 cleavage causing membrane blebbing (Coleman et al. 2001). The activated Rho-kinases phosphorylate several substrates in particular proteins involved in regulation of actin-filament assembly and contractility, such as <u>My</u>osin <u>P</u>hosphatase <u>T</u>argeting subunit (MYPT), LIMKs, and ERM (ezrin-radixin-moesin) proteins. In platelets, three of these Rho-kinase effectors, MLC, MYPT and moesin have been studied in part extensively and suggested to be important for regulating platelet responses during activation. During shape change, the activation of Rho-kinase elevates MLC phosphorylation either directly by phosphorylating MLC or indirectly by phosphorylating MYPT thereby inhibiting myosin phosphatase. This leads to an increased actin-myosin driven contractility (Amano et al. 1996; Kureishi et al. 1997; Shimizu et al. 2005). Also during shape change, Rho-kinase stimulates the phosphorylation of moesin (Retzer and Essler 2000). Recently, it has been stated that Rho-kinase

mediates the destabilization of the cytoskeletal microtubule ring leading to shape change; however the exact mechanism of this process is not known (Paul et al. 2003).

One of the important physiological targets of Rho-kinase is the MYPT subunit of myosin phosphatase (Hartshorne 1998). Myosin phosphatase is a heterotrimeric phosphatase composed of a 38-kDa protein phosphatase (PP) 1cδ type catalytic subunit and two regulatory subunits, a 110-kDa MYPT subunit (Figure 1.6) and a 20-kDa small regulatory subunit (M20). MYPT subunit interacts with PP1cδ type catalytic phosphatase at the N-terminus and with regulatory M20 subunit at the C-terminus, thereby forming the holoenzyme of myosin phosphatase. At the N-terminus, MYPT contains ankyrin repeats that are involved in binding to the target protein, phosphorylated MLC. The PP1cδ-binding motif (KVKF) at the N-terminus margin of the first ankyrin repeat allows the access of PP1cδ phosphatase to dephosphorylate MLC. An alternative myosin binding site also exists at the C-terminal sequence of MYPT. Binding of myosin to both the N-terminal and C-terminal regions of MYPT suggests that the myosin head binds to the N-terminus and the myosin rod portion binds to the C-terminus thereby aligning phosphorylated myosin to the holoenzyme of myosin phosphatase. The function of small M20 subunit has not been established.
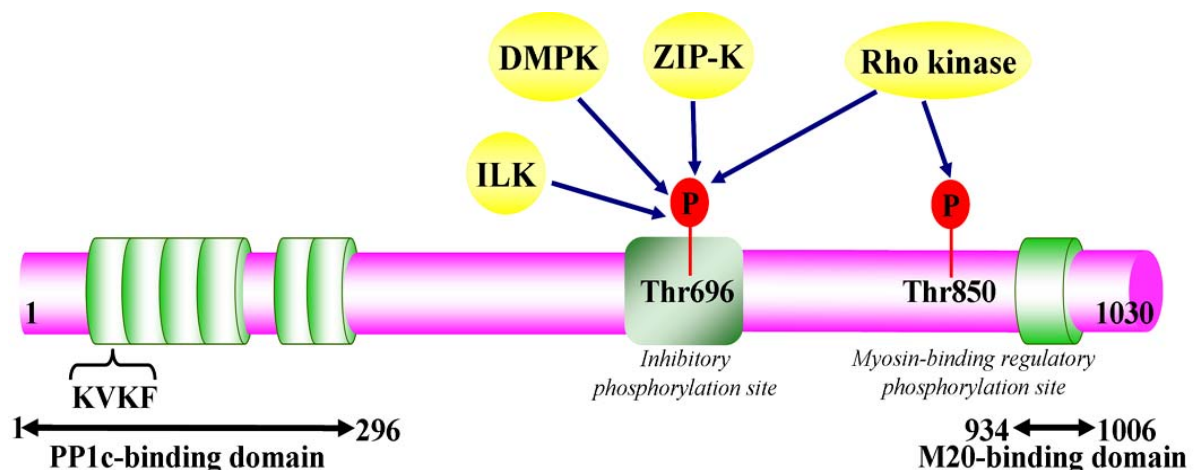
Figure 1.6 Domain structure of human MYPT. MYPT contains PP1cδ-binding domain composed of binding motif (KVKF) and ankyrin repeats, and M20-binding domains. Two major phosphorylation sites shown here are targets of various kinases that regulate MYPT functions.

Multi-phosphorylation site in MYPT are regulatory for inhibiting myosin phosphatase activity, however, the molecular basis for this inhibition is not understood. Human MYPT has two major sites for phosphorylation by Rho-kinase, which contribute for inactivation of myosin phosphatase, the inhibitory phosphorylation site (Thr696) and the myosin-binding regulatory phosphorylation site (Thr853). Phosphorylation of Thr696 is also regulated by several other kinases like ZIP-kinase (more recently termed MYPT1 kinase), integrin-linked kinase, myotonic dystrophy protein kinase (DMPK) and PAK, whereas Thr853 is known to be phosphorylated specifically by Rho-kinase (Ito et al. 2004).

Rho-kinase also phosphorylates LIMKs and enhances their ability to phosphorylate cofilin at Ser3 (Maekawa et al. 1999). Cofilin phosphorylation blocks its actin binding and F-actin depolymerization activity.

1.4.6. LIM-kinases

LIM (for Lin11, Isl1 and Mec3) kinases are serine/threonine kinases involved in the regulation of actin-filament dynamics (Khurana et al. 2002), which were initially identified in a screen for novel members of the c-Met/HGF receptor tyrosine kinase family (Mizuno et al. 1994). LIMKs (~70-kDa) are unique protein kinases that have two repeats of the LIM domain at N-terminus, followed by a PDZ domain, a proline/serine-rich region, and an unusual protein kinase domain at the C-terminus. The LIMK protein family is comprised of two members, LIMK-1 and LIMK-2 (Okano et al. 1995). Comparisons of these LIMK homologue protein sequences reveal variations in amino acid conservation between domains. The kinase domains are most highly conserved between LIMK-1 and LIMK-2 (~70%), followed by the LIM (~50%) and PDZ domains (~46%).

The N-terminal LIM domains play an inhibitory role in the regulation of the kinase activity of LIMK-1 by direct interaction with the kinase domain (Nagata et al. 1999). The LIM domains may fix the kinase domain in an inactive conformation, or inhibit the access of substrates by masking the kinase catalytic site or substrate-binding site. Many serine/threonine kinases are phosphorylated on a residue(s) in the activation loop, which regulates their activity. LIMK-1 and LIMK-2 have Thr508 and Thr505 residues, respectively, in the activation loop as regulatory phosphorylation sites. Rho-kinase phosphorylates LIMK-1 at Thr508 (Ohashi et al. 2000), and LIMK-2 at Thr505 (Sumi et al. 2001) and activates them (Figure 1.7).
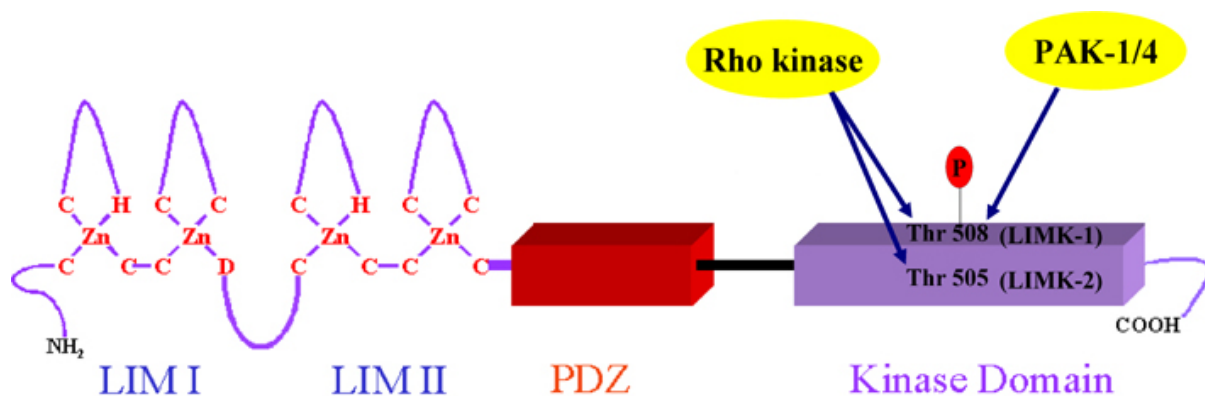
Figure 1.7 Structure and regulatory phosphorylation of LIMKs. LIMKs contain two zinc finger LIM, a PDZ and a kinase domain. LIMK-1 can be phosphorylated and activated by Rho-kinase as well as PAK1/PAK4.

As mentioned above (see section 1.5.1), in addition to the Rho/Rho-kinase pathway, Cdc42 and Rac effectors PAK1 and PAK4 can phosphorylate LIMK-1 at Thr508 (Edwards et al. 1999; Dan et al. 2001). Furthermore, MRCKα a protein downstream of Cdc42 is able to phosphorylate LIMK-1 and LIMK-2 at their respective sites leading to enhanced cofilin phosphorylation (Sumi et al. 2001).

The physiological substrate known for Rho GTPases mediated LIMKs activation is cofilin, an actin dynamizing protein. The knowledge of regulation and activation of cofilin has become an important area to understand actin dynamics underlying different physiological responses by cells.

1.5. Cofilin

Cofilin is a member of actin depolymerization factor (ADF)/cofilin (A/C) family, firstly purified from porcine brain (Maekawa et al. 1984). Proteins in the A/C family are generally small (13-20 kDa), exist in multiple forms, and expressed ubiquitously in all eukaryotic cells. Their main functions include rapid recycling of actin monomers thereby dynamizing the actin scaffold needed for various cellular events such as cell motility, membrane protrusions, polarity of cell migration, or during cytokinesis. The first member of A/C family was the ADF protein, identified and purified from embryonic chick brain extract (Bamburg et al. 1980). Since then, over 30 members of the A/C proteins family have been discovered that are named after their observed functions e.g., ADF or destrin (destroys F-actin), depactin (depolymerizes actin) and cofilin (co-sediments with filamentous actin) (Bamburg 1999). All of these proteins exhibit considerable homology in their amino acids sequence. Proteins of the A/C family from a single organism share about 70% sequence identity. A similar sequence identity is also observed when A/C proteins from mammals are compared with their counterparts in avians. However, the homology decreases to 20-40% when vertebrates are compared with lower eukaryotes. Despite the variation in identity between homologs, vertebrates have genes for only two forms, ADF and cofilin (dos Remedios et al. 2003). Although names of the two proteins indicate a behavioral difference, they are functionally related proteins, as they both can bind and depolymerize F-actin. To differentiate these related proteins, efforts for knowing the kinetic of their activities are in progress. For my thesis, the term cofilin includes both ADF and cofilin. Mammalian A/C family is comprised of one ADF and two cofilin isomers. Cofilin 1 is expressed in most embryonic tissues and adult cells, cofilin 2 is only expressed in muscle cells, and ADF expression is limited to the epithelia and endothelia (Vartiainen et al. 2002). The differential location of these isoforms might be a reason for their specific requirement for actin dynamics in different cell types.

1.5.1. Structure of cofilin

Human cofilin has 72% sequence identity with human ADF. The multiple sequence alignment of human cofilin with other proteins of A/C family shows the conservation of primary sequence and secondary structure elements within the family (Figure 1.8).

Among the most highly conserved regions are the two actin-binding domains, including the single regulatory phosphorylation site. The region of non-homology between divergent members likely occurs in loops between the conserved secondary structures. These insertions are thought merely to increase the length of a protein without having any impact on their three-dimensional structures. Human cofilin (166aa) is larger than its counterpart in plant (139aa) and yeast (143aa). Some of the additional residues contributing to the large size are the nuclear localization signal (NLS) and the extended C-terminus. Similar to other A/C members, human cofilin is made up of a unique actin-binding module, the ADF homology (ADF-H) domain, which is present in three distinct classes of actin binding proteins: ADF/cofilins, twinfilins (two ADF-H domains), and Abp1/drebrins (Lappalainen et al. 1998). ADF-H domain is a ~150 amino acid motif, folds with a central 4 to 6-stranded mixed β-sheet sandwiched between two pairs of α-helices, one on each face. Recently, the structure of human cofilin in solution was determined by multi-dimensional NMR spectroscopy (Figure 1.8B) (Pope et al. 2004).
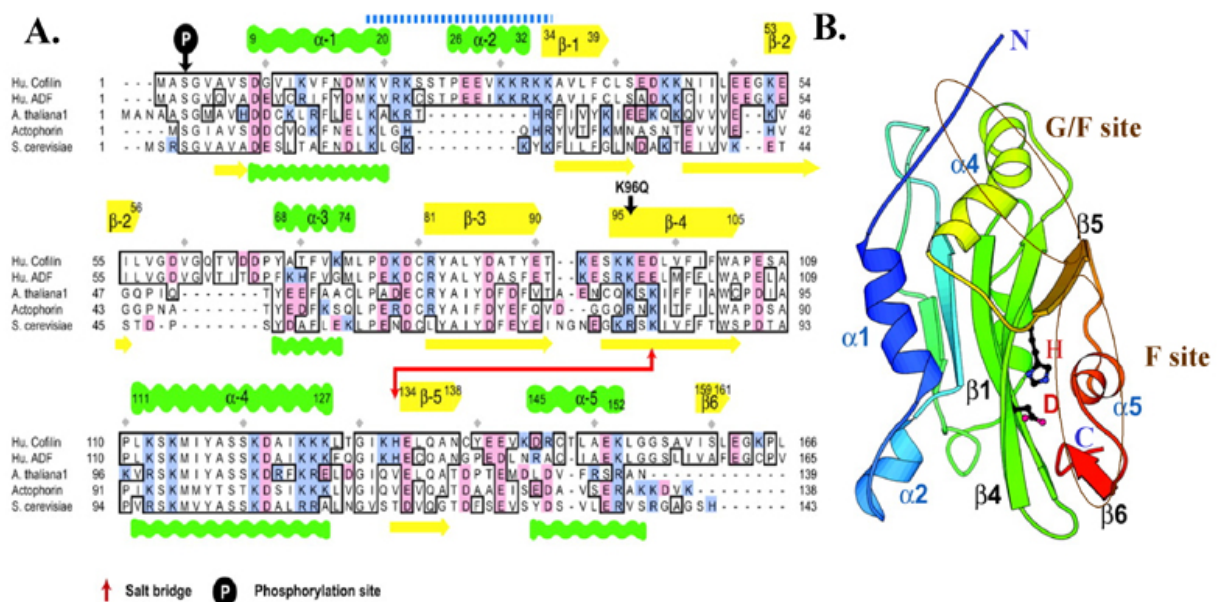
Figure 1.8.A) Sequence alignment of A/C family with known three-dimensional structures. The alignment shows homologous sequences (***boxed***), basic/acidic residues (***blue***/***red***, respectively), α-helices (***green***) and β-strands (***yellow***; above for human cofilin with residue numbering and below for yeast cofilin. The salt bridge (***red arrows***), the phosphorylation site (***circled P***) and the NLS (***blue dotted line***, residues 18-34) are some important features of cofilin for its activity. **B) Ribbon diagram of cofilin structure.** The G/F site is involved in G-/F-actin binding and the F site is involved in F-actin binding (***brown rings***). Residues involved in the salt bridge, Asp98 and His133 are labeled in ***red***. (Pope et al. 2004).

The ADF-H fold in human cofilin possesses the core of a five-stranded mixed β-sheet with four strands anti-parallel and the final pair parallel in arrangement. Four helices (α1-α4) surround the central β-sheet, and a fifth helix (α5) packs against β5-strand. Additionally the C-terminal residue 159-161 forms a short strand (β6), which is unique to cofilin, and results in tighter packing of module. In contrast to the C-terminal β6-strand of cofilin, the corresponding residue in human ADF forms part of a slightly helical coil that might contribute to the different actin depolymerizing activity of these proteins. A salt bridge in cofilin between His133 and Asp98

(Glu98 in ADF), which are conserved in human A/C members, may explain the pH sensitivity of human cofilin and ADF.

1.5.2. <u>Properties and functions of cofilin</u>

Cofilin associates stoichiometrically with actin and reaches saturation at a 1:1 molar ratio (Nishida et al. 1984). The ADF-H domain in cofilin contributes to its role in binding monomeric (G/F site) as well as filamentous actin (G/F site and F site, see Fig 1.6B). The G/F site is covered by the N-terminus, α4-helix and β5-strand, and is responsible for both G-and F-actin binding. The F site includes the C-terminus, α5-helix and β5-strand, and is responsible for F-actin binding and severing activity. The specific amino acid residues participating in these interactions have not been entirely elucidated. However, the recent study by Pope et al. interpreted that the environment of hydrophobic pockets in these sites is important for binding of cofilin with actin (Pope et al. 2004). Residues identified by site directed mutagenesis, Ser3, Lys112 and Lys114 for G/F site and Lys96 for F site, are considered as critical for providing the favorable environment. Phosphorylation of cofilin at Ser3 position or S3D mutation (Moriyama et al. 1996), and replacement of Lys112 and Lys114 by glutamine (Moriyama et al. 1992) inhibited cofilin interaction with actin.
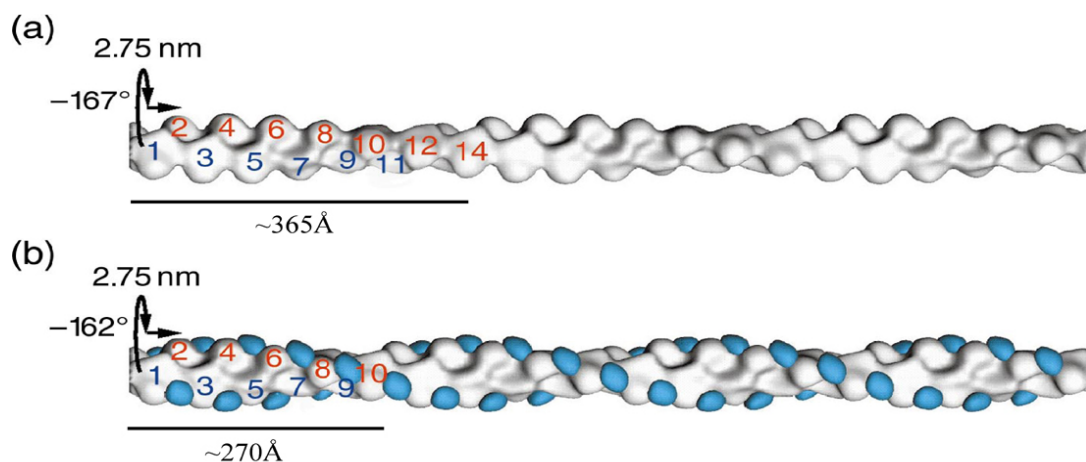
Figure 1.9 Effect of cofilin on actin filament structure. (a) Structure of actin with axial rise per subunit (1-2) of 2.75 nm and a rotation of ~167°. A crossover segment in actin filament is generally observed after ~13 residues. (b) Cofilin binding to actin changes the rotation per subunit to ~162° but the axial rise remains unchanged. After cofilin binding, a crossover is observed after ~10 actin subunits. (Bamburg et al. 1999). Blue and red numbers indicate actin monomers of the intertwined actin helix.

At physiological ionic strength, cofilin binds with the ADP-bound G- or F-actin with an affinity ~100 fold higher than the ATP- or ADP-Pi-bound forms (Carlier et al. 1997). The preferential binding of cofilin with ADP-bound actins makes the pointed end (slowly growing region) of the filament, a more favorable target for cofilin action than the barbed end. Cofilin binds with two actin protomers adjacent to each other along the two-start, polar, and helical actin filament. The interaction of the G/F-site of cofilin with actin domains 1 and 3 (comprise site1) and of the F-site

with the actin domains 1 and 2 (comprise site2) twists the actin filament with a reduction of rotation per actin subunit by about 5°, but no shrinkage in overall length of the filament (McGough et al. 1997), Figure 1.9.

This reduction in twist and a new closed packing of protomers provide intrinsic strength to the actin filament where cofilin is bound (Galkin et al. 2001; Dedova et al. 2004). However, this modification in filament's topology destabilizes both longitudinal and lateral actin-actin contacts in adjacent subunits that are free from cofilin (McGough and Chiu 1999; Bobkov et al. 2002). The weakening of these contacts results in the release of actin protomers and depolymerization of the actin filament. It is not clear whether the actin protomers are released as single forms, with or without cofilin, or whether they exist in an actin pair associated with cofilin. The higher affinity of cofilin for ADP-actin also inhibits the released actin monomer from nucleotide exchange and limits their recycling back to the filament during the process of treadmilling (Nishida 1985; Teubner and Wegner 1998). Thus, cofilin accelerates the off-rate from pointed end of the filament by about 30-fold and on-rate at the barbed end by about 10-fold, under physiological condition (Carlier et al. 1997).

Cofilin binding to actin filaments is highly cooperative (Hawkins et al. 1993; Hayden et al. 1993). Cofilin binding to the site1 on G-actin or F-actin exposes the site2 of actin for additional cofilin binding, which might explain its cooperative binding behavior and intercalation into F-actin (Blondin et al. 2001). Cooperative changes in the conformation of F-actin brought by cofilin binding may modulate the binding of other proteins to actin filament or sequester the F-actin from interaction with these proteins (McGough et al. 1997). Actin filament decorated with cofilin makes the filament brittle at the juncture of decorated and undecorated regions and contribute to the severing activity of cofilin. However, severing activity of cofilin is weaker than gelsolin and raises an argue for cofilin being a true severing protein (Ichetovkin et al. 2000). Furthermore, severing does not occur on short (less than 0.7μm or 250 subunits) gelsolin-capped filaments, suggesting that cofilin requires longer filament with greater flexibility (Yeoh et al. 2002) or gelsolin modulates the filament structure and cofilin binding with actin filament (Ressad et al. 1998). Severing of actin filaments can accelerate the rate of actin depolymerization by increasing the number of depolymerizing ends (Maciver et al. 1998; Moriyama and Yahara 1999). Although, both severing and depolymerizing activities are presumably due to the additional strain on actin filaments, some groups suggested a separation between severing and depolymerizing activities based on residues involved in cofilin-actin complexes (Pope et al. 2000; Ono et al. 2001). Severing of actin filament by cofilin can also generate free barbed ends that can act as nuclei for efficient enhancement of actin polymerization needed for cell motility. Cofilin produces newly polymerized actin filaments that are preferred for dendritic nucleation by the Arp2/3 complex (Ichetovkin et al. 2002). Antibody that blocks the nucleation activity of Arp2/3 complex inhibited the lamellipodia protrusion but did not inhibited the appearance of barbed ends (Chan et al. 2000), whereas function-blocking antibody against cofilin inhibited barbed end

generation (Bailly et al. 2001), indicating that both act together to produce the actin-based motility at the leading edge (DesMarais et al. 2004). Furthermore, recent studies showed that cofilin alone is sufficient to generate free barbed ends leading to actin polymerization and protrusion. These results support a direct role for cofilin severing in initiating and defining the polarity of cell motility (Ichetovkin et al. 2002; Ghosh et al. 2004).

1.5.3. <u>Regulation of cofilin activities</u>

There are several factors that can regulate cofilin activities; these are intracellular pH, competitor proteins for actin binding, interacting proteins, kinases and phosphatases. Some but not all cofilin isoforms are pH-dependent, which regulate cofilin binding, severing and filament depolymerization. At low pH (~6.7), cofilin binds filaments and changes their twist but does not promote disassembly (De La Cruz 2005). At increased pH (7.0-7.5), the critical concentration for the assembly of cofilin-actin complex increases resulting in depolymerization of actin filament (Ressad et al. 1998). The actin-binding and depolymerizing activities of cofilin can also be regulated by PI(4)P and PI(4,5)P2, which inhibit cofilin binding to actin in vitro (Yonezawa et al. 1990) because the binding site for the phospholipids and actin overlap on the surface of cofilin (Ojala et al. 2001). Tropomyosin competes with cofilin for actin binding, increases filament stiffness and protects F-actin from depolymerizing effects of cofilin, thus, it is thought to be a physiological inhibitor for cofilin-dependent actin dynamics (Gunning et al. 2005). Profilin competes with cofilin for G-actin binding and enhances exchange of actin-bound nucleotide in the presence of cofilin, thereby increasing the rate of pointed-end disassembly (by 125 fold) and rate of actin turnover synergistically with cofilin (Didry et al. 1998). Actin-interacting protein 1 (Aip1), which interacts functionally with cofilin as well as actin, actively enhances depolymerizing activity of cofilin (Ono et al. 2004). Cyclase-associated protein (CAP) sequesters G-actin and stimulates nucleotide exchange (ADP to ATP) through C-terminal domain, and accelerates actin depolymerization by binding to actin-cofilin complex through its N-terminal domain (Hubberstey and Mottillo 2002; Moriyama and Yahara 2002). Thus CAP1 speeds up the turnover of actin filaments through its effect on both ends of the actin filament (Figure 1.10).

Cofilin from most organisms are regulated by phosphorylation/dephosphorylation on a highly conserved serine residue; Ser3 in human cofilin isoforms. This phosphorylation inhibits the activity of cofilin by reducing its affinity for actin by 20-fold (Ressad et al. 1998). Several kinases responsible for this inactivation have been characterized. In vertebrates, LIMKs and testicular protein kinases (TESKs) are specific for cofilin and mediate various signals for remodeling of the actin cytoskeleton, for detail of LIMKs see section 1.4.6. TESK-1 and -2 also phosphorylate cofilin on the same serine residue (Toshima et al. 2001), but these kinases seem to be controlled by integrin mediated signaling pathways through 14-3-3 proteins for their activity and subcellular localization (Toshima et al. 2001). 14-3-3zeta proteins interact also with LIMK1 and phosphocofilin, and negatively regulate cofilin by protecting it from phosphatases-mediated

Ser3 dephosphorylation (Gohla and Bokoch 2002; Birkenfeld et al. 2003). Other kinases that phosphorylate cofilin include a neutrophil-specific Ser3 cofilin kinase (Lian et al. 2000), a calmodulin-like domain protein kinase in plants (Allwood et al. 2001) and a NRK/NIK-like embryo-specific kinase (NESK) that belong to the germinal center kinase family (Nakano et al. 2003).
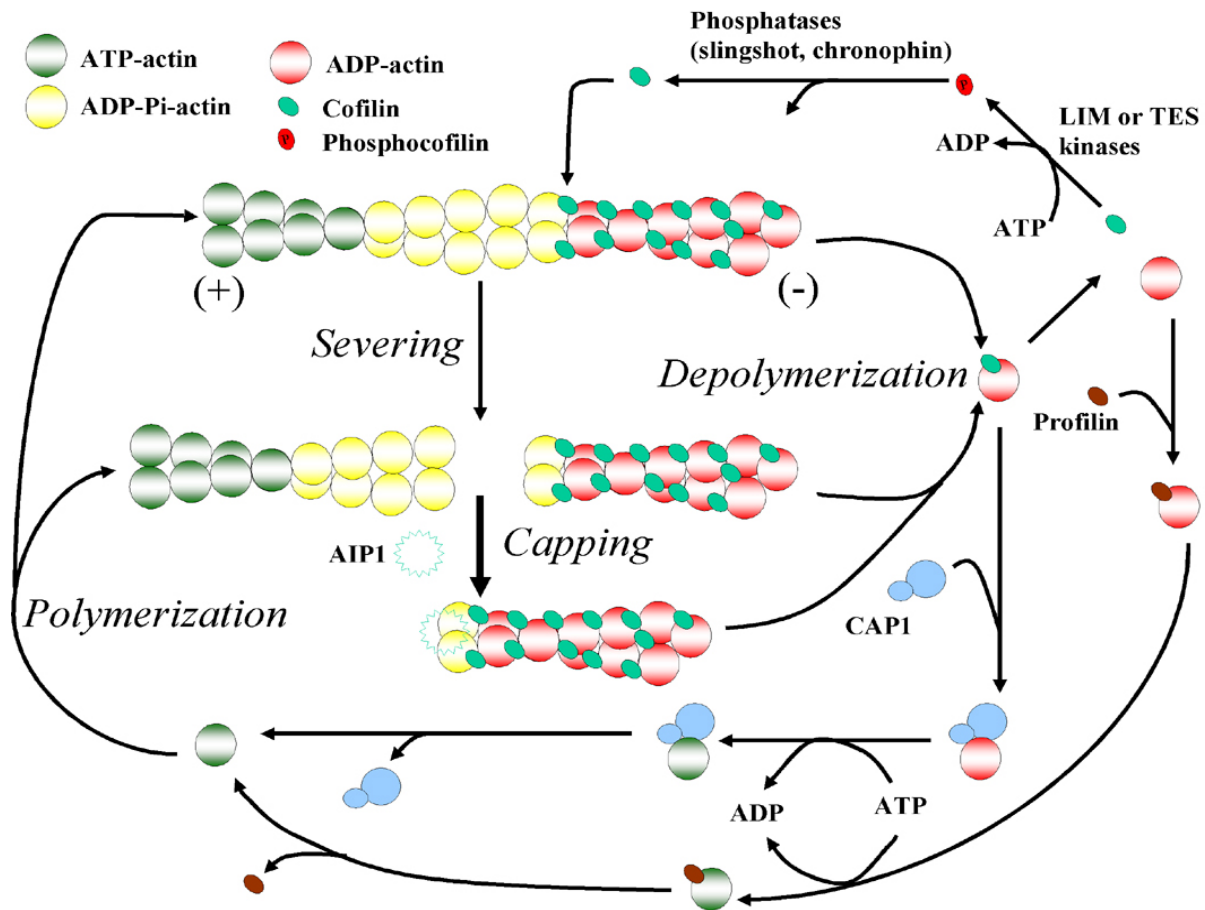
Figure 1.10 Biochemical activity of cofilin and proteins involved in regulating these activities. Cofilin binds cooperatively to F-actin, with highest affinity for ADP-actin subunits at the pointed end of actin filaments. Cofilin sever and depolymerizes actin filaments, and in cooperation with other proteins accelerates the treadmilling process. LIM- or TES-kinases and phosphatases regulate cofilin phosphorylation and dephosphorylation cycle respectively, and thereby regulate cofilin activity.

The activation of cofilin phosphatases can dephosphorylate and activate cofilin. In some cell types, activation of cofilin kinases after cell stimulation induced an increase in net phosphocofilin levels, while in other cells a significant increase in phosphocofilin turnover was observed with no significant change in total phosphocofilin pool (Meberg et al. 1998). This observation suggested that the activity of both cofilin kinases and cofilin phosphatase might are regulated by common upstream stimulatory signals. Cofilin dephosphorylation has been observed in response to various stimuli such as growth factors, chemotactic peptides and agents that increase the intracellular levels of Ca^{2+} and cAMP. Suggested phosphatases for cofilin dephosphorylation include type PP1, PP2A, and calcium-dependent protein phosphatase type PP2B (Meberg et al. 1998; Ambach et al. 2000). However, the effects of pharmacological phosphatase inhibitors on

dephosphorylation of cofilin were not consistent and lead to the suggestion of a specific cofilin phosphatase (Okada et al. 1996; Takuma et al. 1996). Thus, so far two types of cofilin-specific phosphatases have been identified: the Slingshot family of phosphatases, and Chronophin (Niwa et al. 2002; Gohla et al. 2005). A current model for regulation of actin dynamics by cofilin and other proteins is showed above in Figure 1.10.

1.5.4. <u>Cell biological functions of cofilin</u>

The activity of cofilin is fundamental to cells, because inactive mutants of cofilin isoforms from different organisms tested so far are lethal (Moon et al. 1993; McKim et al. 1994; Gunsalus et al. 1995). Cofilin is essential for those cellular processes that require a dynamic actin cytoskeleton such as cell movement (Chen et al. 2001), cytokinesis (Gunsalus et al. 1995; Nagaoka et al. 1995), phagocytosis (Bierne et al. 2001) and endocytosis (Lappalainen and Drubin 1997). Overexpression of cofilin enhances cell motility (Aizawa et al. 1996; Meberg and Bamburg 2000), whereas genetic ablation of cofilin impairs cell motility in vivo (Chen et al. 2001). Furthermore, the importance of cofilin as key regulators of actin dynamics is demonstrated by the fact that cofilin is indispensable for the motility of the small intracellular pathogen *Listeria monocytogenes* in living cells (Loisel et al. 1999). In cells, cofilin is predominantly cytoplasmic, but upon activation it concentrates at the leading edge and ruffling membranes of motile cells. Cofilin also localizes to other structures displaying high actin filament turnover rates such as the contractile ring and neuronal growth cones (Bamburg 1999). Cofilins can be transported to the nucleus after dephosphorylation in response to various stress factors (Ohta et al. 1989; Nebl et al. 1996). Cofilin acts as nuclear transporter for actin, and in the nucleus it forms rods with actin. It has been postulated that rod formation is a mechanism to conserve the nuclear pool of ATP in stress situations by decreasing actin filament dynamics, which is a major consumer of ATP (Bamburg 1999).

It might be important to study the role of cofilin in various human diseases where intracellular or intercellular aberrations due to altered actin structures have been observed. Cofilin might initiate or support cognitive impairment, inflammation, infertility, immune deficiencies, neurodegenerative diseases, Alzheimer's, ischemic kidney diseases, and other pathological defects (Bamburg and Wiggan 2002). Rho-kinase activation has important effects on several cardiovascular diseases therefore regulation of cofilin through Rho-kinase and LIM-kinases cannot be neglected for its possible role in cardiovascular diseases.

2. Aim of the study

Stimulation of platelets with various physiological agonists leads to the different morphological and functional platelet responses such as shape change, spreading, secretion and aggregation. These platelet responses require a dynamic remodeling of the actin structure. A key protein regulating the actin remodeling is cofilin, which has been shown to regulate various important functions in cells, however, the role and regulation of cofilin activity during platelet activation is not known. Cofilin activity is regulated by LIMKs and cofilin phosphatases. The effectors of Rho family GTPases, such as Rho-kinase and PAK can activate LIMKs. So far, only PAK2 has been identified in platelets. Thus, the need for identifying the signaling molecules and pathways regulating cofilin and subsequent importance of cofilin in regulating actin dynamics underlying platelet activation is one of the prime targets of this study. In this study, following questions were raised to answer the role of cofilin in platelets physiological activation.

a) Which forms of LIMKs are expressed in platelets?

b) How is the activation of LIMKs regulated, and whether LIMKs activation leads to cofilin phosphorylation?

c) Whether the cofilin phosphorylation pathway is stimulated during physiological activation of platelets?

d) Which signaling pathways are involved in the regulation of cofilin activity?

e) How does the regulation of cofilin phosphorylation affect its actin binding and filament depolymerizing activities during platelet shape change and secretion/aggregation induced by physiological agonists?

3. <u>Materials and methods</u>

All solutions and media were prepared with ultra-pure water (Milli-Q Plus ultra purification pak, Milli-RO Plus purification pak; Millipore, Molsheim, France). Chemicals otherwise not mentioned are from *Sigma, Munich, Germany*.

3.1. <u>General equipments</u>

Name	*Types and Suppliers*
Aggregometers	*LABOR aggregometer, Labor GmbH (Hamburg, Germany), PICA$^{®}$ (Platelet Ionized Calcium Aggregometer), Chrono-Log Corp. (Havertown, PA)*
Autoclave	*Autoclave 23; MELAG Medizintechnick (Berlin, Germany) Bioclav; Schütt Labortechnik GmbH (Göttingen, Germany)*
Centrifuges	*Biofuge pico, Omnifuge 2.OR, Megafuge 1.ORS, Heraeus (Osterode, Germany) Centrikon H-401, with Rotors A8.24 and A6.9; Kontron-Hermle (Gosheim, Germany)*
Chart recorder	*Servogor 102 chart recorder, Kipp & Zonen (Röntgenweg, The Netherlands)*
Chromatography System	*Automated Econo System; Biorad (Hercules, CA)*
Confocal microscope	*LSM 510META confocal microscope, Zeiss (Jena, Germany)*
Densitometer	*Pharmacia LKB (Sweden)*
Freezes, 4-8 and -20°C	*Robert Bosch GmbH (Stuttgart, Germany)*
Freezer, -70°C	*ULT1706; Revco Scientific (Asheville, NC)*
Gel documentation camera	*Polaroid MP-4 land camera; Polaroid USA*
Gel Electrophoresis	*Biorad (Hercules, CA)*
Incubators	*WTB Binder (Tuttlingen, Germany), Forma Scientific JULABO Labortechnik GmbH*
Magnetic stirrer	*MR3001; Heidolph (Kelheim, Germany)*
Microscope	*IX50; Olympus Optical GmbH (Hamburg, Germany)* *Model RI60P; Sartorius (Göttingen, Germany)*
pH meter	*Model 765 Calimatic; Knick (Berlin, Germany)*
Shaker	*Labquake rotating shaker; Lab Extreme, Inc (Kent City, MI)* *Unimax 2010; Heidolph Instruments GmbH (Schwabach, Germany)*
Sonicator	*SONOPLUS Bandelin electronic GmbH (Berlin, Germany)*
Spectrophotometer	*UVICON 930; Kontron instruments (Echingen, Germany)*
Thermocycler	*Mastercycler gradient; Eppendorf (Hamburg, Germany)*

Thermomixer	*Thermomixer compact; Eppendorf (Hamburg, Germany)*
Ultracentrifuge	*Optima^{TM} TLX with rotor TLA 100.4; BeckMan Instruments (Fullerton, CA)*
Vortexer	*REAX top; Heidolph (Kelheim, Germany)*
Water baths	*GFL GmbH (Burgwedel, Germany)*
UV illuminator	*Model N90M; UniEquip (Martinsried, Germany)*

3.2. Materials

3.2.1. Chemicals

Name	*Suppliers*
Acetic acid	*Merck Biosciences GmbH, Schwalbach, Germany*
Acetylsalicylic acid	*Fluka AG, Buchs, Switzerland*
Acryl/Bis 37.5:1; 40% (w/v) solution	*AMRESCO Inc. USA*
Agar	*Mo Bio Laboratories, USA*
Agarose	*Sigma, Munich, Germany*
Ammonium persulphate	*Sigma, Munich, Germany*
Ampicillin	*Sigma, Munich, Germany*
Apyrase	*Sigma, Munich, Germany*
ATP	*Amersham Biosciences, Freiburg, Germany*
Bromophenol blue	*Sigma, Munich, Germany*
BSA (bovine serum albumin)	*Sigma, Munich, Germany*
Citric acid	*Merck Biosciences GmbH, Schwalbach, Germany*
Coomassie Brilliant Blue G250$^®$	*Serva, Heidelberg, Germany*
Chrono-lumi luciferase luciferin reagent	*Chrono-Log, Havertown, PA*
Dideoxynucleotides	*Stratagene Inc USA*
DMSO	*Sigma, Munich, Germany*
EDTA	*Sigma, Munich, Germany*
EGTA	*Sigma, Munich, Germany*
Ethanol	*Merck Biosciences GmbH, Schwalbach, Germany*
Ethidium Bromide	*Sigma, Munich, Germany*
Isopropanol	*Sigma, Munich, Germany*
Formaldehyde	*Sigma, Munich, Germany*
Glycerol	*Merck Biosciences GmbH, Schwalbach, Germany*

HEPES	*Sigma, Munich, Germany*
IPTG	*peqLab Biotechnologie, Erlangen, Germany*
Kanamycin	*Sigma, Munich, Germany*
KCl	*Sigma, Munich, Germany*
Methanol	*Merck Biosciences GmbH, Schwalbach, Germany*
2-Mercaptoethanol	*Sigma, Munich, Germany*
MnCl$_2$	*Sigma, Munich, Germany*
Protein A Sepharose CL-4B	*Sigma, Munich, Germany*
Polylysine	*Sigma, Munich, Germany*
SDS	*Serva, Heidelberg, Germany*
Sodium Azide	*Serva, Heidelberg, Germany*
Sodium Fluoride	*Sigma, Munich, Germany*
Sodium Orthovanadate	*Merck Biosciences GmbH, Schwalbach, Germany*
TEMED	*Sigma, Munich, Germany*
Tris-HCl	*Serva, Heidelberg, Germany*
Triton X-100	*Sigma, Munich, Germany*
Tryptone	*Sigma, Munich, Germany*
Tween-20	*Sigma, Munich, Germany*

3.2.2. <u>Enzymes and reagents for molecular biology</u>

Name	*Suppliers*
Restriction enzymes	*New England Biolabs GmbH, Frankfurt, Germany*
Taq DNA polymerase	*New England Biolabs GmbH, Frankfurt, Germany*
Pfu Ultra HF DNA polymerase	*Stratagene, Netherlands*
Thermoscript reverse transcriptase	*Invitrogen GmbH, Karlsruhe, Germany*
Calf intestine alkaline phosphatase	*Roche Diagnostic, Mannheim, Germany*
T4 DNA ligase	*New England Biolabs GmbH, Frankfurt, Germany*
DNase I	*Roche Diagnostic, Mannheim, Germany*
Lysozyme	*Sigma, Munich, Germany*
dNTPs	*Stratagene, Netherlands*
T4 Polynucleotide kinase	*New England Biolabs GmbH, Frankfurt, Germany*

3.2.3. Antibodies and fluorescent probes

3.2.3.1. Primary antibodies

a) **Anti-actin** *(Chemicon International, Inc. Temecula, CA)*

Immunogen: Purified chicken gizzard actin.

Source: Mouse   Application: IB (1:50,000)

b) **Anti-cofilin** *(Cytoskeleton, Denver, CO)*

Immunogen: N-terminal 13-22 amino acids of human cofilin.

Source: Rabbit   Application: IB (1:20,000)

c) **Anti-phospho-cofilin** *(Cell Signaling Tech, Baverly, MA)*

Immunogen: Synthetic phospho-peptide (KLH coupled) corresponding to residues surrounding Ser3 of human cofilin.

Source: Rabbit   Application: IB (1:1000)

d) **Anti-LIMK1** *(Cell Signaling Tech, Baverly, MA)*

Immunogen: Synthetic peptide (KLH coupled) corresponding to the C-terminal residues of LIMK-1.

Source: Rabbit   Applications: IB (1:1000) and IP (1:25)

e) **Anti-LIMK2** *(Cell Signaling Tech, Baverly, MA)*

Immunogen: Synthetic peptide (KLH coupled) corresponding to the C-terminal residues of LIMK-2.

Source: Rabbit   Application: IB (1:1000)

f) **Anti-phospho-LIMK1 (Thr508)/LIMK2 (Thr505)**
   (Cell Signaling Tech, Baverly, MA)

Immunogen: Synthetic phospho-peptide (KLH coupled) corresponding to residues surrounding Thr508 of LIMK-1.

Source: Rabbit   Application: IB (1:1000)

g) **Anti-phospho-MYPT1 (Thr696)** *(Upstate Biotech, Lake Placid, NY)*

Immunogen: KLH conjugated synthetic peptide (CQSRRT^{P}QGVTL) corresponding to amino acids 691-701 of human MYPT1.

Source: Rabbit   Application: IB (1:3000)

h) **Anti-phospho-MYPT1 (Thr853)** *(Upstate Biotech, Lake Placid, NY)*

Immunogen: Synthetic peptide corresponding to amino acid residues 848-858 (C-EKRRST^{P}GVSFW) human MYPT1 with an N-terminal cysteine added for conjugation purposes.

Source: Rabbit   Application: IB (1:3000)

i) **Anti-PAK1/2/3** *(Cell Signaling Tech, Baverly, MA)*

Immunogen: Synthetic peptide (KLH coupled) corresponding to the C-terminal residues of human PAK1.

Source: Rabbit   Application: IB (1:1000)

j) **Anti-phospho-PAK1 (Thr423)/PAK2 (Thr402)** *(Cell Signaling Tech, Baverly, MA)*

Immunogen: Synthetic phospho-peptide (KLH coupled) corresponding to residues surrounding Thr423 of human PAK1.

Source: Rabbit   Application: IB (1:1000)

k) **Anti-human CD41a, FITC-conjugated** *(BD-Biosciences, Franklin Lakes, NJ)*

Clone: HIP8   Source: Mouse IgG$_1$

Application: Immunofluorescence (1:1000)

3.2.3.2. Secondary antibodies

a) **Anti-rabbit IgG peroxidase-linked F(ab')$_2$ fragment**

(Amersham Biosciences, Freiburg, Germany).

Immunogen: Purified immunoglobulin fractions from normal rabbit serum.

Source: Donkey   Application: IB (1:5000)

b) **Anti-mouse IgG peroxidase-linked F(ab')$_2$ fragment**

(Amersham Biosciences, Freiburg, Germany).

Immunogen: Purified immunoglobulin fractions from normal mouse serum.

Source: Sheep   Application: IB (1:5000)

3.2.3.3. Fluorescents probes

a) Alexa Fluor-546 phalloidin *(Molecular Probes, Eugene, OR)*

Usage: 20 U/ml for 15 minutes to immunostain F-actin

3.2.3.4. IgG isotype controls and sera

Rabbit IgG   *Sigma, Munich, Germany*

Mouse IgG   *Sigma, Munich, Germany*

Goat serum   *Sigma, Munich, Germany*

FITC-conjugated Mouse IgG$_1$ *BD Biosciences, Franklin Lakes, NJ*

3.2.4. <u>Inhibitors, blockers and agonists</u>

3.2.4.1. Inhibitors and blockers

Merck Biosciences GmbH, Schwalbach, Germany

Compound	Specifications	Conditions (at 37°C)
Y-27632	A highly potent, cell permeable and selective inhibitor of Rho-kinase	20 µM for 30 min
H-1152	A cell-permeable isoquinolinesulfonamide compound that acts as a highly specific, potent, and ATP-competitive inhibitor of Rho-kinase	20 µM for 30 min
Okadaic acid	An ionophore-like polyether derivative of a C_{38} fatty acid compound. Potent inhibitor of PP1A and PP2B type phosphatases.	0.75 µM for 10 min
Latrunculin A	A cell-permeable marine toxin that disrupts actin polymerization	10 µM for 10 min
Na_3VO_4	A broad spectrum potent inhibitor of protein tyrosine phosphatases	1 µM for 10 min
11R-Can-AID (CAID)	A cell-permeable peptide composed of the calcineurin (CaN) autoinhibitory domain (AID) fused to a poly-arginine-based protein transduction domain (11R)	20 µM for 20 min
11R-VIVIT (NFAT)	A highly selective NFAT (Nuclear Factor of Activated T-cells) inhibitor coupled to 11R	20 µM for 20 min
Wortmannin	A cell-permeable, fungal metabolite that acts as irreversible inhibitor of PI3-kinase	50 nM for 20 min
Akt inhibitor IV	A cell-permeable benzimidazole compound that inhibits Akt	10 µM for 20 min
Triciribine	A cell-permeable tricyclic nucleoside that inhibits Akt1/2/3	50 µM for 20 min
BAPTA-AM	Intracellular calcium chelator	20 µM for 5 min
RGDS	Blocks fibrinogen binding to the integrin $\alpha_{IIb}\beta_3$ (*Bachem Biochemica, Heidelberg, Germany*)	0.5 mM for 2 min

3.2.4.2. Inhibitor cocktails

Phosphatase inhibitor cocktail   *Roche Diagnostic, Mannheim, Germany*

Proteases inhibitor cocktail   *Roche Diagnostic, Mannheim, Germany*

3.2.4.3. Agonists

Thrombin (T7009)   *Sigma, Munich, Germany*

18:1 Lysophosphatidic acid (LPA)

1-Oleoyl-2-Hydroxy-sn-Glycero-3-Phosphate   *Avanti polar lipids Inc. USA*

3.2.5. <u>Commercial kits and other materials</u>

QIAquick[TM] PCR-Purification kit   *Qiagen, Hiden, Germany*

QIAquick[TM] Gel-extraction kit   *Qiagen, Hiden, Germany*

QIA[®]Spin Miniprep kit   *Qiagen, Hiden, Germany*

Rapid DNA ligation kit   *Roche Diagnostic, Mannheim, Germany*

Expend High Fidelity PCR system   *Roche Diagnostic, Mannheim, Germany*

Thermoscript[TM] RT-PCR system   *Invitrogen GmbH, Karlsruhe, Germany*

DotMetric[TM]-1µl Protein assay kit   *Genotech Inc. USA*

Hybond[TM]-C extra blotting membrane   *Amersham Biosciences, Germany*

SuperSignal[®]West Pico chemiluminiscent   *Pierce, Rockland, USA*

Substrate

Photographic film   *Polapan; Polaroid, Offenbach, Germany*

Chariot[TM] transfection reagent   *Active Motif, California, USA*

3.2.6. <u>Softwares</u>

a) CELLQuest software for flow cytometry.

b) National Institutes of Health (NIH) ImageJ (1.34s) software for densitometry.

c) Zeiss LSM510 Meta software for confocal microscopy.

3.3. <u>In vitro studies of human platelets</u>

3.3.1. <u>Isolation of washed human platelets</u>

The isolation of human platelets was performed using multi-step centrifugation methods. The principle behind these methods is to separate blood cells based on their differential sedimentation velocity. Platelets, being smaller in size, settle down at high centrifugation speed as compared to other cells.

<u>Method A</u>

Buffer B	20 mM HEPES, 138 mM NaCl, 2.9 mM KCl, 1 mM $MgCl_2.6H_2O$, 0.36 mM NaH_2PO_4, and pH 6.2
Buffer C	Composition same as buffer B except pH 7.4

Both buffers B and C were pre-warmed at 37°C before use.

Blood from healthy volunteers, who did not take any medication, was drawn by cubital venepuncture into a propylene syringe containing tri-sodium citrate (3.13% w/v) in a ratio 1:10 of blood (v/v). The anticoagulant-treated blood was immediately transferred into 50 ml polystyrene tubes and centrifuged at 160x g for 20 minutes (without brake) to separate the platelet rich plasma (PRP) from other blood cells. The top layer of PRP was aspirated carefully without disturbing the buffy coat and the red blood cells layer. The COX inhibitor (aspirin, 1 mM), and ADPase (apyrase, 0.3 U/ml) was added to the PRP and incubated at 37°C for 15 minutes to avoid platelet activation by TxA_2 and ADP released during the isolation, respectively. Subsequently, in order to prevent clotting of the PRP induced by Ca^{2+} released calcium chelators like citric acid (citrate; 9 mM) and EDTA (5 mM) were added to the PRP. The platelets from PRP were isolated by centrifugation at 800x g for 20 minutes (with brake). The platelet pellet was then washed once with buffer B containing apyrase (0.3 U/ml). The volume of buffer B was determined by 10% of the original blood volume. Before the final centrifugation at 800x g for 20 minutes, 10 µl of platelet suspension was mixed with THROMBO PLUS for calculating the number of platelets/µl. The final platelet pellet was resuspended in a volume of buffer C required to obtain the final platelet count of 400,000/µl. Apyrase (0.6 U/ml) and glucose (5 mM) were added prior to the resuspension of platelet pellet.

<u>Method B</u>

ACD buffer	111 mM glucose, 85 mM tri-sodium citrate and 65 mM citric acid
Tyrode buffer	10 mM HEPES, 137 mM NaCl, 2 mM KCl, 0.3 mM NaH_2PO_4, 12 mM $NaHCO_3$, 1 mM $MgCl_2$, 2 mM $CaCl_2$, 5 mM glucose and 0.35% (w/v) BSA and pH 7.6

| **Working buffer** | Composition same as of Tyrode buffer, but with 0.1% BSA |

All buffers were pre-warmed at 37°C before use.

Washed platelet suspension used to study platelet aggregation induced by LPA was prepared according to Cazenave et al (Cazenave JP 1993) and Haserück et al (Haseruck et al. 2004) with some modifications. Tyrode buffer as described by Cazenave et al. was used, except the omission of heparin from first wash buffer and the use of 0.1% albumin concentration in final suspension. The blood anti-coagulated with acid-citrate-dextrose (ACD; 1:6) was centrifuged at 160x g for 20 minutes to prepare PRP. Prostacyclin (PGI_2 25 nM) was added to PRP and incubated at 37°C for 20 minutes in order to prevent the platelet activation during subsequent centrifugation at 1100x g for 8 minutes. The platelets were resuspended in Tyrode buffer (one fifth of initial blood volume) containing PGI_2 (1 µM) and incubated at 37°C for 10 minutes and then re-supplemented with PGI_2 (1 µM). Subsequently, platelets were resuspended in Tyrode buffer containing PGI_2 (1 µM) for a second time and incubated for 10 minutes at 37°C prior to the final centrifugation step (1100x g for 8 minutes). Meanwhile, 10 µl of the platelet suspension was used for calculating the concentration of platelets/µl, in a similar manner as described in method A. Finally, platelets were resuspended in working buffer, and the platelet concentration was adjusted to 400,000/µl. Apyrase (0.02 U/ml) was added to the suspension. The platelet suspension was stored at 37°C under an atmosphere of 5% CO_2 and 95% humidity in a cell incubator, in order to avoid pH changes, during experiment.

3.3.2. <u>Platelet shape change and aggregation by turbidimetric method</u>

This method is based on obstruction or augmentation of the light transmitted through a platelet suspension during activation. During shape change, the turbidity increases due to the discoid-spheroid transformation of discoid platelets and hence the light transmission decreases. During aggregation, an augmentation of the light transmission is observed due to the decrease in number of particulate matters, such as single platelets. Platelet shape change and aggregation were measured in a two-channel LABOR aggregometer. Aliquots of platelet suspension (400,000 platelets/µl) were incubated at 37°C for 5 minutes in translucent plastic cuvettes containing a magnetic stirrer. The platelet suspensions were stirred and further incubated at 37°C for 2 minutes prior to the addition of agonists, antagonists or inhibitors. The change in light transmission was recorded using an analog chart recorder. Unstimulated and stimulated platelet suspensions (100 µl) were transferred from the aggregometer cuvette to an eppendorf cups containing an equal volume of appropriate buffer for performing flow cytometry, biochemical or microscopic studies. During aggregation, the reactions were quenched at a given time point by adding an equal volume of appropriate buffer directly to the platelet suspension.

3.3.3. <u>Measurement of ATP secretion</u>

The ATP secretion during platelet activation was measured in a PICA$^®$ (Platelet Ionized Calcium Aggregometer) lumi-aggregometer that simultaneously monitors aggregation and secretion of ATP within the same platelet sample. This instrument uses the same turbidimetric principle implied for measuring platelet aggregation. In addition, secretion of ATP is measured by coupling ATP to the firefly luciferase system for obtaining luminescence. This luminescence is detected at the right angle to the aggregometer light path. The lumi-aggregometer was pre-adjusted for 37°C temperature, 1000 rpm stirring and for appropriate luminescence gain. Two platelet suspensions of varying concentrations were prepared from the initial platelet suspension (400,000 platelets/µl) for calibrating the instrument. Namely, the platelet rich suspension (PRS) by mixing 15 µl of buffer C to 385 µl of initial platelet suspension and the platelet poor suspension (PPS) by mixing 100 µl of buffer C to 300 µl of platelet suspension. The lumi-aggregometer was set for the base line correction using PRS and PPS. The ATP secreted from dense granules during platelet stimulation with various agonists was measured after addition of 15 µl of Chrono-Lumi luciferase/luciferin reagent. The emitted luminescence converted to electronic signals was recorded using an analog chart reader.

3.4. <u>Flow cytometric analysis of human platelets</u>

The flow cytometry uses the principle of light scattering in combination with light excitation/emission of fluorochrome molecules to generate specific multi-parameter data from particles and cells in the size range of 0.5 μm to 40 μm diameter. The cells are hydro-dynamically focused in a sheath of buffer before intercepting an optically focused light source thereby producing data for each single cell. Lasers are most often used as a light source in flow cytometry. As cells or particles of interest intercept the light source they scatter light and fluorochromes are excited to a higher energy state. Fluorochromes release energy in the form of photons of light with specific spectral properties, which is unique to each fluorochrome. Scattered and emitted light from cells and particles are collected and redirected by a beam splitter to appropriate detectors, which convert the light into electrical pulses. The beam splitter splits the collected light into different wavelengths, which are routed to band pass filters of specified wavelengths that allow them to designated optical detectors. For example, a 525 nm band pass filter placed in the light path prior to the detector will only allow "green" light received by the detector. The most common type of detector used in flow cytometry is the photomultiplier tube (PMT).

3.4.1. <u>Shape change measurement</u>

In flow cytometry, the cells are characterized individually by their physical and/or chemical properties. The physical profile of cells can be observed by combining the forward light scatter (FSC) and the orthogonal or side light scatter (SSC) that are produced by cells intercepting the light beam. In forward light scatter, the intensity of laser beams uninterrupted by the cells and beams that passes around the cells, are measured. This measurement is an indication of the cell's unique refractive index, which depends on its size, organelles, and water and molecular contents. The refractive index (FSC) of a cell can change through cell cycle progression, activation and fixation. The cellular side scatter light is the light that is reflected orthogonal to the laser beam and it is an indication of internal complexity or cell surface granularity (Figure 3.1).
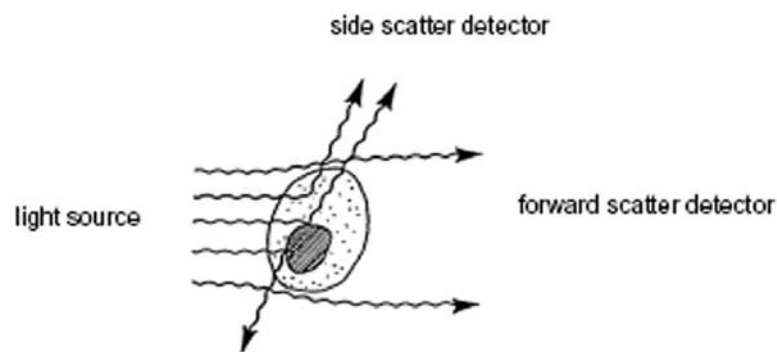
Figure 3.1 Light scattering properties of a cell. The detector in the path of light source detects forward scatter light while the detector placed at 90° to the interception point detects side scatter light.

The side and forward light scatter profiles of unstimulated platelets are different from those of platelets undergoing shape change (Ruf and Patscheke 1995). During shape change, the mean FSC of platelets increases due to a decrease in average cell size, while the mean SSC decreases due to a reduction of surface granularity caused by the centralization of granules after platelet activation. Thus, the ratio of FSC/SSC increases proportionally to the extent of platelet shape change. Aliquots (100 µl) of the stimulated and unstimulated platelet suspensions were transferred to an equal volume of 0.15 M phosphate buffer (pH 7.4) containing 0.2% (w/v) glutaraldehyde for fixation. After 10 minutes, the samples were centrifuged in a microfuge (800x g for 5 minutes) and washed twice with 0.5 ml of Dulbecco's phosphate buffered saline (PBS). The platelet pellets were resuspended in the residual volume and were incubated for 15 minutes in the dark at room temperature with following antibodies: anti-CD41a–FITC antibody binding to the glycoprotein IIb to label platelets and isotype-matched IgG_1-FITC (6 µL diluted 1:100) to determine unspecific binding. Subsequently, platelet samples were then diluted with PBS to get a concentration of platelets less than 10^6 cells/µl. Platelets labeled with anti-CD41a–FITC antibody and showing negative staining for IgG_1-FITC isotype were gated and the mean FSC/SSC ratio of 10,000 platelet events was calculated using the CELLQuest software. The shape change induced by agonists was calculated as an increase in FSC/SSC ratio compared to that of the unstimulated platelets.

3.4.2. F-actin measurement using flow cytometry

Phalloidin, a toxin from the toadstool "Death Cap" (*Amanita phalloides* mushroom) that binds with F-actin in a stoichiometric ratio of 1:1 (Lengsfeld et al. 1974) has provided a very convenient tool to study the distribution of F-actin in permeabilized cells, since fluorescent analogs of phalloidin can be synthesized that retain its actin binding property (Wulf et al. 1979). Phalloidin binds to actin at the junction between subunits and because this is not a site at which many actin-binding proteins bind, most of the F-actin in cells is available for phalloidin labeling.

In the same fixed platelet samples prepared for shape change measurement by flow cytometry, the F-actin content in resting or activated platelets was determined. The fixed platelets were permeabilized with 0.1% Triton X-100 containing 20 U/ml Alexa Fluor-546 phalloidin at 25°C and in dark for a minimum of 15 minutes. The labeled platelets were washed two times with PBS and incubated with anti-CD41a-FITC antibody as described above (section 3.4.1). The samples were resuspended in PBS (1.2 ml), and the platelets labeled with anti-CD41a-FITC were gated and analyzed for Alexa Fluor-546 phalloidin fluorescence to estimate F-actin content in these platelets. The mean fluorescence intensity of Alexa Fluor-546 from 10,000 platelet events was quantified using the CELLQuest software. The correlation of changes in F-actin content after stimulation was calculated by considering F-actin in unstimulated platelets as 40% of the total actin present in platelets.

3.5. Biochemical analysis of human platelets

3.5.1. Platelet lysates for measuring phosphorylation of proteins

SDS-PAGE sample buffer (2x): 100 mM Tris-HCl (pH 6.8), 20% (v/v) glycerol, 4% (w/v) SDS, 0.01% (w/v) bromophenol blue, 10% (v/v) β-mercaptoethanol

During shape change, aliquots (100 μl) of unstimulated and stimulated platelet suspensions were transferred from the aggregometer cuvettes to eppendorf tubes containing equal volume of 2x SDS-PAGE sample buffer. In case of aggregation, the reactions were quenched at given time points by adding an equal volume of 2x SDS-PAGE sample buffer directly to the platelet suspension. Platelet lysates were denatured at 95°C for 5 minutes and immediately used for immunoblotting or stored at -20°C.

3.5.2. Isolation of the total F-actin and actin cytoskeleton from platelets

Lysis buffer (2x): 2% (v/v) Triton X-100, 100 mM Tris-HCl, 10 mM EGTA, 10 mM NaF, 2 mM Na_3VO_4, phosphatase cocktail inhibitor-I (1:100

dilution), complete-mini protease inhibitor (1 tablet/10 ml of buffer) and pH adjusted to 7.4

The F-actin cytoskeleton of platelets based on its structure can be subdivided into two fractions: a membrane skeleton and a cytoskeleton (see section 1.3.1). The membrane skeleton can be isolated at a high g-force (100,000x g) while the actin cytoskeleton can be isolated at a low g-force (15,000x g), Figure 3.2.
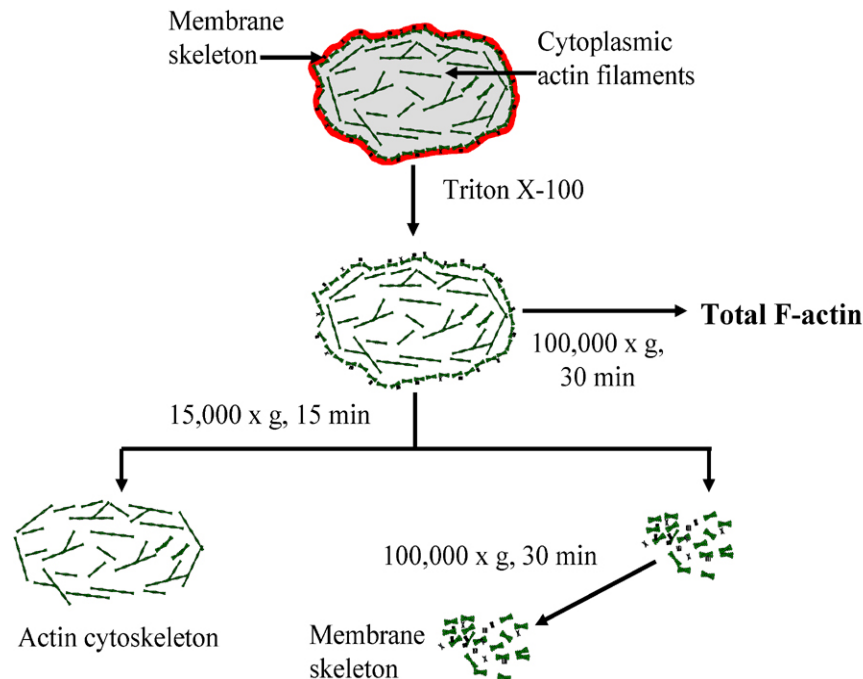
Figure 3.2 Schematic representation for the separation of platelet F-actin fractions. Platelets after lysis with Triton X-100 retain their cytoskeletal contours. Total F-actin comprises the actin cytoskeleton and membrane skeleton. Proteins engaged in these structures also remain associated with actin F-actin fractions.

To isolate the total F-actin content of platelets, a method as described previously (Kovacsovics and Hartwig 1996) was used with slight modifications such as platelet lysis time, centrifugation speed and omission of phalloidin from the platelet lysis buffer. The F-actin isolated from platelets was also used for analyzing proteins associated with F-actin during shape change and secretion. Aggregation of platelets was blocked using integrin $\alpha_{IIb}\beta_3$ blocker RGDS to avoid possible artifacts such as unspecific trapping of protein in the platelet aggregates and inefficient lysis of platelets. Aliquots (100 µl) of unstimulated and stimulated platelet suspensions were lysed with an equal volume of lysis buffer. After 5 minutes of lysis, the total F-actin was separated from the Triton X-100 insoluble fraction by centrifugation at 100,000x g for 30 minutes at 4°C using a tabletop ultracentrifuge. For isolating only the actin cytoskeleton, samples were centrifuged at 15,000x g for 15 minutes at 4°C in a tabletop centrifuge. The residual pellets were washed twice with ice cold PBS and dissolved in SDS-PAGE sample buffer. The proteins were separated on polyacrylamide gels and detected by Coomassie staining or by immunoblotting.

3.5.3. Immunoprecipitation of LIMK-1 from platelets

Beads swelling buffer: 20 mM NaH_2PO_4, 0.15 M NaCl, and 0.1% (w/v) NaN_3, 2% (w/v) BSA, and pH 8.0.

Lysis buffer (2x):   2% (v/v) NP40, 300 mM NaCl, 20 mM Tris, 2 mM EGTA, 2 mM EDTA, 5 mM Na_3VO_4, 0.1% (w/v) SDS, phosphatase cocktail (1:100 dilution), complete mini protease inhibitor (1 tablet/10 ml of buffer), and pH 7.5.

The underlying strategy behind making the immunoprecipitation a successful method for isolating and characterizing an antigen or for identifying protein-protein interactions is the use of antibodies high affinity for their antigens. Protein A or protein G, which interacts specifically with the Fc-regions of antibodies, are covalently linked to a matrix like agarose or sepharose beads, and utilized to isolate and purify antibody-antigen complexes. The unspecific molecules interacting with the beads or with the antibody-antigen complexes are removed by applying different stringent conditions during immunoprecipitation.

The experiments were carried out in the presence of RGDS to avoid platelet aggregation. The platelet suspensions (4×10^8/mL, 0.4 ml) stimulated with agonists in the presence or absence of inhibitors were lysed in an equal volume of 2x-immunoprecipitation lysis buffer for 45 minutes on ice. The lysates were clarified by centrifugation at 16,000x g for 15 minutes. To preclear the supernatant, 40 µl 50% protein A-sepharose slurry was added to the supernatants and incubated for 1 hour at 4°C with an end to end rotation using a rotating shaker. The protein A-sepharose slurry was prepared by incubating the beads in swelling buffer that contained 2% BSA to block unspecific binding. The precleared supernatants were incubated overnight with anti-LIMK-1 antibody (1:50 dilution) followed by addition of 80 µl 50% protein A-sepharose slurry and incubation at 4°C for 1 hour with an end to end rotation using a rotating shaker. The immunoprecipitates were collected by centrifugation at 16,000x g for 25 seconds, washed 3 times with 1 ml ice-cold 1x immunoprecipitation lysis buffer, and processed for immunoblot analysis or for the kinase assay.

3.5.4. LIMK-1 kinase assay

Kinase buffer: 50 mM HEPES, 5 mM $MgCl_2$, 5 mM $MgCl_2$, 10 mM NaF, 1 mM Na_3VO_4, and pH 7.5

Preparation of cofilin as substrate:

His-tagged cofilin (section 3.7) was incubated with 20 units of λ-phosphatase for 30 minutes at 37°C to dephosphorylate cofilin and to ensure that cofilin is present only in its non-phosphorylated state. The λ-phosphatase was then heat inactivated at 65°C for 1 hour.

LIMK-1 immunoprecipitates from unstimulated or stimulated platelets were washed twice with kinase buffer prior to performing the kinase reaction. The protein concentration of the immunoprecipitated samples was measured using dotMETRIC^{TM} protein assay kit and equal amount of corresponding immunoprecipitated beads suspended in 100 µl of kinase buffer was taken to perform the kinase reaction. The reaction was started by adding ATP (10 mM) and λ-phosphatase-treated His-tagged cofilin (16 µg), and incubating the reaction mixture for 1 hour at 37°C. The reactions were quenched by adding 100 µl 2x SDS-PAGE sample buffer. The samples were then immunoblotted with anti-phospho-cofilin and anti-cofilin antibodies. The activity of LIMK-1 was measured by cofilin phosphorylation.

3.5.5. <u>Measurement of protein concentration</u>

dotMETRIC^{TM} 1µl Protein assay

This is a chromatographic capture method where the flat surface of the test strip acts as the solid matrix or support. Protein solution is applied to a specific protein binding test strip by point of contact capillary action. As the protein enters into the matrix of the test strip it binds instantly and saturates the matrix. The protein solution diffuses into the test strip in a uniform manner to produce a circular spot. The circular protein imprint is developed into visible protein spots using a protein specific dye, whose diameter is proportional to the concentration of protein applied. By measuring the diameter of the protein spots with a pre-developed measuring gauge, the amount of protein in the spot can be estimated (as shown in Figure 3.3). This method requires only 1 µl of the sample and is resistant to most common laboratory reagents such as Triton-X100, Triton-X114, Thesit, Tween-20, NP-40 and SDS, reducing agents such as β-mercaptoethanol and DTT, sugars, cobalt, EDTA, Tris buffers, and others. This assay is independent of protein-to-protein variation and can be performed even if the protein sample is in a SDS-PAGE gel-loading buffer.
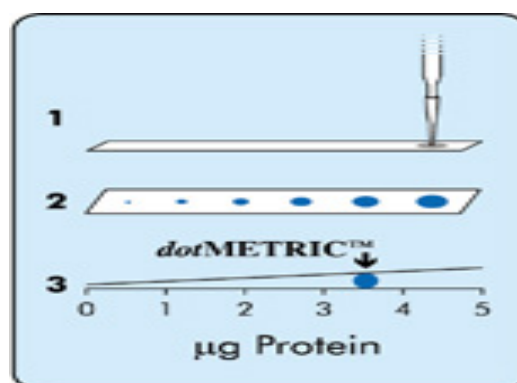
Figure 3.3 Steps involved in protein estimation: Protein solution (1-5µl) is applied to the test strip (1), Protein imprints are developed into compact and symmetrical spots on the strip (2), and the diameter of protein spots proportional to their protein concentration is measured using dotMETRICTM scale (3). The dotMETRICTM scale, supplied with each kit, is calibrated for diameter of spots per µg of protein.

The protein amount was estimated by dotMETRIC^{TM} protein assay kit according to the manufacturer's instructions. A small volume (2 µl) of protein sample was diluted to 10 µl with

the dilution buffer provided in the kit. Using the common pipette man with ultra fine tip, 2 µl and 4 µl of diluted sample was spotted on the test strip. The loaded protein sample was then fixed on the test strip by incubating the strip in a diluted fixer (0.8 ml of Fixer-A stock + 7.0 ml of water) for 2 minutes at room temperature. The fixed strip was transferred to the diluted developer solution (0.8 ml of developer-B stock + 7.0 ml of water) containing an unknown protein stain. The strips were gently shook for 30 seconds and incubated for 2-4 minutes or longer at room temperature to develop the spots. The spots were read for their diameter and corresponding protein concentrations using the dotMETRIC™ scale. To neglect pipetting errors and to reproduce the results, 2 spots for each sample were produced and each spot was read twice, measured a long and a short diameter of each spot, and calculated the mean average diameter for each sample.

3.5.6. <u>SDS-PAGE</u>

Electrophoresis buffer (10x): 30 gm Tris-base, 142 gm glycine and 10 gm SDS dissolved in 1 liter of double distilled water.

Table 3.1 Composition of stacking and resolving gel.

Components	Stacking gel 5% (5ml final vol.)	Resolving gel 10% (10ml final vol.)	Resolving gel 12% (10ml final vol.)
Water	3.2 ml	4.0 ml	3.3 ml
40% (w/v) acrylamide/bis-acrylamide ratio 37.5:1	0.83 ml	3.3 ml	4.0 ml
1.5 M Tris (pH8.8)		2.5 ml	2.5 ml
1.0 M Tris (pH6.8)	0.63ml		
10% (w/v) SDS	0.05 ml	0.1 ml	0.1 ml
10% (w/v) APS	0.05 ml	0.1 ml	0.1 ml
TEMED	0.005 ml	0.004 ml	0.004 ml

The protein samples were resolved for analytical purposes by polyacrylamide gel electrophoresis (PAGE). The principle behind resolving proteins on SDS-PAGE is the very strong interaction between the dodecylsulphate detergent and the protein peptide chain that causes the SDS-protein complexes to migrate as one well-defined identity. The migration of proteins on SDS-PAGE is directly proportional to their molecular mass. The polyacrylamide gels were prepared by polymerization of acrylamide in the presence of a bi-functional cross-linking agent such as *N,N'*-methylene bisacrylamide. *N,N,N',N'*-tetramethylethylenediamine (TEMED) catalyzes the formation of free radicals from chemical decay of ammonium persulphate (APS) and accelerates

the polymerization. This process gives a three dimensional network within the gels. Varying the ratio of acrylamide to the crosslinking agent permits the formation of gels with predictable average pore size and texture. The electrophoresis towards the anode was carried out in a discontinuous system where SDS-protein complexes were first concentrated within a stacking gel before they migrate into the resolving gel. The size of different proteins was determined by comparing their mobility with that of a protein standard.

The preparation of polyacrylamide gels and the electrophoretic separation were done using Mini-PROTEAN 3 electrophoresis system (Bio-Rad, Hercules, CA). Clean glass plates with permanent bonded spacers were aligned and clamped into a casting frame. The resolving gel solution was prepared according to composition given in Table 3.1, poured between two glass plates and overlaid with water. After polymerization, the top of the gel was washed with water and the residual water was removed by soaking with filter papers. A freshly prepared stacking gel solution was poured on top of the polymerized resolving gel. A plastic comb of appropriate well dentures was inserted in poured stacking gel and allowed to polymerize. After the stacking gel was polymerized, the comb was removed and the wells were flushed with water to remove traces of unpolymerized acrylamide. Subsequently, the gel was placed in a vertical electrophoresis apparatus filled with 1x electrophoresis buffer. A denatured protein standard and protein samples were loaded into the wells of the SDS-PAGE gel. The electrophoresis was carried out at a constant voltage of 200 V. The resolving gel was subsequently subjected to western blot analysis or gel staining. Low molecular weight proteins (<55 kDa) were resolved with 12% SDS-PAGE gels, whereas high molecular weight proteins (>55 kDa) were resolved with 10% SDS-PAGE gels.

3.5.7. Isoelectric focusing (IEF)

IEF is an electrophoretic technique in which compounds are fractionated according to their pIs along a continuous pH gradient. The gradient is created and maintained by the passage of current through a solution of amphoteric compounds with closely spaced pIs, encompassing a given pH range. The surface charge of an amphoteric compound in IEF keeps decreasing, as it moves along the pH gradient approaching its equilibrium position where pH matches its pI and stops moving further.

Cofilin and phosphocofilin in resting platelets were separated by isoelectric focusing electrophoresis. The isoelectric focusing gels of 0.4 mm thickness consisting a mixture of ampholytes (Serva, Heidelberg, Germany) of pH range 7-9 (4%) and pH range 3-10 (1%), 5% glycerol, 6% acrylamide and 6 M urea were polymerized with 0.015% ammonium persulphate, 0.0005% riboflavin 5-phosphate and 0.03% TEMED. Lysates of unstimulated platelets were loaded on these gels and were separated electrophoretically for 30 minutes at 100 V, 30 minutes at 200 V, and 2 hours at 450 V. The separated proteins were detected by anti-cofilin immunoblot.

3.5.8. Detection of protein on gel

3.5.8.1. Silver staining of the polyacrylamide gels

Fixing solution: Ethanol: glacial acetic acid: H_2O (30:10:60)

Silver nitrate solution: 1% (w/v) $AgNO_3$

Developing solution: 2.5% (w/v) Na_2CO_3 and 0.02% (w/v) formaldehyde

*All solutions were prepared freshly.

Silver staining of polyacrylamide gels allows the detection of proteins separated by SDS-PAGE to a limit of 0.1-1 ng of polypeptide in a single band. In silver staining, the gel is impregnated with soluble silver ions and developed by treatment with formaldehyde, which reduces silver ions to form an insoluble brown precipitate of metallic silver. This reduction of silver ions is promoted by the side chains of amino acids in proteins.

The proteins separated by SDS-PAGE were fixed by incubating the gel with a fixing solution for 4 hours at 25°C or overnight at 4°C with gentle shaking. The fixing solution was discarded, and at least 5 gel volumes of 30% ethanol was added to dehydrate the gel by incubating it for 30 minutes at room temperature with gentle shaking. This step was repeated once more to ensure complete dehydration of gel. The gel was then washed thrice with 10 gel volumes of deionized H_2O for 10 minutes at 25°C with gentle shaking. The gel swells during rehydration. Carefully, a silver nitrate solution was added and the gel was incubated for 30 minutes at 25°C. After incubation, the silver nitrate solution was discarded and both sides of the gel were washed (20 seconds each) under a stream of deionized H_2O. A sufficient volume of a developing solution was added and the gel was incubated with gentle agitation until stained bands of protein with desired contrast are obtained. Subsequently, the reaction was quenched by washing the gel in 1% (v/v) acetic acid for a few minutes and several times with deionized H_2O.

For storage purpose, the stained polyacrylamide gel was placed between a wet Whatman 3MM paper (bottom) and a cellophane sheet (top), and dried under vacuum for 2 hours at 85°C.

3.5.8.2. Coomassie staining of the polyacrylamide gels

Staining solution: 0.25 gm Coomassie Brilliant Blue R-250 dissolved in 100ml of methanol, H_2O and acetic acid solution (50:40:10 v/v ratio) and filtered through Whatman No. 1 filter to remove any particulate matter

Destaining solution: Methanol, H_2O and acetic acid solution in a ratio of 30:60:10 (v/v)

Coomassie Brilliant Blue is an aminotriarylmethane dye that forms strong but not covalent complexes with proteins, most probably by a combination of van der Waals forces and

electrostatic interactions with NH_3^+ groups. Coomassie blue binds to proteins approximately stoichiometrically, thus this staining method is preferable when relative amounts of protein need to be determined by densitometry. Coomassie staining allows the detection of proteins to a limit of 0.1-0.5 μg of polypeptide in a single band.

The polyacrylamide gel was immersed in at least 5 gel volumes of the coomassie staining solution and placed on a slow rotating platform for 15-30 minutes at room temperature. The gel was destained in destaining solution with three to four changes of fresh destaining solution. The rapid destaining can also be achieved by placing the stained gel in hot water (80°C). The remaining background was removed by leaving the gel overnight in water.

3.5.9. <u>Immunoblotting</u>

Transfer buffer: 48 mM Tris-base, 39 mM glycine, and 20% (v/v) methanol.

TBST buffer: 10 mM Tris-base, 150 mM NaCl, 0.1% (v/v) Tween-20, and pH adjusted to 7.6

Blocking solution: 5% (w/v) non-fat dry milk (BioRad) in TBST

Immunoblotting combines the resolution of proteins by gel electrophoresis with the specificity of immunochemical detection and can detect proteins levels down to 0.1 ng. The strategy behind the immunoblotting technique is to transfer the proteins electrophoretically out of the gel onto a membrane support, thus making a replica of the separated proteins. The nitrocellulose membrane is the most commonly used support although it does have certain disadvantages such as non-covalent binding of the proteins and brittleness, especially when it is dry. The target protein immobilized on membrane is identified by probing the membrane with a specific primary antibody and a horseradish peroxidase (HRP)-conjugated secondary antibody directed against the primary antibody. The detection of the antigen-antibody-antibody complex occurs by HRP-mediated oxidation of the chemiluminescent substrate luminol, a cyclic diacylhydrazide. The reaction product exhibits an excited state which decays to ground state via a light emitting pathway, and is detectable by exposure of the membrane to an autoradiography film.

The proteins were blotted to nitrocellulose membranes using the Mini Trans-Blot electrophoresis cell (Bio-Rad, Hercules, CA). After SDS-PAGE, the gel, nitrocellulose membrane pads and electrode papers were equilibrated with transfer buffer. The gel and nitrocellulose membrane were sandwiched between 7 electroblotting papers and a fiber pad on each side, and clamped in the electroblotting cassette as shown in Figure 3.4.
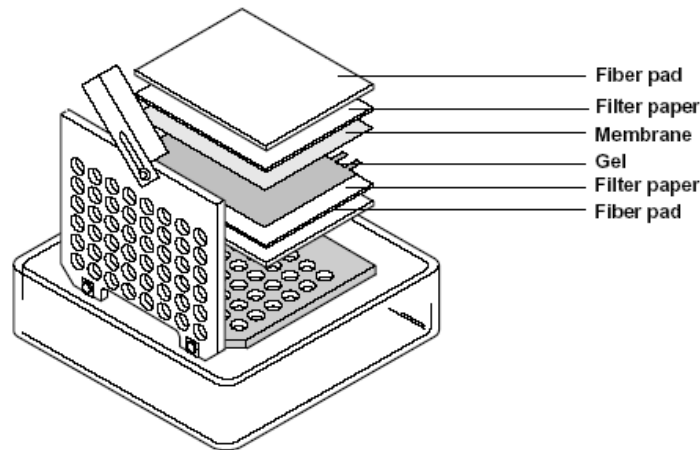
Figure 3.4 Arrangement of the gel and the membrane in the cassette.

The firmly closed cassette was put into the blotting module and then placed into the electroblotting buffer tank with an ice cooling unit. The proteins were transferred to the membrane at 200 mA for 1 hour at 4°C in ice-cooled transfer buffer with continuous stirring. The blotted membrane was blocked for the non-specific binding sites on the membrane by incubating it with gentle shaking in blocking solution for 2 hours at room temperature. After blocking, the membrane was washed thrice with TBST for 5 minutes each wash. The washed membrane was sealed in a polystyrene bag containing sufficient volume of the primary antibody and was incubated at 4°C for over night with an end-to-end shaking. The membrane was washed thrice for 5 minutes each and incubated with the secondary antibody diluted in blocking solution for 1 hour. The membrane was again washed thrice for 5 minutes each wash. Subsequently, the freshly prepared Super Signal West Pico Chemiluminescent substrate solution (Pierce) was added to the upper surface of the blotted membrane (approx. 0.2 ml/cm^2) and incubated for 3 minutes at room temperature. The membrane was wrapped in plastic foil and exposed in the darkroom for an appropriate time to an autoradiographic film that was subsequently developed in dark room conditions.

3.5.10. <u>Densitometric analysis of immunoblots</u>

The films were scanned into TIF format using ScanJet 5300C (Hewlett-Packard Company, Palo Alto, CA). The calibration of the scanner to an optical density scale (Kodak step tablet st34, Eastman Kodak Company, Rochester, NY) and the densitometric analysis of proteins were done using the public domain of National Institutes of Health (NIH) ImageJ (1.34s) software. To measure the extent of protein phosphorylation, the densitometric values of phosphorylated proteins were divided by the corresponding values of unphosphorylated proteins, respectively. Absorption of proteins in unstimulated control samples was set to 100%. Data were expressed as mean±S.D. of individual experiments from different blood donors.

3.6. Microscopic study of human platelets

3.6.1. Principle of confocal microscopy

In confocal laser scanning microscopes, a light beam with short wavelength generated by a laser is reflected by a beam-splitter/diachronic mirror and is led by flexible mirrors over the object field to scan a custom region. Excited chromophores scatter light of a longer wavelength back through the beam-splitter/diachronic mirror and produce in the focal plane a characteristic diffraction pattern from which the center, the so called "Airy disc" is selected by a detector pinhole. Because light beams projected from regions above and below the focal plane will not pass the detector pinhole, this step leads to a strong suppression of out of focus information, known as the confocal principle. A laser beam scans the specimen pixel-by-pixel and line-by-line. The pixel data are then assembled into an image that is an optical section through the specimen, distinguished by high contrast and high resolution in x, y and z planes. Number of images generated with the focal plane shifted in small steps can be combined into a 3-dimensional image stack, which is available for digital processing.

3.6.2. Preparation of poly-lysine coated coverslips

Coating buffer: 150 mM NaCl, 50 mM Na_2HPO_4, 50 mM NaH_2PO_4, and pH adjusted to 8.0

Glass coverslips were cleaned, rinsed with isopropanol and dried. Poly-lysine (200 µg/ml) was diluted with an equal volume of coating buffer to get a concentration of 100 µg/ml. On a plane surface of parafilm, drops of diluted poly-lysine (100 µl) were poured and glass coverslips were slowly mounted on these drops, and incubated for 20 minutes at room temperature. Poly-lysine coated coverslips were inverted with coated surface facing up and then washed thrice with 4 ml of H_2O and dried at room temperature for overnight.

3.6.3. F-Actin staining of human platelets

An equal volume of PBS containing 7.4% (w/v) formaldehyde was added to resting and activated platelet suspension for fixation and incubated for 10 minutes at room temperature. Fixed platelet samples were directly spun onto polylysine-coated coverslips at 800x g for 5 minutes. The coverslips were washed thrice with 1 ml of PBS. Because phalloidin probes for F-actin staining are not cell permeable, platelets were permeabilized with PBS containing 0.2% Triton X-100 for 5 minutes and washed thrice with PBS. In a humid chamber, the coverslips were inverted and loaded on drops of Alexa Fluor 546 phalloidin (60 nM) and incubated for 15 minutes to stain F-actin. The platelet immunofluorescence was observed using a Zeiss LSM510 confocal laser-scanning microscope.

3.7. <u>Expression and purification of recombinant cofilins</u>

3.7.1. <u>Work with *E.coli*</u>

3.7.1.1. Bacterial strains

Escherichia coli DH5α   F⁻φ80d*lac*ZΔM15 Δ(*lac*ZYA-*arg*F)U169 *deo*R *rec*A1 *end*A1 *hsd*R17(r_k^-, m_k^+) *pho*A *sup*E44λ−*thi*-1

Escherichia coli M15 Nal^s str^s rif^s thi^- lac^- ara^+ gal^+ mtl^- F⁻ $recA^+$ uvr^+ lon^+ contains pREP4 (Kan^R) plasmid

3.7.1.2. Media for bacterial culture

LB-medium   1.0% (w/v) tryptone, 0.5 % (w/v) yeast extract, 1.0 % (w/v) NaCl, pH 7.2.

(1.5% agar was added to the LB medium to make agar plates)

The following concentrations of the antibiotics were used if required:

Antibiotic	Stock solution	Working concentration
Ampicillin	100 mg/ml in water	100 µg/ml
Kanamycin	10 mg/ml in water	30 µg/ml

Table 3.2 Antibiotic stock solutions and its working concentration

3.7.1.3. General

E. coli was cultured at 37°C in LB medium. Bacteria transformed with an antibiotic resistance-conferring plasmid were selectively propagated in the LB medium supplemented with respective antibiotic (see Table 3.2). All solutions and supplements used for work with *E. coli* were autoclaved for 20 minutes at 121°C or filter-sterilized. Bacterial strains were long-term stored at -70°C in the LB medium supplemented with glycerol to a final concentration of 15%.

3.7.1.4. Culturing bacteria

3.7.1.4.1 Growth on solid media

The solidified LB agar plates were used for platting bacterial culture. Single bacterial colony or bacterial suspension was platted with even spreading using a sterile inoculation loop or a glass spreader, respectively, to achieve single colony growth. The plates were incubated inverted overnight at 37°C.

3.7.1.4.2 Growth of liquid cultures

For small liquid culture, 5-10 ml of LB or LB/antibiotic medium was inoculated with a single bacterial colony and incubated overnight at 37°C on a shaking platform. Starter culture was incubated for 8-12 hours and used to inoculate fresh and large volume of liquid medium. For a liquid culture of 100-250 ml of LB or LB/antibiotic medium, a starter culture to a dilution of 1:50-1:100 was inoculated and incubated overnight at 37°C with shaking. Bacteria were harvested by centrifugation at 2500x g for 15 minutes.

3.7.1.4.3 Monitoring the bacterial growth

The growth of the bacteria in liquid culture was measured at a wavelength of 600 nm (OD_{600}) in plastic cuvettes against pure medium as a blank in a spectrophotometer. Each OD_{600} unit of 0.1 corresponds to approximately 10^8 cells/ml, valid until $OD_{600} < 1$.

3.7.1.5. Preparation of ultra-competent cells by Inoue method

Inoue transformation buffer: 55 mM $MnCl_2 \cdot H_2O$, 15 mM $CaCl_2 \cdot 2H_2O$, 250 mM KCl, 10 mM PIPES (pH 6.7) and sterilized by filtration through a 0.4 μM Nalgene filter.

LB medium (100 ml) was inoculated with an overnight culture of *E. coli* cells and grown at 37°C with shaking to an OD_{600} of 0.55. The culture vessel was immediately transferred to an ice water bath and incubated for 10 minutes. Cells were harvested by centrifugation at 2500x g for 10 minutes at 4°C. The cell pellet was washed once with 8 ml ice-cold Inoue transformation buffer and finally resuspended in 2 ml ice-cold Inoue transformation buffer and 150 μl of glycerol was added to the cell suspension. Working quickly, aliquots of 200 μl were dispensed into chilled and sterile microfuge tubes, and snap-froze by immersing the tightly closed tubes in a bath of liquid nitrogen, which were later stored at -70°C until needed.

3.7.1.6. Heat shock transformation of plasmid into *E.coli*

Treatment of competent bacterial cells with a brief heat shock enables transformation of DNA. Plasmid DNA or a plasmid ligation reaction mixture (not more than 15 ng or 2.5 μl in volume) was mixed with 50 μl of thawed competent bacteria and incubated for 30 minutes on ice. The bacterial suspension was then subjected to heat shock at 42°C for 90 seconds and placed immediately on ice for 1-2 minutes. The transformed bacterial suspension was diluted 10-fold with 950 μl of LB medium and incubated for 1 hour at 37°C with shaking to recover bacteria from the heat shock. An aliquot of 50-200 μl of this bacterial suspension was spread on LB/antibiotic agar plate and incubated overnight at 37°C in order to select transformed bacteria. In case of ligation mixtures, the transformed cells were pellet down by centrifugation at 13,000 rpm for 30 seconds, and resuspended in the residual LB medium. The whole resuspended bacterial cells were spread on the agar plate.

3.7.2. Sub-cloning of cofilin and GFP cDNA

3.7.2.1. Cofilin and GFP cDNA amplification

The polymerase chain reaction (PCR) constitutes an enzymatic *in vitro* amplification of specific cDNA segments.   Amplification occurs in automated, temperature-controlled cycles of denaturation, annealing and elongation in a thermal cycler.   Initially, double-stranded template DNA is separated into its complementary single strands by heating (denaturation).   At a lower temperature two oligonucleotides primers, flanking the DNA region to be amplified, hybridize to their respective complementary sequences on opposite strands (annealing) and serve as primers for DNA synthesis in a 5'→3' direction (elongation).   Primer extension is catalyzed at a slightly increased temperature by a thermostable DNA polymerase that add deoxyribonucleotide triphosphates (dNTPs) to the recessed 3'-hydroxyl end of extending strands, thereby generating new double-stranded DNA across the primer-flanked region.   The products of each reaction cycle are then denatured to permit a new amplification cycle.   Theoretically, for n cycles a 2^n-fold amplification of a specific DNA sequence is obtained.

Primer for amplification of cofilin cDNA was commercially synthesized (MWG Biotech, Ebersberg, Germany).   It was designed corresponding to the DNA segment to be amplified, provided with restriction sites for endonuclease digestion. Pairs of primers were designed to have equivalent melting temperatures (Tm), calculated according to the formula

Tm [°C] = (A+T) ×2 + (G+C) ×4.

Where A, T, G, and C are the 2'-deoxyribonucleosides; adenosine (A), thymidine (T), guanosine (G) and cytidine (C) with in the primer sequence.

Following cofilin primers containing respective sites for restriction endonuclease (underlined) were designed to amplify cofilin cDNA from plasmid pEGFP-C1-cofilin:

Sense primer (*Nco I*)   5'-ATTATT<u>CCATGG</u>ATGGCCTCCGGTGTGGC-3'
Antisense primer (*BamH I*)   5'-TTATT<u>GGATCC</u>TCACAAAGGCTTGCCC-3'

Whereas to amplify GFP cDNA from same plasmid (pEGFP-C1-cofilin), following GFP primers were used:
Sense primer (*BamH I*)   5'-ATTA<u>GGATCC</u>CCGGTCGCCACCATG-3'
Antisense primer (*Bgl II*)   5'-AGAATTCGAAGCTTGAGCTCGAGATCTGAGTCC-3'

The annealing temperature for each PCR was typically estimated experimentally.   For preparative DNA amplification as part of cloning strategies, High fidelity DNA polymerase was used in preference to *Taq* DNA polymerase, due to its 3'→5' proofreading exonuclease activity which minimizes the risk of nucleotide miss-incorporation during elongation.

PCR reaction composition for DNA amplification was as follows:

Template DNA	20-50 ng (Plasmid pEGFP-C1-cofilin)
Sense primer (forward)	100 pmoles
Antisense primer (reverse)	100 pmoles
dNTPs	200 µM each
PCR reaction buffer	1x
DMSO	5-10% (Optional, to increase yield, specificity, consistency)
DNA polymerase	1-2.5 units
Final reaction volume	100 µl (preparative PCR), 20-50 µl (analytical PCR)

Thermal cycle parameters for PCR were as follows:

Lid temperature	105°C
Initial denaturation	94°C, 5 minutes
Denaturation	94°C, 30 seconds
Annealing	50-55°C (primer pair and template specific), 1minute
Elongation	72°C, 1 minute/kb
Cycles	30
Final elongation	72°C, 10 minutes

The PCR amplified products were analyzed by agarose gel electrophoresis. Cofilin cDNA was further processed for cloning into the pQE-60 vector (Qiagen, Hiden, Germany). The resultant pQE-60-cofilin plasmid was used as backbone to ligate the GFP cDNA between the C-terminus of cofilin and the His-tag to get the pQE-60-cofilin-GFP plasmid.

3.7.2.2. Agarose gel electrophoresis for isolating cDNA

Buffers and solutions

TBE buffer (0.5x): 45 mM Tris-base, 45 mM boric acid, 1 mM EDTA (pH 8.0)

TE buffer: 10 mM Tris-base and 1 mM EDTA (pH 8.0)

DNA loading buffer (6x): 0.25% (w/v) bromophenol blue, 0.25% (w/v) xylene cyanol, 30% (v/v) glycerol, and 50 mM EDTA

Agarose gel electrophoresis was used separate and purify DNA fragments from PCR reaction mixtures. This method uses the migration of negatively charged DNA towards the anode in an electric field. The fragments migrate through the gel matrix at rates inversely proportional to the logarithm ($\log_{10}$) of the number of base pairs. The agarose gel was prepared by melting 1-2% (w/v) agarose in 0.5x TBE electrophoresis buffer, adding 0.5 µg/ml ethidium bromide to the melted agarose and casting in a tray of desired size. A plastic comb of desired thickness and well number was inserted before the solidification of agarose gel. After solidification, the gel was placed in an electrophoresis tank and submerged in 0.5x TBE buffer. The DNA samples were mixed with DNA loading buffer and loaded into the gel wells. In adjacent to the samples, 5 µl of a DNA standard (SmartLadder[TM] Eurogentec GmbH, Germany) was loaded. Horizontal

electrophoresis was carried out at approximately 100 V. DNA bands were visualized within agarose gel by illumination of DNA-intercalated fluorescent dye ethidium bromide under UV light. The length of DNA fragments were determined by comparing their mobility with that of DNA standards. The stained gel was photographed under UV light.

3.7.2.3. DNA recovery from agarose gel

For preparative purposes DNA fragments of interest were cut out from stained agarose gels with a sharp scalpel under UV illumination. The gel slices were solubilized and DNA was purified by using the QIAquick Gel extraction kit (Qiagen) according to the manufacturer's instructions. Agarose gel slices were weighed (1 volume) and dissolved in 3 volumes of solubilization buffer QG by incubating at 50°C for 10 minutes. A volume of isopropanol was added and mixed. The whole solution was applied to a silica-gel embedded in QIAquick spin column and centrifuged at 13,000 rpm for 1 minute in order to bind DNA. The column was washed once by adding 0.75 ml wash buffer PE and centrifuging at 13,000 rpm for 1 minute. An additional 1 minute centrifugation was done to remove residual buffer. DNA was eluted by adding 30-50 µl water or TE to the column followed by incubation for 2 minutes at room temperature and then centrifugation at 13,000 rpm for 1 minute. All the buffers were provided in the QIAquick Gel extraction kit.

3.7.2.4. Restriction endonuclease digestion of DNA

For sub-cloning cofilin into pQE-60 vector, 1-5 µg PCR amplified cofilin cDNA and pQE-60 vector were digested with 1-20 U of restriction enzymes (BamHI and NcoI) in 10-50 µl of reaction buffer. For construction of pQE-60-cofilin-GFP, the resultant pQE-60-cofilin plasmid and GFP cDNA were digested with BglII and BamHI restriction endonucleases. Complete digestion was confirmed by agarose gel electrophoresis. For analytical purposes, 0.2-1 µg DNA were digested with 1-5 U of enzyme in a volume of 10-20 µl of reaction buffer. In both cases digests were incubated for 3 hours at 37°C. Reaction buffers were supplied by the manufacturer. Enzymes were heat-inactivated as recommended by the supplier or removed by purifying the digested DNA using QIAquick PCR purification kit.

3.7.2.5. Dephosphorylation of linearized plasmid DNA by CIP

In order to prevent self-ligation of vector ends, linearized plasmid DNA was treated with calf intestine alkaline phosphatase (CIP). CIP catalyzes the hydrolysis of 5'-phosphate to generate 5'-hydroxyl ends. T4 DNA ligase requires 5'-phosphate residues to catalyze new phosphodiester bonds. After hydrolysis of vector's 5'-phosphate ends, ligation is only possible between vector and inserts ends, but not between vector-ends themselves. Dephosphorylation was carried out directly following plasmid linearization. CIP was added to the digested mixture at a concentration of 1 U per pmole of linearized vector DNA and incubated at 37°C for 45 minutes.

3.7.2.6. Purification of the digested DNA

To inactivate and remove the proteins e.g. restriction enzymes, digested DNA were purified using the QIAquick PCR purification kit (Qiagen) and according to the manufacturer's instructions with slight modification. Buffers were provided in the kit and all centrifugation steps were carried out at 13,000 rpm at 25°C using a tabletop micro-centrifuge. To the DNA solutions sought purification, 5 volume of buffer PB and one volume of isopropanol were added. The mixed solution was then applied to QIAquick spin column (Qiagen) and centrifuged for 1 minute in order to bind DNA. The column was washed with 0.75 ml buffer PE and centrifuged for 1 minute. Flow through was discarded and an additional centrifugation was done to remove the residual ethanol present in buffer PE. The column was then placed into a clean 1.5 ml eppendorf tube and the purified DNA was eluted with 30-50 µl of buffer TE or water as described for QIAquick Gel extraction kit (section 3.7.2.3).

3.7.2.7. Ligation of DNA fragments

DNA fragments of bearing either sticky or blunt ends can be ligated *in vitro* with bacteriophage T4 DNA ligase. This enzyme catalyzes the formation of new phosphodiester bonds between a 5'-phosphate residue of one and a 3'-hydroxyl residue of another double-stranded DNA fragment generated by restriction endonucleases.

Ligation was carried out using Rapid DNA ligation kit (Roche) according to the manufacturer's instructions with slight modification. All the buffers were provided in the kit. A 2-5 molar excess of PCR amplified cofilin cDNA relative to the linearized and dephosphorylated pQE-60 vector DNA were taken and mixed. The vector and insert DNA mixture was diluted to a final volume of 10 µl using dilution buffer. To the diluted mixture, 10µl of ligation buffer and 5 units of T4 DNA ligase were added and mixed thoroughly. The ligation reaction mixture was then incubated at 20°C for 10 minutes subsequently used for transformation. An aliquot of 5 µl was used for transformation of 200 µl DH5α competent cells. Positive bacterial colonies were selected, screened by restriction digestion or PCR, and confirmed by DNA sequencing.

3.7.2.8. Quantification of DNA solution

The concentration of nucleic acid solutions was determined by spectrophotometry. The UV absorption was measured at a wavelength of 260 nm (OD_{260}) using a quartz cuvette of 1 cm width. For double-stranded DNA an OD_{260}=1.0 corresponds to approximately 50 µg DNA/ml. In addition the OD_{260} was measured to estimate the purity of the nucleic acid sample. A ratio OD_{260}/OD_{280} of significantly less than 1.8-2.0 indicates protein contamination.

3.7.2.9. DNA sequencing

The sequence of specific target regions in recombinant plasmid DNA was determined by a commercial sequencing service (Agowa GmbH Berlin, Germany). The sequence data were verified on the basis of the corresponding fluorescence.

3.7.3. In vitro expression of His-tagged cofilin

The vector pQE-60 was selected for construction of recombinant cofilin and cofilin-GFP with 6xHis tag placed at C-terminus of the protein. The presence of 6 consecutive histidine residues facilitates the purification of protein by nickel-nitrilotriacetic acid (Ni-NTA) metal-affinity chromatography. Plasmid DNA containing cofilin cDNA as insert was purified from DH5α bacterial culture by alkaline lysis of cells using QIAprep Spin miniprep kit according to the manufacture instructions.

Purified plasmid DNA was transformed into *E. coli* M15 [pREP4] ultra-competent cells for high expression of his-tagged cofilin. Colonies resistant to kanamycin, as a selection marker for cells containing plasmid pREP4, were selected. A small culture of bacteria (15 ml) was grown overnight in order to make starter culture. A large volume of LB medium (500 ml) was inoculated with 10 ml of the starter culture and incubated at 37°C with vigorous shaking (250 rpm) until OD_{600} reached ~0.5-0.6. Cells were induced with 1 mM IPTG and incubated at 37°C for 5 hours. Aliquots (100 µl) of samples before and after every hour of IPTG induction were collected and corrected for equal number of cells with PBS. IPTG-induced samples were lysed with 1x SDS-PAGE buffer for analyzing expression of protein by gel electrophoresis. The cells overexpressing cofilin-GFP were easy to identify since the pellet of these cells appeared fluorescent green in color. The cells were harvested by centrifugation at 4000x g for 20 minutes and stored at -20°C until used.

3.7.4. Purification by Ni-NTA affinity chromatography

3.7.4.1. Working principle of Ni-NTA affinity chromatography

Proteins containing one or more 6xHis affinity tags, located at either the amino and/or carboxyl terminus of the protein, can bind to the Ni-NTA groups on the matrix with an affinity far greater than that of antibody–antigen or enzyme–substrate interactions. Binding of the 6xHis tag does not depend on the three-dimensional structure of the protein. Untagged proteins that have histidine residues in close proximity on their surface could also bind to Ni-NTA, but in most cases these interactions are much weaker than the binding of the 6xHis tag. These non-specific bindings can be reduced under conditions that introduce competition for the binding sites, i.e. at a slightly reduced pH or in the presence of low imidazole concentrations (10-20 mM). The binding of untagged proteins can further be reduced by washing the matrix under stringent conditions

such as increased imidazole concentration (10-50 mM) in washing buffer or lowering the pH to 6.3. The histidine residues in the 6xHis tag have a pKa of approximately 6.0 and will become protonated if the pH is reduced to pH 4.5-5.3. Under these conditions the 6xHis-tagged protein can no longer bind to the nickel ions and will dissociate from the Ni-NTA resin. Similarly, if the imidazole concentration is increased to 100-250 mM, the 6xHis-tagged proteins will also dissociate because they can no longer compete for binding sites on the Ni-NTA resin.

3.7.4.2. Preparation of Ni-NTA affinity column

A Ni-NTA Superflow resin (Qiagen, Hiden, Germany) column was prepared for FPLC purification of the His-tagged cofilin in a cold room ambient. Briefly, a chromatography glass column was cleaned, rinsed with isopropanol and dried. The column was clamped in a test tube holder stand and slurry of 50% Ni-NTA Superflow beads was slowly poured avoiding any trapping of air bubbles into the column. The column and bed size was calculated depending on the amount of His-tagged protein to be purified. Generally, the binding capacity of Ni-NTA superflow is 5-10 mg protein per ml resin. The resin was allowed to settle by allowing the buffer to flow through by uncapping the bottom outlet. After the column was nicely packed, it was attached to the peristaltic pump of Econo System (Bio-Rad) with a flow rate of 1ml/minute and equilibrated with 10 column volumes of the lysis buffer.

3.7.4.3. Purification of His-tagged recombinant cofilins

Lysis buffer:	50 mM NaH_2PO_4, 300 mM NaCl, 0.05% (w/v) NaN_3, 10 mM imidazole, and complete mini EDTA-free protease inhibitor (2 tablets/10 ml of buffer).
Wash buffer:	50 mM NaH_2PO_4, 300mM NaCl, 0.05% (w/v) NaN3, and 50 mM imidazole.
Elution buffer:	50 mM NaH_2PO_4, 300 mM NaCl, 0.05% (w/v) NaN_3, and 250 mM imidazole.

All buffers were adjusted to pH 8.0 and stored at 4°C.

The cell pellet was thawed for 15 minutes on ice and resuspended in 2-5 ml of lysis buffer per gram wet weight. Cells were lysed by adding lysozyme to 1 mg/ml (final concentration) and incubated on ice for 30 minutes. After incubation, cell lysate was sonicated on ice for ten times with 20 seconds bursts of 200-300 W and a 20 seconds cooling period between each bursts. When the lysate was very viscous, DNaseI was added at concentration 5 μg/ml and incubated on ice for 10-15 minutes. Lysate was centrifuged at 10,000x g for 1 hour in order to separate the cellular debris. Supernatant was collected in ice-cold 50-ml plastic tubes applied to the Ni-NTA Superflow column with a flow rate of 0.5 ml/minute. The eluate was passed through an Econo UV Monitor (280 nm) to check elution of proteins. The column was washed with lysis buffer until the A_{280} became stable. Binding of non-specific proteins to the Ni-NTA resin was

minimized by washing the column with wash buffer until the eluate showed a low and stable A_{280}. The bounded His-tagged proteins were eluted with elution buffer and eluate fractionated into approx. 1ml each was collected in clean glass tubes using Model 2110 Fraction Collector. All collected fractions were subjected to SDS-PAGE and those that contain high amount of purified his-tagged proteins (>97%) were selected. The purified his-tagged cofilin is shown in Figure 3.5A (fraction 3+4). The purified his-tagged cofilin and cofilin-GFP analyzed for protein degradation using anti-cofilin immunoblot are shown in Figure 3.5B. Protein was concentrated using Centricon® Plus-20 centrifugal filter device (Millipore) with molecular weight cut off (MWCO) of 5-kDa at 4000 rpm, 4°C until a desired concentrated volume was achieved. Protein concentration was measured using dotMETRIC™ protein assay kit.
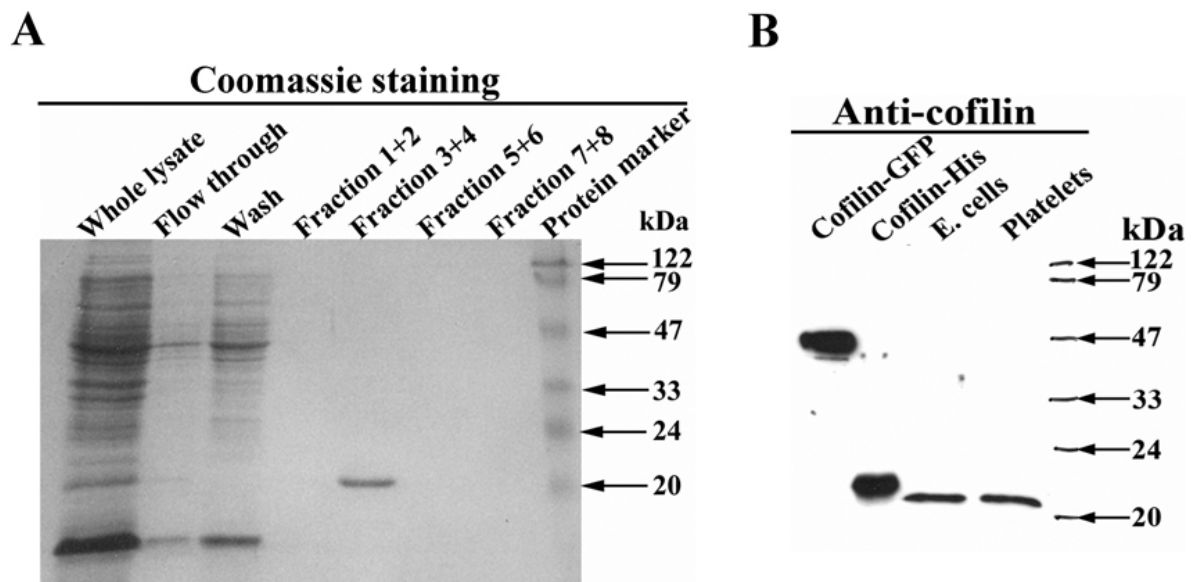
Figure 3.5 Purification of His-tagged cofilins by Ni-NTA affinity chromatography. **(A)** Samples from different steps during protein purification of his-tagged cofilin were subjected to SDS-PAGE and probed with coomassie brilliant blue staining. The purified his-tagged cofilin (20-kDa) was eluted in fraction 3+4. **(B)** The purified his-tagged cofilin and cofilin-GFP along with lysates of endothelial cell and platelets were subjected to anti-cofilin immunoblotting for analyzing protein degradation. Single bands of his-tagged cofilin and cofilin-GFP indicate no degradation of these proteins.

3.8. <u>Peptide and protein delivery into platelets</u>

Platelets do not contain any defined transcriptional machinery and therefore the genetic manipulation methods to overexpress proteins of interest in platelet are not feasible. Moreover, platelets are very sensitive to their external milieu and therefore platelet is a difficult system to manipulate by delivering peptides and proteins using current transfection techniques. Recently, novel methods to deliver peptide or proteins into cells using cell-permeable peptides such as TAT, penetratin, and cationic poly-arginine have been reported and commercialized (Deshayes et al. 2005). We chemically synthesized poly-arginine (R9) conjugated N-terminal cofilin peptide

(1-16 amino acids), a reverse peptide and a peptide mimicking cofilin phosphorylation (S3D). These peptides were used to study the regulation of LIMK-1 in intact platelets. The N-terminal cofilin peptide has been shown to inhibit LIMK-1 in neuronal cells (Aizawa et al. 2001). Different concentrations of these peptides were incubated with platelets at 37°C for 30 minutes and 1 hr and then induced with thrombin (0.5 U/ml). Activated platelets were lysed by adding equal volume of SDS-PAGE lysis buffer and were analyzed for cofilin phosphorylation by immunoblotting.

Chariot, a revolutionary new transfection reagent (Morris et al. 2001), which has been successfully used to deliver proteins into mammalian cells, was studied to deliver cofilin-GFP into platelets. Unlike current peptide based transfection techniques, which require covalent coupling of these membrane permeable peptides with peptide/proteins of interest, Chariot forms a non-covalent complex with protein, peptide or antibody of interest and is a comparatively faster method. The Chariot-macromolecule complex stabilizes the macromolecule and helps to protect it from degeneration during the transfection process. Upon internalization, the complex dissociates and the macromolecule becomes free to proceed to its target organelle. Purified cofilin-GFP was delivered into platelets so that the efficiency of transfection could be easily monitored using confocal microscopy. Chariot transfection reagent (10 µL) was diluted in 60 µl of 20% DMSO/H_2O solution. Cofilin-GFP (2 µg) was added to 50 µL of H_2O and mixed with 60 µl of diluted Chariot reagent. In order to assemble Chariot-cofilin-GFP complex, the mixture (110 µl) was incubated at 37°C for 30 minutes. After complex formation, the reaction mixture was added to 100 µl of platelet suspension (5% DMSO final concentration) and incubated for 2 hours at 37°C. Platelets were then washed twice with PBS and resuspended in 100 µl of buffer C. The transfected platelets were directly spun onto polylysine-coated coverslips at 800x g for 5 minutes and allowed to spread for 15 minutes at 37°C. Spread platelets were then fixed, permeabilized and probed for F-actin staining using Alexa-546, and observed by confocal microscopy as described in section 3.6.3

4. <u>Results</u>

4.1. <u>Identification of cofilin and LIMK-1 in human platelets</u>

4.1.1. <u>Cofilin</u>

In cells, cofilin exists in two forms, unphosphorylated (cofilin) and phosphorylated at Ser3 position (phospho-cofilin). Platelets are known to contain cofilin in both forms (Davidson and Haslam 1994). However, the extent of cofilin phosphorylation in resting platelets is not clear. These two different forms of cofilin have a different pI and can be easily separated by isoelectric focusing (IEF). Phospho-cofilin due to the negatively charged phosphate group has a lower pI than cofilin and it therefore moves faster towards the anode. The two forms present in lysates of resting platelets were separated using IEF and subsequently immunoblotted with anti-cofilin antibody to quantify the amount of phospho-cofilin by densitometry. It was found that one third of the total cofilin is present in its phosphorylated form in resting platelets (Figure 4.1).
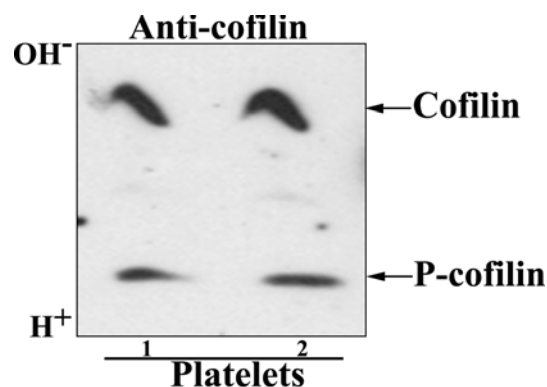
Figure 4.1 Identification of cofilin in its unphosphorylated and phosphorylated states in resting platelets. Resting platelet lysates were subjected to IEF electrophoresis and subsequently immunoblotted with anti-cofilin antibody.

4.1.2. <u>LIMK-1</u>

It was not known, whether platelets contain LIM-kinases, and which type of LIM-kinase is expressed in platelets. A polyclonal antibody against the recombinant kinase domain of LIMK-2 was produced and used for immunoblotting. A 72-kDa protein was identified in platelets, which shows that LIM-kinases are expressed in platelets (data not shown). Since this antibody did probably not distinguish between LIMK-1 and LIMK-2 due to the high homology in the kinase domain, specific peptide antibodies against the two forms of LIMKs were used. The specificity of the anti-LIMK-1 and anti-LIMK-2 was probed by immunoblotting endothelial cells transfected with different GFP-LIMK-2 constructs (Goyal 2005). The anti-LIMK-2 antibody identified the

different GFP-LIMK-2 constructs at their respective positions in the immunoblot, while the anti-LIMK-1 antibody did not. After immunoblotting platelet lysates with these specific LIM kinase antibodies, only LIMK-1 but not LIMK-2 expression was found in platelets (Figure 4.2). In contrast to platelets, endothelial cells contain both LIMK-1 and LIMK-2 (Goyal 2005).
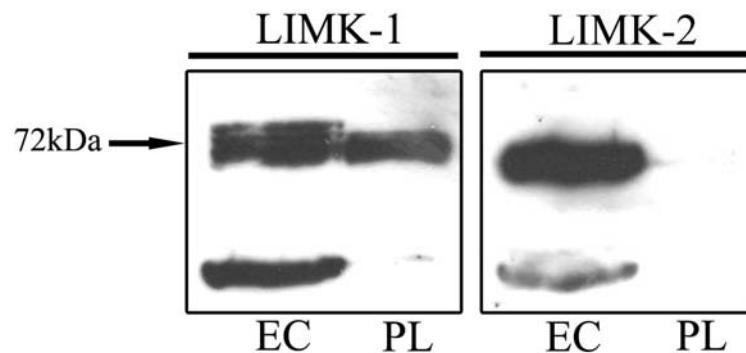
Figure 4.2 LIMK-1 but not LIMK-2 is expressed in platelets. Lysates of endothelial cells (EC) and platelets (PL) were immunoblotted with specific anti-LIMK-1 and anti-LIMK-2 antibodies. Endogenous LIMK-1 and LIMK-2 are expressed in endothelial cells but platelet expresses only LIMK-1 (both LIMK-1 and LIMK-2 have molecular mass of 72-kDa). The lower bands detected by both LIMK-1 and LIMK-2 in endothelial cells could be a truncated form of LIM-kinases.
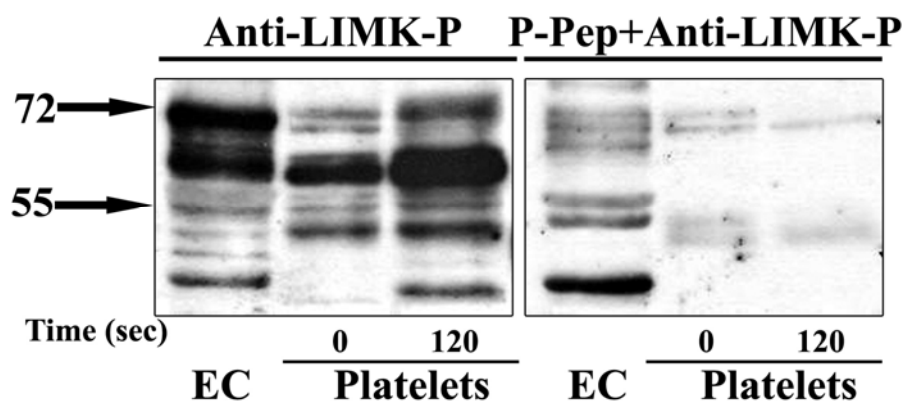
Figure **4.3 Specificity of phospho-LIMK-1/LIMK-2 antibody.** Lysates of endothelial cell, resting platelets and platelets stimulated for 120 seconds with thrombin (0.5U/ml) were immunoblotted with phospho-LIMK-1/LIMK-2 antibody pre-incubated or not incubated with the 7.5μM of synthetic phospho-peptide (CKNDRKKRYTPVVG, P-Pep) for 1 hour at 37°C.

LIMK-1 in cells is activated by phosphorylation of Thr508 in the kinase domain. In order to analyze the activation of LIMK-1 we used a specific anti-phospho-LIMK antibody raised against a KLH-coupled synthetic phospho-peptide corresponding to residues surrounding phospho-Thr508 of human LIMK-1. This antibody recognizes both LIMK-1 and LIMK-2 phosphorylated at Thr508 and Thr505, respectively. In endothelial cells, the antibody recognized a phosphorylated 72-kDa protein, and an additional protein of approx molecular mass 56-kDa was detected. The phosphorylation of the 72-kDa protein as well as three additional proteins was increased in thrombin-activated platelets. The specificity of the anti-phospho-LIMK antibody

was probed using the respective synthetic unphosphorylated and phosphorylated peptides (CKNDRKKRYTVVGN; amino acid 500-512) of LIMK1. Preincubation of phospho-LIMK antibody with the unphopshorylated peptide did not block the detection of these proteins (data not shown), whereas with the phospho-peptide the signal of phosphorylated LIMK-1 was suppressed in endothelial cells and platelets (Figure 4.3). Additionally, the phospho-peptide also blocked the signals of the 56-kDa protein in endothelial cells and the other three proteins in resting and activated platelets (Figure 4.3). These results show that the anti-phospho-LIMK antibody identifies phosphorylated LIMK-1 and other unknown proteins in endothelial cells and platelets. Some of these proteins could be truncated forms of LIMK-1 as observed by Soosairajah et al (Suppliment 1)(Soosairajah et al. 2005).

4.2. Platelet shape change induced by thrombin

4.2.1. Shape change studied by decrease in light transmission
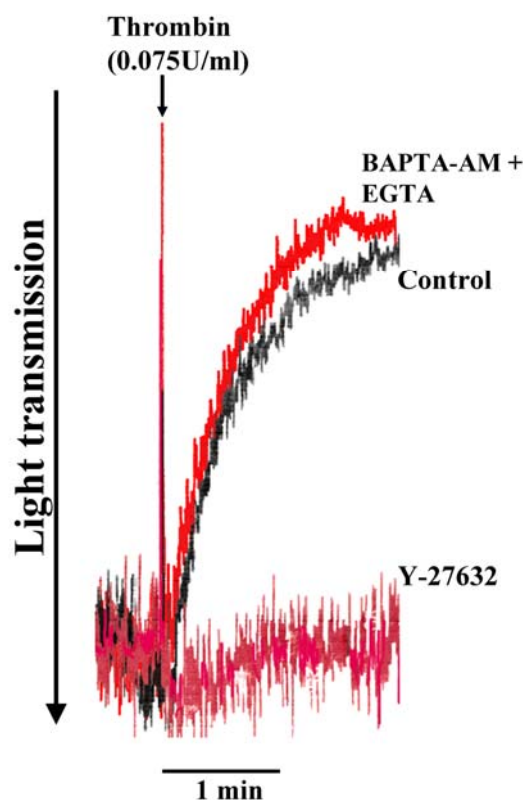
Figure 4.4 Rho-kinase-mediated platelet shape change induced by thrombin (0.075U/ml). Shape change was measured by the decrease in light transmission. Preincubation of platelets with the Rho-kinase inhibitor Y-27632 but not with BAPTA-AM/EGTA inhibited platelet shape change induced by this concentration of thrombin (black). For incubation conditions see section 3.2.4.1.

Physiological stimuli such as thrombin at a low concentration range of 0.01-0.04 U/ml, induce shape change through a pathway that is apparently independent of an increase in cytosolic Ca^{2+}(Bauer et al. 1999). At higher concentrations of thrombin, Ca^{2+} influx through the plasma membrane and mobilization of Ca^{2+} from intracellular stores are observed. However, I found

even a high concentration of thrombin (0.075U/ml) induced a Ca^{2+}-independent Rho-kinase-mediated shape change. Pretreatment of platelets with the Rho-kinase inhibitor Y-27632 completely inhibited this shape change (Figure 4.4). In contrast, preincubation of platelets with the intracellular Ca^{2+} chelator BAPTA-AM in combination with the extracellular Ca^{2+} chelator EGTA did not affected thrombin-induced shape change indicating that Ca^{2+} influx through the plasma membrane or Ca^{2+} mobilization from intracellular stores is not involved (Figure 4.4).

Serotonin, ATP and ADP secreted after platelet stimulation with thrombin might affect the platelet shape change by reinforcing signal transduction pathways through outside-in signaling by activating their respective platelet receptors. However, no ATP secretion was observed, indicating that thrombin-induced shape change is independent of platelet activators released by dense granule secretion (e.g. ADP, serotonin).

4.2.2. <u>Shape change studied by confocal microscopy</u>

In the non-activated state platelets have a typical discoid shape, and activation of platelets by agonists such as thrombin leads to a spheroid shape with the formation of pseudopods. Confocal microscopic studies of resting and thrombin-stimulated platelets (for 2 minutes) that were stained for F-actin with Alexa-546 phalloidin showed that the smooth and regular structure of disc-like resting platelets (diffusely stained for F-actin) changed to an irregular and smaller spherical structure (more intensely stained for F-actin) of activated platelets. Pretreatment of platelets with the Rho-kinase inhibitor Y-27632 completely blocked the shape change further supporting that shape change induced by thrombin involves a Rho-kinase mediated signaling pathway (Figure 4.5).
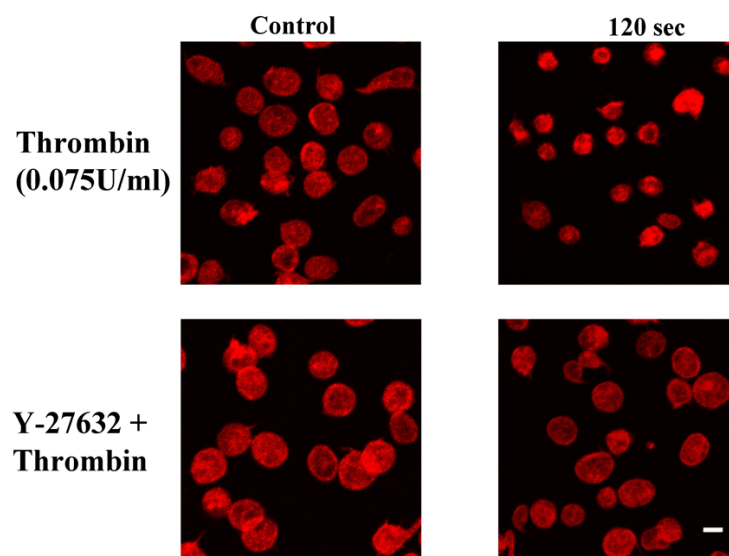

Figure 4.5 Confocal fluorescence microscopy of platelets. Platelets in the absence or presence of Rho-kinase inhibitor Y-27632 are stimulated with thrombin (0.075U/ml). Platelets are stained for F-actin with Alexa Fluor 546 phalloidin (Bar=2μm).

4.2.3. <u>F-actin increase in thrombin-stimulated platelets</u>

Platelet activation is associated with changes in the actin cytoskeleton such as an increase of F-actin content. During the Rho-kinase-mediated platelet shape change induced by thrombin (0.075 U/ml), the change in platelet F-actin was analyzed.

Activation of F-actin depolymerizing and severing proteins like cofilin and gelsolin result in the formation of small F-actin filaments from the existing large filaments. Moreover, stimulation of actin polymerization during shape change may also generate F-actin filaments of various lengths. Platelet F-actin, upon its sediment properties can be divided into a low-speed (15,000x g) and a high-speed (100,000x g) Triton X-100-insoluble fraction. To measure the total F-actin content, platelets were lysed for 5 minutes on ice, and both the low-speed and high-speed Triton-X100 insoluble fractions were pelleted together by centrifugation at 150,000x g for 30 minutes. The F-actin content of platelets undergoing shape change was measured by separation of proteins using SDS-PAGE, probing them with Coomassie brilliant blue (CBB®), and subsequent densitometry. The F-actin content was calculated as percentage of the total actin. Thrombin induced an increase in F-actin from 43±2% of total in resting platelets to 55±3% (mean± SD, n= 4) 30 sec after thrombin stimulation. The increase of F-actin content in thrombin-stimulated platelets was inhibited by Y-27632 (Figure 4.6). These results suggest that thrombin-stimulated platelet shape change is accompanied by an increase in F-actin content, which is Rho-kinase dependent. Interestingly, Y-27632 increased significantly the F-actin content in unstimulated platelets.
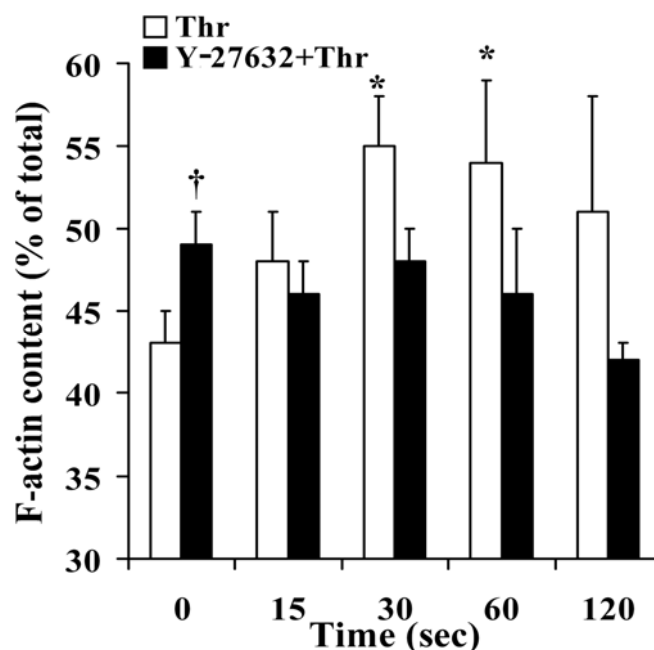

Figure 4.6 Effect of Y-27632 on F-actin content during shape change induced by thrombin (0.075U/ml). Values are mean+SD of 4 independent experiments. Asterisks (*) denote statistical significance with respect to non-activated controls (0 seconds); *P*<0.05. (†) Denotes significance between control (□) and Y-27632 (■) treated unstimulated platelets.

4.2.4. <u>Activation of Rho-kinase (MYPT phosphorylation)</u>

In order to analyze Rho-kinase activation during thrombin-induced platelet shape change, phosphorylation of one of its substrates, the <u>m</u>yosin <u>p</u>hosphatase <u>t</u>argeting subunit (MYPT) was measured. The human MYPT has Thr696 and Thr853 as sites of phosphorylation for Rho-kinase (see Figure 1.6), which can be measured by specific anti-MYPT1 (Thr696) and anti-MYPT1 (Thr853) antibodies.

The measurement of MYPT phosphorylation at Thr696 (data not shown) and Thr853 (Figure 4.7) was used to estimate Rho-kinase activation during platelet shape change. Thrombin induced a rapid increase of MYPT phosphorylation at Thr853, reaching a maximal (about 2-fold) within 1 minute after platelet stimulation. The MYPT phosphorylation was irreversible after 2 minutes of thrombin stimulation. The established Rho-kinase inhibitor Y-27632 reduced the MYPT phosphorylation in non-activated platelets and completely abolished the thrombin-induced increase of MYPT phosphorylation. These results together with the results showed in section 4.2.3 (Figure 4.6) indicate that Rho-kinase is activated during shape change and mediates the F-actin increase underlying platelet shape change (Figure 4.7).
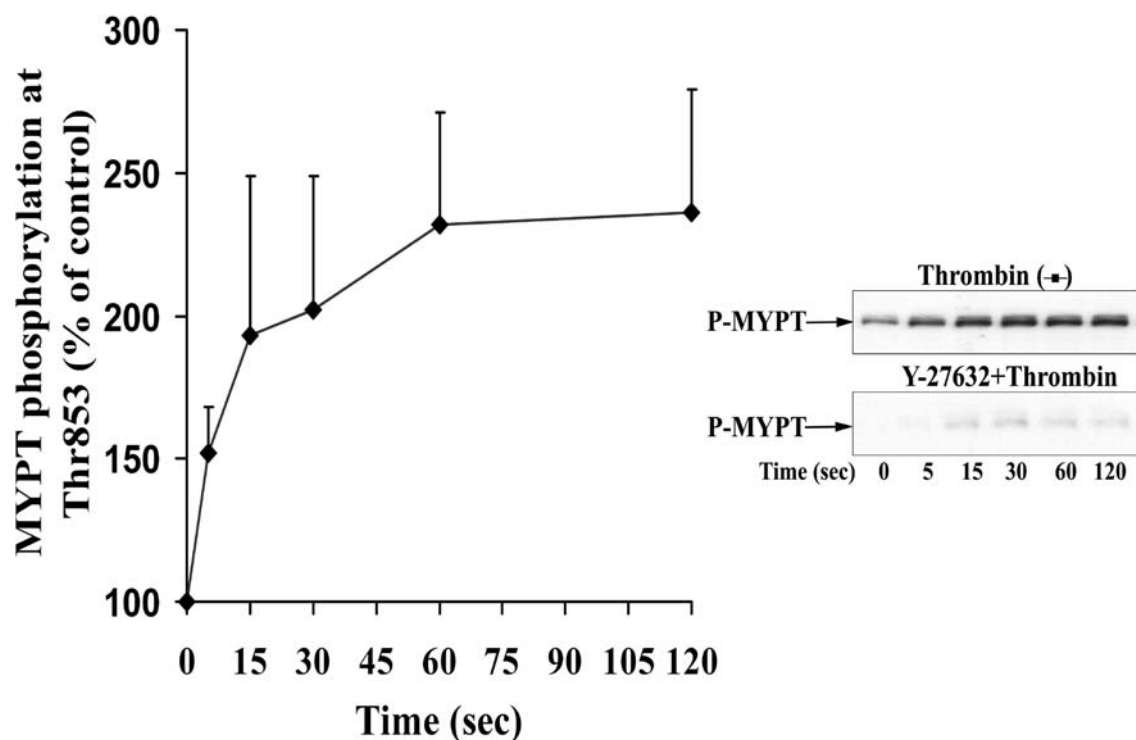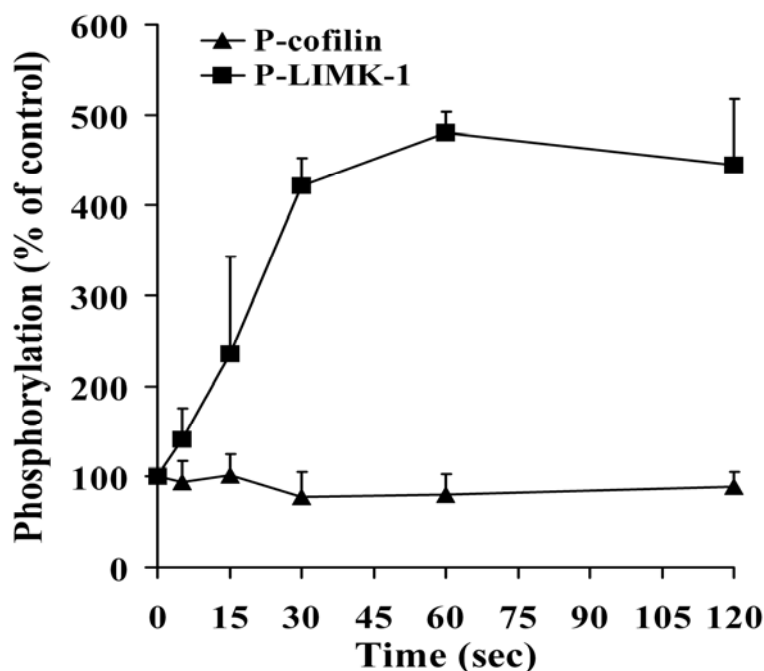

Figure 4.7 MYPT phosphorylation during thrombin-stimulated platelet shape change. Platelet lysates were immunoblotted with anti-phopsho-Thr853-MYPT antibody. (Left) Graphical representation of the results evaluated by densitometry. Values are mean + SD of 3 independent experiments. (Right) Representative immunoblots of MYPT phosphorylation.

4.2.5. <u>LIMK-1 and cofilin phosphorylation</u>

Rho-kinase also phosphorylates LIMK-1 at Thr508 leading to the activation of this enzymes (Ohashi et al. 2000; Sumi et al. 2001). Activated LIMK-1 phosphorylates cofilin at Ser3 and thereby inactivates cofilin for its actin binding, severing and actin depolymerization activities. LIMK-1 can also be phosphorylated by Rac-activated PAKs (p21 activated kinases) (Edwards et al. 1999). Both Rac and PAK are stimulated during platelet activation (Teo et al. 1995; Azim et al. 2000). We investigated whether Rho-mediated Rho-kinase activation or Rac-mediated PAK activation stimulates LIMK-1. We also analyzed whether LIMK-1 activation leads to cofilin phosphorylation, and whether a Rho-kinase/LIM-kinase/cofilin pathway might regulate the increase of F-actin underlying platelet shape change stimulated by thrombin. LIMK-1 phosphorylation was quantified using a specific anti-phospho-LIMK antibody.

LIMK-1-Thr508 phosphorylation increased during shape change. LIMK-1 phosphorylation was rapid and irreversible reaching a maximum (4-5 fold) within 1 minute of thrombin stimulation. The kinetic of LIMK-1 phosphorylation was similar to the kinetics of MYPT1 phosphorylation (Rho-kinase activation) except LIMK-1 phosphorylation was slightly slower than MYPT phosphorylation (compare with Figure 4.7). In platelets pre-treated with the Rho-kinase inhibitor Y-27632, which does not affect the activity of PAK even at high concentrations (Uehata et al. 1997), the increase in LIMK-1 phosphorylation was completely blocked. These results show that the increase of LIMK-1 phosphorylation during shape change was completely Rho-kinase dependent (Figure 4.8).

Figure 4.8 LIMK-1 and cofilin phosphorylation during platelet shape change induced by thrombin (0.075U/ml). Graphical representation of the result for LIMK-1 (-■-) and cofilin (-▲-) phosphorylation. Values are presented as mean + SD of three experiments with platelets from different donors.

To investigate whether LIM-kinase activation might phosphorylate cofilin in thrombin–stimulated platelets, cofilin phosphorylation was measured by using a specific anti-phospho cofilin antibody. Unexpectedly, despite the rapid and pronounced Rho-kinase activation and subsequent LIMK-1 phosphorylation, we could not observe a concomitant increase in cofilin phosphorylation during shape change. Cofilin phosphorylation during thrombin-induced platelet shape change was unchanged (Figure 4.8 and Figure 4.9A, upper immunoblots).

Preincubation of platelets with Y-27632, which completely inhibited LIMK-1 phosphorylation, decreased cofilin phosphorylation by (20%) in resting platelets (Figure 4.9). A gradual dephosphorylation of cofilin was noticed when platelets pretreated with Y-27632 were stimulated by thrombin (Figure 4.9B). In thrombin-stimulated platelets, cofilin phosphorylation decreased from 76±10% to 54±12% of control after 2 minutes of stimulation. These results suggest that cofilin dephosphorylation by a cofilin phosphatase might mask the concomitant stimulation of cofilin phosphorylation by LIMK-1 during thrombin-stimulated platelet shape change.
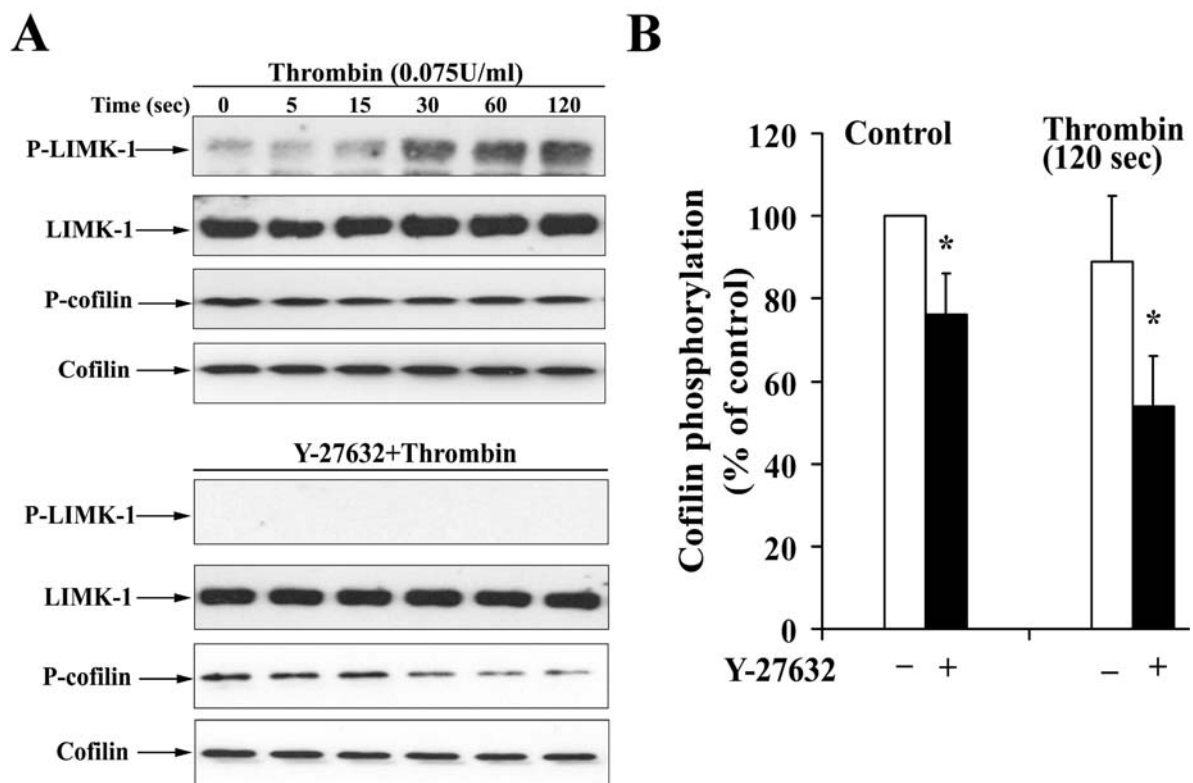
Figure 4.9 Effect of Y-27632 on LIMK-1 and cofilin phosphorylation during shape change stimulated by thrombin. Platelet lysates from platelets treated or non-treated with Y-27632 and then stimulated with thrombin (0.075U/ml) were immunoblotted with anti-phospho-LIMK-1/LIMK-2, anti-LIMK-1, anti-P-cofilin and anti-cofilin antibodies. (Left) Representative immunoblots. (Right) Bar diagram showing cofilin phosphorylation of non-treated (□) and Y-27632 (■) treated platelets in control and after thrombin stimulation (120 sec). Values for cofilin phosphorylation in resting platelets and activated platelets are mean + S.D of eight and four independent experiments, respectively. Asterisks (*) denote statistical significance *P*<0.05 with respect to control, not treated with Y-27632 (right).

4.2.6. <u>Rapid association of cofilin with F-actin during shape change</u>

Since there was no net increase in the total phospho-cofilin pool during the shape change, where an increase of F-actin was observed, we wondered whether the association of active unphosphorylated cofilin with F-actin was changed. We thus analyzed the cofilin association with F-actin at different time intervals during shape change. A method described by Kovacsovics and Hartwig (Kovacsovics and Hartwig 1996) was used for isolating F-actin with few modifications such as platelet lysis time, centrifugation speed and omission of phalloidin from the platelet lysis buffer. Platelets were lysed only for 5 minutes and not for 1 hour on ice to avoid changes after lysis such as depolymerization of F-actin (Carlsson et al. 1979).
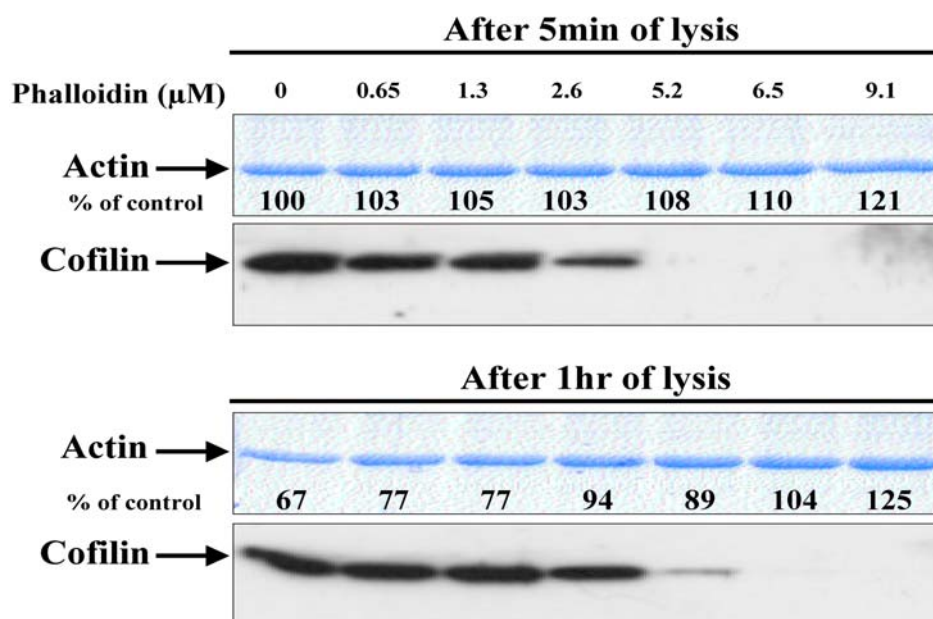

Figure 4.10 Effect of phalloidin and platelet lysis time on platelets F-actin content and cofilin association with F-actin. The total F-actin from platelets lysed for 5min (upper) and 1hr (lower) in lysis buffer containing increasing concentration of phalloidin was isolated by centrifugation at 150,000x g for 30 minutes and subjected to actin staining by coomassie brilliant blue, or immunoblotting with anti-cofilin antibody. Values determined by densitometry are presented in percent of control by setting 100% for platelets lysed for 5 minutes and 0 µM phalloidin.

A decrease of 30% in F-actin content was observed when incubation time for lysis was 1 hour compared to the lysis for 5 minutes (Figure 4.10). Phalloidin was omitted from the lysis buffer, because it was found that the presence of phalloidin in the lysis buffer increased the formation of F-actin depending on the incubation time for platelet lysis (Figure 4.10). After 5 minutes of lysis, phalloidin (9.1 µM) increased F-actin from 100% to 121%, whereas after 1 hour of lysis, the same concentration of phalloidin increased F-actin from 67% to 125 %. This effect of phalloidin was concentration dependent. It was found that by increasing the phalloidin concentration in the lysis buffer the associated cofilin was displaced proportionally from F-actin, and concentrations above 6 µM completely removed cofilin from the F-actin (Figure 4.10). Phalloidin, although it binds to F-actin at a position different than cofilin, has been reported to inhibit the binding of

cofilin to actin (Yonezawa et al. 1988). Once phalloidin is bound and has stabilized the F-actin, cofilin is no longer able to interact with F-actin (McGough et al. 1997). Therefore we used for the experiments subsequently shown a lysis time of 5 minutes and omitted phalloidin from the lysis buffer.
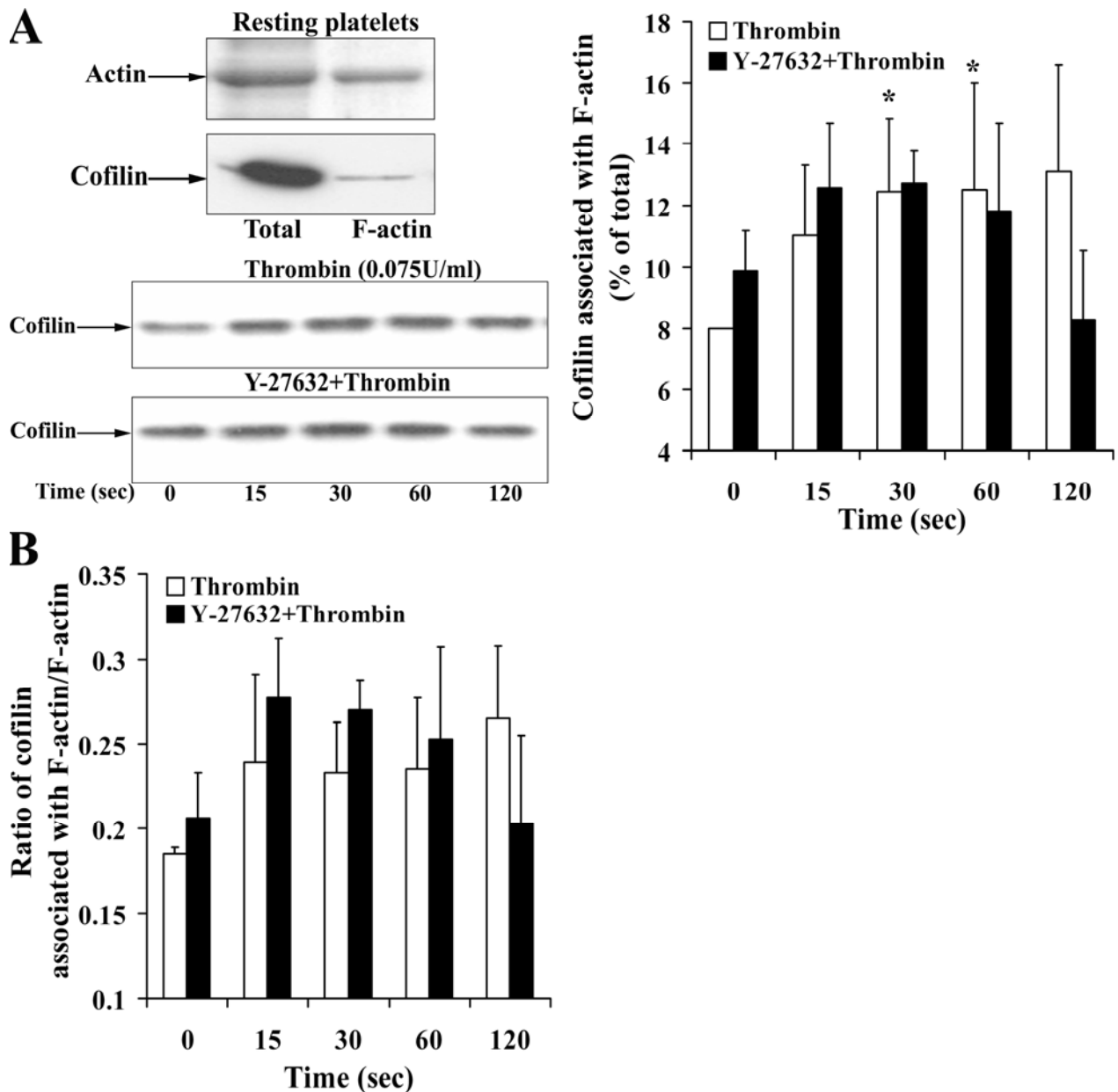
Figure 4.11 Cofilin association with F-actin during thrombin-induced platelet shape change. (A, left, top) Representative gel and immunoblot of F-actin and cofilin, respectively. Total indicate whole platelets; F-actin, F-actin fraction of the same number of platelets. (Left, bottom) Immunoblot of cofilin associated with F-actin during thrombin induced shape change in the absence or presence of Y-27632. (Right) Graphic representation of the results. Values are the mean + S.D for four independent experiments. Asterisks (*) denote statistical significance $P<0.05$ with respect to time 0 sec in nontreated samples. (B) Bar diagram showing the ratio of cofilin associated with F-actin to F-actin in non-treated platelets (□) and platelets treated with Y-27632 (■) during thrombin-induced shape change. Values are the mean + S.D for four independent experiments.

Cofilin only in its unphosphorylated form binds with F-actin while the phosphorylated cofilin does not (Lee et al. 2000). We also found in platelets that cofilin only in its unphosphorylated form bound with F-actin, while the phosphorylated cofilin did not (data not shown). A small amount of cofilin (about 8% of total) was bound with F-actin in non-activated platelets. During shape change, we found a significant small increase of cofilin association with F-actin (to about 13% of total). However, cofilin relative to F-actin did not significantly increase as measured by the ratio of F-actin- associated cofilin with F-actin at various time points of shape change (Figure 4.11B). Furthermore, pre-treatment of platelets with Y-27632 increased significantly the cofilin association with F-actin in resting platelets, and the subsequent increase during thrombin-stimulation was not significant. Y-27632 which resulted in cofilin dephosphorylation of 40% 2 min after thrombin stimulation (Figure 4.9B), rather decreased than increased the association of cofilin with F-actin at this time point (Figure 4.11 A and B). These results indicate that the F-actin increase and the association of the small pool of cofilin with F-actin (5%) during shape change are regulated by a mechanism other than cofilin phosphorylation. No association of LIMK-1 and phospho-LIMK-1 with the actin cytoskeleton could be detected in resting or activated platelets (data not shown).

4.3. Platelet secretion and aggregation induced by thrombin

4.3.1. Effect of Y-27632 on platelet secretion and aggregation

Stimulation of platelets with thrombin (0.5 U/ml) induced rapid dense granule secretion and platelet aggregation (Figure 4.12). Pretreatment of platelets with Y-27632 (20 µM) inhibited thrombin-induced secretion and platelet aggregation. Y-27632 reduced platelet aggregation and made it partly reversible during platelet stimulation with 0.5 U/ml thrombin, but failed to inhibit aggregation induced by higher concentration (1.0 U/ml) of thrombin (data not shown). ADP secreted from dense granule during platelet stimulation with the low concentration of thrombin might augment the thrombin response. To answer, whether the Rho-kinase inhibitor Y-27632 inhibits primarily secretion or whether it affects integrin $\alpha_{IIb}\beta_3$ activation leading to a reduced ATP secretion, the integrin $\alpha_{IIb}\beta_3$ antagonist RGDS was used to inhibit platelet aggregation. Prevention of platelet aggregation by RGDS did not inhibit the thrombin-induced ATP secretion suggesting that the outside-in signaling through integrin $\alpha_{IIb}\beta_3$ does not regulate dense granule secretion in thrombin-stimulated platelets.

Interestingly, even in the presence of RGDS, Y-27632 inhibited ATP-secretion from platelet indicating that inhibition of aggregation by Y-27632 is due to inhibition of secretion and thereby attenuating platelet aggregation. These results suggest a role of Rho-kinase in dense granule secretion from activated platelets.
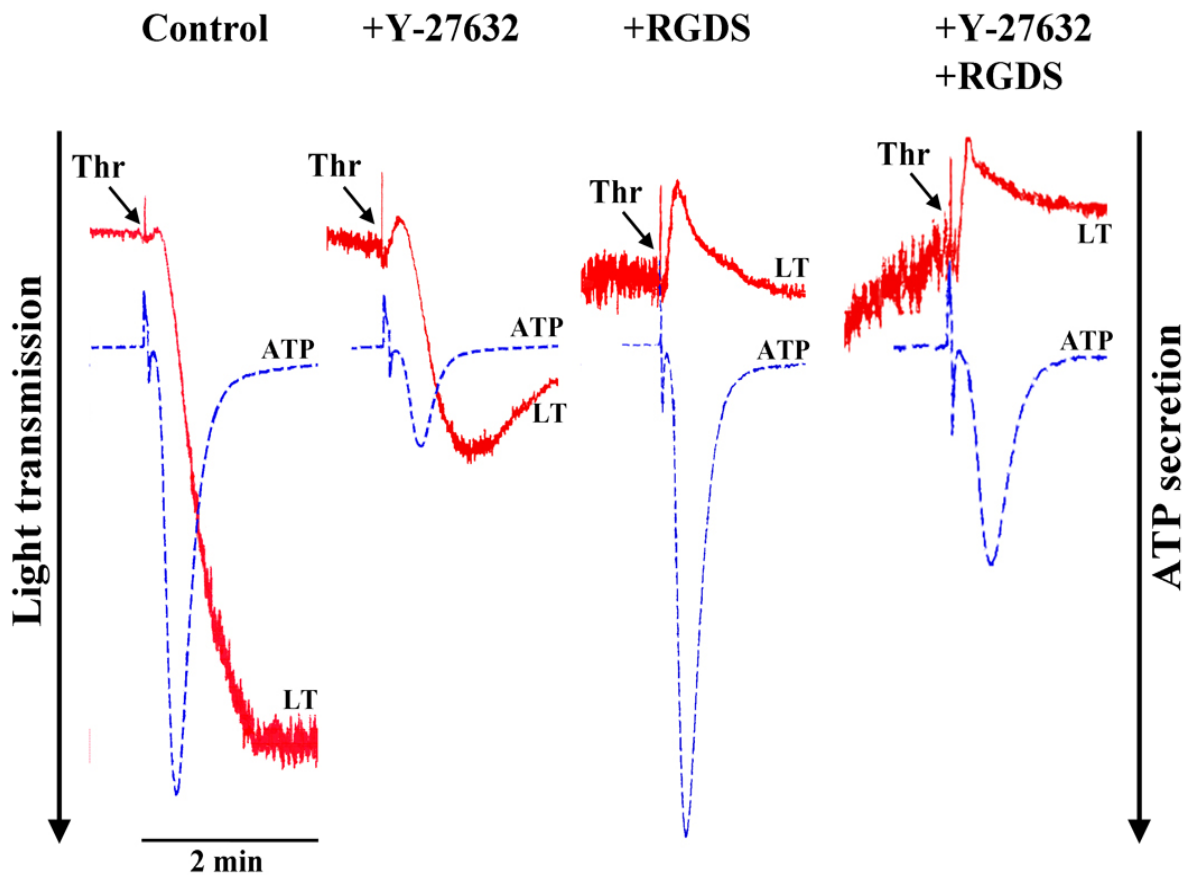
Figure 4.12 Inhibition of thrombin-induced aggregation and secretion by the Rho-kinase inhibitor Y-27632.
Platelets were stimulated with thrombin (0.5 U/ml) in the absence or presence of the integrin $\alpha_{IIb}\beta_3$ blocker RGDS (0.5 mM) and the Rho-kinase inhibitor Y-27632 (20 μM). Representative tracings for change in light transmission (LT, red)) and ATP secretion (blue) are shown.

4.3.2. Rho-kinase activation (MYPT phosphorylation)

Rho-kinase activation was determined by measuring the MYPT phosphorylation at its Thr696 and Thr853 residues as described previously during thrombin-induced platelet shape change (section 4.2.4). Estimation of MYPT phosphorylation at both sites (Thr696 and Thr853) gave identical results. MYPT phosphorylation was rapid reaching a maximum (2-3 fold) 5 seconds after thrombin (0.5 U/ml) stimulation and then decreased to the level below control after 1-2 minutes. The peak of MYPT phosphorylation was similar as during thrombin-induced shape change. The rapid increase of MYPT phosphorylation at both Thr696 (Figure 4.13) and Thr853 (data not shown) was not only inhibited by Y-27362 (Figure 4.15), but also by the new specific Rho-kinase inhibitor H-1152 (20 μM; data not shown). The reversible MYPT phosphorylation pattern during platelet aggregation was different from the irreversible time course of MYPT phosphorylation during shape change. These differences might be explained by an aggregation-dependent stimulation of dephosphorylation of MYPT phosphorylated at Thr696 and Thr853. To investigate the role of outside-in signaling through integrin $\alpha_{IIb}\beta_3$ in regulating MYPT phosphorylation, RGDS was used or platelets were activated in the absence of stirring. Under the

conditions, which blocked platelet aggregation but not secretion, MYPT phosphorylation was irreversible (Figure 4.13). Therefore in thrombin-aggregated platelets, the rapid increase of MYPT phosphorylation is due activation of Rho-kinase, and the subsequent and pronounced decrease of MYPT phosphorylation is due to activation of a phosphatase acting on MYPT Thr696 and Thr853 phosphorylation sites that is activated by engagement of the integrin $\alpha_{IIb}\beta_3$.
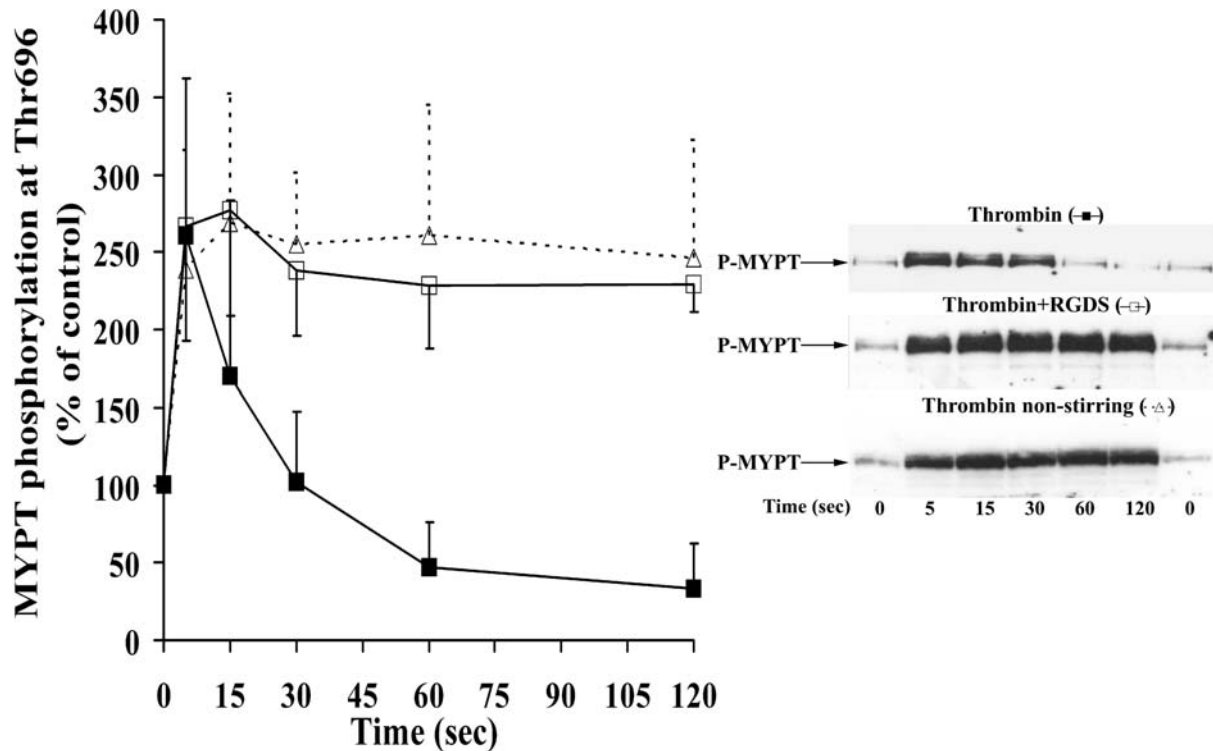
Figure 4.13 Thrombin induced a reversible or irreversible MYPT phosphorylation during aggregation or secretion, respectively. Platelet suspensions were not treated (stirring (-■-) and non-stirring (-Δ-) conditions) or treated with RGDS (0.5mM) (-□-) for 2 minutes before stimulation with thrombin (0.5 U/ml). (A) Thrombin-induced MYPT phosphorylation. Platelet lysates were immunoblotted with anti-phospho-Thr696-MYPT antibody. Left, graphic representation of results. Values are mean + SD or mean – SD of 3 independent experiments. Right, representative immunoblot of MYPT phosphorylation.

4.3.3. LIMK-1 phosphorylation and activation

4.3.3.1. LIMK-1 phosphorylation measured by immunoblotting

During thrombin-induced platelet aggregation, LIMK-1 phosphorylation was rapid and irreversible and reached a maximum after 15 seconds of stimulation. The increase of LIMK-1 phosphorylation was higher during aggregation (13-fold) than during shape change (5-fold) induced by thrombin (compare Figure 4.14 and Figure 4.8). To examine, whether outside-in signaling through integrin $\alpha_{IIb}\beta_3$ could affect LIMK-1 phosphorylation, LIMK-1 activation was measured in the presence of RGDS or by the absence of platelet stirring. LIMK-1 phosphorylation during aggregation was independent of integrin $\alpha_{IIb}\beta_3$ engagement, since the pattern of LIMK-1 phosphorylation was unchanged in the presence of RGDS or by the absence of

platelet stirring. The phosphorylation of LIMK-1 in thrombin-stimulated platelets was Rho-kinase dependent, since it was completely inhibited by Y-27632 and H-1152 (Figure 4.15A and data not shown).
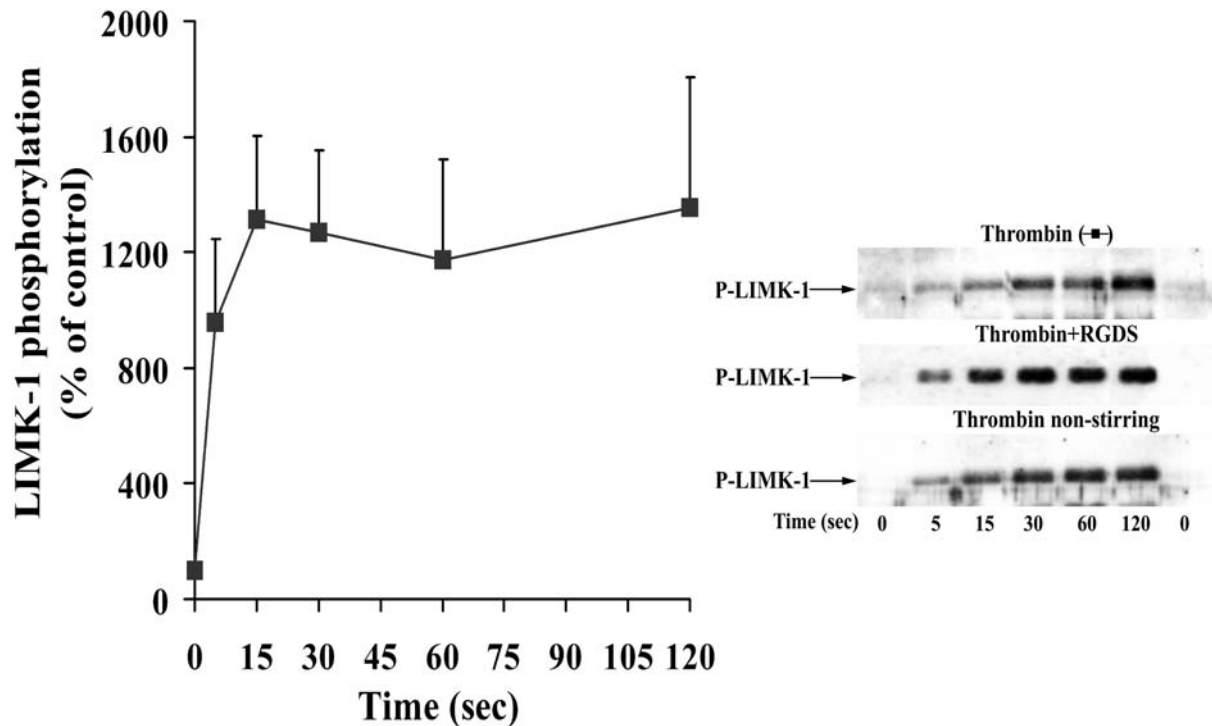
Figure 4.14 LIMK-1 phosphorylation during thrombin (0.5U/ml) induced platelet secretion/aggregation. Platelet lysates were immunoblotted with anti-phospho-LIMK-1/LIMK-2 (Thr508/505) antibody. Left, graphic representation of LIMK-phosphorylation during aggregation. Right, representative immunoblots for LIMK-1 phosphorylation in platelets non-treated (stirring and non-stirring conditions) and treated with RGDS.

4.3.3.2. LIMK-1 activation

In cell lines, it has been shown that LIMK-1 can be activated by upstream kinases like PAK or Rho-kinase after phosphorylating LIMK-1 at Thr508 in its kinase domain (Edwards et al. 1999; Ohashi et al. 2000). To confirm that LIMK-1 phosphorylation reflects its activation, LIMK-1 from platelets was immunoprecipitated, and in parallel analyzed for its phosphorylation and kinase activity. Platelets were stimulated and lysed in the presence of RGDS to avoid platelet aggregation and thereby reducing the possibility of insufficient lysis and trapping of proteins in these platelet aggregates. Immunoprecipitates of LIMK-1 were immunoblotted with anti-phospho-LIMK antibody to observe the LIMK-1 phosphorylation. LIMK-1 phosphorylation was increased in platelets stimulated with thrombin (0.5 U/ml) for 2 minutes. Y-27632 completely inhibited LIMK-1 phosphorylation in unstimulated platelets and did not show any increase of LIMK-1 phosphorylation after stimulation with thrombin (Figure 4.15B). Immunoblotting the total lysates of the same samples also showed inhibition of MYPT phosphorylation (Rho-kinase activation) and LIMK-1 phosphorylation by Y-27632 (Figure 4.15A).
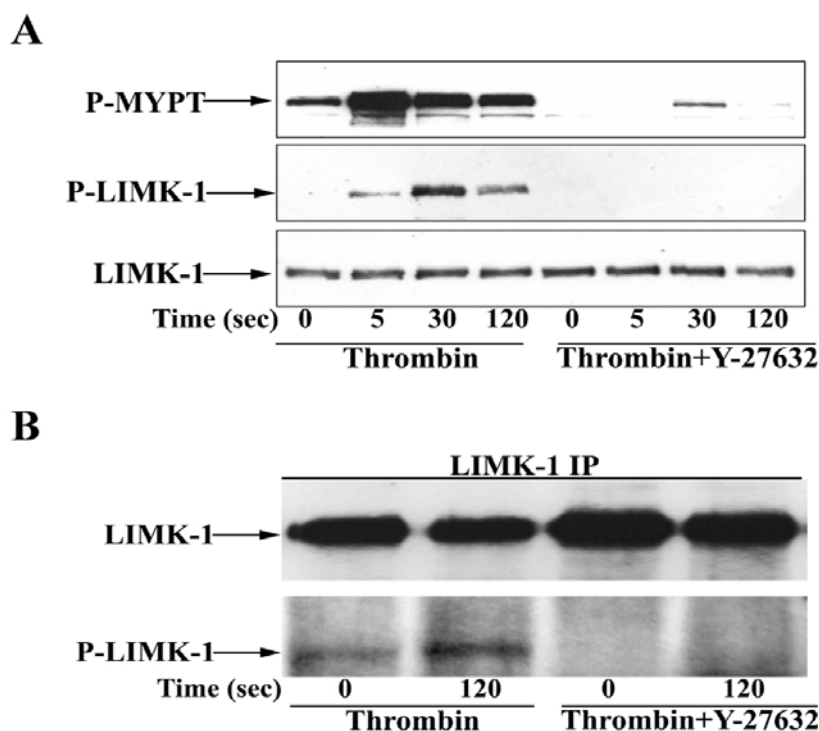
Figure 4.15 Inhibition of MYPT and LIMK-1 phosphorylation during thrombin-stimulated platelet secretion/aggregation. A) Platelet samples stimulated by thrombin (0.5 U/ml) in the absence or presence of Y-27632 (20 μM) were immunoblotted with anti-phospho-MYPT, anti-phospho-LIMK-1/LIMK-2 (Thr508/505) and anti-LIMK-1 antibodies. **B)** Immunoprecipitates from platelets non-treated or treated with Y-27632 and stimulated with thrombin for 2 minutes were immunoblotted with ant-LIMK-1 and anti-phospho-LIMKs antibodies.

The LIMK-1 immunoprecipitates were also analyzed for their kinase activity using His-tagged cofilin as substrate. LIMK-1 immunoprecipitates from thrombin-stimulated platelets showed an increase in cofilin phosphorylation (after 2 minutes) confirming that increase in LIMK-1 phosphorylation reflects its increased kinase activity.   In Y-27632-treated platelets LIMK-1 activity stimulated by thrombin was drastically reduced (Figure 4.16).   These results show that LIMK-1 phosphorylation correlates with its activity, which is regulated in a Rho-kinase dependent manner.
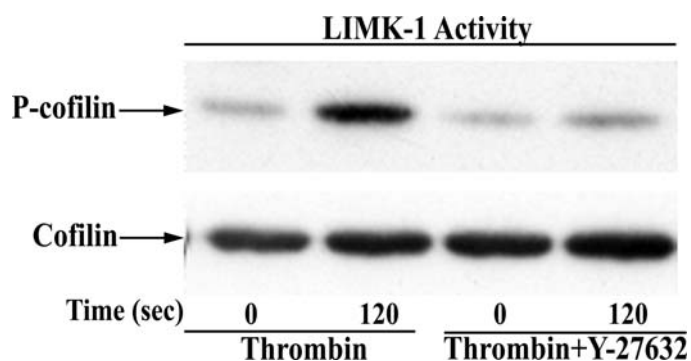
Figure 4.16 Effect of the Rho-kinase inhibitor Y-27632 on LIMK-1 activity. LIMK-1 immunoprecipitates were subjected for LIMK-1 kinase reaction using His-tagged cofilin as substrate. The Rho-kinase inhibitor Y-27632 inhibited the LIMK-1 activity.

4.3.4. Reversible cofilin dephosphorylation during thrombin-induced secretion and aggregation

Despite Rho-kinase and LIMK-1 activation, cofilin phosphorylation rapidly decreased after thrombin-stimulation of platelets. The decrease of cofilin phosphorylation was about 60% 30 seconds after thrombin addition, and was followed by slow rephosphorylation (Figure 4.17). Blocking of the integrin $\alpha_{IIb}\beta_3$ by RGDS or in the absence of stirring during stimulation with thrombin did not change the kinetics of cofilin de- and rephosphorylation (Figure 4.17), indicating that they are independent of integrin $\alpha_{IIb}\beta_3$ engagement. Cofilin phosphorylation in thrombin-stimulated platelets might be regulated either by activation and then inactivation of a cofilin phosphatase or by activation of a cofilin phosphatase and subsequently LIMK-1, which mediates cofilin rephosphorylation.
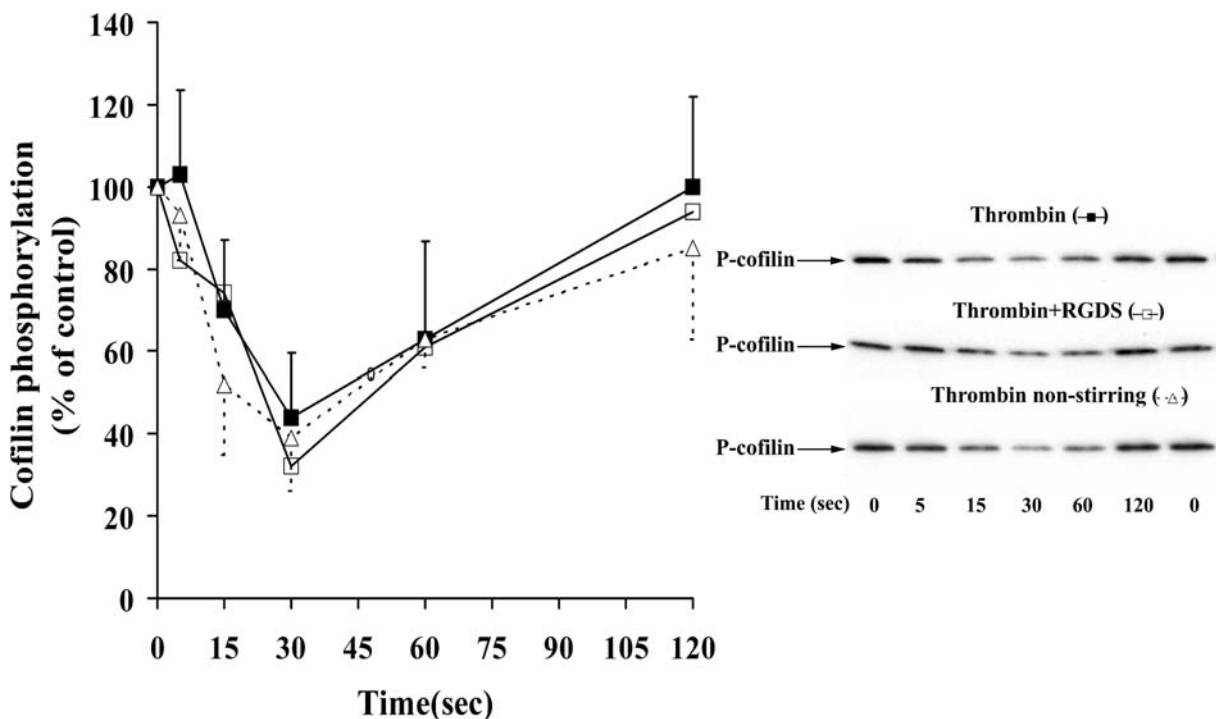
Figure 4.17 Thrombin-induced reversible dephosphorylation of cofilin is independent of integrin $\alpha_{IIb}\beta_3$ engagement. Platelets samples were not treated (stirring (-■-) and non-stirring (-Δ-) conditions) or treated with RGDS (0.5 mM) (-□-) for 2 minutes before stimulation with thrombin (0.5 U/ml). Lysates of thrombin-stimulated platelets were immunoblotted with anti-phospho-cofilin and anti-cofilin antibodies. Left, graphical representation of results. Values are mean + SD or mean – SD of three independent experiments. Right, representative immunoblots for cofilin phosphorylation.

4.3.5. Inhibition of cofilin rephosphorylation by Rho-kinase inhibitors

The result of the rapid and sustained activation of Rho-kinase and LIMK1, but rapid decrease of cofilin phosphorylation raised the question concerning the role of these kinases in regulating cofilin phosphorylation. Preincubation of platelets with Y-27632 and H-1152, which inhibited Rho-kinase and LIMK-1 activation did not inhibit the initial cofilin dephosphorylation suggesting

that dephosphorylation of cofilin is not regulated by Rho-kinase and LIMK-1. These results indicate that cofilin phosphatase is activated independently of this pathway in thrombin-stimulated platelets. However, thrombin-induced cofilin rephosphorylation was completely inhibited by Y-27632 (Figure 4.18) and H-1152 (data not shown), which inhibit LIMK-1 phosphorylation and LIMK-1 activity (Figure 4.16). Hence, these results strongly suggest that in thrombin-stimulated platelets the Rho-kinase/LIMK-1 pathway mediates cofilin rephosphorylation.
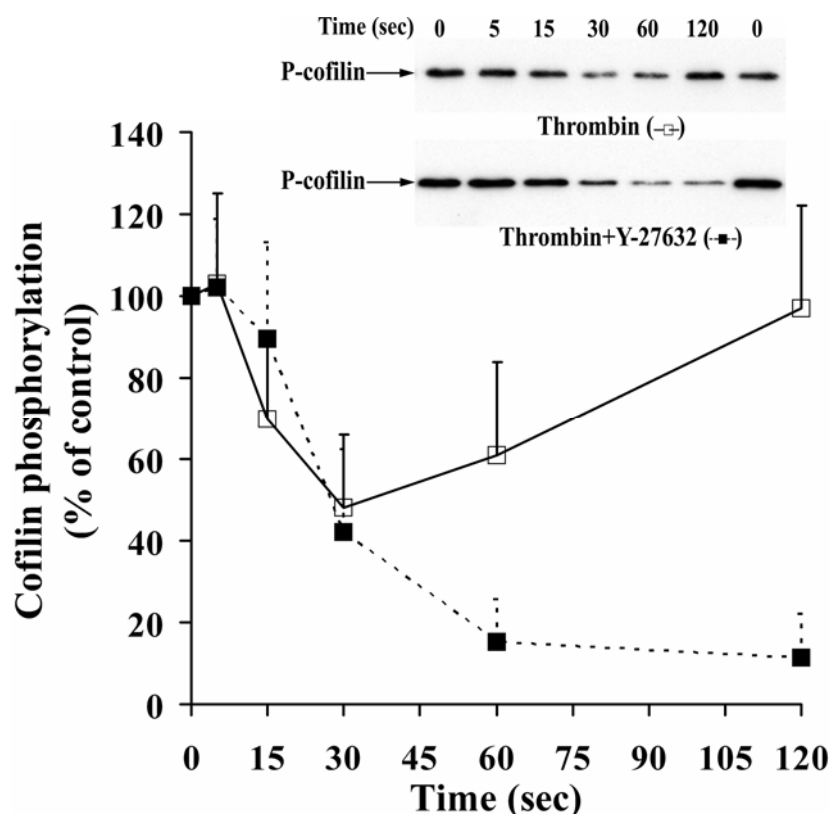
Figure 4.18 Inhibition of cofilin rephosphorylation by the Rho-kinase inhibitor Y-27632 during stimulation of platelets with thrombin (0.5U/ml). Lysates of thrombin-stimulated platelets in the absence (-□-) or presence of Y-27632 (-■-) were immunoblotted with anti-P-cofilin and anti-cofilin antibodies and analyzed by densitometry. Graphic representation of the results with values presented in mean + SD of three independent experiments. Inset, representative immunoblots against anti-P-cofilin antibody.

4.3.6. F-actin increase in thrombin-stimulated platelet secretion/aggregation

Platelet aggregation and secretion induced by thrombin (0.5 U/ml) is associated with a different actin reorganization pattern as compared to shape change induced by low concentration of thrombin (0.075 U/ml). The rapid activation of cofilin during stimulation of platelets with a high concentration of thrombin (0.5 U/ml) could modulate F-actin content differently leading to secretion and aggregation. The changes in F-actin content of unstimulated and stimulated platelets were analyzed in the presence of RGDS, which does not affect the kinetics of cofilin de- and rephosphorylation (Figure 4.17), to avoid possible artifacts described in section 4.3.3.2. The

increase in F-actin was higher during platelet secretion as compared to shape change: F-actin increased from 34±1% in resting platelets to 56±5% of total 30sec after addition of thrombin (Figure 4.19). These results suggest that the rapid cofilin dephosphorylation (maximum at 30sec) generating more active cofilin increases F-actin during platelet secretion. However, the F-actin increase was irreversible and was not reduced during cofilin rephosphorylation 2 minutes after thrombin-stimulation. Pretreatment of platelets with Y-27632 increased the total F-actin in resting platelets, reduced the increase after thrombin-activation, and made the F-actin increase reversible (Figure 4.19). Inhibition of cofilin rephosphorylation by Y-27632 might destabilize F-actin at 60 and 120 minutes of thrombin-stimulation. Thus, these results indicate that a Rho-kinase dependent pathway is involved in F-actin increase in thrombin-stimulated platelets.
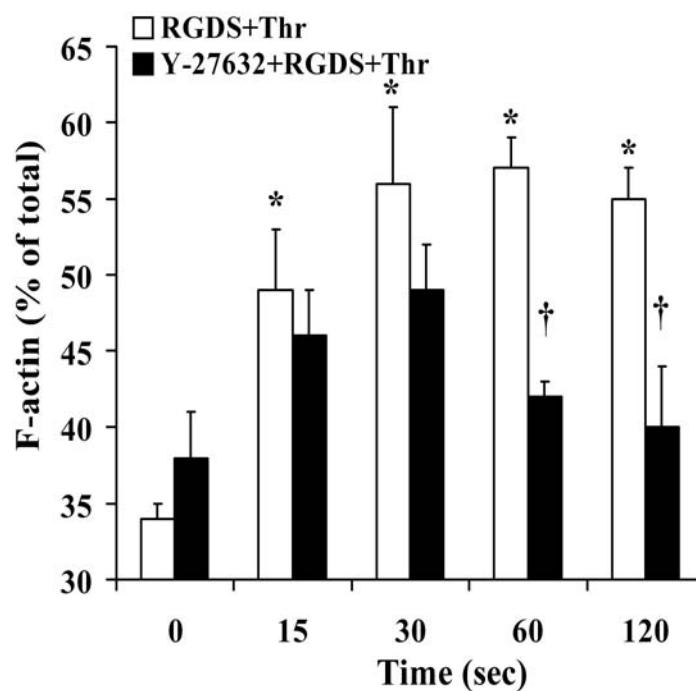
Figure 4.19 Inhibition of F-actin increase by Y-27632 during thrombin-induced platelet secretion. Platelets treated with H_2O (□) or Y-27632 (■) were stimulated with thrombin (0.5 U/ml) in the presence of the integrin $\alpha_{IIb}\beta_3$ blocker RGDS (0.5 mM) and lysed with 1% TritonX-100 for isolation of F-actin. F-actin and cofilin associated with F-actin (% of total) were measured. The result is presented in bar diagram. Values are the mean + S.D for four independent experiments. Asterisks (*) denote statistical significance $P<0.05$ with respect to non-treated samples at time 0 seconds, and (†) denotes significance between control (□) and Y-27632 (■) treated platelets.

4.3.7. <u>Cofilin association with F-actin</u>

Since cofilin was rapidly dephosphorylated during platelet secretion (in the absence or presence of aggregation), we wondered, whether the association of cofilin with F-actin was increased. Cofilin association with the total F-actin pool increased from 8±2% in resting platelets to 29±5% (Figure 4.20A). This increase was a net increase because the ratio of F-actin-associated cofilin relative to F-actin increased 3-fold from 0.23 in resting platelets to 0.64 30 seconds after addition

of thrombin (Figure 4.20B). These results suggest that the rapid cofilin dephosphorylation (maximum at 30 seconds) generating more active cofilin enhances its association with F-actin. Since at the same time, platelet F-actin content also increased (about 1.7 fold) after addition of thrombin it appears that cofilin association with F-actin might regulate F-actin increase during platelet secretion (Figure 4.19 and Figure 4.20). Cofilin remained associated with F-actin 60 and 120 seconds after thrombin stimulation, indicating that LIMK-1-mediated cofilin rephosphorylation did not cause cofilin dissociation from F-actin. Inhibition of Rho-kinase/LIMK-1 lead to a reduced F-actin increase at 30 seconds, did not reduce the rapid cofilin dephosphorylation and cofilin association with F-actin during the first 30 seconds, and reversed the increase of F-actin and the cofilin association with F-actin. These results indicate that Rho-kinase regulates the F-actin increase during platelet secretion through a mechanism other than cofilin phosphorylation and association with F-actin.
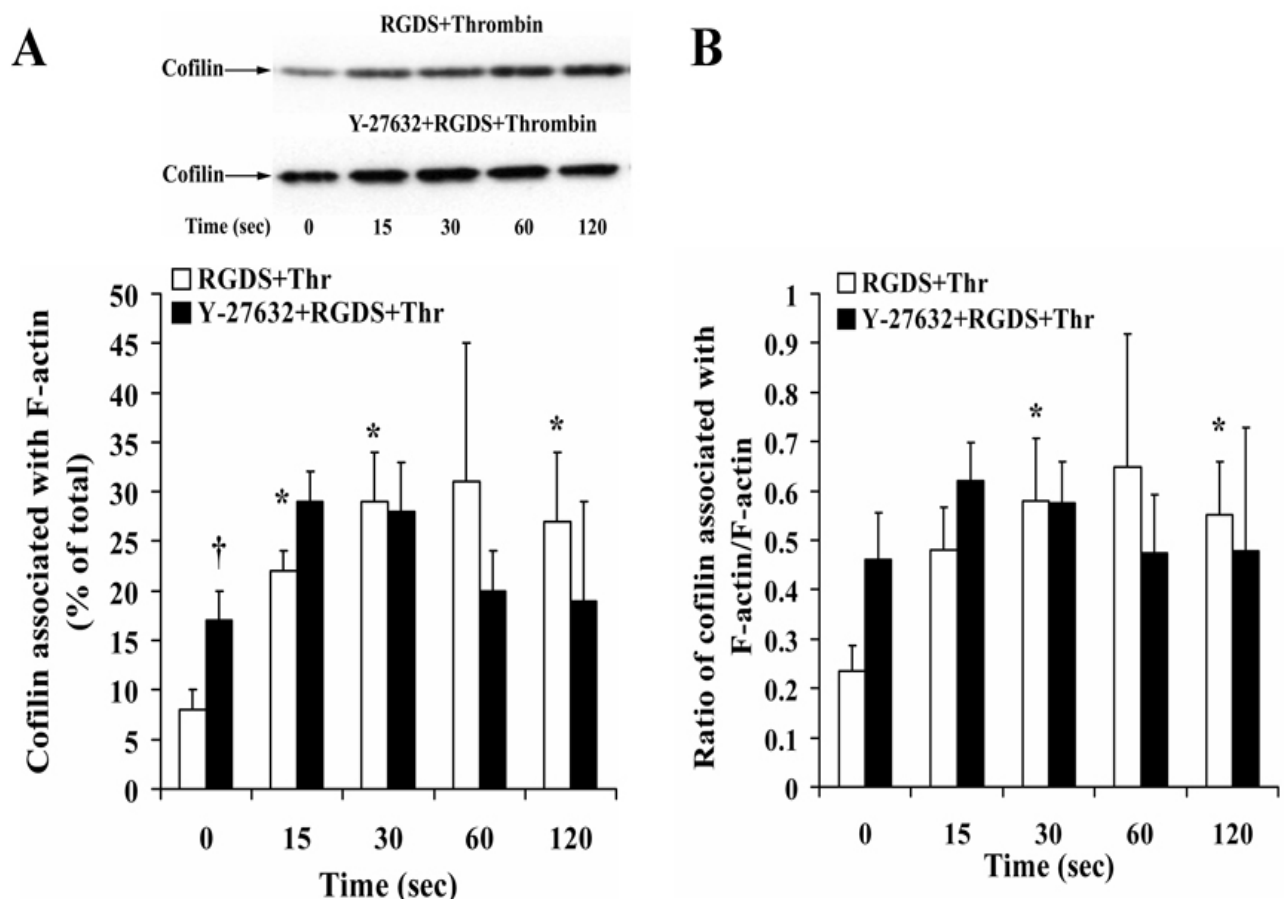
Figure 4.20 Association of cofilin with F-actin during thrombin-induced secretion. The total F-actin isolated from platelets pretreated with RGDS in the absence or presence of Y-27632 and stimulated with thrombin (0.5 U/ml) were immunoblotted with the anti-cofilin antibody. A) Top, representative immunoblots. Bottom, bar diagram showing association of cofilin with F-actin. B) Bar diagram for the ratio of F-actin-associated cofilin to F-actin. Values are mean + SD of 4 independent experiments. Asterisks (*) denote statistical significance $P<0.05$ with respect to nonstimulated samples at 0 seconds, and (†) denotes significance between control (□) and Y-27632 (■) treated platelets.

4.4. Platelet shape change induced by LPA

4.4.1. LPA-stimulated platelet shape change and actin polymerization are Rho-kinase dependent

LPA at low concentrations (10–100 nM) induces platelet shape change without any increase in the cytosolic Ca^{2+} concentration (Retzer and Essler 2000). Washed platelets were stimulated with low concentrations of LPA (0.1 µM) to induce platelet shape change selectively without inducing platelet secretion or aggregation. LPA induced a rapid and reversible platelet shape change with a maximum at 15 seconds after stimulation (Figure 4.21). As previously observed, we also found that LPA-induced shape change is mediated by through the Rho/Rho-kinase pathway (Retzer and Essler 2000), since Y-27632 (20 µM) completely inhibited LPA-induced shape change. Latrunculin-A (10 µM), a small molecule that binds to the monomeric actin thereby facilitating actin cytoskeleton disassembly and inhibiting actin polymerization (Spector et al. 1999), completely blocked the LPA-induced shape change indicating that actin polymerization is required for shape change.
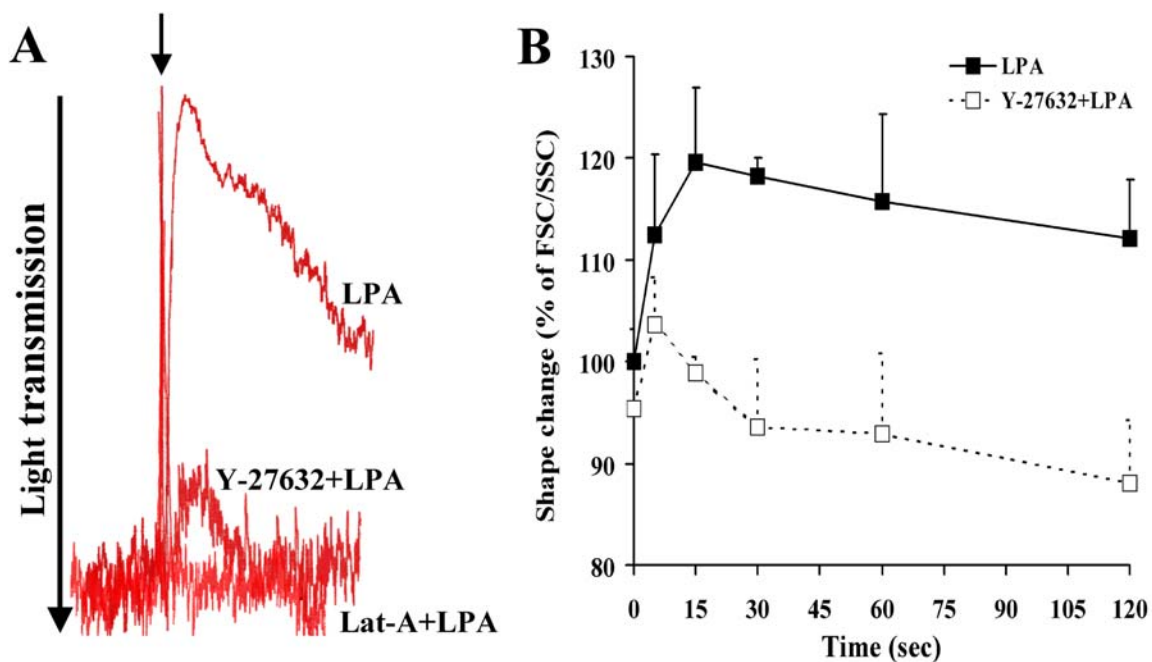
Figure 4.21 LPA-induced shape change is Rho-kinase dependent and requires actin polymerization. A) Shape change studied by the decrease in light transmission. Platelets pre-incubated with H20, Y-27632, and latrunculin-A (Lat-A), were stimulated with LPA (0.1 µM). **B)** Shape change studied by the changes in FSC/SSC ratio using flow cytometry. The FSC/SSC ratio of unstimulated platelets not treated with Y-27632 was set to 100%. Values are mean + SD of three independent experiments.

Shape change was also measured by estimating the change in light scattering properties of platelets using flow cytometry. During platelet shape change, the mean forward scattering (FSC) of light increases while the mean side scattering (SSC) of light decreases and hence, the ratio of FSC/SSC increases proportionally to the platelet shape change (Ruf and Patscheke 1995). LPA-

induced platelet shape change measured by flow cytometry correlated well with shape change measured by light transmission of the same samples (Figure 4.21 A and B). Preincubation of platelets with Y-27632 (Figure 4.21B) as well as latrunculin-A (data not shown) inhibited the LPA-induced increase of FSC/SSC ratio confirming the study made by the turbidimetric method.

We investigate, whether F-actin increased during LPA-induced shape change. During shape change, LPA induced a reversible F-actin increase with a maximum at 15 seconds after stimulation. Preincubation of platelets with Y-27632 inhibited the F-actin increase induced by LPA (Figure 4.22). This suggests that the activation of Rho-kinase might be involved in regulation of actin polymerization underlying platelet shape change. Interestingly, Y-27632 increased the F-actin content significantly in unstimulated platelets.
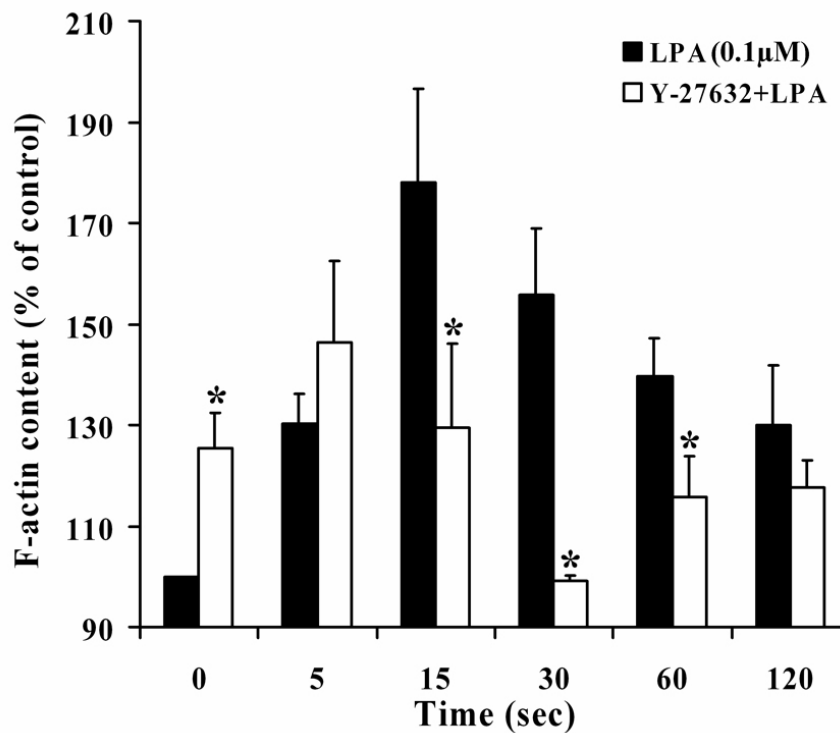
Figure 4.22 The Rho-kinase inhibitor Y-27632 inhibited the actin polymerization in LPA-stimulated platelets. F-actin content was quantified by Alexa Fluor 546 phalloidin binding. Values are mean + S.D of 4 independent experiments. Asterisks (*) denote statistical significance $P<0.05$ between untreated (■) and Y-27632-treated (□) platelets.

4.4.2. <u>Activation of Rho-kinase during LPA-induced shape change</u>

LPA induced a rapid (maximum after 5 seconds) and reversible increase of MYPT phosphorylation at Thr696 (4-5 fold) and Thr853 (4-5 fold) during shape change (Figure 4.23, and data not shown). The rapid and reversible MYPT phosphorylation was Rho-kinase dependent. The specific Rho-kinase inhibitors Y-27632 and H-1152 (20 µM) completely abolished the LPA-induced increase of MYPT phosphorylation (Figure 4.23, inset and data not

shown). The rapid activation of Rho-kinase (5 seconds) preceded the maximum increase of F-actin content (15 seconds) during shape change. Together, these results indicate that LPA-induced Rho-kinase activation is upstream of and mediates the F-actin increase underlying shape change.
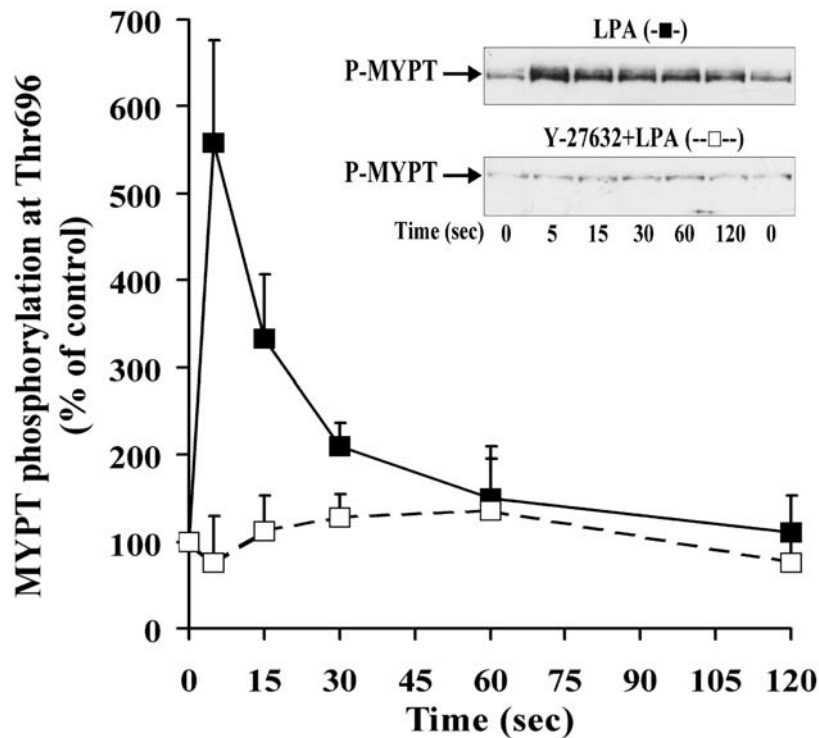
Figure 4.23 MYPT phosphorylation during LPA induced platelet shape change. Platelet lysates were immunoblotted with anti-phospho-MYPT antibody. Graphic representation of the result of MYPT phosphorylation in the absence (-■-) and presence (-□-) of Y-27632 evaluated by densitometry. Values are presented in mean + S.D, n=3. Inset, representative western blot of MYPT phosphorylation in the absence and presence of Y-27632.

4.4.3. Regulation of LIMK-1 and cofilin phosphorylation during shape change

To analyze, how Rho-kinase activation regulates the increase of F-actin in LPA-stimulated platelets, the activation of LIMK-1 known to phosphorylate and inactivate cofilin was analyzed. During LPA-induced shape change, a rapid and reversible LIMK-1 phosphorylation was observed. LIMK-1 phosphorylation reached a maximum (5-fold) after 5 seconds and then decreased to the resting level after 2 minutes of platelet stimulation (Figure 4.24A). The kinetics of MYPT phosphorylation and LIMK-1 phosphorylation induced by LPA were similar, rapid and reversible. This observation suggests that Rho-kinase mediates phosphorylation of LIMK-1 during LPA-induced shape change. LIMK-1 phosphorylation was completely abolished in the presence of Rho-kinase inhibitors Y-27632 and H-1152 (Figure 4.24B and data not shown), indicating that Rho-kinase is upstream of LIMK-1 and is responsible for LIMK-1 phosphorylation during shape change.

A

B
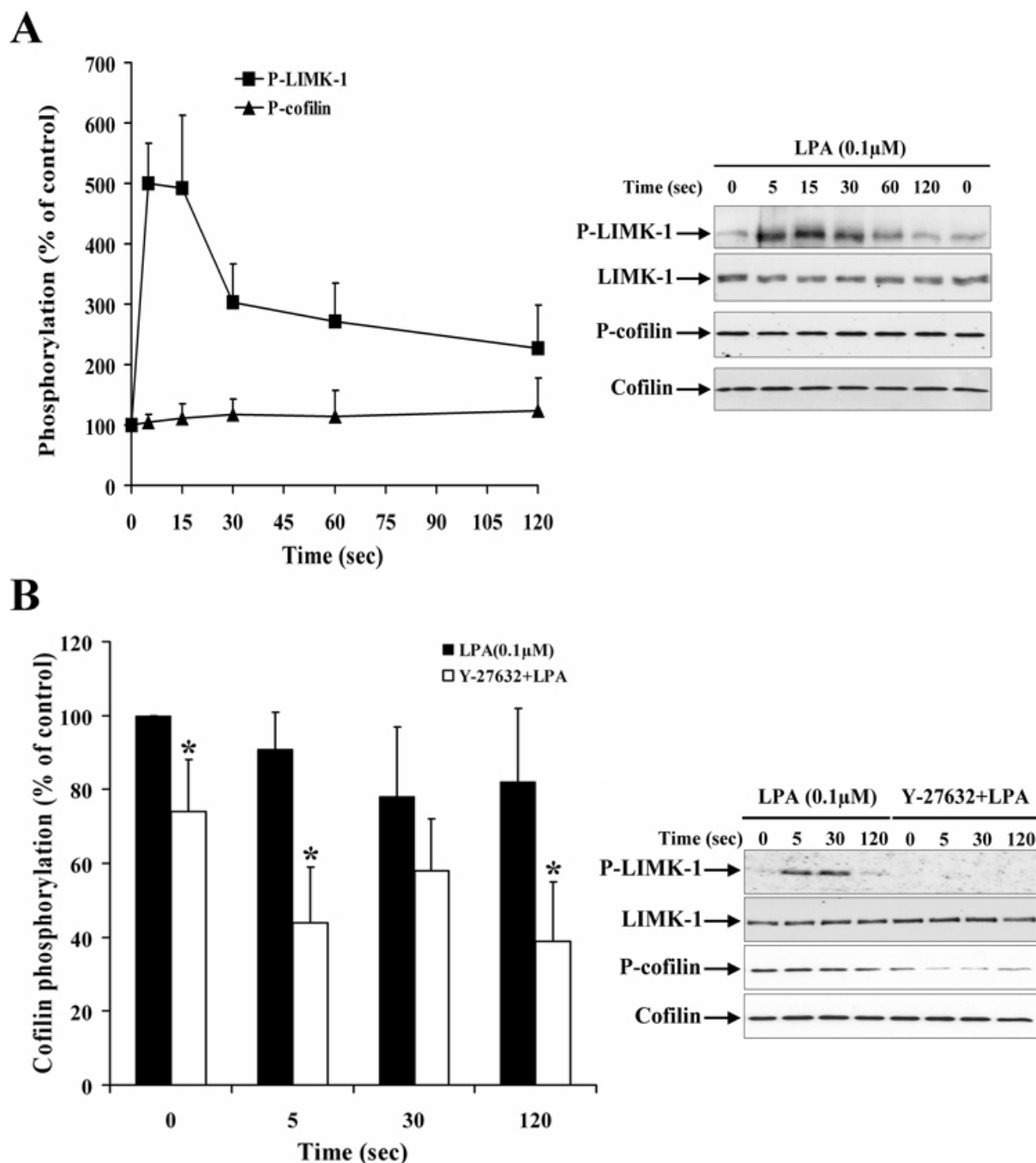
Figure 4.24 Rho-kinase dependent LIMK-1 phosphorylation but no subsequent cofilin phosphorylation during LPA-induced platelet shape change. A) LIMK-1 and cofilin phosphorylation during platelet shape change. Left, graphical representation of the result for LIMK-1 (-■-) and cofilin (-▲-) phosphorylation. Values are mean+SD for LIMK-1; n=3 and cofilin; n=3. Right, Representative immunoblots for LIMK-1 and cofilin in their unphosphorylated and phosphorylated states. **B)** Effect of Y-27632 on LIMK-1 and cofilin phosphorylation. Left, Cofilin dephosphorylation in the presence of Y-27632 in resting and LPA-stimulated platelet shape change Right, Representative immunoblots Asterisks (*) denote statistical significance $P<0.05$ between untreated (■) and Y-27632-treated (□) platelets..

During shape change, in spite of LIMK-1 activation, we could not observe a concomitant increase in cofilin phosphorylation (Figure 4.24A). Preincubation of platelets with Y-27632 decreased cofilin phosphorylation in resting platelets. Interestingly, a further significant decrease of cofilin phosphorylation ($P<0.05$) was observed in Y-27632 treated platelets 5 and 120 seconds after LPA stimulation (Figure 4.24B). These results suggested that cofilin dephosphorylation by a cofilin

phosphatase occurs during shape change which is masked by the concomitant stimulation of cofilin phosphorylation due to Rho-kinase/LIMK-1 activation. Thus, increased phospho-cycling of cofilin during LPA-induced shape change might occur reflecting an accelerated shuttling of this protein between its inactive and active forms.

4.4.4. LPA-induced PAK phosphorylation does not regulate LIMK-1 activation during shape change.

LIMK-1 could also be phosphorylated and activated by Rac-activated PAK (Edwards et al. 1999). To examine whether PAK is activated during LPA-induced shape change, the specific phospho-PAK1/2 (Thr423/Thr402) antibody was used. A significant increase of PAK phosphorylation was observed only at 30 seconds after platelet stimulation with LPA (0.1 μM). The kinetic of PAK phosphorylation was much slower (Figure 4.25) than LIMK-1 phosphorylation (Figure 4.24A) indicating that PAK1/2 is unlikely to be involved in phosphorylating LIMK-1 during LPA-induced shape change. In the presence of Y-27632, LPA-stimulated PAK phosphorylation was, albeit but not significantly, reduced (Figure 4.25) indicating that Rho-kinase might be involved in PAK1/2 phosphorylation.
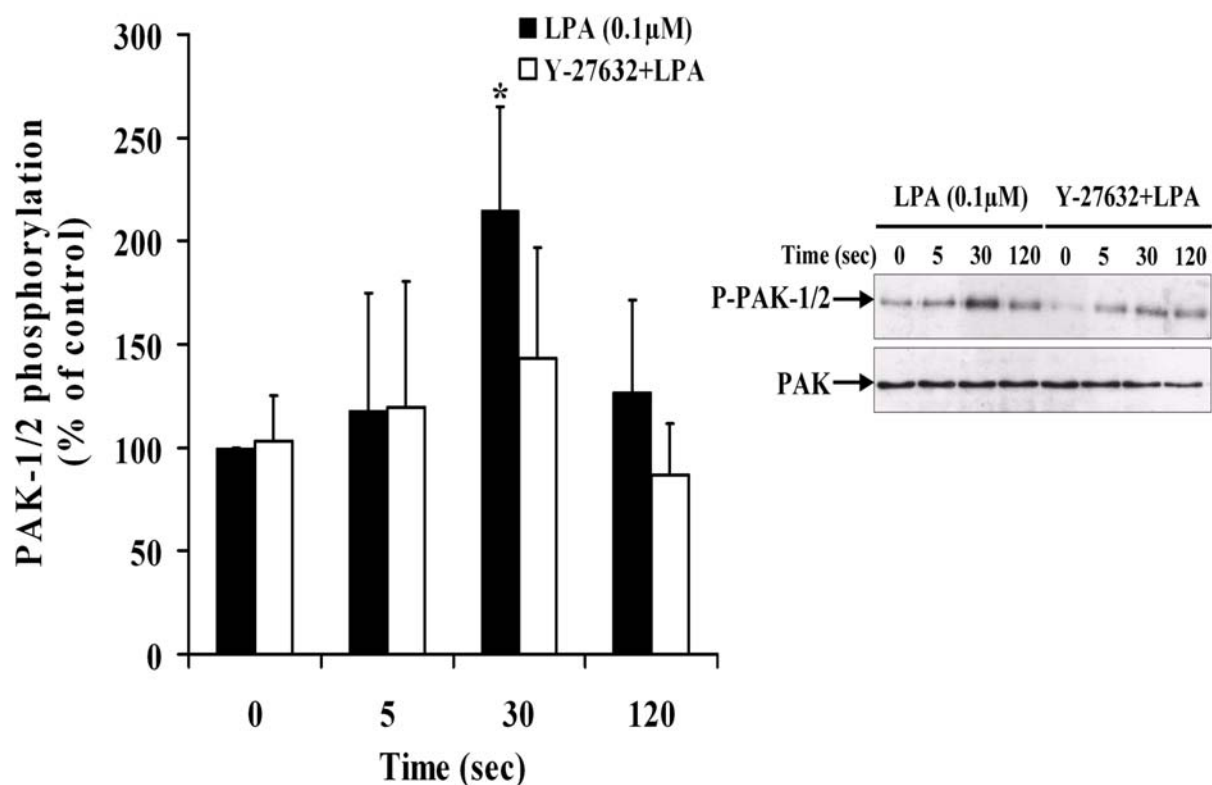
Figure 4.25 PAK-1/2 phosphorylation during LPA-induced shape change. Left, bar diagram showing PAK phosphorylation during LPA-stimulation of platelets untreated with (-■-) and treated with Y-27632 (-□-). Asterisk denotes statistical significance *P*<0.05 with respect to non-treated control (mean + S.D, n=4). Right, representative immunoblots showing non-significant reduction of PAK phosphorylation by the Rho-kinase inhibitor Y-27632 (20 μM) during shape change induced by LPA (0.1 μM).

4.4.5. LPA induced a rapid association of cofilin with actin cytoskeleton

It is known that active, unphosphorylated cofilin binds to the actin cytoskeleton, while the phosphorylated cofilin does not (Lee et al. 2000). Because cofilin net phosphorylation during LPA-induced shape was not increased, we explored the possibility that cofilin might associate with the F-actin cytoskeleton during shape change. The actin cytoskeleton of unstimulated and LPA-stimulated platelets was isolated and immunoblotted with anti-cofilin antibody. In resting platelets 10±4 % (mean±SD, n=4) of total cofilin was associated with the actin cytoskeleton. LPA stimulation of platelets induced a rapid and reversible increase of cofilin in the actin cytoskeleton (Figure 4.26). Cofilin association was maximal 2-fold already at 5 seconds after stimulation, and then decreased after 1 min below the level of resting platelets (50% of control). In contrast, the increase of F-actin in the platelet cytoskeleton was maximal at 15 seconds after stimulation (136 ± 12%) and showed a slow decline thereafter (117 ± 6%, after 2 minutes). No association of phospho-cofilin, LIMK-1 and phospho-LIMK-1 with the actin cytoskeleton could be detected in resting or LPA-stimulated platelets (data not shown).
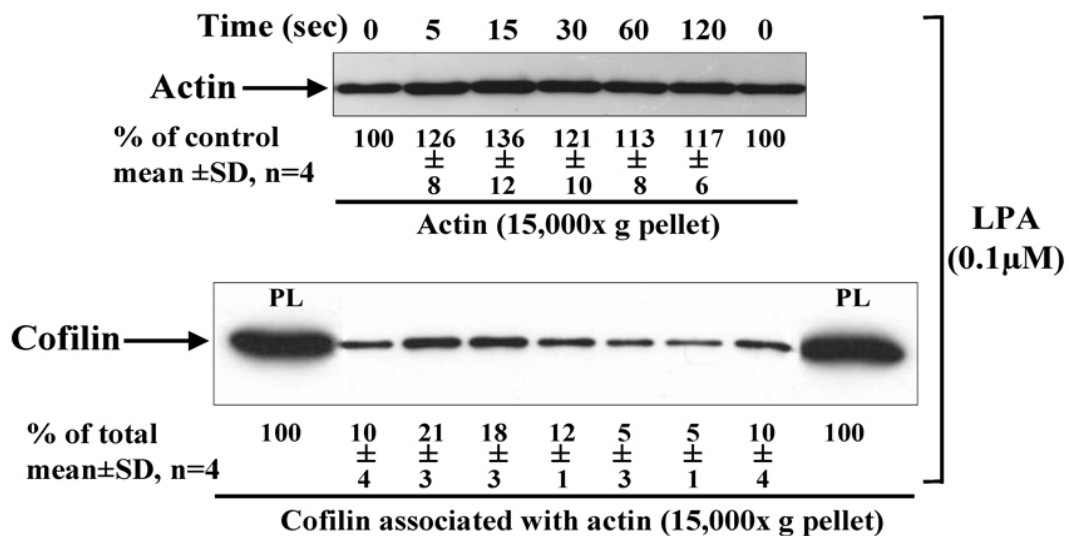
Figure 4.26 Rapid association of cofilin with the actin cytoskeleton during platelet shape change. Samples of actin cytoskeleton isolated from platelets stimulated with LPA (0.1 μM) for various times were immunoblotted with anti-actin and anti-cofilin antibodies. Amount of protein association with actin cytoskeleton was determined densitometrically. Values are mean ± SD (n = 4) with respect to control. PL, whole platelet lysate.

4.5. LPA-mediated platelet secretion and aggregation

4.5.1. Platelet secretion and aggregation studied in Lumi-aggregometer

LPA at higher concentrations and in the presence of fibrinogen induces aggregation of washed platelets. The LPA-mediated platelet aggregation is the result of synergism between LPA and secreted ADP during platelet activation (Haseruck et al. 2004). Unlike platelet suspensions

prepared for analyzing LPA-stimulated platelet shape change, washed platelets were prepared to observe LPA-induced aggregation using a method described by Cazenave et al (Cazenave JP 1993). This method was modified such as omission of heparin from the first wash buffer and the use of 0.1% albumin instead of 0.35% concentration in the final suspension (see method). LPA (10 μM) alone induced platelet shape change, but no secretion of ATP and aggregation (Figure 4.27). However, when platelets were stimulated with LPA in the presence of fibrinogen (0.5 μg/ml) they secreted ATP and underwent aggregation (Figure 4.27). LPA induced platelet aggregation was reversible or irreversible depending on the extent of ATP secreted from the stimulated platelets (data not shown). Preincubation of platelets with Y-27632 completely blocked the LPA-induced dense granule secretion and inhibited platelet aggregation (Figure 4.27). These results indicate that the inhibition of LPA-mediated platelet aggregation is largely due to inhibition of dense granule secretion from stimulated platelets, which is mediated by Rho-kinase activation. Based on these results we concluded that Rho-kinase mediated signaling pathways might be upstream of secretion and subsequently, aggregation.
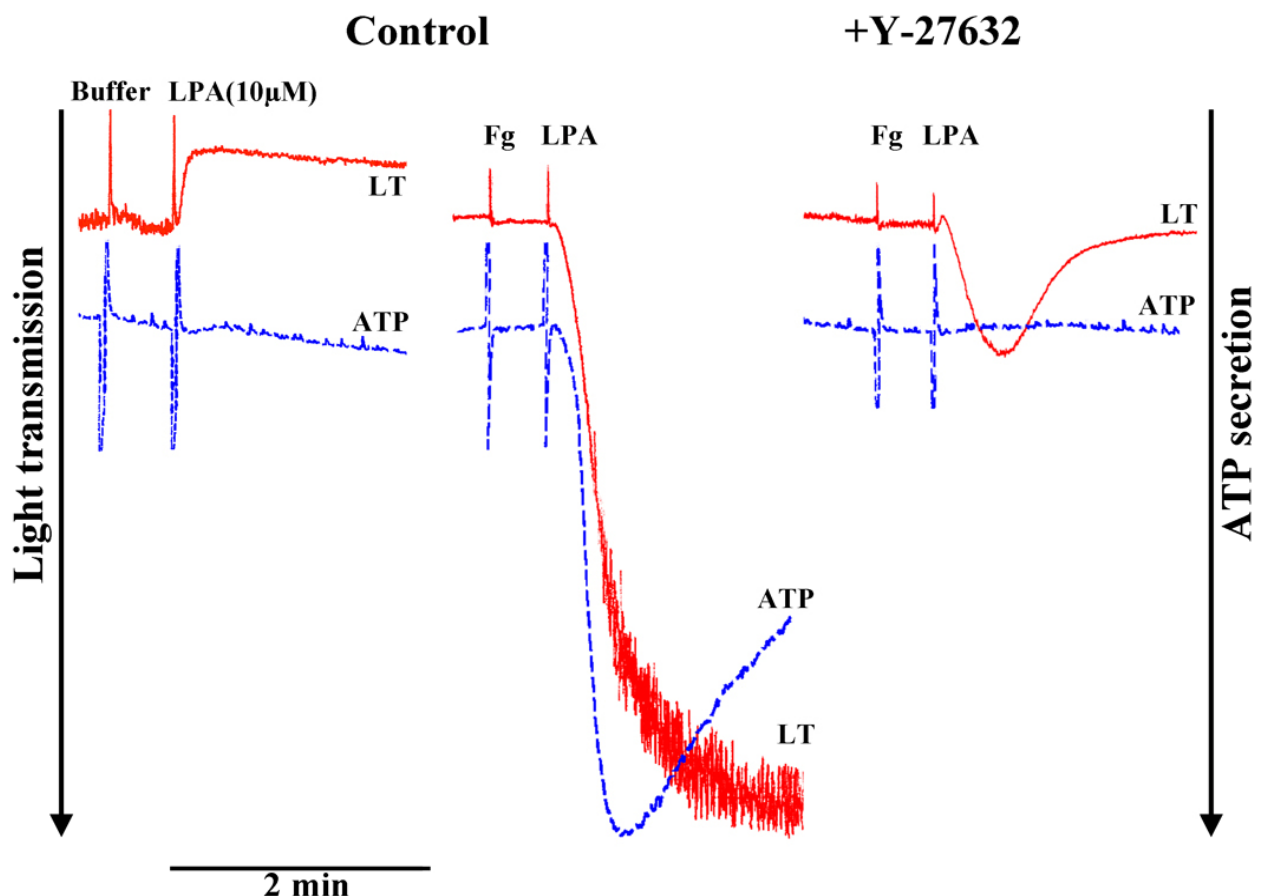
Figure 4.27 Inhibition of dense granule secretion and platelet aggregation by Y-27632. Platelets were stimulated with LPA (10 μM) in the absence and presence of fibrinogen (0.5 mg/ml) and the Rho-kinase inhibitor Y-27632 (20 μM). Representative tracings for change in light transmission (red) and ATP secretion (blue) by LPA.

4.5.2. <u>MYPT phosphorylation during LPA-stimulated platelet secretion and aggregation</u>

MYPT phosphorylation at Thr853 was measured to analyze Rho-kinase activation during LPA-stimulated platelet secretion and aggregation. LPA (10 µM) in the absence of fibrinogen induced a rapid and partly reversible MYPT phosphorylation (Figure 4.28). MYPT phosphorylation increased to a maximum of 3-fold after 5 seconds and then slowly decreased to 2 fold after 2 minutes of platelet stimulation. Platelets stimulated with LPA in the presence of fibrinogen showed similar kinetics for MYPT phosphorylation (data not shown). This result indicates that Rho-kinase activation is upstream and independent of dense granule secretion and integrin $\alpha_{IIb}\beta_3$ involvement. MYPT phosphorylation at Thr853 was Rho-kinase dependent since Y-27632 reduced the MYPT phosphorylation in non-activated platelets and further inhibited its increase during platelet secretion/aggregation induced by LPA (Figure 4.28).
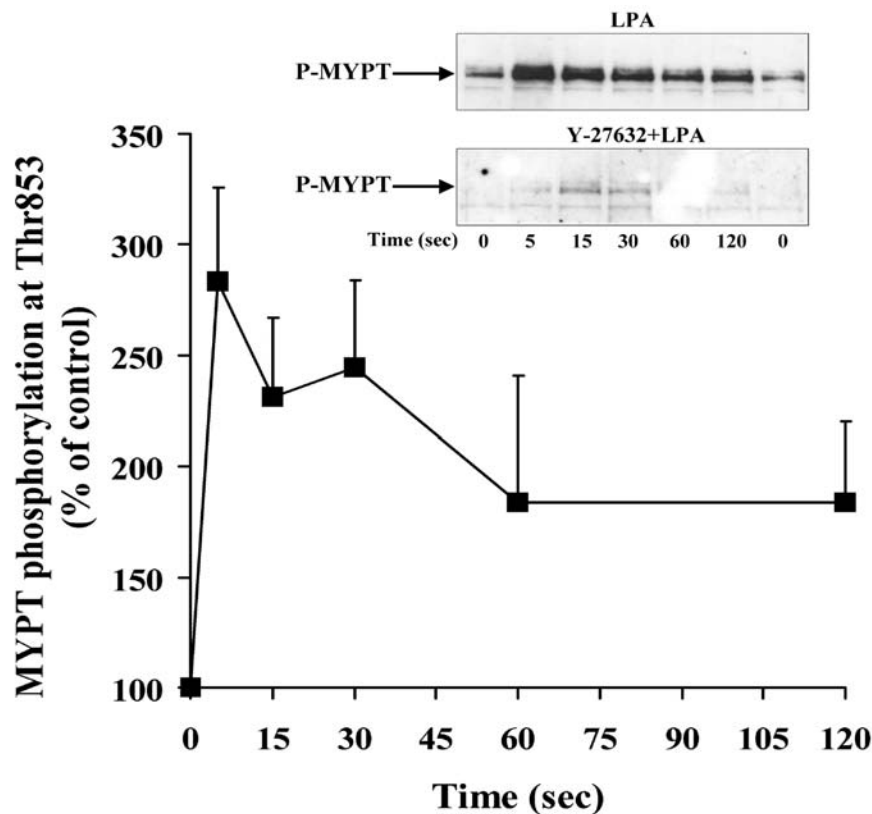
Figure 4.28 MYPT phosphorylation in LPA-stimulated secretion/aggregation. Platelets stimulated with LPA (10µM) were immunoblotted with anti-phospho-MYPT and analyzed using densitometry. Values are mean + SD of three independent experiments. Inset, representative immunoblots showing MYPT phosphorylation in LPA-stimulated platelets in the absence or presence of Y-27632.

4.5.3. <u>Regulation of LPA-induced cofilin de-and rephosphorylation</u>

Washed platelets used to study LPA-mediated platelet secretion/aggregation were resuspended in a buffer containing 0.1% BSA. BSA of molecular mass 68-kDa co-migrated electrophoretically with LIMK-1 (72-kDa) and masked the detection of LIMK-1 in platelets by immunoblot and immunoprecipitation. Therefore we could not measure LIMK-1 activation under these conditions of LPA (10 µM)-induced secretion/aggregation (data not shown).

We observed that after platelet stimulation with 10 µM LPA, cofilin was rapidly dephosphorylated with a maximum at 60 seconds and then slowly rephosphorylated to the level of resting platelets (Figure 4.29). This finding was similar to the one we observed for platelets stimulated with thrombin (0.5 U/ml). Cofilin de- and rephosphorylation showed similar kinetics in the absence and presence of fibrinogen indicating that the kinetics of cofilin phosphorylation is independent of integrin $\alpha_{IIb}\beta_3$ engagement as well as of dense granule secretion. Y-27632 inhibited the cofilin rephosphorylation completely indicating that the Rho-kinase/LIMK-1 pathway mediates cofilin rephosphorylation and might be involved in regulating LPA-stimulated secretion/aggregation.
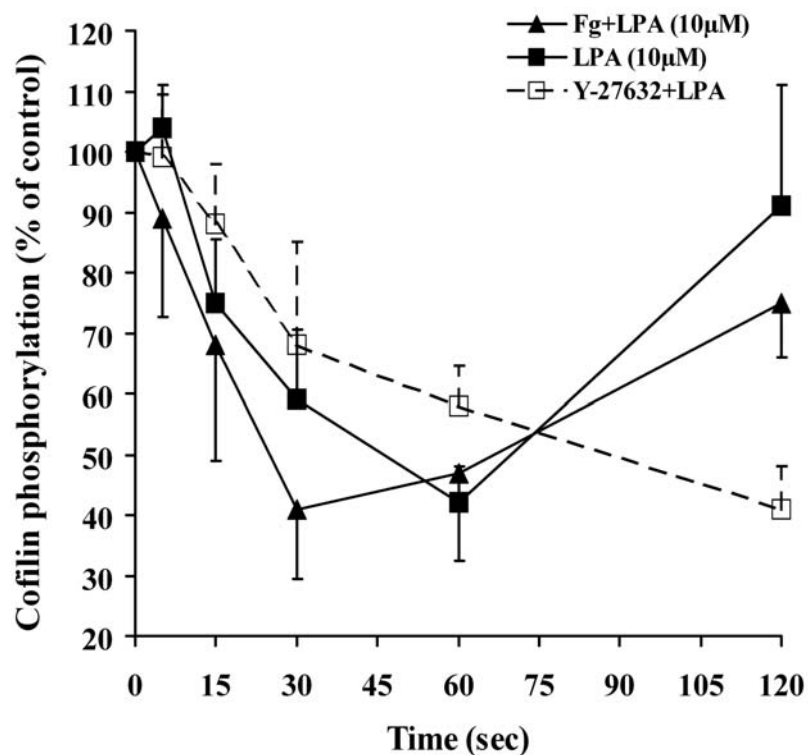
Figure 4.29 LPA (10 µM) induced cofilin de- and rephosphorylation in platelets is independent of secretion and aggregation. Cofilin rephosphorylation is inhibited by Y-27632. Graphic representation of the results of cofilin phosphorylation after platelet stimulation with LPA in the presence (-▲-) and absence (-■-) of fibrinogen, and inhibition of cofilin rephosphorylation in Y-27632-treated (-□-) platelets. Values are mean + S.D for three independent experiments.

4.6. Signaling for cofilin dephosphorylation

4.6.1. Effect of phosphatase inhibitors on cofilin dephosphorylation

To explore which type of phosphatase is responsible for cofilin dephosphorylation, we tested the broad-spectrum protein phosphatase inhibitor sodium orthovanadate Na_3VO_4, and the PP1/PP2A type specific phosphatase inhibitor okadaic acid. Pretreatment of platelets with Na_3VO_4 (1 μM) and okadaic acid (0.75 μM) inhibited thrombin-induced platelet aggregation (data not shown). In the presence of Na_3VO_4, cofilin dephosphorylation was completely inhibited but no increase of cofilin phosphorylation in resting and platelets stimulated with thrombin was observed. As vanadate is known to inhibit non-specifically ATPases and kinases, inhibition of cofilin dephosphorylation might be due to in fact inhibition of Rho-kinase/LIMK-1 pathway. In the presence of okadaic acid, thrombin-induced initial cofilin dephosphorylation was not affected, but surprisingly the subsequent cofilin rephosphorylation was completely blocked. These results indicate that cofilin phosphatase present in platelets is different from the conventional PP1/PP2A type phosphatase. The inhibition of cofilin rephosphorylation by okadaic acid was similar to that we found in the presence of Rho-kinase inhibitors Y-27632 and H-1152 (compare Figure 4.30 and Figure 4.18). These results led us to investigate, whether okadaic acid might inhibit the Rho-kinase-mediated LIMK-1 activation.
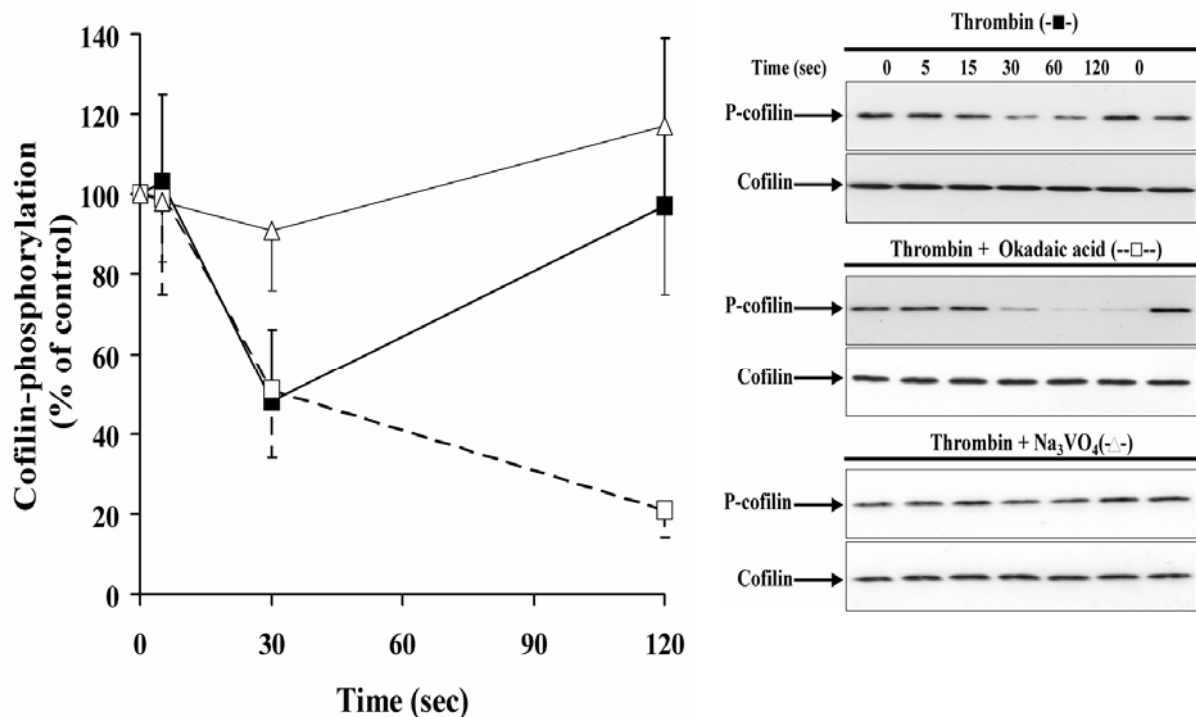
Figure 4.30 Effect of phosphatase inhibitors on cofilin dephosphorylation during platelet stimulation by thrombin (0.5U/ml). Lysates of platelets not treated (■) or pretreated with Na3VO4 (Δ) and okadaic acid (OA, □), and then stimulated by thrombin were immunoblotted with anti-cofilin and anti-phospho-cofilin antibodies. Left, graphical representation of the results, values are mean +SD or mean – SD of three independent experiments. Right, representative immunoblots for cofilin phosphorylation.

To examine the effect of okadaic acid on LIMK-1 activation, LIMK-1 immunoprecipitates from platelets non-treated or treated with okadaic acid and then stimulated with thrombin for 2 minutes were analyzed for LIMK-1 phosphorylation and LIMK-1 kinase activity. Unlike Y-27632-treated platelets, pretreatment of platelets with okadaic acid did not decrease, but increased the phosphorylation of LIMK-1 immunoprecipitates (Figure 4.31, left). These results suggest that okadaic acid might lead to an inhibition of LIMK-1 phosphatase resulting in a further increase of LIMK-1 phosphorylation. LIMK-1 immunoprecipitates from okadaic acid-treated platelets showed an increased phosphorylation of His-tagged cofilin when assayed for kinase reaction. Cofilin phosphorylation by LIMK-1 immunoprecipitates was proportional to the extent of LIMK-1 phosphorylation. These results indicate that inhibition of cofilin rephosphorylation by okadaic acid was not due to the inhibition of LIMK-1 activity. Cofilin phosphatase is not a PP1/PP2A type phosphatase and an okadaic acid sensitive PP1/PP2A type phosphatase might be involved in regulating the cofilin phosphatase negatively in thrombin-stimulated platelets (Figure 4.31).
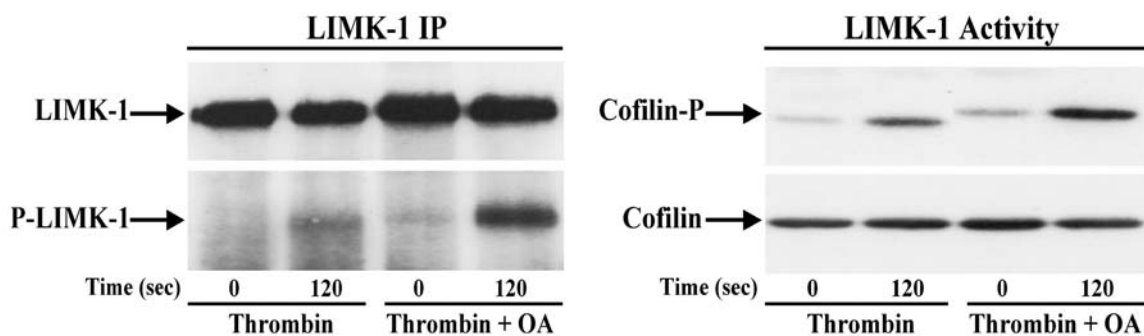
Figure 4.31 Effect of okadaic acid (OA) on LIMK-1 phosphorylation and kinase activity in thrombin-stimulated platelets. Left, immunoprecipitates from platelets non-treated or treated with OA and stimulated with thrombin for 2 minutes were immunoblotted with anti-LIMK-1 and anti-phospho-LIMKs antibodies. Right, LIMK-1 immunoprecipitates were subjected for LIMK-1 kinase reaction using His-tagged cofilin as substrate. Anti-cofilin and anti-phospho-cofilin antibodies were used to measure cofilin phosphorylation. The PP1/PP2A type phosphatase inhibitor OA augmented the LIMK-1 activity.

4.6.2. <u>Inhibition of cofilin dephosphorylation by calcineurin inhibitor</u>

Various phosphatases act in a calcium dependent manner. Many studies showed that an increase in sub-cellular Ca^{2+} concentration induces cofilin dephosphorylation in cells (Davidson and Haslam 1994; Wang et al. 2005). Therefore, we studied whether calcineurin, a calcium-dependent phosphatase, is involved in regulating cofilin dephosphorylation in thrombin-stimulated platelets. A cell-permeable peptide composed of the calcineurin (CaN) auto inhibitory domain (AID) fused with a poly-arginine-based protein transduction domain (11R) (CAID) was used inhibit calcineurin. Preincubation of platelets with CAID-peptide (20 μM) blocked thrombin-induced platelet aggregation (data not shown). The CAID-peptide also completely inhibited thrombin-induced cofilin dephosphorylation (Figure 4.32). A peptide inhibitor of nuclear factor of activated T-cells (NFAT) fused with poly-arginine (11R) was used as a negative

control for CAID-peptide. NFAT-peptide neither affected platelet aggregation nor the cofilin de- and rephosphorylation during platelets stimulation with thrombin (data not shown). These results indicate that calcineurin or intracellular Ca^{2+} release might be involved in facilitating the initial cofilin dephosphorylation in thrombin-stimulated platelets.
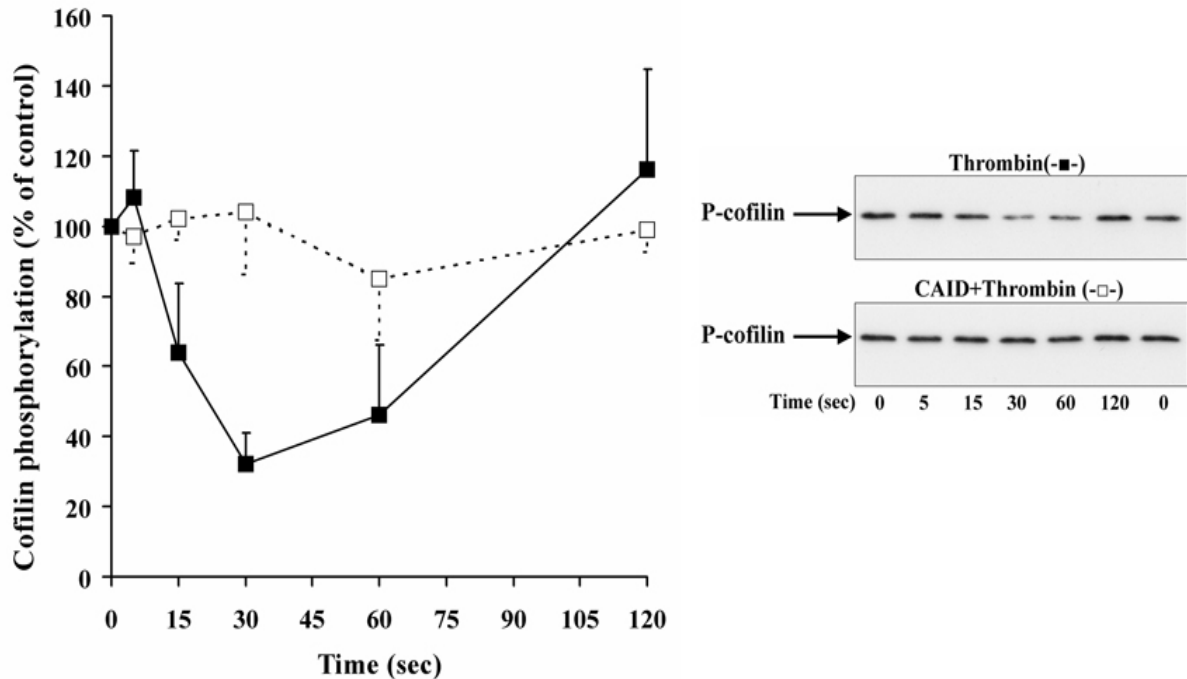
Figure 4.32 Effect of CAID on cofilin dephosphorylation in thrombin-stimulated platelets. Platelet samples not treated (-■-) or pretreated with CAID (20 μM) (-□-) and stimulated with thrombin (0.5 U/ml) were immunoblotted with anti-cofilin and anti-phospho-cofilin antibodies. Left, graphical representation of the results. Values are mean + SD or mean – SD of three independent experiments. Right, representative immunoblots for cofilin phosphorylation.

4.6.3. <u>Inhibition of LPA-induced cofilin dephosphorylation by BAPTA-AM</u>

Since cofilin dephosphorylation induced by thrombin was inhibited by CAID peptide, which inhibits Ca^{2+}-dependent calcineurin activation, we speculate that LPA-induced cofilin dephosphorylation might be due to increase in cytosolic Ca^{2+} after LPA stimulation. In LPA-stimulated platelets, cofilin dephosphorylation was observed only with 100-times higher concentration of LPA. At these high concentrations LPA increases the cytosolic Ca^{2+} concentration mainly through Ca^{2+} influx across the plasma membrane (Maschberger et al. 2000; Rother et al. 2003). In order to investigate whether an increase of cytosolic Ca^{2+} could mediate the rapid dephosphorylation of cofilin, platelets were pre-treated with the intracellular Ca^{2+} chelator BAPTA-AM, which blocks the cytosolic Ca^{2+} increase in activated platelets, as described previously (Bauer et al. 1999). BAPTA-AM (20 μM) inhibited ATP secretion, and blocked the aggregation and cofilin dephosphorylation in LPA-stimulated platelets indicating that a Ca^{2+}-dependent phosphatase might be involved in dephosphorylating cofilin, which in turn might regulate secretion and aggregation (Figure 4.33).
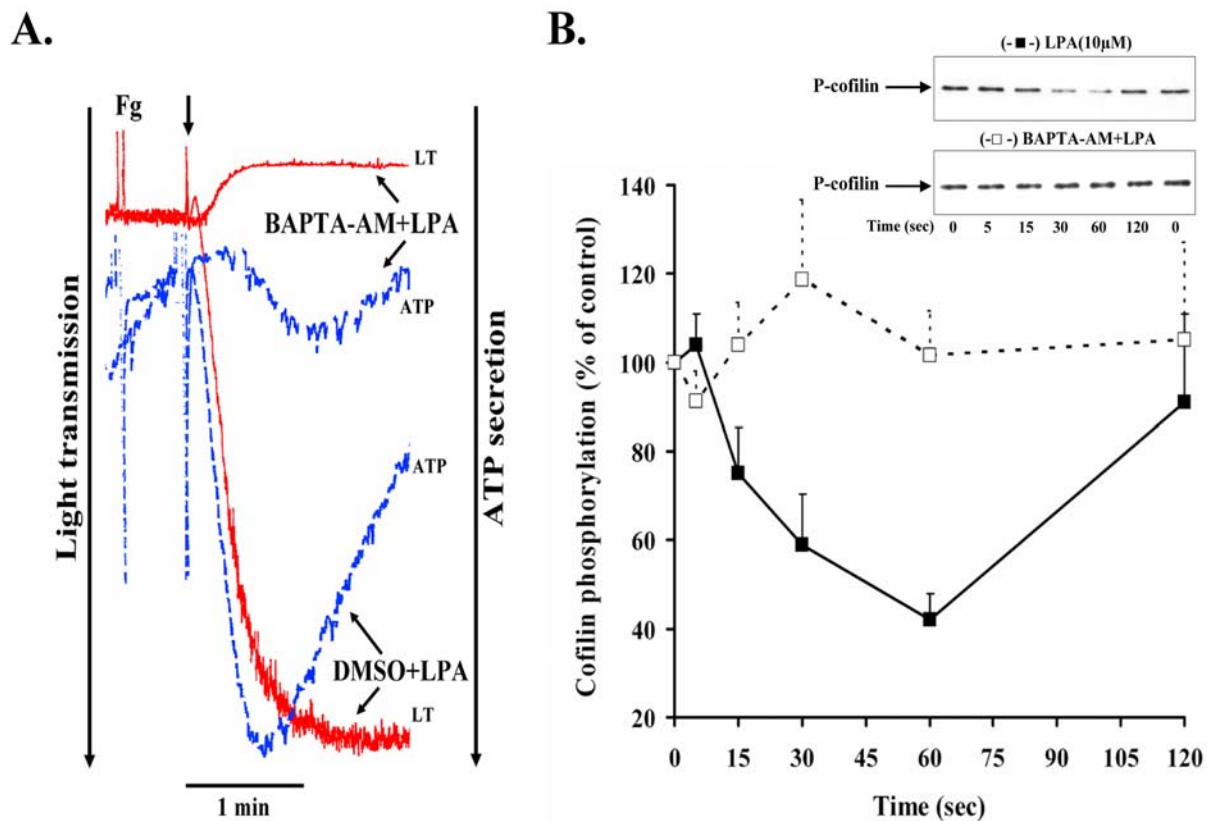
Figure 4.33 Inhibition of LPA (10μM)-induced secretion, aggregation and cofilin dephosphorylation by BAPTA-AM. (**A**) Tracings for light transmission (red) and ATP secretion (blue) of LPA-stimulated platelet aggregation and dense granule secretion in the presence of DMSO (0.1%, control) or BAPTA-AM (20 μM), respectively. (**B**) Graphical representation of the results of cofilin phosphorylation after platelet stimulation with LPA in the absence (-■-) and presence (-□-) of BAPTA-AM. Values for cofilin phosphorylation are mean + S.D of three independent experiments. Inset, representative immunoblots showing inhibition of LPA-induced cofilin dephosphorylation by BAPTA-AM.

4.6.4. <u>Inhibition of cofilin dephosphorylation by PI3-kinase inhibitor</u>

A recent study showed that PI3-kinase is involved in the regulation of slingshot (a cofilin phosphatase) activation in insulin-stimulated cells (Nishita et al. 2004). In order to analyze the role of PI3-kinase in regulating cofilin dephosphorylation, an irreversible inhibitor of PI3-kinase, wortmannin, was used. Wortmannin, which is a fungal metabolite, acts as a potent, selective and cell-permeable inhibitor for PI3-kinase without affecting the upstream signaling events. Pretreatment of platelets with wortmannin (50 nM) resulted in a reduced and reversible aggregation of platelets stimulated with thrombin. Wortmannin (50 nM) blocked PI3-kinase completely as measured by the inhibition of Akt phosphorylation at Ser473 (data not shown). The initial cofilin dephosphorylation in thrombin-stimulated platelet was inhibited in the presence of wortmannin indicating that PI3-kinase might be involved in regulating the activity of cofilin phosphatase (Figure 4.34). We also analyzed the role of Akt kinase, which is activated downstream of PI3-kinase, for cofilin dephosphorylation induced by thrombin. We pretreated platelets with Akt inhibitors (Akt inhibitor IV and Triciribine, 20 μM each) and then stimulated

with thrombin. These inhibitors blocked the Akt activation as measured by the inhibition of phosphorylation of its substrate, glucose synthase kinase (GSK), at Ser21. However, inhibition of Akt did not block the thrombin-induced cofilin dephosphorylation (data not shown). Therefore, it seems that PI3-kinase mediated cofilin dephosphorylation does not involve the PI3-kinase/Akt pathway.
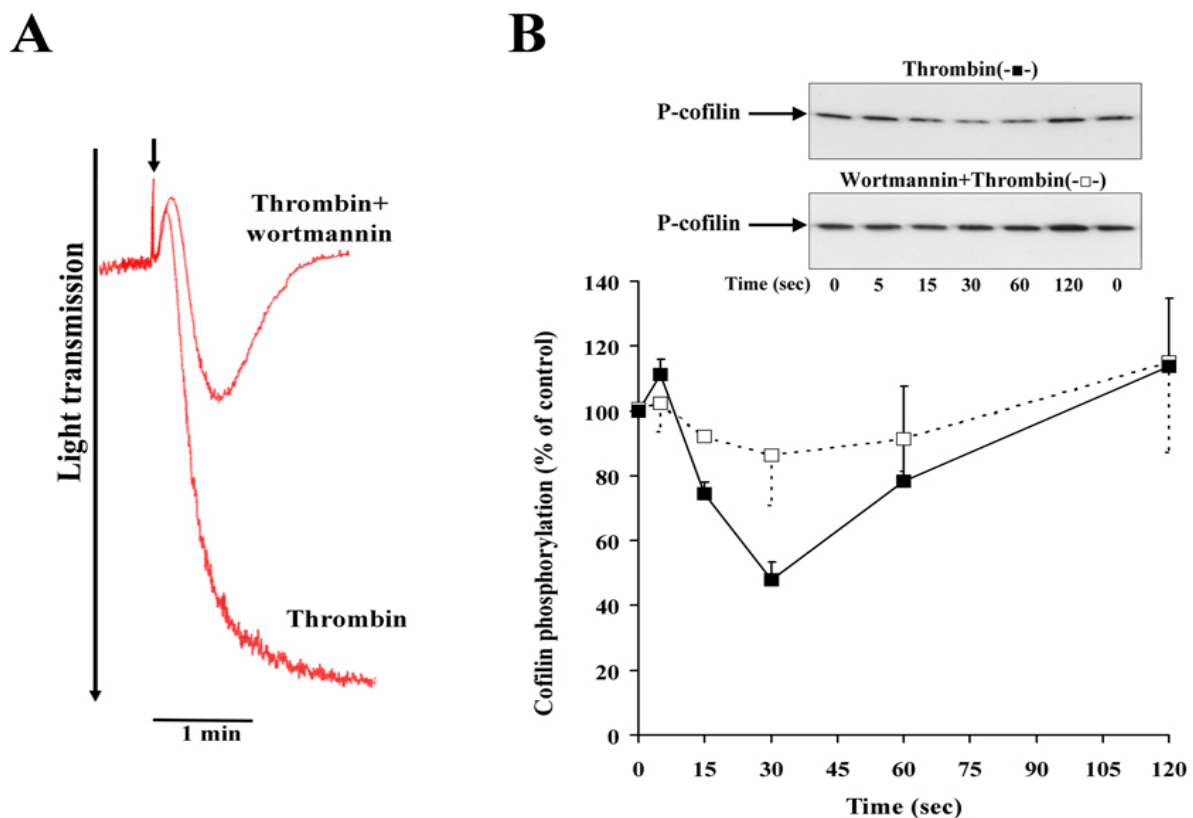
Figure 4.34 Effect of wortmannin on platelet aggregation and cofilin dephosphorylation induced by thrombin. Platelet samples not treated (-■-) or pretreated with wortmannin (50 nM) (-□-) and stimulated with thrombin (0.5 U/ml). Left, light transmission tracings showing platelet aggregation. Right top, representative immunoblots blotted with anti-phospho-cofilin antibody. Right bottom, graphical representation of the results. Values are mean + SD or mean – SD of three independent experiments.

4.7. Peptide or protein transfection into platelets

4.7.1. Poly-arginine based peptide transfection

A peptide with consecutive nine L-arginine residues (R9) can be efficiently taken up into the cells (Wender et al. 2000). In order to inhibit LIMK-1 mediated cofilin phosphorylation in platelets, a peptide corresponding to the N-terminal of cofilin containing the Ser3 (underlined) phosphorylation site (MA_S_GVAVSDGVIKVFN) and coupled to R9 peptide at its C-terminal was synthesized. In a similar manner, the reverse peptide (NFVKIVGDSVAVGSAM) and the pseudo-phosphorylated peptide (Ser3 replaced by Asp, MA_D_GVAVSDGVIKVFN) were

synthesized and used as control peptides. Incubation of platelets with these R9-peptides (80 µM) did not change the phosphorylation level of cofilin (data not shown). These results indicate that either the R9-peptides did not penetrate the platelets or they did not reached the site of action of LIMK-1 inside the platelets.

4.7.2. Protein transfection by Chariot^{TM}

Chariot^{TM} is a commercial transfection reagent that efficiently transports biologically active proteins, peptides and antibodies directly into cultured mammalian cells (Morris et al. 2001). In order to standardize and observe the protein transfection by Chariot^{TM} into platelets, His-tagged cofilin coupled to the green fluorescent protein (GFP) at its C-terminal was subcloned, expressed and purified, and used for transfection. Incubation of cofilin-GFP-Chariot^{TM} mixture with platelet suspension successfully transferred cofilin-GFP into platelets as observed by confocal microscopy of spread platelets. Cofilin-GFP was present as clusters, and not evenly distributed in the spread platelets (Figure 4.35). Although this method for proteins transfection into platelets needs further standardization, it seems to be a good tool to transfer proteins into platelets, which is otherwise difficult to perform using the existing transfection methods.

Alexa 546-phalloidin   **GFP-cofilin**   **Merge**
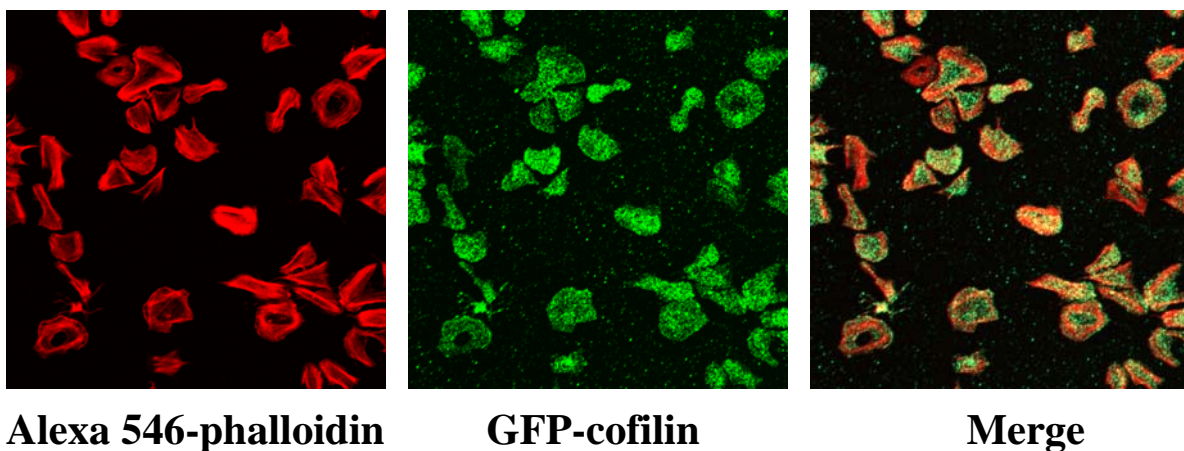
Figure 4.35 Transfection of GFP-cofilin into platelets using Chariot^{TM} protein/peptide transfection reagent. GFP-cofilin transfected platelets were allowed to spread for 15 minutes on glass cover slip and then probed with Alexa 546 phalloidin to stain F-actin. Right, F-actin staining with Alexa-546 phalloidin. Middle, GFP-cofilin fluorescence. Left, merge of Alexa-546 phalloidin and GFP-cofilin fluorescence.

5. <u>Discussion</u>

5.1. <u>Role of Rho-kinase in activated platelets</u>

The alteration of the actin cytoskeleton leads to morphological changes underlying the different platelet responses, i.e., shape change, secretion of granule contents and aggregation. Members of the Rho family GTPases such as Rho, Rac, and Cdc42 are involved in reorganizing the actin cytoskeleton during platelet activation. However, the downstream signaling pathways regulating the reorganization of the actin cytoskeleton through these Rho family GTPases in activated platelets have only been partially characterized. In this study, the role of Rho-kinase in regulating LIMK-1 activity and cofilin phosphorylation leading to changes in the actin cytoskeleton during shape change, secretion and aggregation was studied using functional and biochemical approaches.

Along with the classical turbidimetric method for measuring platelet shape change and aggregation, shape change was also monitored by two other methods, flow cytometry and microscopy. The microscopic analysis of platelets immunostained for F-actin showed that the discoid platelets with a smooth surface got transformed into spheroid cells with an irregular surface after activation. The spheroid form and irregularity of the platelet surface during shape change result in changes in the light scattering properties of platelets. The analysis of platelets by flow cytometry showed that activated platelets scattered more light in forward direction (FSC) and less in perpendicular (SSC) to the incident light (see method section 3.4.1). Thus, the ratio of FSC/SSC increased proportionally to the extent of platelet shape change. The flow cytometry method can also be applied to easily measure platelet shape change in whole blood (Haseruck et al. 2004). Pre-treatment of platelets with the specific Rho-kinase inhibitor Y-27632 blocked the platelet shape change in blood (Haseruck et al. 2004) and also the shape change of washed platelets monitored by all three methods (present thesis) indicating that the activation of Rho-kinase is important for platelet shape change.

5.1.1. <u>Activation of Rho-kinase</u>

Rho-kinase activation is known to augment MLC phosphorylation directly or indirectly by phosphorylating the MYPT and thereby inhibiting myosin phosphatase activity. Taking this into consideration, the activation of Rho-kinase in platelets was measured using a new approach, i.e. by quantifying the phosphorylation of the substrate MYPT on Thr696 or Thr853 (Ito et al. 2004). During shape change induced by LPA as well as by low concentration of thrombin, a rapid phosphorylation of MYPT at Thr696 and Thr853 was observed. Phosphorylation of these Rho-kinase-targeted sites were inhibited by specific inhibitors of Rho-kinase, Y-27632 and H-1152, confirming and extending previous results that Rho-kinase activation mediates Ca^{2+}-independent

shape change induced by thrombin and LPA (Bauer et al. 1999; Retzer and Essler 2000). The kinetics of MYPT phosphorylation was similar during platelet stimulation with low (0. 1μM) as well as high (10 μM) concentrations of LPA (both in the presence and absence of fibrinogen), except that the extent of MYPT phosphorylation with 0.1 μM LPA was comparatively higher than with 10 μM LPA. Probably, this reduction is caused by the activation of a MYPT phosphatase after platelet stimulation with the high dose of LPA.

MYPT phosphorylation during shape change induced by thrombin was slower and irreversible as compared to a rapid and reversible MYPT phosphorylation during aggregation induced by thrombin. The difference in kinetics of MYPT phosphorylation induced by different concentrations of thrombin might be due to the different sensitivity of PAR receptors. Out of the two thrombin-stimulated receptors on human platelets, PAR-1 is easily cleaved and activated by low thrombin concentrations while PAR-4 requires 10- to 100-fold higher concentrations of thrombin (Covic et al. 2000; Brass 2003). Probably, the slow MYPT phosphorylation during shape change is due to the partial activation of PAR-1 and the more rapid response during secretion and aggregation is due to the complete activation of PAR-1 and additional activation of PAR-4. After the rapid increase, MYPT phosphorylation at Thr696 and Thr853 decreased due to integrin $\alpha_{IIb}\beta_3$ engagement during thrombin-stimulated platelet aggregation. This indicates that the engagement of the integrin $\alpha_{IIb}\beta_3$ during platelet activation might stimulate a phosphatase acting on these Rho-kinase specific sites in MYPT and thus, this method to measure Rho-kinase activity is not appropriate. The initial increase in MYPT phosphorylation was independent of integrin $\alpha_{IIb}\beta_3$ engagement, which in agreement with a previous study, shows that Rho and Rho-kinase activation in platelets are upstream of integrin $\alpha_{IIb}\beta_3$ (Gratacap et al. 2001).

LPA-stimulated MYPT phosphorylation was more rapid and reversible as compared to irreversible MYPT phosphorylation during thrombin-induced platelet shape change. This difference in MYPT phosphorylation indicates that LPA (through LPA receptors) and thrombin (through PAR-1 receptor) activate Rho-kinase with different kinetics during platelet shape change.

5.1.2. <u>Rho-kinase activation mediates F-actin increase during shape change</u>

Platelet stimulation by agonists induces a rapid increase in actin polymerization (Kometani et al. 1986; Oda et al. 1992). These new actin filaments fill in the filopodia and form a contractile network underlying platelet shape change. It was observed that thrombin as well as LPA induced a rapid increase in F-actin content during platelet shape change. The inhibition of F-actin increase by latrunculin A, which binds to G-actin and thereby facilitates F-actin depolymerization and inhibits further actin polymerization, blocked the shape change induced by LPA. Similar studies that explore the alteration of actin dynamics by other actin-assembly inhibitors the cytochalasins, which bind to the barbed end of filament and inhibit actin polymerization, showed

an inhibition of platelet shape change and pseudopod extensions after stimulation with agonists (Kometani et al. 1986; Natarajan et al. 2000). Therefore, actin polymerization is a vital process for platelet shape change. Together with an increase in F-actin, other cytoskeletal events such as an increase in actin-myosin filament formation and contraction due to MLC phosphorylation (Retzer and Essler 2000) and disruption of the microtubule ring (Paul et al. 2003) are equally involved in the transformation of discoid platelets into spheroid cells. Preincubation of platelets with Y-27632, a specific Rho-kinase inhibitor, abolishes MLC phosphorylation and disassembly of the microtubule ring (Paul et al. 2003). In the present study, the Ca^{2+}-independent platelet shape change and increase of F-actin induced by low concentrations of thrombin and LPA were inhibited by Y-27632. Together, our results and results of previous studies show that Rho-kinase acts as a central molecule signaling to actin polymerization, actomyosin contraction and microtubule disruption underlying platelet shape change. Furthermore, the kinetics of Rho-kinase activation, F-actin increase and shape change, which were irreversible after platelet activation with thrombin and reversible after platelet activation with LPA suggest that the kinetic of Rho-kinase activation determines the pattern of F-actin increase and platelet shape change.

5.1.3. <u>Rho-kinase is involved in secretion and platelet aggregation</u>

The actin polymerization during dense granule secretion is substantially more than during shape change (Lefebvre et al. 1993). Confirming this previous observation, a higher increase of F-actin during secretion (170% of control) as compared during shape change (128% of control) in platelets stimulated with thrombin was observed. Although many signaling pathways induced during secretion might contribute to the cytoskeletal changes, the inhibition of F-actin increase and a reduction in dense granule secretion in thrombin-stimulated platelets by Y27632 indicate that the Rho-kinase-mediated actin polymerization is involved in dense granule secretion. This conclusion is supported by recent studies where secretion induced by agonists was blocked by inhibiting actin polymerization using cytochalasins (Diaz-Ricart et al. 2002; Flaumenhaft et al. 2005). However, earlier studies also using cytochalasins contradicted the necessity of F-actin formation for dense granule secretion, and even suggested that an intact actin cytoskeleton acts as barrier for granule secretion (Kirkpatrick et al. 1980; Cox 1988). In addition to inhibition of F-actin formation, Y-27632 also inhibits actomyosin contraction, which is an important process for secretion and therefore Rho-kinase activation might be needed for efficient actin dynamics underlying dense granule secretion from platelets.

Previously, it was observed that Rho-kinase is involved in irreversible platelet aggregation, but not in secretion after platelet stimulation with the PAR-1 activating peptide, SFLLRNP (Missy et al. 2001). However, another study showed that Y-27632 and H-1152 inhibited dose-dependently dense granule secretion induced by the thromboxane A_2 mimetic SAT_2 and low, but not higher concentrations of thrombin (≥ 0.1U/ml) (Suzuki et al. 1999). In our study, Y-27632 dose-dependently inhibited ATP secretion (data not shown) and reduced the secretion induced by

thrombin concentrations as high as 0.5U/ml. The difference in inhibition of thrombin-induced secretion by Rho-kinase inhibitors in these two studies might be for two reasons. First, in our platelet preparation the presence of apyrase (ADPase) in the final resuspension buffer could degrade ATP and hence these Rho-kinase inhibitors could effectively block secretion induced by higher concentrations of thrombin as compared to the study by Suzuki et al. Second, in our study, platelet suspensions were incubated with these inhibitors at 37°C for 30 minutes, whereas in study by Suzuki et al., they were incubated for 3 minutes, which might result in inefficient inhibition of Rho-kinase. The inhibition of secretion by Y-27632 was incomplete suggesting that apart from Rho-kinase other signaling pathways are important in dense granule secretion induced by thrombin.

Inhibition of thrombin-induced secretion by the Rho-kinase inhibitor Y-27632 was accompanied by a reduced and reversible platelet aggregation. To distinguish whether in thrombin-stimulated platelets Rho-kinase regulates secretion or aggregation the integrin $\alpha_{IIb}\beta_3$-blocker RGDS was used to inhibit aggregation. No reduction of ATP secretion was observed under these conditions. These results indicate that Rho-kinase regulates primarily secretion, which then amplifies platelet aggregation. Stimulation of platelets with strong physiological agonist thrombin induces the release of fibrinogen and thrombospondin from α-granules, which are known to initiate and stabilize platelet aggregation, respectively (Leung 1984; Bornstein 2001). Inhibition of thrombin-induced platelet aggregation by Y-27632 might then be due to less fibrinogen release from α-granules, and the reversibility of platelet aggregate formation might be a consequence of less secretion of thrombospondin from these granules.

It has been observed that Rho-kinase contributes to a greater extent for platelet secretion induced by weaker agonists. LPA is a weak agonist as compared to thrombin and induces only shape change of washed platelets even at high concentrations (10 μM). However, LPA in the presence of external fibrinogen, induced secretion and platelet aggregation. Pretreatment of platelets with Y-27632 completely abolished the secretion and reduced platelet aggregation induced by LPA. The complete inhibition of LPA-induced secretion by Y-27632 indicates that dense granule secretion is mainly regulated by Rho-kinase in LPA-stimulated platelets.

LPA-induced platelet aggregation in platelet suspensions and blood is mediated by synergism with ADP secreted from dense granules (Haseruck et al. 2004). We also showed a reduced and reversible platelet aggregation after complete inhibition of dense granule secretion by Y-27632 in LPA-stimulated platelets supporting that ADP secreted from dense granules potentiates LPA-induced platelet aggregation by positive feedback through purinergic ADP receptors. However, on the other hand there are evidences that $\alpha_{IIb}\beta_3$-mediated outside-in signaling elicits secretion induced by physiological agonists such as ADP and thromboxane A_2 (Krishnamurthi et al. 1989; Moritani et al. 2002; Li et al. 2003). The lack of ATP secretion observed after platelet stimulation with LPA in the absence of fibrinogen supports these previous findings. Thus, fibrinogen binding to the $\alpha_{IIb}\beta_3$ integrin and signaling pathways activated due to this binding are

required for ADP secretion, which then can amplify, propagate and perpetuate platelet aggregation in LPA-stimulated platelets. Together these studies also show that granule secretion and platelet aggregation are interdependent events, and are difficult to arrange in hierarchy after platelet stimulation. These studies also infer that Rho-kinase activation is an important signaling event for shape change, granule secretion and platelet aggregation and thus can be a target for the development of anti-thrombotic drugs.

5.2. Identification and regulation of LIMK-1 in human platelets

5.2.1. LIMK-1 but not LIMK-2 expressed in platelets

In other cell types, Rho-kinase is known to phosphorylate and activate LIM-kinases, a target other than MLC and myosin phosphatase (Maekawa et al. 1999). There exist two types of LIM kinases namely, LIMK-1 and LIMK-2 that are widely expressed in all tissues and cell types (Foletta et al. 2004; Acevedo et al. 2006). The similar function of LIMKs to phosphorylate cofilin suggests that they might be redundant in cells expressing both enzymes, but might be essential in cells expressing only one of them. So far, the presence of different LIM kinase isoforms in platelets was not known. This study using specific antibodies against LIMK-1 and LIMK-2 showed that only LIMK-1 is expressed in platelets. In addition, endothelial cells that contain both LIMK-1 and LIMK-2 showed an extra lower band recognized by both of these antibodies, which were absent in platelets. These bands might be similar to the spliced variants of LIMK-2, described in mouse tissues (Ikebe et al. 1997; Ikebe et al. 1998). Exclusive expression of LIMK-1 in platelets suggests that megakaryocytes that produce platelets might also contain only LIMK-1. The other possibility is that megakaryocytes express both LIMK-1 and LIMK-2, and that these cells suppress LIMK-2 expression during differentiation. Concerning the first possibility, the expression of LIMK-1 is found in human erythroleukaemia cell line, which is thought to differentiate into megakaryocytes (Konakahara et al. 2004). Supporting the second possibility that selective proteins are expressed in megakaryocytes and platelets, it has been shown that the cytosolic protein paxillin is expressed in megakaryocytes, but is lost during maturation of megakaryocytes into platelets, and is functionally replaced by another homologous protein hic-5 in platelets (Hagmann et al. 1998). Our results also infer that LIMK-1 might be the only relevant LIM-kinase for physiological activation of platelets. It would be interesting to know whether also mouse platelets express only LIMK-1 or both forms of LIMKs. Dependent on this result, the physiological role of LIMK-1 and LIMK-2 could be probed in the future by performing functional studies on platelets from LIMK-1 and LIMK-2 null mice. LIMK-1 deficient mice are viable, but have abnormal spine morphology, synaptic regulation, and brain functions (Meng et al. 2002). LIMK-2 knockout mice are also viable, but showed impaired spermatogenesis and an increase in apoptosis of germ cells (Meng et al. 2004). Mice lacking both LIMKs have the same defects, but are also viable and fertile suggesting that other kinases

such as TESK-1 and 2 might functionally compensate for the lack of LIMKs in these mice. The LIMK-1/2 double knockout mice were, however, more severely impaired in cofilin phosphorylation and synaptic functions (Meng et al. 2004). LIMK-1/2 deficiency causes apparently no major bleeding problems leading to premature death indicating that in these mice the platelet number was not drastically reduced, and therefore platelet production from megakaryocytes is not severely impaired. It remains an open question, however, whether LIMK-1 plays a function for specific platelet responses or is involved in pathological thrombus formation.

5.2.2. <u>Rho-kinase activation leads to LIMK-1 phosphorylation</u>

Most of the studies suggest that during physiological cell activation, Rho-kinase-mediates LIMK-2 activity, whereas PAKs are responsible for LIMK-1 activity. Our study is to our knowledge the first to provide evidence that Rho-kinase activates LIMK-1 in LPA- and thrombin-stimulated platelets. LIMK-1 was rapidly phosphorylated during shape change and secretion/aggregation. The kinetics of LIMK-1 phosphorylation during shape change and secretion were similar to the kinetics of Rho-kinase activation as measured by MYPT phosphorylation, suggesting that Rho-kinase phosphorylates LIMK-1 in intact platelets. Moreover, LIMK-1 phosphorylation was completely inhibited by two different Rho-kinase inhibitors, Y-27632 and H-1152. These Rho-kinase inhibitors completely blocked LIMK-1 phosphorylation during thrombin-induced platelet shape change, secretion and aggregation, and inhibited the activity of LIMK-1 in immunoprecipitates from thrombin-stimulated platelets.

It has been reported using transfected cells that LIMK-1 can be phosphorylated and activated either by PAKs (Edwards et al. 1999) or Rho-kinase (Ohashi et al. 2000). PAK2 has been shown to be activated during platelet shape change (Teo et al. 1995) and aggregation (Vidal et al. 2002). Moreover, LPA that mainly activates the Rho/Rho-kinase pathway has also been reported in few studies to stimulate PAK in a Rac- or Cdc42-dependent manner (Schmitz et al. 2002; Rhee and Grinnell 2006). These studies raised the possibility that PAK might also be activated and contribute to LIMK-1 activation in LPA-stimulated platelets. In our study, LPA induced rapidly Rho-kinase activation and slower PAK activation during shape change. We found that during LPA-stimulated platelet shape change LIMK-1 activation coincides with and was completely dependent on Rho-kinase activation, whereas PAK activation was unlikely to be involved. These results also infer that PAK activation in platelets might have targets other than LIMK-1, for example MLC-kinase or directly MLC (Bokoch 2003). However, since specific cell-permeable PAKs inhibitors are not available, we cannot rule out a transient Rho-kinase dependent, PAK-mediated LIMK-1 phosphorylation in LPA-stimulated platelets. Supporting this possibility we found that PAK1/2 phosphorylation was reduced by Y-27632, albeit not significantly. Y-27632 is a specific inhibitor of Rho-kinase and does not inhibit PAK activation in vitro even at high concentrations (100 μM) (Uehata et al. 1997). Recently, Rac activation in TRAP-stimulated platelets was reported to be slightly enhanced by Y-27632 pretreatment suggesting that Rho-

kinase down-regulates Rac and possibly PAK activation (Soulet et al. 2005). However, our study suggests that Rho-kinase might rather stimulate then inhibit PAK-activation in LPA-stimulated platelets.

Rac and Cdc42 in platelets regulate distinct morphological structures, spreading and filopodia formation, respectively (Vidal et al. 2002; Chang et al. 2005). This difference in their specific role indicates that they might be regulated differently. In activated platelets, the G_q/PLCβ/Ca^{2+} pathway and G_i activation mediate stimulation of Rac (Azim et al. 2000; Gratacap et al. 2001; Suzuki-Inoue et al. 2001; Vidal et al. 2002; Soulet et al. 2005), whereas Cdc42 activation was independent of the PLC/Ca^{2+} pathway (Soulet et al. 2001) and could contribute to filopodia formation during Ca^{2+}-independent platelet shape change after LPA and thrombin stimulation. Low concentrations of LPA do not stimulate G_q and G_i, and do not increase cytosolic Ca^{2+} during shape change (Maschberger et al. 2000; Haseruck et al. 2004), raising the possibility that Cdc42, and not Rac stimulates PAK phosphorylation. Another possibility is that PAK is stimulated through the PI3-kinase/Akt pathway, which is activated by $G_{\beta\gamma}$ subunits independently of Rac1/Cdc42 (Menard and Mattingly 2004). Whether Cdc42/PAK pathway contributes to filopodia formation during the LPA-induced platelet shape change is an open question, since inhibition of Rho-kinase reversed the spheroid morphology but could not block the filopodia formation during ADP-induced platelet shape change (Paul et al. 2003). These authors observed that Y-27632-treated platelets after ADP stimulation returned to discoid shape, but still possessed extended filopodia. It is possible that Rho-kinase- and Rac/Cdc42-mediated pathways specifically controls the spheroid and filopodia formation during agonists-induced shape change, respectively.

LIMK-1 phosphorylation was not changed by the integrin $\alpha_{IIb}\beta_3$ blocker RGDS and by the absence of stirring during thrombin-stimulation of platelets. This indicates that unlike MYPT, LIMK-1 activation is not influenced by integrin $\alpha_{IIb}\beta_3$ engagement and occurs therefore upstream of integrin $\alpha_{IIb}\beta_3$ activation in thrombin-stimulated platelets. Hence, measuring LIMK-1 (Thr508) phosphorylation might be a better tool than MYPT (Thr696 and Thr853) phosphorylation for analysis of Rho-kinase activation in stimulated platelets, since MYPT is dephosphorylated in aggregated platelets.

5.3. <u>Regulation of cofilin activities</u>

Cofilin phosphorylation by LIMKs inhibits its actin depolymerizing activity and modulates its binding to F-actin. In agreement with observations made previously (Davidson and Haslam 1994), we found that about one third of the total cofilin is phosphorylated in resting platelets. We observed a significant decrease of cofilin phosphorylation in resting platelets after treatment with Y-27632 indicating that the Rho-kinase/LIMK-1 pathway is needed to maintain this basal level of cofilin phosphorylation. The presence of both cofilin and phospho-cofilin suggests that cofilin

phosphorylation in resting platelets is under influence of both Rho-kinase/LIMK-1 and a cofilin phosphatase.

Surprisingly, the activation of LIMK-1 failed to increase cofilin phosphorylation during shape change induced by LPA as well as thrombin. The lack of subsequent increase in cofilin phosphorylation could be explained by simultaneous activation of a cofilin phosphatase. In support of this explanation, we found that inhibition of the Rho-kinase/LIMK-1 pathway revealed a further decrease of phospho-cofilin during shape change 5 seconds to 120 seconds after stimulation with LPA and thrombin, indicating that the simultaneous activation of a cofilin phosphatase counteracts the effect of LIMK-1 for phosphorylating cofilin during shape change. Thus, the phosphocycling on cofilin might be increased without any substantial changes in cofilin net phosphorylation due to the simultaneous activation of these counteracting pathways. In support of this hypothesis, Meberg et al showed that EGF-induced membrane ruffling in human epithelial cells was not associated with a changed ratio of phosphorylated to dephosphorylated cofilin, however the rate of phosphocycling on cofilin was increased (Meberg et al. 1998). A further possibility for the lack of stimulation of cofilin phosphorylation by LIMK-1 during shape change is the presence of another LIMK-1 substrate in platelets, such as destrin, another protein of the ADF family and known to be phosphorylated by LIM-kinases. However, in thrombin-stimulated platelets destrin was observed to be dephosphorylated after 60 sec along with cofilin (Marcus et al. 2003). Thus, destrin behaves similar to cofilin in activated platelets, not being well accessible to phosphorylation by LIMK-1.

During platelet aggregation and secretion induced by thrombin, cofilin was rapidly dephosphorylated and subsequently rephosphorylated; the latter phase was due to Rho-kinase and LIMK-1 activation. Cofilin dephosphorylation/ rephosphorylation occurred independently whether platelets aggregated or not indicating that the regulation of cofilin phosphorylation was independent of the integrin $\alpha_{IIb}\beta_3$ involvement. The rapid cofilin dephosphorylation observed in thrombin-stimulated platelets is similar to a previous study and recent findings (Davidson and Haslam 1994; Falet et al. 2005). However, in TRAP-stimulated platelets no decrease of cofilin phosphorylation, only an increase 3 to 5 minutes after activation was found (Kashiwagi et al. 2005). In contrast to our results, the study of Falet et al showed that during thrombin-induced platelet aggregation, cofilin remained dephosphorylated suggesting that integrin $\alpha_{IIb}\beta_3$ activation leads to sustained cofilin dephosphorylation. Also, a recent study in epithelial cells showed that β_3 overexpression reduced phospho-cofilin levels (Danen et al. 2005). A possible explanation for the discrepancies between the study of Falet et al and our study might be the different methods used to isolate washed platelets such as use of a metrizamide gradient in the study of Falet el al. We further validated the independency of cofilin dephosphorylation from integrin $\alpha_{IIb}\beta_3$ engagement by our results in LPA-stimulated platelets. Platelets stimulated with a high concentration of LPA (10 μM), did not show any dense granule secretion and no platelet aggregation, but exhibited cofilin de- and rephosphorylation, similar to that observed for platelets

stimulated with high concentration of thrombin. These data clearly indicate an integrin $\alpha_{IIb}\beta_3$-independent regulation of cofilin phosphorylation in activated platelets.

In thrombin-stimulated platelets, the possible role of dense granule secretion in inducing the rapid cofilin dephosphorylation was not clear. Davidson and Haslam had previously shown that cofilin dephosphorylation occurs later than dense granule secretion in thrombin-stimulated platelets suggesting that dephosphorylation of cofilin is a consequence of secretion (Davidson and Haslam 1994). However, in the same study the dephosphorylation of cofilin in the absence of secretion after platelet stimulation with ionophore A23187 was not explained. Our study clearly shows that cofilin dephosphorylation is independent and upstream of secretion since the onset of cofilin dephosphorylation is as rapid as secretion in thrombin-stimulated platelets and also occurs in the absence of dense granule secretion, when platelets were stimulated with LPA (10 μM) in the absence of fibrinogen. Moreover, a very recent study using the quench-flow technique showed that thrombin (0.1 U/ml) evoked a rapid cofilin dephosphorylation that commenced within 100 milliseconds, reached a maximum at 0.9 seconds, which was then followed by subsequent rephosphorylation exceeding the resting level about 1.5 seconds after platelet activation (Redondo et al. 2006). Secretion-like store-operated calcium entry (SOCE) occurred later than cofilin dephosphorylation in that study supporting our data of secretion-independent regulation of cofilin dephosphorylation in activated platelets.

Cofilin dephosphorylation during platelet stimulation with high concentrations of LPA and thrombin was followed by Rho-kinase/LIMK-1-mediated cofilin rephosphorylation to the level observed in resting platelets within 2 minutes. The results of inhibition of the Rho-kinase/LIMK-1-mediated cofilin rephosphorylation with Y-27632 indicate that this pathway regulates primarily secretion, not aggregation. Y-27632 did not inhibit cofilin dephosphorylation up to 30 seconds. These results also suggest that during platelet secretion/aggregation, the two counteracting pathways regulating cofilin phosphorylation, i.e. cofilin phosphatase and LIMK-1, sequentially act on cofilin. The rapid and large dephosphorylation of cofilin shows that a cofilin phosphatase is activated very rapidly, and that this enzyme has a better access to its substrate phospho-cofilin than LIMK-1 (which is also activated rapidly) to cofilin. Since LIMK-1 is rapidly activated in thrombin-stimulated platelets, but cofilin is rapidly dephosphorylated, one has also to assume a compartmentalization in order to explain these results. LIMK-1 is known to bind to a number of different proteins including the cofilin phosphatase slingshot (Soosairajah et al. 2005), 14-3-3 (Birkenfeld et al. 2003), heat shock protein 90 (Li et al. 2006) and some transmembrane receptors (Foletta et al. 2003), so even in its activated form it may not have direct access to cofilin. Based on our results, we interpret the cofilin phosphorylation data in platelets stimulated with high concentrations of thrombin (0.5 U/ml) and LPA (10 μM) by a rapid activation of a cofilin phosphatase generating active cofilin, which after 30-60 seconds is rephosphorylated and inactivated by LIMK-1. However, the presence of other kinases than LIMK-1 that can

phosphorylate cofilin in intact platelets cannot be excluded, since LIMK-1 was not inhibited directly, only indirectly through Rho-kinase inhibition.

Our study shows that cofilin is maximally dephosphorylated at 30 seconds and then rephosphorylated to the basal level within 2 minutes of platelet stimulation with thrombin (0.5 U/ml). The kinetics of cofilin phospho-cycle in LPA (10 µM)-stimulated platelets was similar except the maximal dephosphorylation occurred at 60 sec after LPA induction. The study by Falet et al, showed that cofilin after initial dephosphorylation is rephosphorylated slowly and commencing not later that 2 minutes of platelet stimulation with thrombin (1 U/ml) in the presence of RGDS and in the absence of stirring (Falet et al. 2005). Using rapid quench-flow technique, Redondo et al showed that in thrombin (0.1 U/ml)-stimulated platelets the phospho-cycle of cofilin is completed within 1.5 seconds (Redondo et al. 2006). This very early onset and shorter time frame for the cofilin phospho-cycle in the study by Redondo et al might be explained by the use of different experimental set-ups. Similarity in these studies, first de- and rephosphorylation of cofilin although with different kinetics, suggests that cofilin phospho-cycle is an important regulatory process for rapid actin dynamics underlying different morphological and functional changes of platelets.

5.3.1. <u>Cofilin association with F-actin</u>

Cofilin in its dephosphorylated and activated form binds with filamentous actin (Nagaoka et al. 1996). We investigated, how cofilin phosphorylation was related to the increase of F-actin, and to the association of cofilin with F-actin. The results with Y-27632 in resting platelets suggested that LIMK-1-mediated cofilin phosphorylation might reduce F-actin content and cofilin association with F-actin. However, during thrombin-induced shape change there was no relation of the unchanged phospho-cofilin levels in platelets with the rapid increase of F-actin (11%) and the increase of cofilin association with F-actin (5 %) of platelets. During the initial phase of thrombin-induced secretion (up to 30 seconds), cofilin dephosphorylation was associated with a larger increase of F-actin (22 %) and a higher amount of cofilin associated with F-actin (21 %) as compared to shape change. Confirming our results, Falet et al (Falet et al. 2005) showed that only cofilin but not phospho-cofilin binds to F-actin and the initial cofilin dephosphorylation was accompanied with an increase in F-actin content and increased association of cofilin with F-actin in thrombin-stimulated platelets. However, cofilin rephosphorylation after 30 seconds did not decrease F-actin, and cofilin association with F-actin. Moreover, Y-27632 pre-treatment reversed the increase of F-actin and cofilin association with F-actin, which was associated with an inhibition of cofilin rephosphorylation. These results show that LIMK-1-mediated cofilin phosphorylation does not regulate the F-actin increase and cofilin association with F-actin in thrombin-activated platelets. In contrast, the study by Falet et al contradicts our findings showing that cofilin rephosphorylation 5-10 minutes after thrombin stimulation was paralleled by its dissociation from F-actin. This difference in the study by Falet et al and ours might be due to

different lysis methods used for isolation of F-actin. We observed that phalloidin, which was not used in our method but in the study by Falet et al, displaced cofilin from F-actin and caused F-actin increase during lysis. The incubation time for platelet lysis is also critical to avoid changes that occur after platelet lysis (Carlsson et al. 1979).

During LPA-induced platelet shape change, we studied the association of cofilin with F-actin of the actin cytoskeleton instead of association of cofilin to the whole F-actin content of platelets. We found that cofilin very rapidly associated with the actin cytoskeleton. The maximal cofilin association with actin cytoskeleton occurred before the maximal F-actin increase, suggesting that cofilin association with F-actin might regulate the turnover and actin polymerization during platelet shape change. Cofilin association with actin filaments during shape change might generate more free barbed ends that can be utilized for further polymerization of actin filaments by the Arp2/3 complex (Pollard and Beltzner 2002). In contrary to the actin depolymerizing activity of cofilin, such a concept might also explain the simultaneous increase rather than decrease in F-actin content accompanied with the activation of cofilin during thrombin-stimulated dense granule secretion. Such an explanation is supported by a recent data demonstrating that cofilin promotes rather than decreases actin polymerization, generates protrusions, and determines the direction of cell migration (Ghosh et al. 2004).

5.3.2. <u>Possible factors regulating cofilin dephosphorylation</u>

Even after years of study, the identification of specific cofilin phosphatases and signaling pathways regulating cofilin dephosphorylation remain unclear. Cofilin dephosphorylation could result from either the inactivation of cofilin kinases (LIMKs), activation of the cofilin phosphatase, or a combination of these reactions. Some recent studies in human cell lines and neurons suggested that down-regulation of the Rho-kinase/LIMK-1 pathway induces cofilin dephosphorylation (Jung et al. 2006; Zhang et al. 2006). In agreement to this observation, we found that the inhibition of Rho-kinase reduced cofilin phosphorylation in resting platelets and subsequently unrevealed cofilin dephosphorylation in activated platelets. However, even when Rho-kinase and LIMK-1 were rapidly activated during platelet stimulation with thrombin and LPA, either no increase in cofilin phosphorylation during shape change or a rapid cofilin dephosphorylation during secretion and aggregation was observed. A similar observation of cofilin net dephosphorylation in parallel to LIMK-1 activation induced by insulin in human epidermoid carcinoma KB cells has been reported (Arai and Atomi 2003). However, they found that the apparent insulin-induced cofilin dephosphorylation was due to suppression of cofilin phosphorylation and not due to enhanced cofilin dephosphorylation. In contrast, our results suggest that cofilin dephosphorylation is the result of stimulation of a phosphatase and not due to the inhibition of Rho-kinase/LIMK-1 pathway, since the cofilin dephosphorylation was not affected by Y-27632.

Davidson and Haslam observed that GTPγS induced cofilin dephosphorylation in electro-permeabilized platelets suggesting that GTP-binding proteins are involved in this process (Davidson and Haslam 1994). Recently, a study by Tanaka et al showed that constitutively active RhoA induced slingshot-mediated cofilin dephosphorylation in Xenopus zygote (Tanaka et al. 2005). The activation of slingshot was dependent on an increase of F-actin induced by Rho signaling. Inhibition of actin polymerization by latrunculin A (sequesters G-actin) and facilitation of actin polymerization by jasplakinolide (stabilizes F-actin) resulted in inhibition and augmentation of cofilin dephosphorylation, respectively (Tanaka et al. 2005). This observation might explain our findings of simultaneous increase in F-actin and enhanced cofilin dephosphorylation during thrombin-induced secretion. F-actin formation might enhance cofilin phosphatase activity and thereby induce cofilin dephosphorylation. However, by using Y-27632 we did not observed an effect on cofilin dephosphorylation in thrombin-stimulated platelets, despite of the inhibition of F-actin increase.

Another recent study on axon growth in Drosophila showed that Rac through a PAK-independent pathway antagonizes the effect of LIMK-1 over-expression on cofilin phosphorylation, probably due to activation of a cofilin phosphatase (Ng and Luo 2004). These studies altogether suggest that signaling induced by agonists bifurcate downstream of Rho-GTPases into simultaneous activation of a Rho/Rho-kinase/LIMK-1 and cofilin phosphatase that later converge on a common downstream target, cofilin and thus, influencing its phosphorylation. Whether and how Rho-GTPases are involved in regulating cofilin dephosphorylation and which Rho-GTPase is actually involved in this process would be of great interest in future studies.

Cofilin dephosphorylation was inhibited by the non-specific phosphatase inhibitor sodium orthovanadate but not by the PP1/PP2A type phosphatase inhibitor okadaic acid suggesting that cofilin phosphatase is not a PP1/PP2A type phosphatase. Earlier, Davidson and Haslam also made a similar observation in thrombin-stimulated platelets (Davidson and Haslam 1994). In contrast to these observations, few studies suggested that these okadaic acid-sensitive phosphatases are capable of associating with cofilin and dephosphorylating it, for example in T-lymphocytes (Samstag et al. 1996; Ambach et al. 2000). However, in other cell types okadaic acid failed to inhibit cofilin dephosphorylation (Takuma et al. 1996; Heyworth et al. 1997). Our results showing that okadaic acid did not affect the cofilin dephosphorylation support the idea that cofilin might be dephosphorylated by a specific cofilin phosphatase such as the recently identified "slingshot", which is insensitive to inhibition by okadaic acid (Niwa et al. 2002) or "chronophin", a novel HAD-type serine protein phosphatase (Gohla et al. 2005). However, the presence of slingshot family (SSH) proteins and chronophin in platelets is not known. Recently, a transcriptome study identified the presence of SSH2 mRNA in platelets, whereas mRNA of SSH1 and SSH3 was not found indicating that SSH2 might be present in platelets (Bugert and Kluter 2006).

Surprisingly, in some studies inhibitors of PP1/PP2A type phosphatases (okadaic acid and calyculin A) themselves induced cofilin dephosphorylation (Okada et al. 1996; Takuma et al. 1996; Djafarzadeh and Niggli 1997). In our study, also okadaic acid and calyculin A induced cofilin dephosphorylation in resting platelets (data not shown), and cofilin rephosphorylation was completely abolished in thrombin-stimulated platelets that were pretreated with okadaic acid, although LIMK-1 immunoprecipitates from okadaic acid-treated platelets showed an increased LIMK-1 activity towards cofilin. Hence, these results rule out the possibility of okadaic acid inhibiting LIMK-1-mediated cofilin rephosphorylation in thrombin-stimulated platelets. These observations suggest that PP1/PP2A type phosphatases might negatively regulate the cofilin phosphatase either by dephosphorylation of some mediator protein or the cofilin phosphatase itself.

Davidson and Haslam had shown that calcium ionophore A23187 induces cofilin dephosphorylation in platelets (Davidson and Haslam 1994). The cAMP-stimulated dephosphorylation of cofilin in a neuronal cell line was inhibited by PP1 and PP2A phosphatases inhibitor calyculin A (Meberg et al. 1998). In addition, cofilin dephosphorylation by chemotactic peptide in leukocytes was inhibited by the PI3-kinase inhibitor wortmannin. However, wortmannin did not block phorbol ester-induced cofilin dephosphorylation, which was inhibited by inhibitors of calcium-independent forms of PKC (Okada et al. 1996). Thus, these studies show that multiple signaling pathways involving calcium, cAMP, PKC and PI3-kinase can mediate stimulus-induced cofilin dephosphorylation in different cell types. Recently, most of these cofilin-dephosphorylating pathways have now been linked to the activation of slingshot. One study showed that insulin-induced cofilin dephosphorylation in MCF-7 cells is due to PI3-kinase-mediated activation of slingshot. Our results of inhibition of thrombin-induced cofilin dephosphorylation by wortmannin in platelets similarly suggest that a PI3-kinase mediates cofilin dephosphorylation. However, the lack of inhibition of cofilin dephosphorylation by specific inhibitors of Akt, a downstream protein kinase target of PI3-kinase, indicates that PI3-kinase regulates cofilin dephosphorylation not through the Akt signaling pathway. One possibility is that the lipid target of PI3-kinase-mediated signaling PIP_2 is involved. PIP_2 is known to bind cofilin (inhibiting its activity) as well as phospho-cofilin (Moriyama et al. 1996). PIP_3, the product of PIP_2 phosphorylation by PI3-kinase has a slightly lower affinity towards cofilin binding as compared to PIP_2 (Ojala et al. 2001). Phosphorylation of PIP_2 to PIP_3 might lead to dissociation of phospho-cofilin from the complex and thereby could facilitate cofilin dephosphorylation. In support of such a relation of PIP_3/cofilin dephosphorylation and PIP_2/cofilin phosphorylation, it has been shown that cells overexpressed with PTEN (phosphatase and tensin homolog deleted in chromosome 10), which dephosphorylates PIP_3 to PIP_2, showed an increase of cofilin phosphorylation, whereas PTEN deficient cells showed a decrease in cofilin phosphorylation (Nishita et al. 2004).

Cofilin undergoes dephosphorylation in response to extracellular stimuli that elevate intracellular Ca^{2+} concentrations. An increase of cytosolic Ca^{2+} concentration after platelet stimulation with Ca^{2+} ionophores leads to cofilin dephosphorylation and secretion (Siess 1989; Davidson and Haslam 1994; Wang et al. 2005). Platelets stimulated with high concentrations of LPA (>1μM) and thrombin, which showed a rapid cofilin dephosphorylation, are associated with a rise in intracellular Ca^{2+} (Maschberger et al. 2000). Preincubation of platelets with the intracellular Ca^{2+} chelator BAPTA-AM completely blocked the LPA-stimulated cofilin dephosphorylation suggesting a role of Ca^{2+} for regulating cofilin phosphatase. Recently, calcium-induced cofilin dephosphorylation was observed being mediated via calcineurin-dependent activation of slingshot (Wang et al. 2005). Calcineurin is a calcium-regulated protein phosphatase, also known as PP2B. In our study, the treatment of platelets with the calcineurin autoinhibitory domain (CAID) coupled to a membrane penetrating peptide sequence completely blocked the thrombin-induced cofilin dephosphorylation suggesting that calcium-mediated activation of calcineurin is involved in stimulating the cofilin phosphatase in platelets. Vice versa, it has recently been shown in thrombin-stimulated platelets that the rapid cofilin dephosphorylation could through changes in actin dynamics enhances cytosolic Ca^{2+} concentration through stimulation of the store-operated Ca^{2+} entry (Redondo et al. 2006).

The present study shows that the activation of cofilin phosphatase in platelets is regulated by several factors: an increase in intracellular Ca^{2+} and an activation of calcineurin and PI3-kinase positively regulates, whereas the activation of PP1/PP2A type phosphatase negatively regulates the activity of cofilin phosphatase (Figure 5.1).
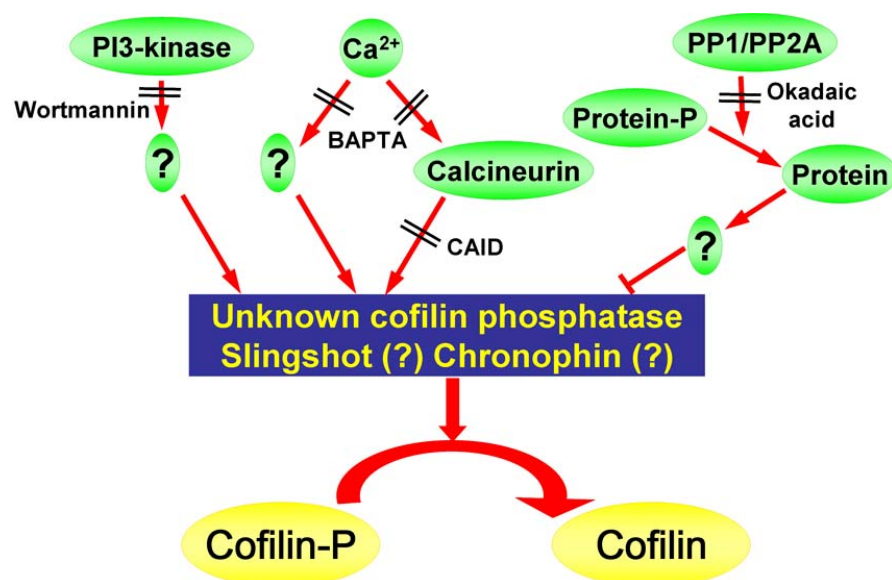
Figure 5.1 Possible factors regulating the activity of the unknown cofilin phosphatase in platelets. Cofilin dephosphorylation during platelet activation seems to be regulated by an increase in intracellular Ca2+ and by activation of calcineurin and PI3-kinase, whereas the activation of PP1/PP2A type phosphatase negatively regulates the activity of cofilin phosphatase. These factors might regulate cofilin phosphatase directly or indirectly through unidentified intermediates. Calcineurin auto inhibitory domain; CAID.
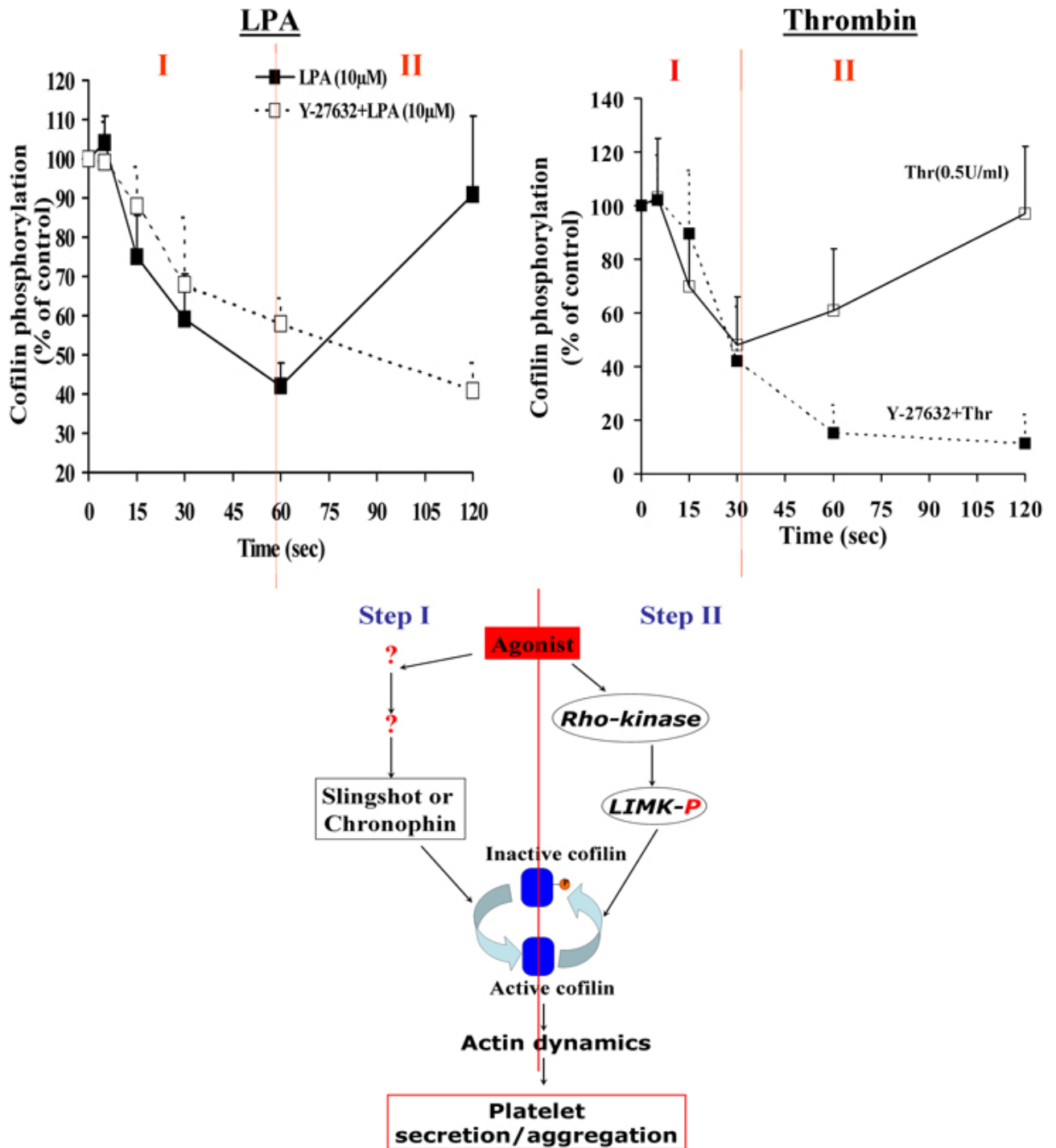
5.4. <u>Two-step model for cofilin phospho-cycle</u>

In conclusion, this study shows that Rho-kinase mediates rapid LIMK-1 activation and the increase of F-actin during shape change and aggregation/secretion induced by platelet activating agents such as thrombin and LPA. The rapid LIMK-1 activation did, however, not lead to an increased cofilin phosphorylation during shape change and the early phase of secretion. This might be explained by the simultaneous activation of two counteracting pathways regulating cofilin phosphorylation, cofilin phosphatase and LIMK-1, and by compartmentalization of LIMK-1 with reduced accessibility to cofilin in intact platelets. During secretion and aggregation the simultaneous activation of cofilin phosphatase and LIMK-1 resulted in a sequential dephosphorylation and then rephosphorylation of cofilin. LIMK-1 activation and the pathways regulating cofilin de- and rephosphorylation were independent of dense granule secretion and integrin $\alpha_{IIb}\beta_3$ activation. The early cofilin dephosphorylation by an okadaic-acid insensitive cofilin phosphatase seems to be regulated at least in part by an increase in intracellular Ca^{2+} and by PI3-kinase, and it will be interesting to examine how these pathways regulate the cofilin phosphatase, which is still to be identified (Figure 5.1). Cofilin rephosphorylation by Rho-kinase/LIMK-1 activation suggests a late influence of this pathway on cofilin-mediated rearrangement of actin cytoskeleton during platelet activation. At last, since the kinetics of cofilin phospho-cycle is similar in LPA- as well as in thrombin-stimulated platelets, we hypothesize a general two-step regulatory process for cofilin phospho-cycle underlying primarily secretion, and subsequently platelet aggregation: dephosphorylation by a cofilin phosphatase and then rephosphorylation by the Rho-kinase/LIMK-1 pathway (Figure 5.2).

Figure 5.2. Model for regulation of cofilin phospho-cycle in platelets. Top left, graphical representation for cofilin phospho-cycle during LPA-stimulated secretion and platelet aggregation. Top right, graphical representation for cofilin phospho-cycle during thrombin-stimulated secretion and aggregation. Bottom center, based on these two results, the hypothetical two-step model for cofilin-phosphocycle: initial dephosphorylation (step I) and then rephosphorylation (step II), for regulating actin dynamics beneath various platelet responses.

6. <u>Summary</u>

The activation of platelets is a central step during the physiological process of hemostasis and its understanding may lead us to control the pathophysiological process of intra-arterial thrombus formation and vascular occlusion, which can cause acute coronary syndrome and myocardial infarction. One of the important aspects of platelet activation is to understand the dynamic regulation and rearrangement of the cytoskeleton after stimulation. The morphological and functional changes of platelets require a drastic remodeling of the actin cytoskeleton regulated by numerous actin-binding proteins and signaling molecules such as the family of Rho-GTPases. The small GTPase Rho can regulate several aspects of cellular function, predominantly through its downstream effector Rho-kinase. One of the well established Rho-kinase-mediated signaling pathways is the phosphorylation of myosin light chain (MLC) and its counteracting MLC phosphatase. Rho-kinase regulates a second pathway that involves activation of LIM-kinases (LIMKs) and subsequent phosphorylation and inactivation of cofilin, an actin dynamizing protein. Dephosphorylation and activation of cofilin lead to severing and depolymerization of existing actin filaments. The signaling pathway Rho-kinase/LIMKs/cofilin phosphorylation during platelet activation and the question, how the phosphorylation of cofilin affects the actin dynamics underlying platelet activation, has not previously been studied. The physiological agonist thrombin and the pathophysiological relevant agonist lysophosphatidic acid (LPA), which is the main platelet-activating lipid in atherosclerotic plaque, were used as platelet stimuli to address these questions.

It was found that the activation of Rho-kinase is important for an increase in F-actin content underlying Ca^{2+}-independent platelet shape change. The activation of Rho-kinase was found to be upstream to secretion and integrin $\alpha_{IIb}\beta_3$ activation. The rapid activation of Rho-kinase during secretion leads to a further increase in F-actin content as compared to shape change. It was observed that LPA-stimulated dense granule secretion is mainly regulated by Rho-kinase, whereas secretion induced by thrombin was only in part Rho-kinase-dependent. Together, these results show that Rho-kinase regulates the F-actin increase underlying shape change and secretion, but it is not directly involved in aggregation.

This study for the first time demonstrates that platelet expresses only LIMK-1 and not LIMK-2. LIMK-1 can be activated by Rho-kinase as well as by p21-activated kinases (PAKs). Our study shows that LIMK-1 activation was mainly Rho-kinase dependent in LPA- and thrombin-stimulated platelets. Although, PAK-1/2 activation was observed during LPA-stimulated platelet shape change, PAKs are unlikely to be involved in LIMK-1 activation in these cells. Like Rho-kinase activation, it was also found that LIMK-1 activation was independent and upstream of integrin $\alpha_{IIb}\beta_3$ activation. Surprisingly, the activation of LIMK-1 failed to increase cofilin phosphorylation during shape change induced by LPA as well as by thrombin. Inhibition of the Rho-kinase/LIMK-1 pathway unmasked cofilin dephosphorylation suggesting that during shape change the simultaneous activation of a cofilin phosphatase counteracts the effect of LIMK-1 for

phosphorylating cofilin. During secretion and aggregation induced by LPA and thrombin, cofilin was rapidly dephosphorylated and subsequently rephosphorylated; the latter phase was due to Rho-kinase/LIMK-1 activation. After stimulation with LPA and thrombin under conditions, where platelet aggregation could not occur, the kinetics of cofilin de- and rephosphorylation were unperturbed indicating their independence of integrin $\alpha_{IIb}\beta_3$ engagement. Furthermore, the results clearly showed that cofilin dephosphorylation is also independent and upstream of secretion, since the onset of cofilin dephosphorylation was as rapid as secretion in thrombin-stimulated platelets and also occurred in the absence of dense granule secretion in LPA (10 μM)-stimulated platelets. Since the kinetics of cofilin phospho-cycle was similar during secretion and platelet aggregation in LPA- and thrombin-stimulated cells, I propose a general two-step regulatory process for cofilin phospho-cycle underlying primarily secretion, and subsequently platelet aggregation: dephosphorylation by a cofilin phosphatase and then rephosphorylation by the Rho-kinase/LIMK-1 pathway.

Our results showing that only dephosphorylated (activated) cofilin binds with F-actin support previous observations that the state of cofilin phosphorylation determines its association with F-actin. The effect of Y-27632 in resting platelets showing a reduction in cofilin phosphorylation, and an increase of F-actin content and cofilin association with F-actin suggested that LIMK-1-mediated cofilin phosphorylation reduces the F-actin content and cofilin association with F-actin in resting platelets. In contrast, during shape change, cofilin that showed no change in its phosphorylation was rapidly associated with the actin cytoskeleton. The maximal cofilin association with actin cytoskeleton occurred before the maximal F-actin increase, suggesting that cofilin association with F-actin might regulate the turnover and actin polymerization during platelet shape change. It is an open question, whether cofilin is locally dephosphorylated before binding to F-actin during shape change.

Previous studies in other cells could correlate cofilin dephosphorylation (activation) with the depolymerization of F-actin. However, in our studies cofilin dephosphorylation during the initial phase of thrombin-induced secretion (up to 30 seconds) was associated with a large increase of F-actin and a high amount of cofilin association with F-actin. Cofilin rephosphorylation after 30 seconds did not decrease F-actin content and cofilin association with F-actin. Together, in activated platelets the association of cofilin with F-actin and the F-actin increase do not simply correlate to the cofilin phosphorylation state: it seems to be more complex. It is assumed that the cofilin phosphorylation and actin dynamics are regulated in specific compartments during platelet activation.

The rapid cofilin dephosphorylation in platelets was mediated by an okadaic-acid insensitive phosphatase. The activation of the cofilin phosphatase seemed to be regulated at least in part by an increase in intracellular Ca^{2+} and by PI3-kinase. Cofilin de- and rephosphorylation occurring upstream of secretion and platelet aggregation suggests that the enzymes regulating the cofilin phospho-cycle could be potential targets for the development of anti-thrombotic drugs.

7. <u>Zusammenfassung</u>

Die Aktivierung von Blutplättchen spielt sowohl während der physiologischen Hämostase als auch bei pathologischen Prozessen wie der intraarteriellen Thrombenbildung und des damit verbundenen Gefäßverschlusses eine zentrale Rolle.

Einer der wichtigen Aspekte der Plättchenaktivierung ist die Dynamik und Umorganisation des Zytoskelettes nach Stimulation der Thrombozyten. Die morphologischen und funktionellen Veränderungen der Plättchen erfordern eine drastische Umorganisation des Aktin-Zytoskelettes, welches durch eine Vielzahl Aktin-bindender Proteine und Signalmoleküle, wie zum Beispiel Moleküle der Familie der Rho-GTPasen, gesteuert wird. Die kleine GTPase Rho reguliert verschiedenste Zellfunktionen, hauptsächlich durch ihren nachgeschalteten Effektor Rho-Kinase. Einer der Signaltransduktionswege der Rho-Kinase verläuft über die Phosphorylierung der *myosin light chain* (MLC) und deren Gegenspieler der MLC-Phosphatase. Ein zweiter Signalweg involviert die Aktivierung von LIM-Kinasen (LIMK) und die nachfolgende Phosphorylierung und Inaktivierung von Cofilin, einem Aktin dynamisierendem Protein. Dephosphorylierung und Aktivierung von Cofilin resultiert in einer Spaltung und Depolymerisation von Aktinfilamenten.

Es ist bisher nicht untersucht worden, ob während der Thrombozytenaktivierung der Signalweg über die Rho-kinase/LIM-kinase/Cofilin-Phosphorylierung aktiviert wird und wie die Cofilinaktivierung die Aktindynamik, welche der Plättchenaktivierung zugrunde liegt, beeinflusst. Um diese Fragestellungen zu beantworten wurde der physiologische Agonist Thrombin und der pathophysiologisch relevante Agonist Lysophosphatidsäure (LPA), welche als thrombogene Substanz in atherosklerotischen Plaques enthalten ist, als Plättchenstimuli eingesetzt und die nachfolgende Regulierung des Rho-Kinase/LIM-Kinase/Cofilin-Phosphorylierungsweges untersucht.

In unseren Untersuchungen konnten wir zeigen, dass die Aktivierung der Rho-Kinase für einen Anstieg des F-Aktin-Gehaltes während der kalziumunabhängigen Konformationsänderung der Thrombozyten, induziert durch LPA oder Thrombin, von Bedeutung ist. Die Aktivierung der Rho-Kinase war einer Sekretion der Plättchengranula und einer Integrin $\alpha_{IIb}\beta_3$-Aktivierung vorgeschaltet. Die schnelle Aktivierung der Rho-Kinase führte während der Sekretion der Granulainhaltstoffe und der Thrombozytenaggregation zu einem vermehrten Anstieg des F-Aktin-Gehaltes im Vergleich zum shape change. Es konnte beobachtet werden, dass die durch LPA stimulierte Sekretion der dichten Granula in den Plättchen hauptsächlich durch Rho-Kinase reguliert wurde, während die Sekretion die durch Thrombin induziert wurde, nur teilweise Rho-Kinase abhängig war. Diese Resultate zeigen zusammen, dass Rho-Kinase den F-Aktin-Anstieg, der einer Formänderung und der Sekretion der Plättchen zu Grunde liegt, reguliert, aber nicht direkt an der Aggregation beteiligt ist.

Zum ersten Mal konnte durch diese Arbeit gezeigt werden, dass Plättchen nur LIMK-1 exprimieren und nicht LIMK-2. Erstere kann durch die Rho-Kinase sowie durch p21-aktivierte Kinasen (PAKs) aktiviert werden. Wir konnten zeigen, dass die LIMK-1 Aktivierung in stimulierten Plättchen ausschließlich von der Rho-Kinase abhängig ist. Obwohl eine PAK1/2 Aktivierung während des LPA-stimulierten *shape change* beobachtet werden kann, sind in LPA-stimulierten Plättchen PAKs wahrscheinlich nicht an einer LIMK-1-Aktivierung beteiligt. Es wurde gezeigt, dass die LIMK-1-Aktivierung genau wie die Rho-Kinase-Aktivierung unabhängig von der Integrin $\alpha_{IIb}\beta_3$-Aktivierung ist und die Rho-Kinase-Aktivierung einer LIMK-1-Aktivierung vorgeschaltet ist.

Überraschenderweise führte die durch Thrombin und LPA aktivierte LIMK-1 nicht zu einem Anstieg der Phosphorylierung von Cofilin während des *shape change*. Durch Hemmung des Rho-Kinase/LIM-Kinase Signalweges wurde eine Cofilin-Dephosphorylierung deutlich, was darauf hindeutete, dass die gleichzeitige Stimulierung von Cofilin-Phosphatasen der Wirkung einer LIMK-1 vermittelten Cofilin-Phosphorylierung entgegenwirkt. Während der LPA- und Thrombin-induzierten Plättchensekretion und Aggregation wurde Cofilin zuerst sehr schnell dephosphoryliert und anschließend, infolge der LIMK-1 Aktivierung, rephosphoryliert. Nach Stimulation mit LPA und Thrombin unter Bedingungen, unter denen keine Plättchen-aggregation auftritt, war die Cofilin-Phosphorylierung und Dephosphorylierung unverändert, was zeigt, dass Kinetik des Cofilin-Phosphorylierungszyklus unabhängig von der Integrin $\alpha_{IIb}\beta_3$ Einbindung ist.

Weiterhin wird durch diese Ergebnisse gezeigt, dass die Cofilin-Dephosphorylierung unabhängig von der Sekretion abläuft und dieser vorgeschaltet ist, da die Dephosphorylierung von Cofilin ebenso schnell wie die Sekretion in Thrombin-stimulierten Plättchen auftrat und auch in Abwesenheit einer dichten Granula-Sekretion nachgewiesen werden konnte, wenn Plättchen ohne Fibrinogen mit LPA (10 µM) stimuliert wurden. Da die Kinetik des Cofilin Phosphorylierungszyklus ähnlich in LPA- als auch in Thrombin-stimulierten Plättchen ist, schlage ich einen generellen Zwei-Schritt Regulationsmechanismus vor: Zuerst eine Dephosphorylierung durch eine Cofilin-Phosphatase und nachfolgend eine Rephosphorylierung durch den Rho-Kinase/ LIMK-1 Signalweg. Dieser Cofilin-Phosphorylierungszyklus reguliert primär die Sekretion und sekundär die Aggregation.

Unsere Beobachtungen, die zeigen, dass nur dephosphoryliertes, aktiviertes Cofilin an F-Aktin bindet, stützen vorherige Resultate, dass der Cofilin-Phosphorylierungsstatus die F-Aktin-Assoziation bestimmt. Der Effekt von Y-27632 in ruhenden Plättchen, welches eine Reduktion der Cofilin Phosphorylierung, einen F-Aktin-Anstieg und eine Steigerung in der Cofilin-Aktin-Assoziation bewirkt, lässt vermuten, dass die LIMK-1 vermittelte Cofilin-Phosphorylierung den F-Aktin Gehalt und auch die Cofilin-Aktin-Assoziation in ruhenden Plättchen reduziert. Die Situation ist anders als in aktivierten Thrombozyten: hier zeigte das Cofilin, welches keine Veränderung seiner Phosphorylierung während des Gestaltwandels von Plättchen aufwies, eine schnelle Assoziation mit F-Aktin. Die maximale Cofilin-Aktinzytoskelett-Interaktion fand vor

dem maximalen F-Aktin-Anstieg statt, was auf eine Regulation des Aktin-*turnove*r und der Aktinpolymerisation durch Cofilin während der Konformationsänderung der Thrombozyten hinweist. In bisherigen Studien an anderen Zellen wird die Dephosphorylierung von Cofilin, also dessen Aktivierung, vor allem mit einer Aktindepolymerisation in Verbindung gebracht. Hingegen konnten wir in unseren Studien belegen, dass während der Anfangsphase der Thrombin induzierten Sekretion eine Cofilindephosphorylierung mit einem enormen Anstieg des F-Aktin-Gehaltes und einer starken Cofilin-F-Aktin-Interaktion assoziiert war. Durch die Rephosphorylierung von Cofilin 30 Sekunden bis 2 min nach Stimulation zeigte sich kein Rückgang im F-Aktin-Gehalt oder in der Assoziation von Cofilin mit dem Aktin-Zytoskelett. Zusammengenommen zeigen diese Ergebnisse die Komplexität der Regulation der Cofilin-Phosphorylierung und dessen Assoziation mit F-Aktin.

Die schnelle Cofilin-Dephosphorylierung in Plättchen wurde durch eine Okadaic-Säure insensitive Phosphatase katalysiert. Die Aktivierung dieser Phosphatase schien zumindest teilweise durch einen Anstieg des intrazellulären Kalziums und durch die PI3-Kinase reguliert zu sein. Die Enzyme, die den Cofilin-Phosphorylierungs-Dephosphorylierungszyklus regulieren, welcher der Sekretion der Plättchengranula und der Plättchenaggregation vorgeschaltet ist, könnten als potentielle medikamentöse Ziele für antithrombotische Medikamente dienen

8. <u>References</u>

Acevedo, K., N. Moussi, R. Li, P. Soo and O. Bernard (2006). "LIM kinase 2 is widely expressed in all tissues." <u>J Histochem Cytochem</u> **54**(5): 487-501.

Aizawa, H., K. Sutoh and I. Yahara (1996). "Overexpression of cofilin stimulates bundling of actin filaments, membrane ruffling, and cell movement in Dictyostelium." <u>J Cell Biol</u> **132**(3): 335-44.

Aizawa, H., S. Wakatsuki, A. Ishii, K. Moriyama, Y. Sasaki, K. Ohashi, Y. Sekine-Aizawa, A. Sehara-Fujisawa, K. Mizuno, Y. Goshima and I. Yahara (2001). "Phosphorylation of cofilin by LIM-kinase is necessary for semaphorin 3A-induced growth cone collapse." <u>Nat Neurosci</u> **4**(4): 367-73.

Allwood, E. G., A. P. Smertenko and P. J. Hussey (2001). "Phosphorylation of plant actin-depolymerising factor by calmodulin-like domain protein kinase." <u>FEBS Lett</u> **499**(1-2): 97-100.

Amano, M., M. Ito, K. Kimura, Y. Fukata, K. Chihara, T. Nakano, Y. Matsuura and K. Kaibuchi (1996). "Phosphorylation and activation of myosin by Rho-associated kinase (Rho-kinase)." <u>J Biol Chem</u> **271**(34): 20246-9.

Ambach, A., J. Saunus, M. Konstandin, S. Wesselborg, S. C. Meuer and Y. Samstag (2000). "The serine phosphatases PP1 and PP2A associate with and activate the actin-binding protein cofilin in human T lymphocytes." <u>Eur J Immunol</u> **30**(12): 3422-31.

Arai, H. and Y. Atomi (2003). "Suppression of cofilin phosphorylation in insulin-stimulated ruffling membrane formation in KB cells." <u>Cell Struct Funct</u> **28**(1): 41-8.

Arber, S., F. A. Barbayannis, H. Hanser, C. Schneider, C. A. Stanyon, O. Bernard and P. Caroni (1998). "Regulation of actin dynamics through phosphorylation of cofilin by LIM-kinase." <u>Nature</u> **393**(6687): 805-9.

Aszodi, A., A. Pfeifer, M. Ahmad, M. Glauner, X. H. Zhou, L. Ny, K. E. Andersson, B. Kehrel, S. Offermanns and R. Fassler (1999). "The vasodilator-stimulated phosphoprotein (VASP) is involved in cGMP- and cAMP-mediated inhibition of agonist-induced platelet aggregation, but is dispensable for smooth muscle function." <u>Embo J</u> **18**(1): 37-48.

Azim, A. C., K. Barkalow, J. Chou and J. H. Hartwig (2000). "Activation of the small GTPases, rac and cdc42, after ligation of the platelet PAR-1 receptor." <u>Blood</u> **95**(3): 959-64.

Bailly, M., I. Ichetovkin, W. Grant, N. Zebda, L. M. Machesky, J. E. Segall and J. Condeelis (2001). "The F-actin side binding activity of the Arp2/3 complex is essential for actin nucleation and lamellipod extension." <u>Curr Biol</u> **11**(8): 620-5.

Ballem, P. J., A. Belzberg, D. V. Devine, D. Lyster, B. Spruston, H. Chambers, P. Doubroff and K. Mikulash (1992). "Kinetic studies of the mechanism of thrombocytopenia in patients with human immunodeficiency virus infection." <u>N Engl J Med</u> **327**(25): 1779-84.

Bamburg, J. R. (1999). "Proteins of the ADF/cofilin family: essential regulators of actin dynamics." <u>Annu Rev Cell Dev Biol</u> **15**: 185-230.

Bamburg, J. R., H. E. Harris and A. G. Weeds (1980). "Partial purification and characterization of an actin depolymerizing factor from brain." <u>FEBS Lett</u> **121**(1): 178-82.

Bamburg, J. R., A. McGough and S. Ono (1999). "Putting a new twist on actin: ADF/cofilins modulate actin dynamics." <u>Trends Cell Biol</u> **9**(9): 364-70.

Bamburg, J. R. and O. P. Wiggan (2002). "ADF/cofilin and actin dynamics in disease." <u>Trends Cell Biol</u> **12**(12): 598-605.

Barkalow, K., W. Witke, D. J. Kwiatkowski and J. H. Hartwig (1996). "Coordinated regulation of platelet actin filament barbed ends by gelsolin and capping protein." J Cell Biol **134**(2): 389-99.

Bauer, M., M. Retzer, J. I. Wilde, P. Maschberger, M. Essler, M. Aepfelbacher, S. P. Watson and W. Siess (1999). "Dichotomous regulation of myosin phosphorylation and shape change by Rho-kinase and calcium in intact human platelets." Blood **94**(5): 1665-72.

Bennett, J. S., S. Zigmond, G. Vilaire, M. E. Cunningham and B. Bednar (1999). "The platelet cytoskeleton regulates the affinity of the integrin alpha(IIb)beta(3) for fibrinogen." J Biol Chem **274**(36): 25301-7.

Bierne, H., E. Gouin, P. Roux, P. Caroni, H. L. Yin and P. Cossart (2001). "A role for cofilin and LIM kinase in Listeria-induced phagocytosis." J Cell Biol **155**(1): 101-12.

Birkenfeld, J., H. Betz and D. Roth (2003). "Identification of cofilin and LIM-domain-containing protein kinase 1 as novel interaction partners of 14-3-3 zeta." Biochem J **369**(Pt 1): 45-54.

Blondin, L., V. Sapountzi, S. K. Maciver, C. Renoult, Y. Benyamin and C. Roustan (2001). "The second ADF/cofilin actin-binding site exists in F-actin, the cofilin-G-actin complex, but not in G-actin." Eur J Biochem **268**(24): 6426-34.

Bobkov, A. A., A. Muhlrad, K. Kokabi, S. Vorobiev, S. C. Almo and E. Reisler (2002). "Structural effects of cofilin on longitudinal contacts in F-actin." J Mol Biol **323**(4): 739-50.

Bokoch, G. M. (2003). "Biology of the p21-activated kinases." Annu Rev Biochem **72**: 743-81.

Bornstein, P. (2001). "Thrombospondins as matricellular modulators of cell function." J Clin Invest **107**(8): 929-34.

Brass, L. F. (2003). "Thrombin and platelet activation." Chest **124**(3 Suppl): 18S-25S.

Brill, S., S. Li, C. W. Lyman, D. M. Church, J. J. Wasmuth, L. Weissbach, A. Bernards and A. J. Snijders (1996). "The Ras GTPase-activating-protein-related human protein IQGAP2 harbors a potential actin binding domain and interacts with calmodulin and Rho family GTPases." Mol Cell Biol **16**(9): 4869-78.

Bugert, P. and H. Kluter (2006). "Profiling of gene transcripts in human platelets: an update of the platelet transcriptome." Platelets **17**(7): 503-4.

Carlier, M. F., V. Laurent, J. Santolini, R. Melki, D. Didry, G. X. Xia, Y. Hong, N. H. Chua and D. Pantaloni (1997). "Actin depolymerizing factor (ADF/cofilin) enhances the rate of filament turnover: implication in actin-based motility." J Cell Biol **136**(6): 1307-22.

Carlsson, L., F. Markey, I. Blikstad, T. Persson and U. Lindberg (1979). "Reorganization of actin in platelets stimulated by thrombin as measured by the DNase I inhibition assay." Proc Natl Acad Sci U S A **76**(12): 6376-80.

Carpenter, C. L., K. F. Tolias, A. C. Couvillon and J. H. Hartwig (1997). "Signal transduction pathways involving the small G proteins rac and Cdc42 and phosphoinositide kinases." Adv Enzyme Regul **37**: 377-90.

Carvalho, A. C., R. W. Colman and R. S. Lees (1974). "Platelet function in hyperlipoproteinemia." N Engl J Med **290**(8): 434-8.

Cazenave JP, M. J., Sutter-Bay A, Gachet C, Toti F and Beretz A (1993). A centrifugation techniques for the preparation of suspensions of non activated washed human platelets, Kluwer Academics Publishers.

Chan, A. Y., M. Bailly, N. Zebda, J. E. Segall and J. S. Condeelis (2000). "Role of cofilin in epidermal growth factor-stimulated actin polymerization and lamellipod protrusion." J Cell Biol **148**(3): 531-42.

Chang, J. C., H. H. Chang, C. T. Lin and S. J. Lo (2005). "The integrin alpha6beta1 modulation of PI3K and Cdc42 activities induces dynamic filopodium formation in human platelets." J Biomed Sci **12**(6): 881-98.

Chaponnier, C. and G. Gabbiani (2004). "Pathological situations characterized by altered actin isoform expression." J Pathol **204**(4): 386-95.

Chen, J., S. De, D. S. Damron, W. S. Chen, N. Hay and T. V. Byzova (2004). "Impaired platelet responses to thrombin and collagen in AKT-1-deficient mice." Blood **104**(6): 1703-10.

Chen, J., D. Godt, K. Gunsalus, I. Kiss, M. Goldberg and F. A. Laski (2001). "Cofilin/ADF is required for cell motility during Drosophila ovary development and oogenesis." Nat Cell Biol **3**(2): 204-9.

Chen, J. and J. A. Lopez (2005). "Interactions of platelets with subendothelium and endothelium." Microcirculation **12**(3): 235-46.

Chernoff, A., R. F. Levine and D. S. Goodman (1980). "Origin of platelet-derived growth factor in megakaryocytes in guinea pigs." J Clin Invest **65**(4): 926-30.

Choi, W., Z. A. Karim and S. W. Whiteheart (2006). "Arf6 plays an early role in platelet activation by collagen and convulxin." Blood **107**(8): 3145-52.

Chrzanowska-Wodnicka, M., S. S. Smyth, S. M. Schoenwaelder, T. H. Fischer and G. C. White, 2nd (2005). "Rap1b is required for normal platelet function and hemostasis in mice." J Clin Invest **115**(3): 680-7.

Cohen, I. (1979). "The contractile system of blood platelets and its function." Methods Achiev Exp Pathol **9**: 40-86.

Coleman, M. L., E. A. Sahai, M. Yeo, M. Bosch, A. Dewar and M. F. Olson (2001). "Membrane blebbing during apoptosis results from caspase-mediated activation of ROCK I." Nat Cell Biol **3**(4): 339-45.

Cotteret, S. and J. Chernoff (2002). "The evolutionary history of effectors downstream of Cdc42 and Rac." Genome Biol **3**(2): REVIEWS0002.

Covic, L., A. L. Gresser and A. Kuliopulos (2000). "Biphasic kinetics of activation and signaling for PAR1 and PAR4 thrombin receptors in platelets." Biochemistry **39**(18): 5458-67.

Cox, A. C. (1988). "Cytochalasin E enhances the protein kinase C-dependent process of secretion." Biochem Biophys Res Commun **150**(2): 745-51.

Cunningham, J. G., S. C. Meyer and J. E. Fox (1996). "The cytoplasmic domain of the alpha-subunit of glycoprotein (GP) Ib mediates attachment of the entire GP Ib-IX complex to the cytoskeleton and regulates von Willebrand factor-induced changes in cell morphology." J Biol Chem **271**(19): 11581-7.

Dan, C., A. Kelly, O. Bernard and A. Minden (2001). "Cytoskeletal changes regulated by the PAK4 serine/threonine kinase are mediated by LIM kinase 1 and cofilin." J Biol Chem **276**(34): 32115-21.

Danen, E. H., J. van Rheenen, W. Franken, S. Huveneers, P. Sonneveld, K. Jalink and A. Sonnenberg (2005). "Integrins control motile strategy through a Rho-cofilin pathway." J Cell Biol **169**(3): 515-26.

Daniel, J. L. and R. S. Adelstein (1976). "Isolation and properties of platelet myosin light chain kinase." Biochemistry **15**(11): 2370-7.

Daniel, R.-S. S. a. D. (1981). Platelets in Biology and Pathology-2. North Holland, Elsevier/North-Holland Biomedical Press.

Davidson, M. M. and R. J. Haslam (1994). "Dephosphorylation of cofilin in stimulated platelets: roles for a GTP-binding protein and Ca2+." Biochem J **301 (Pt 1)**: 41-7.

De La Cruz, E. M. (2005). "Cofilin binding to muscle and non-muscle actin filaments: isoform-dependent cooperative interactions." J Mol Biol **346**(2): 557-64.

De La Cruz, E. M. and T. D. Pollard (1995). "Nucleotide-free actin: stabilization by sucrose and nucleotide binding kinetics." Biochemistry **34**(16): 5452-61.

Dedova, I. V., O. P. Nikolaeva, V. V. Mikhailova, C. G. dos Remedios and D. I. Levitsky (2004). "Two opposite effects of cofilin on the thermal unfolding of F-actin: a differential scanning calorimetric study." Biophys Chem **110**(1-2): 119-28.

Deshayes, S., M. C. Morris, G. Divita and F. Heitz (2005). "Cell-penetrating peptides: tools for intracellular delivery of therapeutics." Cell Mol Life Sci **62**(16): 1839-49.

DesMarais, V., M. Ghosh, R. Eddy and J. Condeelis (2005). "Cofilin takes the lead." J Cell Sci **118**(Pt 1): 19-26.

DesMarais, V., F. Macaluso, J. Condeelis and M. Bailly (2004). "Synergistic interaction between the Arp2/3 complex and cofilin drives stimulated lamellipod extension." J Cell Sci **117**(Pt 16): 3499-510.

Diaz-Ricart, M., G. Arderiu, E. Estebanell, S. Perez-Pujol, M. Lozano, J. G. White, G. Escolar and A. Ordinas (2002). "Inhibition of cytoskeletal assembly by cytochalasin B prevents signaling through tyrosine phosphorylation and secretion triggered by collagen but not by thrombin." Am J Pathol **160**(1): 329-37.

Didry, D., M. F. Carlier and D. Pantaloni (1998). "Synergy between actin depolymerizing factor/cofilin and profilin in increasing actin filament turnover." J Biol Chem **273**(40): 25602-11.

Disanza, A., A. Steffen, M. Hertzog, E. Frittoli, K. Rottner and G. Scita (2005). "Actin polymerization machinery: the finish line of signaling networks, the starting point of cellular movement." Cell Mol Life Sci **62**(9): 955-70.

Djafarzadeh, S. and V. Niggli (1997). "Signaling pathways involved in dephosphorylation and localization of the actin-binding protein cofilin in stimulated human neutrophils." Exp Cell Res **236**(2): 427-35.

Dorsam, R. T., S. Kim, J. Jin and S. P. Kunapuli (2002). "Coordinated signaling through both G12/13 and G(i) pathways is sufficient to activate GPIIb/IIIa in human platelets." J Biol Chem **277**(49): 47588-95.

Dorsam, R. T., M. Tuluc and S. P. Kunapuli (2004). "Role of protease-activated and ADP receptor subtypes in thrombin generation on human platelets." J Thromb Haemost **2**(5): 804-12.

dos Remedios, C. G., D. Chhabra, M. Kekic, I. V. Dedova, M. Tsubakihara, D. A. Berry and N. J. Nosworthy (2003). "Actin binding proteins: regulation of cytoskeletal microfilaments." Physiol Rev **83**(2): 433-73.

Edwards, D. C., L. C. Sanders, G. M. Bokoch and G. N. Gill (1999). "Activation of LIM-kinase by Pak1 couples Rac/Cdc42 GTPase signalling to actin cytoskeletal dynamics." Nat Cell Biol **1**(5): 253-9.

Escolar, G., M. Krumwiede and J. G. White (1986). "Organization of the actin cytoskeleton of resting and activated platelets in suspension." Am J Pathol **123**(1): 86-94.

Escolar, G. and J. G. White (1991). "The platelet open canalicular system: a final common pathway." Blood Cells **17**(3): 467-85; discussion 486-95.

Falet, H., G. Chang, B. Brohard-Bohn, F. Rendu and J. H. Hartwig (2005). "Integrin alpha(IIb)beta3 signals lead cofilin to accelerate platelet actin dynamics." Am J Physiol Cell Physiol **289**(4): C819-25.

Falet, H., K. M. Hoffmeister, R. Neujahr and J. H. Hartwig (2002). "Normal Arp2/3 complex activation in platelets lacking WASp." Blood **100**(6): 2113-22.

Flaumenhaft, R. (2003). "Molecular basis of platelet granule secretion." Arterioscler Thromb Vasc Biol **23**(7): 1152-60.

Flaumenhaft, R., J. R. Dilks, N. Rozenvayn, R. A. Monahan-Earley, D. Feng and A. M. Dvorak (2005). "The actin cytoskeleton differentially regulates platelet alpha-granule and dense-granule secretion." Blood **105**(10): 3879-87.

Foletta, V. C., M. A. Lim, J. Soosairajah, A. P. Kelly, E. G. Stanley, M. Shannon, W. He, S. Das, J. Massague and O. Bernard (2003). "Direct signaling by the BMP type II receptor via the cytoskeletal regulator LIMK1." J Cell Biol **162**(6): 1089-98.

Foletta, V. C., N. Moussi, P. D. Sarmiere, J. R. Bamburg and O. Bernard (2004). "LIM kinase 1, a key regulator of actin dynamics, is widely expressed in embryonic and adult tissues." Exp Cell Res **294**(2): 392-405.

Fox, J. E. (1993). "The platelet cytoskeleton." Thromb Haemost **70**(6): 884-93.

Fox, J. E. (1999). "On the role of calpain and Rho proteins in regulating integrin-induced signaling." Thromb Haemost **82**(2): 385-91.

Fox, J. E. (2001). "Cytoskeletal proteins and platelet signaling." Thromb Haemost **86**(1): 198-213.

Fox, J. E., S. J. Shattil, R. L. Kinlough-Rathbone, M. Richardson, M. A. Packham and D. A. Sanan (1996). "The platelet cytoskeleton stabilizes the interaction between alphaIIbbeta3 and its ligand and induces selective movements of ligand-occupied integrin." J Biol Chem **271**(12): 7004-11.

Fox, J. E., R. G. Taylor, M. Taffarel, J. K. Boyles and D. E. Goll (1993). "Evidence that activation of platelet calpain is induced as a consequence of binding of adhesive ligand to the integrin, glycoprotein IIb-IIIa." J Cell Biol **120**(6): 1501-7.

Freson, K., R. De Vos, C. Wittevrongel, C. Thys, J. Defoor, L. Vanhees, J. Vermylen, K. Peerlinck and C. Van Geet (2005). "The TUBB1 Q43P functional polymorphism reduces the risk of cardiovascular disease in men by modulating platelet function and structure." Blood **106**(7): 2356-62.

Gachet, C. (2001). "ADP receptors of platelets and their inhibition." Thromb Haemost **86**(1): 222-32.

Galkin, V. E., A. Orlova, N. Lukoyanova, W. Wriggers and E. H. Egelman (2001). "Actin depolymerizing factor stabilizes an existing state of F-actin and can change the tilt of F-actin subunits." J Cell Biol **153**(1): 75-86.

Gawaz, M. (2001). Blood platelets: physiology, pathophysiology, membrane receptors, antiplatelet principles, and therapy for atherothrombotic diseases, Georg Thieme Verlag.

Ghosh, M., X. Song, G. Mouneimne, M. Sidani, D. S. Lawrence and J. S. Condeelis (2004). "Cofilin promotes actin polymerization and defines the direction of cell motility." Science **304**(5671): 743-6.

Gohla, A., J. Birkenfeld and G. M. Bokoch (2005). "Chronophin, a novel HAD-type serine protein phosphatase, regulates cofilin-dependent actin dynamics." Nat Cell Biol **7**(1): 21-9.

Gohla, A. and G. M. Bokoch (2002). "14-3-3 regulates actin dynamics by stabilizing phosphorylated cofilin." Curr Biol **12**(19): 1704-10.

Goldschmidt-Clermont, P. J., M. I. Furman, D. Wachsstock, D. Safer, V. T. Nachmias and T. D. Pollard (1992). "The control of actin nucleotide exchange by thymosin beta 4 and profilin. A potential regulatory mechanism for actin polymerization in cells." Mol Biol Cell **3**(9): 1015-24.

Goyal, P. (2005). Dual function of LIMK2 in endothelial cells. Institut für Prophylaxe und Epidermiologie der Kreislaufkrankheiten. Munich, Ludwig-Maximillians Universität: 138.

Gratacap, M. P., B. Payrastre, B. Nieswandt and S. Offermanns (2001). "Differential regulation of Rho and Rac through heterotrimeric G-proteins and cyclic nucleotides." J Biol Chem **276**(51): 47906-13.

Gunning, P. W., G. Schevzov, A. J. Kee and E. C. Hardeman (2005). "Tropomyosin isoforms: divining rods for actin cytoskeleton function." Trends Cell Biol **15**(6): 333-41.

Gunsalus, K. C., S. Bonaccorsi, E. Williams, F. Verni, M. Gatti and M. L. Goldberg (1995). "Mutations in twinstar, a Drosophila gene encoding a cofilin/ADF homologue, result in defects in centrosome migration and cytokinesis." J Cell Biol **131**(5): 1243-59.

Hagmann, J., M. Grob, A. Welman, G. van Willigen and M. M. Burger (1998). "Recruitment of the LIM protein hic-5 to focal contacts of human platelets." J Cell Sci **111 (Pt 15)**: 2181-8.

Hartshorne, D. J. (1998). "Myosin phosphatase: subunits and interactions." Acta Physiol Scand **164**(4): 483-93.

Hartwig, J. and J. Italiano, Jr. (2003). "The birth of the platelet." J Thromb Haemost **1**(7): 1580-6.

Hartwig, J. H., K. Barkalow, A. Azim and J. Italiano (1999). "The elegant platelet: signals controlling actin assembly." Thromb Haemost **82**(2): 392-8.

Hartwig, J. H., G. M. Bokoch, C. L. Carpenter, P. A. Janmey, L. A. Taylor, A. Toker and T. P. Stossel (1995). "Thrombin receptor ligation and activated Rac uncap actin filament barbed ends through phosphoinositide synthesis in permeabilized human platelets." Cell **82**(4): 643-53.

Haseruck, N., W. Erl, D. Pandey, G. Tigyi, P. Ohlmann, C. Ravanat, C. Gachet and W. Siess (2004). "The plaque lipid lysophosphatidic acid stimulates platelet activation and platelet-monocyte aggregate formation in whole blood: involvement of P2Y1 and P2Y12 receptors." Blood **103**(7): 2585-92.

Hashimoto, K., K. Kawarabayashi, K. Hashimoto and N. Tatsumi (1986). "Inhibition of platelet secretion of ATP by phalloidin." Cell Biol Int Rep **10**(1): 41-7.

Haslam, R. J., M. M. Davidson and M. D. McClenaghan (1975). "Cytochalasin B, the blood platelet release reaction and cyclic GMP." Nature **253**(5491): 455-7.

Hauser, W., K. P. Knobeloch, M. Eigenthaler, S. Gambaryan, V. Krenn, J. Geiger, M. Glazova, E. Rohde, I. Horak, U. Walter and M. Zimmer (1999). "Megakaryocyte hyperplasia and enhanced agonist-induced platelet activation in vasodilator-stimulated phosphoprotein knockout mice." Proc Natl Acad Sci U S A **96**(14): 8120-5.

Hawkins, M., B. Pope, S. K. Maciver and A. G. Weeds (1993). "Human actin depolymerizing factor mediates a pH-sensitive destruction of actin filaments." Biochemistry **32**(38): 9985-93.

Hayden, S. M., P. S. Miller, A. Brauweiler and J. R. Bamburg (1993). "Analysis of the interactions of actin depolymerizing factor with G- and F-actin." Biochemistry **32**(38): 9994-10004.

Heyworth, P. G., J. M. Robinson, J. Ding, B. A. Ellis and J. A. Badwey (1997). "Cofilin undergoes rapid dephosphorylation in stimulated neutrophils and translocates to ruffled

membranes enriched in products of the NADPH oxidase complex. Evidence for a novel cycle of phosphorylation and dephosphorylation." Histochem Cell Biol **108**(3): 221-33.

Holmes, K. C., D. Popp, W. Gebhard and W. Kabsch (1990). "Atomic model of the actin filament." Nature **347**(6288): 44-9.

Holmsen, H., K. L. Kaplan and C. A. Dangelmaier (1982). "Differential energy requirements for platelet responses. A simultaneous study of aggregation, three secretory processes, arachidonate liberation, phosphatidylinositol breakdown and phosphatidate production." Biochem J **208**(1): 9-18.

Hubberstey, A. V. and E. P. Mottillo (2002). "Cyclase-associated proteins: CAPacity for linking signal transduction and actin polymerization." Faseb J **16**(6): 487-99.

Ichetovkin, I., W. Grant and J. Condeelis (2002). "Cofilin produces newly polymerized actin filaments that are preferred for dendritic nucleation by the Arp2/3 complex." Curr Biol **12**(1): 79-84.

Ichetovkin, I., J. Han, K. M. Pang, D. A. Knecht and J. S. Condeelis (2000). "Actin filaments are severed by both native and recombinant dictyostelium cofilin but to different extents." Cell Motil Cytoskeleton **45**(4): 293-306.

Ikebe, C., K. Ohashi, T. Fujimori, O. Bernard, T. Noda, E. J. Robertson and K. Mizuno (1997). "Mouse LIM-kinase 2 gene: cDNA cloning, genomic organization, and tissue-specific expression of two alternatively initiated transcripts." Genomics **46**(3): 504-8.

Ikebe, C., K. Ohashi and K. Mizuno (1998). "Identification of testis-specific (Limk2t) and brain-specific (Limk2c) isoforms of mouse LIM-kinase 2 gene transcripts." Biochem Biophys Res Commun **246**(2): 307-12.

Ishizaki, T., M. Maekawa, K. Fujisawa, K. Okawa, A. Iwamatsu, A. Fujita, N. Watanabe, Y. Saito, A. Kakizuka, N. Morii and S. Narumiya (1996). "The small GTP-binding protein Rho binds to and activates a 160 kDa Ser/Thr protein kinase homologous to myotonic dystrophy kinase." Embo J **15**(8): 1885-93.

Ito, M., T. Nakano, F. Erdodi and D. J. Hartshorne (2004). "Myosin phosphatase: structure, regulation and function." Mol Cell Biochem **259**(1-2): 197-209.

Jackson, S. P., W. S. Nesbitt and S. Kulkarni (2003). "Signaling events underlying thrombus formation." J Thromb Haemost **1**(7): 1602-12.

Jaffe, A. B. and A. Hall (2005). "Rho GTPases: biochemistry and biology." Annu Rev Cell Dev Biol **21**: 247-69.

Jantzen, H. M., D. S. Milstone, L. Gousset, P. B. Conley and R. M. Mortensen (2001). "Impaired activation of murine platelets lacking G alpha(i2)." J Clin Invest **108**(3): 477-83.

Jung, J., M. Kim, S. Choi, M. J. Kim, J. K. Suh, E. C. Choi and K. Lee (2006). "Molecular mechanism of cofilin dephosphorylation by ouabain." Cell Signal **18**(11): 2033-40.

Kabsch, W. and K. C. Holmes (1995). "The actin fold." Faseb J **9**(2): 167-74.

Kanaji, T., S. Russell and J. Ware (2002). "Amelioration of the macrothrombocytopenia associated with the murine Bernard-Soulier syndrome." Blood **100**(6): 2102-7.

Kashiwagi, H., M. Shiraga, H. Kato, T. Kamae, N. Yamamoto, S. Tadokoro, Y. Kurata, Y. Tomiyama and Y. Kanakura (2005). "Negative regulation of platelet function by a secreted cell repulsive protein, semaphorin 3A." Blood **106**(3): 913-21.

Khaitlina, S. Y. (2001). "Functional specificity of actin isoforms." Int Rev Cytol **202**: 35-98.

Khurana, T., B. Khurana and A. A. Noegel (2002). "LIM proteins: association with the actin cytoskeleton." Protoplasma **219**(1-2): 1-12.

Kirkpatrick, J. P., L. V. McIntire, J. L. Moake and P. L. Cimo (1980). "Differential effects of cytochalasin B on platelet release, aggregation and contractility: evidence against a contractile mechanism for the release of platelet granular contents." Thromb Haemost **42**(5): 1483-9.

Klages, B., U. Brandt, M. I. Simon, G. Schultz and S. Offermanns (1999). "Activation of G12/G13 results in shape change and Rho/Rho-kinase-mediated myosin light chain phosphorylation in mouse platelets." J Cell Biol **144**(4): 745-54.

Kometani, M., T. Sato and T. Fujii (1986). "Platelet cytoskeletal components involved in shape change and secretion." Thromb Res **41**(6): 801-9.

Konakahara, S., K. Ohashi, K. Mizuno, K. Itoh and T. Tsuji (2004). "CD29 integrin- and LIMK1/cofilin-mediated actin reorganization regulates the migration of haematopoietic progenitor cells underneath bone marrow stromal cells." Genes Cells **9**(4): 345-58.

Kovacsovics, T. J. and J. H. Hartwig (1996). "Thrombin-induced GPIb-IX centralization on the platelet surface requires actin assembly and myosin II activation." Blood **87**(2): 618-29.

Krishnamurthi, S., T. A. Dickens, Y. Patel, C. P. Wheeler-Jones and V. V. Kakkar (1989). "The fibrinogen-derived peptide (RGDS) prevents proteolytic degradation of protein kinase C in platelets by inhibiting platelet aggregation." Biochem Biophys Res Commun **163**(3): 1256-64.

Kunapuli, S. P., R. T. Dorsam, S. Kim and T. M. Quinton (2003). "Platelet purinergic receptors." Curr Opin Pharmacol **3**(2): 175-80.

Kureishi, Y., S. Kobayashi, M. Amano, K. Kimura, H. Kanaide, T. Nakano, K. Kaibuchi and M. Ito (1997). "Rho-associated kinase directly induces smooth muscle contraction through myosin light chain phosphorylation." J Biol Chem **272**(19): 12257-60.

Lappalainen, P. and D. G. Drubin (1997). "Cofilin promotes rapid actin filament turnover in vivo." Nature **388**(6637): 78-82.

Lappalainen, P., M. M. Kessels, M. J. Cope and D. G. Drubin (1998). "The ADF homology (ADF-H) domain: a highly exploited actin-binding module." Mol Biol Cell **9**(8): 1951-9.

Lee, K. H., S. C. Meuer and Y. Samstag (2000). "Cofilin: a missing link between T cell co-stimulation and rearrangement of the actin cytoskeleton." Eur J Immunol **30**(3): 892-9.

Lefebvre, P., J. G. White, M. D. Krumwiede and I. Cohen (1993). "Role of actin in platelet function." Eur J Cell Biol **62**(2): 194-204.

Lengsfeld, A. M., I. Low, T. Wieland, P. Dancker and W. Hasselbach (1974). "Interaction of phalloidin with actin." Proc Natl Acad Sci U S A **71**(7): 2803-7.

Leung, L. L. (1984). "Role of thrombospondin in platelet aggregation." J Clin Invest **74**(5): 1764-72.

Leung, T., X. Q. Chen, E. Manser and L. Lim (1996). "The p160 RhoA-binding kinase ROK alpha is a member of a kinase family and is involved in the reorganization of the cytoskeleton." Mol Cell Biol **16**(10): 5313-27.

Li, F. and H. N. Higgs (2003). "The mouse Formin mDia1 is a potent actin nucleation factor regulated by autoinhibition." Curr Biol **13**(15): 1335-40.

Li, R., J. Soosairajah, D. Harari, A. Citri, J. Price, H. L. Ng, C. J. Morton, M. W. Parker, Y. Yarden and O. Bernard (2006). "Hsp90 increases LIM kinase activity by promoting its homo-dimerization." Faseb J **20**(8): 1218-20.

Li, Z., E. S. Kim and E. L. Bearer (2002). "Arp2/3 complex is required for actin polymerization during platelet shape change." Blood **99**(12): 4466-74.

Li, Z., G. Zhang, G. C. Le Breton, X. Gao, A. B. Malik and X. Du (2003). "Two waves of platelet secretion induced by thromboxane A2 receptor and a critical role for phosphoinositide 3-kinases." J Biol Chem **278**(33): 30725-31.

Lian, J. P., P. G. Marks, J. Y. Wang, D. L. Falls and J. A. Badwey (2000). "A protein kinase from neutrophils that specifically recognizes Ser-3 in cofilin." J Biol Chem **275**(4): 2869-76.

Lind, S. E., H. L. Yin and T. P. Stossel (1982). "Human platelets contain gelsolin. A regulator of actin filament length." J Clin Invest **69**(6): 1384-7.

Loisel, T. P., R. Boujemaa, D. Pantaloni and M. F. Carlier (1999). "Reconstitution of actin-based motility of Listeria and Shigella using pure proteins." Nature **401**(6753): 613-6.

Lokeshwar, V. B. and L. Y. Bourguignon (1992). "The involvement of Ca2+ and myosin light chain kinase in collagen-induced platelet activation." Cell Biol Int Rep **16**(9): 883-97.

Maciver, S. K., B. J. Pope, S. Whytock and A. G. Weeds (1998). "The effect of two actin depolymerizing factors (ADF/cofilins) on actin filament turnover: pH sensitivity of F-actin binding by human ADF, but not of Acanthamoeba actophorin." Eur J Biochem **256**(2): 388-97.

Madaule, P., M. Eda, N. Watanabe, K. Fujisawa, T. Matsuoka, H. Bito, T. Ishizaki and S. Narumiya (1998). "Role of citron kinase as a target of the small GTPase Rho in cytokinesis." Nature **394**(6692): 491-4.

Maekawa, M., T. Ishizaki, S. Boku, N. Watanabe, A. Fujita, A. Iwamatsu, T. Obinata, K. Ohashi, K. Mizuno and S. Narumiya (1999). "Signaling from Rho to the actin cytoskeleton through protein kinases ROCK and LIM-kinase." Science **285**(5429): 895-8.

Maekawa, S., E. Nishida, Y. Ohta and H. Sakai (1984). "Isolation of low molecular weight actin-binding proteins from porcine brain." J Biochem (Tokyo) **95**(2): 377-85.

Marcus, K., J. Moebius and H. E. Meyer (2003). "Differential analysis of phosphorylated proteins in resting and thrombin-stimulated human platelets." Anal Bioanal Chem **376**(7): 973-93.

Maschberger, P., M. Bauer, J. Baumann-Siemons, K. J. Zangl, E. V. Negrescu, A. J. Reininger and W. Siess (2000). "Mildly oxidized low density lipoprotein rapidly stimulates via activation of the lysophosphatidic acid receptor Src family and Syk tyrosine kinases and Ca2+ influx in human platelets." J Biol Chem **275**(25): 19159-66.

McCarty, O. J., M. K. Larson, J. M. Auger, N. Kalia, B. T. Atkinson, A. C. Pearce, S. Ruf, R. B. Henderson, V. L. Tybulewicz, L. M. Machesky and S. P. Watson (2005). "Rac1 is essential for platelet lamellipodia formation and aggregate stability under flow." J Biol Chem **280**(47): 39474-84.

McGough, A. and W. Chiu (1999). "ADF/cofilin weakens lateral contacts in the actin filament." J Mol Biol **291**(3): 513-9.

McGough, A., B. Pope, W. Chiu and A. Weeds (1997). "Cofilin changes the twist of F-actin: implications for actin filament dynamics and cellular function." J Cell Biol **138**(4): 771-81.

McKim, K. S., C. Matheson, M. A. Marra, M. F. Wakarchuk and D. L. Baillie (1994). "The Caenorhabditis elegans unc-60 gene encodes proteins homologous to a family of actin-binding proteins." Mol Gen Genet **242**(3): 346-57.

McNicol, A. and S. J. Israels (1999). "Platelet dense granules: structure, function and implications for haemostasis." Thromb Res **95**(1): 1-18.

Meberg, P. J. and J. R. Bamburg (2000). "Increase in neurite outgrowth mediated by overexpression of actin depolymerizing factor." <u>J Neurosci</u> **20**(7): 2459-69.

Meberg, P. J., S. Ono, L. S. Minamide, M. Takahashi and J. R. Bamburg (1998). "Actin depolymerizing factor and cofilin phosphorylation dynamics: response to signals that regulate neurite extension." <u>Cell Motil Cytoskeleton</u> **39**(2): 172-90.

Menard, R. E. and R. R. Mattingly (2004). "Gbetagamma subunits stimulate p21-activated kinase 1 (PAK1) through activation of PI3-kinase and Akt but act independently of Rac1/Cdc42." <u>FEBS Lett</u> **556**(1-3): 187-92.

Meng, Y., H. Takahashi, J. Meng, Y. Zhang, G. Lu, S. Asrar, T. Nakamura and Z. Jia (2004). "Regulation of ADF/cofilin phosphorylation and synaptic function by LIM-kinase." <u>Neuropharmacology</u> **47**(5): 746-54.

Meng, Y., Y. Zhang, V. Tregoubov, C. Janus, L. Cruz, M. Jackson, W. Y. Lu, J. F. MacDonald, J. Y. Wang, D. L. Falls and Z. Jia (2002). "Abnormal spine morphology and enhanced LTP in LIMK-1 knockout mice." <u>Neuron</u> **35**(1): 121-33.

Missy, K., M. Plantavid, P. Pacaud, C. Viala, H. Chap and B. Payrastre (2001). "Rho-kinase is involved in the sustained phosphorylation of myosin and the irreversible platelet aggregation induced by PAR1 activating peptide." <u>Thromb Haemost</u> **85**(3): 514-20.

Mizuno, K., I. Okano, K. Ohashi, K. Nunoue, K. Kuma, T. Miyata and T. Nakamura (1994). "Identification of a human cDNA encoding a novel protein kinase with two repeats of the LIM/double zinc finger motif." <u>Oncogene</u> **9**(6): 1605-12.

Moers, A., B. Nieswandt, S. Massberg, N. Wettschureck, S. Gruner, I. Konrad, V. Schulte, B. Aktas, M. P. Gratacap, M. I. Simon, M. Gawaz and S. Offermanns (2003). "G13 is an essential mediator of platelet activation in hemostasis and thrombosis." <u>Nat Med</u> **9**(11): 1418-22.

Moon, A. L., P. A. Janmey, K. A. Louie and D. G. Drubin (1993). "Cofilin is an essential component of the yeast cortical cytoskeleton." <u>J Cell Biol</u> **120**(2): 421-35.

Moore, P. B., H. E. Huxley and D. J. DeRosier (1970). "Three-dimensional reconstruction of F-actin, thin filaments and decorated thin filaments." <u>J Mol Biol</u> **50**(2): 279-95.

Moritani, Y., K. Sato, T. Shigenaga, N. Hisamichi, M. Ichihara, S. Akamatsu, K. Suzuki, T. Nii, S. Kaku, T. Kawasaki, Y. Matsumoto, O. Inagaki, K. Tomioka and I. Yanagisawa (2002). "Pharmacological properties of YM-57029, a novel platelet glycoprotein IIb/IIIa antagonist." <u>Eur J Pharmacol</u> **439**(1-3): 43-52.

Moriyama, K., K. Iida and I. Yahara (1996). "Phosphorylation of Ser-3 of cofilin regulates its essential function on actin." <u>Genes Cells</u> **1**(1): 73-86.

Moriyama, K. and I. Yahara (1999). "Two activities of cofilin, severing and accelerating directional depolymerization of actin filaments, are affected differentially by mutations around the actin-binding helix." <u>Embo J</u> **18**(23): 6752-61.

Moriyama, K. and I. Yahara (2002). "Human CAP1 is a key factor in the recycling of cofilin and actin for rapid actin turnover." <u>J Cell Sci</u> **115**(Pt 8): 1591-601.

Moriyama, K., N. Yonezawa, H. Sakai, I. Yahara and E. Nishida (1992). "Mutational analysis of an actin-binding site of cofilin and characterization of chimeric proteins between cofilin and destrin." <u>J Biol Chem</u> **267**(11): 7240-4.

Morris, M. C., J. Depollier, J. Mery, F. Heitz and G. Divita (2001). "A peptide carrier for the delivery of biologically active proteins into mammalian cells." <u>Nat Biotechnol</u> **19**(12): 1173-6.

Nachmias, V. T. (1980). "Cytoskeleton of human platelets at rest and after spreading." J Cell Biol **86**(3): 795-802.

Nagaoka, R., H. Abe, K. Kusano and T. Obinata (1995). "Concentration of cofilin, a small actin-binding protein, at the cleavage furrow during cytokinesis." Cell Motil Cytoskeleton **30**(1): 1-7.

Nagaoka, R., H. Abe and T. Obinata (1996). "Site-directed mutagenesis of the phosphorylation site of cofilin: its role in cofilin-actin interaction and cytoplasmic localization." Cell Motil Cytoskeleton **35**(3): 200-9.

Nagata, K., K. Ohashi, N. Yang and K. Mizuno (1999). "The N-terminal LIM domain negatively regulates the kinase activity of LIM-kinase 1." Biochem J **343 Pt 1**: 99-105.

Nakagawa, O., K. Fujisawa, T. Ishizaki, Y. Saito, K. Nakao and S. Narumiya (1996). "ROCK-I and ROCK-II, two isoforms of Rho-associated coiled-coil forming protein serine/threonine kinase in mice." FEBS Lett **392**(2): 189-93.

Nakano, K., M. Kanai-Azuma, Y. Kanai, K. Moriyama, K. Yazaki, Y. Hayashi and N. Kitamura (2003). "Cofilin phosphorylation and actin polymerization by NRK/NESK, a member of the germinal center kinase family." Exp Cell Res **287**(2): 219-27.

Natarajan, P., J. A. May, H. M. Sanderson, M. Zabe, P. Spangenberg and S. Heptinstall (2000). "Effects of cytochalasin H, a potent inhibitor of cytoskeletal reorganisation, on platelet function." Platelets **11**(8): 467-76.

Nebl, G., S. C. Meuer and Y. Samstag (1996). "Dephosphorylation of serine 3 regulates nuclear translocation of cofilin." J Biol Chem **271**(42): 26276-80.

Nemoto, Y., T. Namba, T. Teru-uchi, F. Ushikubi, N. Morii and S. Narumiya (1992). "A rho gene product in human blood platelets. I. Identification of the platelet substrate for botulinum C3 ADP-ribosyltransferase as rhoA protein." J Biol Chem **267**(29): 20916-20.

Ng, J. and L. Luo (2004). "Rho GTPases regulate axon growth through convergent and divergent signaling pathways." Neuron **44**(5): 779-93.

Nieswandt, B., V. Schulte, A. Zywietz, M. P. Gratacap and S. Offermanns (2002). "Costimulation of Gi- and G12/G13-mediated signaling pathways induces integrin alpha IIbbeta 3 activation in platelets." J Biol Chem **277**(42): 39493-8.

Nishida, E. (1985). "Opposite effects of cofilin and profilin from porcine brain on rate of exchange of actin-bound adenosine 5'-triphosphate." Biochemistry **24**(5): 1160-4.

Nishida, E., S. Maekawa and H. Sakai (1984). "Cofilin, a protein in porcine brain that binds to actin filaments and inhibits their interactions with myosin and tropomyosin." Biochemistry **23**(22): 5307-13.

Nishita, M., Y. Wang, C. Tomizawa, A. Suzuki, R. Niwa, T. Uemura and K. Mizuno (2004). "Phosphoinositide 3-kinase-mediated activation of cofilin phosphatase Slingshot and its role for insulin-induced membrane protrusion." J Biol Chem **279**(8): 7193-8.

Niwa, R., K. Nagata-Ohashi, M. Takeichi, K. Mizuno and T. Uemura (2002). "Control of actin reorganization by Slingshot, a family of phosphatases that dephosphorylate ADF/cofilin." Cell **108**(2): 233-46.

Nurden, A. T. and J. P. Caen (1975). "Specific roles for platelet surface glycoproteins in platelet function." Nature **255**(5511): 720-2.

Nurden, P., E. Heilmann, A. Paponneau and A. Nurden (1994). "Two-way trafficking of membrane glycoproteins on thrombin-activated human platelets." Semin Hematol **31**(3): 240-50.

Oda, A., J. F. Daley, C. Cabral, J. H. Kang, M. Smith and E. W. Salzman (1992). "Heterogeneity in filamentous actin content among individual human blood platelets." Blood **79**(4): 920-7.

Offermanns, S. (2000). "The role of heterotrimeric G proteins in platelet activation." Biol Chem **381**(5-6): 389-96.

Offermanns, S., K. L. Laugwitz, K. Spicher and G. Schultz (1994). "G proteins of the G12 family are activated via thromboxane A2 and thrombin receptors in human platelets." Proc Natl Acad Sci U S A **91**(2): 504-8.

Offermanns, S., C. F. Toombs, Y. H. Hu and M. I. Simon (1997). "Defective platelet activation in G alpha(q)-deficient mice." Nature **389**(6647): 183-6.

Ohashi, K., K. Nagata, M. Maekawa, T. Ishizaki, S. Narumiya and K. Mizuno (2000). "Rho-associated kinase ROCK activates LIM-kinase 1 by phosphorylation at threonine 508 within the activation loop." J Biol Chem **275**(5): 3577-82.

Ohta, Y., E. Nishida, H. Sakai and E. Miyamoto (1989). "Dephosphorylation of cofilin accompanies heat shock-induced nuclear accumulation of cofilin." J Biol Chem **264**(27): 16143-8.

Ojala, P. J., V. Paavilainen and P. Lappalainen (2001). "Identification of yeast cofilin residues specific for actin monomer and PIP2 binding." Biochemistry **40**(51): 15562-9.

Okada, K., H. Takano-Ohmuro, T. Obinata and H. Abe (1996). "Dephosphorylation of cofilin in polymorphonuclear leukocytes derived from peripheral blood." Exp Cell Res **227**(1): 116-22.

Okano, I., J. Hiraoka, H. Otera, K. Nunoue, K. Ohashi, S. Iwashita, M. Hirai and K. Mizuno (1995). "Identification and characterization of a novel family of serine/threonine kinases containing two N-terminal LIM motifs." J Biol Chem **270**(52): 31321-30.

Okita, J. R., D. Pidard, P. J. Newman, R. R. Montgomery and T. J. Kunicki (1985). "On the association of glycoprotein Ib and actin-binding protein in human platelets." J Cell Biol **100**(1): 317-21.

Ono, S., A. McGough, B. J. Pope, V. T. Tolbert, A. Bui, J. Pohl, G. M. Benian, K. M. Gernert and A. G. Weeds (2001). "The C-terminal tail of UNC-60B (actin depolymerizing factor/cofilin) is critical for maintaining its stable association with F-actin and is implicated in the second actin-binding site." J Biol Chem **276**(8): 5952-8.

Ono, S., K. Mohri and K. Ono (2004). "Microscopic evidence that actin-interacting protein 1 actively disassembles actin-depolymerizing factor/Cofilin-bound actin filaments." J Biol Chem **279**(14): 14207-12.

Paul, B. Z., S. Kim, C. Dangelmaier, C. Nagaswami, J. Jin, J. H. Hartwig, J. W. Weisel, J. L. Daniel and S. P. Kunapuli (2003). "Dynamic regulation of microtubule coils in ADP-induced platelet shape change by p160ROCK (Rho-kinase)." Platelets **14**(3): 159-69.

Phillips, D. R. and M. Jakabova (1977). "Ca2+-dependent protease in human platelets. Specific cleavage of platelet polypeptides in the presence of added Ca2+." J Biol Chem **252**(16): 5602-5.

Pollard, T. D. and C. C. Beltzner (2002). "Structure and function of the Arp2/3 complex." Curr Opin Struct Biol **12**(6): 768-74.

Pollard, T. D. and G. G. Borisy (2003). "Cellular motility driven by assembly and disassembly of actin filaments." Cell **112**(4): 453-65.

Pollard, T. D. and J. A. Cooper (1986). "Actin and actin-binding proteins. A critical evaluation of mechanisms and functions." Annu Rev Biochem **55**: 987-1035.

Pope, B. J., S. M. Gonsior, S. Yeoh, A. McGough and A. G. Weeds (2000). "Uncoupling actin filament fragmentation by cofilin from increased subunit turnover." J Mol Biol **298**(4): 649-61.

Pope, B. J., K. M. Zierler-Gould, R. Kuhne, A. G. Weeds and L. J. Ball (2004). "Solution structure of human cofilin: actin binding, pH sensitivity, and relationship to actin-depolymerizing factor." J Biol Chem **279**(6): 4840-8.

Redondo, P. C., M. T. Harper, J. A. Rosado and S. O. Sage (2006). "A role for cofilin in the activation of store-operated calcium entry by de novo conformational coupling in human platelets." Blood **107**(3): 973-9.

Rendu, F. and B. Brohard-Bohn (2001). "The platelet release reaction: granules' constituents, secretion and functions." Platelets **12**(5): 261-73.

Ressad, F., D. Didry, G. X. Xia, Y. Hong, N. H. Chua, D. Pantaloni and M. F. Carlier (1998). "Kinetic analysis of the interaction of actin-depolymerizing factor (ADF)/cofilin with G- and F-actins. Comparison of plant and human ADFs and effect of phosphorylation." J Biol Chem **273**(33): 20894-902.

Retzer, M. and M. Essler (2000). "Lysophosphatidic acid-induced platelet shape change proceeds via Rho/Rho kinase-mediated myosin light-chain and moesin phosphorylation." Cell Signal **12**(9-10): 645-8.

Rhee, S. and F. Grinnell (2006). "P21-activated kinase 1: convergence point in PDGF- and LPA-stimulated collagen matrix contraction by human fibroblasts." J Cell Biol **172**(3): 423-32.

Rodriguez Del Castillo, A., M. L. Vitale, L. Tchakarov and J. M. Trifaro (1992). "Human platelets contain scinderin, a Ca(2+)-dependent actin filament-severing protein." Thromb Haemost **67**(2): 248-51.

Rother, E., R. Brandl, D. L. Baker, P. Goyal, H. Gebhard, G. Tigyi and W. Siess (2003). "Subtype-selective antagonists of lysophosphatidic Acid receptors inhibit platelet activation triggered by the lipid core of atherosclerotic plaques." Circulation **108**(6): 741-7.

Ruf, A. and H. Patscheke (1995). "Flow cytometric detection of activated platelets: comparison of determining shape change, fibrinogen binding, and P-selectin expression." Semin Thromb Hemost **21**(2): 146-51.

Ruggeri, Z. M. (2002). "Platelets in atherothrombosis." Nat Med **8**(11): 1227-34.

Saitoh, M., M. Naka and H. Hidaka (1986). "The modulatory role of myosin light chain phosphorylation in human platelet activation." Biochem Biophys Res Commun **140**(1): 280-7.

Samstag, Y., E. M. Dreizler, A. Ambach, G. Sczakiel and S. C. Meuer (1996). "Inhibition of constitutive serine phosphatase activity in T lymphoma cells results in phosphorylation of pp19/cofilin and induces apoptosis." J Immunol **156**(11): 4167-73.

Sanders, L. C., F. Matsumura, G. M. Bokoch and P. de Lanerolle (1999). "Inhibition of myosin light chain kinase by p21-activated kinase." Science **283**(5410): 2083-5.

Schmidt, V. A., L. Scudder, C. E. Devoe, A. Bernards, L. D. Cupit and W. F. Bahou (2003). "IQGAP2 functions as a GTP-dependent effector protein in thrombin-induced platelet cytoskeletal reorganization." Blood **101**(8): 3021-8.

Schmitz, U., K. Thommes, I. Beier and H. Vetter (2002). "Lysophosphatidic acid stimulates p21-activated kinase in vascular smooth muscle cells." Biochem Biophys Res Commun **291**(3): 687-91.

Schoenwaelder, S. M., Y. Yuan, P. Cooray, H. H. Salem and S. P. Jackson (1997). "Calpain cleavage of focal adhesion proteins regulates the cytoskeletal attachment of integrin

alphaIIbbeta3 (platelet glycoprotein IIb/IIIa) and the cellular retraction of fibrin clots." <u>J Biol Chem</u> **272**(3): 1694-702.

Schwer, H. D., P. Lecine, S. Tiwari, J. E. Italiano, Jr., J. H. Hartwig and R. A. Shivdasani (2001). "A lineage-restricted and divergent beta-tubulin isoform is essential for the biogenesis, structure and function of blood platelets." <u>Curr Biol</u> **11**(8): 579-86.

Shattil, S. J., J. S. Bennett, R. W. Colman and R. A. Cooper (1977). "Abnormalities of cholesterol-phospholipid composition in platelets and low-density lipoproteins of human hyperbetalipoproteinemia." <u>J Lab Clin Med</u> **89**(2): 341-53.

Shattil, S. J. and L. F. Brass (1987). "Induction of the fibrinogen receptor on human platelets by intracellular mediators." <u>J Biol Chem</u> **262**(3): 992-1000.

Shimizu, Y., D. Thumkeo, J. Keel, T. Ishizaki, H. Oshima, M. Oshima, Y. Noda, F. Matsumura, M. M. Taketo and S. Narumiya (2005). "ROCK-I regulates closure of the eyelids and ventral body wall by inducing assembly of actomyosin bundles." <u>J Cell Biol</u> **168**(6): 941-53.

Siess, W. (1989). "Molecular mechanisms of platelet activation." <u>Physiol Rev</u> **69**(1): 58-178.

Siess, W. and G. Tigyi (2004). "Thrombogenic and atherogenic activities of lysophosphatidic acid." <u>J Cell Biochem</u> **92**(6): 1086-94.

Siess, W., K. J. Zangl, M. Essler, M. Bauer, R. Brandl, C. Corrinth, R. Bittman, G. Tigyi and M. Aepfelbacher (1999). "Lysophosphatidic acid mediates the rapid activation of platelets and endothelial cells by mildly oxidized low density lipoprotein and accumulates in human atherosclerotic lesions." <u>Proc Natl Acad Sci U S A</u> **96**(12): 6931-6.

Soosairajah, J., S. Maiti, O. Wiggan, P. Sarmiere, N. Moussi, B. Sarcevic, R. Sampath, J. R. Bamburg and O. Bernard (2005). "Interplay between components of a novel LIM kinase-slingshot phosphatase complex regulates cofilin." <u>Embo J</u> **24**(3): 473-86.

Soulet, C., S. Gendreau, K. Missy, V. Benard, M. Plantavid and B. Payrastre (2001). "Characterisation of Rac activation in thrombin- and collagen-stimulated human blood platelets." <u>FEBS Lett</u> **507**(3): 253-8.

Soulet, C., B. Hechler, M. P. Gratacap, M. Plantavid, S. Offermanns, C. Gachet and B. Payrastre (2005). "A differential role of the platelet ADP receptors P2Y1 and P2Y12 in Rac activation." <u>J Thromb Haemost</u> **3**(10): 2296-306.

Spector, I., F. Braet, N. R. Shochet and M. R. Bubb (1999). "New anti-actin drugs in the study of the organization and function of the actin cytoskeleton." <u>Microsc Res Tech</u> **47**(1): 18-37.

Sumi, T., K. Matsumoto and T. Nakamura (2001). "Specific activation of LIM kinase 2 via phosphorylation of threonine 505 by ROCK, a Rho-dependent protein kinase." <u>J Biol Chem</u> **276**(1): 670-6.

Sumi, T., K. Matsumoto, A. Shibuya and T. Nakamura (2001). "Activation of LIM kinases by myotonic dystrophy kinase-related Cdc42-binding kinase alpha." <u>J Biol Chem</u> **276**(25): 23092-6.

Suzuki-Inoue, K., Y. Yatomi, N. Asazuma, M. Kainoh, T. Tanaka, K. Satoh and Y. Ozaki (2001). "Rac, a small guanosine triphosphate-binding protein, and p21-activated kinase are activated during platelet spreading on collagen-coated surfaces: roles of integrin alpha(2)beta(1)." <u>Blood</u> **98**(13): 3708-16.

Suzuki, Y., M. Yamamoto, H. Wada, M. Ito, T. Nakano, Y. Sasaki, S. Narumiya, H. Shiku and M. Nishikawa (1999). "Agonist-induced regulation of myosin phosphatase activity in human platelets through activation of Rho-kinase." <u>Blood</u> **93**(10): 3408-17.

Tadokoro, S., S. J. Shattil, K. Eto, V. Tai, R. C. Liddington, J. M. de Pereda, M. H. Ginsberg and D. A. Calderwood (2003). "Talin binding to integrin beta tails: a final common step in integrin activation." Science **302**(5642): 103-6.

Takuma, T., T. Ichida, N. Yokoyama, S. Tamura and T. Obinata (1996). "Dephosphorylation of cofilin in parotid acinar cells." J Biochem (Tokyo) **120**(1): 35-41.

Tanaka, K., Y. Okubo and H. Abe (2005). "Involvement of slingshot in the Rho-mediated dephosphorylation of ADF/cofilin during Xenopus cleavage." Zoolog Sci **22**(9): 971-84.

Teo, M., E. Manser and L. Lim (1995). "Identification and molecular cloning of a p21cdc42/rac1-activated serine/threonine kinase that is rapidly activated by thrombin in platelets." J Biol Chem **270**(44): 26690-7.

Teubner, A. and A. Wegner (1998). "Kinetic evidence for a readily exchangeable nucleotide at the terminal subunit of the barbed ends of actin filaments." Biochemistry **37**(20): 7532-8.

Torti, M., A. Bertoni, I. Canobbio, F. Sinigaglia, E. G. Lapetina and C. Balduini (1999). "Rap1B and Rap2B translocation to the cytoskeleton by von Willebrand factor involves FcgammaII receptor-mediated protein tyrosine phosphorylation." J Biol Chem **274**(19): 13690-7.

Toshima, J., J. Y. Toshima, K. Takeuchi, R. Mori and K. Mizuno (2001). "Cofilin phosphorylation and actin reorganization activities of testicular protein kinase 2 and its predominant expression in testicular Sertoli cells." J Biol Chem **276**(33): 31449-58.

Toshima, J. Y., J. Toshima, T. Watanabe and K. Mizuno (2001). "Binding of 14-3-3beta regulates the kinase activity and subcellular localization of testicular protein kinase 1." J Biol Chem **276**(46): 43471-81.

Uehata, M., T. Ishizaki, H. Satoh, T. Ono, T. Kawahara, T. Morishita, H. Tamakawa, K. Yamagami, J. Inui, M. Maekawa and S. Narumiya (1997). "Calcium sensitization of smooth muscle mediated by a Rho-associated protein kinase in hypertension." Nature **389**(6654): 990-4.

Van Aelst, L. and C. D'Souza-Schorey (1997). "Rho GTPases and signaling networks." Genes Dev **11**(18): 2295-322.

van Leeuwen, F. N., S. van Delft, H. E. Kain, R. A. van der Kammen and J. G. Collard (1999). "Rac regulates phosphorylation of the myosin-II heavy chain, actinomyosin disassembly and cell spreading." Nat Cell Biol **1**(4): 242-8.

Vartiainen, M. K., T. Mustonen, P. K. Mattila, P. J. Ojala, I. Thesleff, J. Partanen and P. Lappalainen (2002). "The three mouse actin-depolymerizing factor/cofilins evolved to fulfill cell-type-specific requirements for actin dynamics." Mol Biol Cell **13**(1): 183-94.

Vidal, C., B. Geny, J. Melle, M. Jandrot-Perrus and M. Fontenay-Roupie (2002). "Cdc42/Rac1-dependent activation of the p21-activated kinase (PAK) regulates human platelet lamellipodia spreading: implication of the cortical-actin binding protein cortactin." Blood **100**(13): 4462-9.

Wang, Y., F. Shibasaki and K. Mizuno (2005). "Calcium signal-induced cofilin dephosphorylation is mediated by Slingshot via calcineurin." J Biol Chem **280**(13): 12683-9.

Wegner, A. (1976). "Head to tail polymerization of actin." J Mol Biol **108**(1): 139-50.

Wender, P. A., D. J. Mitchell, K. Pattabiraman, E. T. Pelkey, L. Steinman and J. B. Rothbard (2000). "The design, synthesis, and evaluation of molecules that enable or enhance cellular uptake: peptoid molecular transporters." Proc Natl Acad Sci U S A **97**(24): 13003-8.

Wennerberg, K. and C. J. Der (2004). "Rho-family GTPases: it's not only Rac and Rho (and I like it)." J Cell Sci **117**(Pt 8): 1301-12.

White, J. G. and G. H. Rao (1982). "Effects of a microtubule stabilizing agent on the response of platelets to vincristine." <u>Blood</u> **60**(2): 474-83.

White, J. G. and G. H. Rao (1983). "Influence of a microtubule stabilizing agent on platelet structural physiology." <u>Am J Pathol</u> **112**(2): 207-17.

Williamson, D., I. Pikovski, S. L. Cranmer, P. Mangin, N. Mistry, T. Domagala, S. Chehab, F. Lanza, H. H. Salem and S. P. Jackson (2002). "Interaction between platelet glycoprotein Ibalpha and filamin-1 is essential for glycoprotein Ib/IX receptor anchorage at high shear." <u>J Biol Chem</u> **277**(3): 2151-9.

Winder, S. J. and K. R. Ayscough (2005). "Actin-binding proteins." <u>J Cell Sci</u> **118**(Pt 4): 651-4.

Woulfe, D., H. Jiang, A. Morgans, R. Monks, M. Birnbaum and L. F. Brass (2004). "Defects in secretion, aggregation, and thrombus formation in platelets from mice lacking Akt2." <u>J Clin Invest</u> **113**(3): 441-50.

Wulf, E., A. Deboben, F. A. Bautz, H. Faulstich and T. Wieland (1979). "Fluorescent phallotoxin, a tool for the visualization of cellular actin." <u>Proc Natl Acad Sci U S A</u> **76**(9): 4498-502.

Yang, S. A., C. L. Carpenter and C. S. Abrams (2004). "Rho and Rho-kinase mediate thrombin-induced phosphatidylinositol 4-phosphate 5-kinase trafficking in platelets." <u>J Biol Chem</u> **279**(40): 42331-6.

Yeoh, S., B. Pope, H. G. Mannherz and A. Weeds (2002). "Determining the differences in actin binding by human ADF and cofilin." <u>J Mol Biol</u> **315**(4): 911-25.

Yonezawa, N., E. Nishida, K. Iida, I. Yahara and H. Sakai (1990). "Inhibition of the interactions of cofilin, destrin, and deoxyribonuclease I with actin by phosphoinositides." <u>J Biol Chem</u> **265**(15): 8382-6.

Yonezawa, N., E. Nishida, S. Maekawa and H. Sakai (1988). "Studies on the interaction between actin and cofilin purified by a new method." <u>Biochem J</u> **251**(1): 121-7.

Zhang, J., W. G. King, S. Dillon, A. Hall, L. Feig and S. E. Rittenhouse (1993). "Activation of platelet phosphatidylinositide 3-kinase requires the small GTP-binding protein Rho." <u>J Biol Chem</u> **268**(30): 22251-4.

Zhang, Z., A. K. Ottens, S. F. Larner, F. H. Kobeissy, M. L. Williams, R. L. Hayes and K. K. Wang (2006). "Direct Rho-associated kinase inhibiton induces cofilin dephosphorylation and neurite outgrowth in PC-12 cells." <u>Cell Mol Biol Lett</u> **11**(1): 12-29.

Acknowledgements

List of Publications

Original articles

1. Haseruck N, Erl W, **Pandey D**, Tigyi G, Ohlmann P, Ravanat C, Gachet C, and Siess W. The plaque lipid lysophosphatidic acid stimulates platelet activation and platelet-monocyte aggregate formation in whole blood: involvement of P2Y1 and P2Y12 receptors. *Blood.* 2004 Apr 1;103(7):2585-92.

2. Goyal P, **Pandey D**, Behring A, and Siess W. Inhibition of nuclear import of LIMK2 in endothelial cells by protein kinase C-dependent phosphorylation at Ser-283. *J Biol Chem.* 2005 Jul 29;280(30):27569-77.

3. Tyagi NK, Goyal P, Kumar A, **Pandey D**, Siess W, and Kinne RK. High-Yield Functional Expression of Human Sodium/d-Glucose Cotransporter1 in Pichia pastoris and Characterization of Ligand-Induced Conformational Changes as Studied by Tryptophan Fluorescence. *Biochemistry.* 2005 Nov 29;44(47):15514-15524.

4. **Pandey D,** Goyal P, Bamburg JR, and Siess W. Regulation of LIM-kinase 1 and cofilin in thrombin-stimulated platelets. *Blood.* 2006 Jan 15;107(2):575-583.

5. Goyal P, **Pandey D**, and Siess W. Phosphorylation-dependent regulation of unique nuclear and nucleolar localization signals of LIM-kinase 2 in endothelial cells. *J Biol Chem.* 2006 Sep 1;281(35):25223-30.

6. **Pandey D**, Goyal P, and Siess W. Lysophosphatidic acid-stimulation of platelets rapidly induces Ca^{2+}-dependent dephosphorylation of cofilin that is independent of dense granule secretion and aggregation. *Blood Cell Molecules and Diseases.* 2007; *In press.*

7. Kumar A, Tyagi NK, Goyal P, **Pandey D**, Siess W, and Kinne RK. Sodium-Independent Low Affinity D-Glucose Transport by the Human Sodium/D-Glucose Cotransporter1: Critical Role of Tryptophan 561. *Biochemistry* 2007; *In press.*

Presentations at scientific meetings

Oral Presentations

1. **D. Pandey**, P. Goyal, J. R. Bamburg, and W. Siess. Regulation of cofilin during shape change and aggregation. XVIIth European Platelet meeting, Eberbach, Germany, October 10th-12th, 2002. *Platelets* 13(8): 499-513, 2002.

2. **D. Pandey**, P. Goyal, J. R. Bamburg, and W. Siess. Regulation of LIMK-1 and cofilin during platelet activation. XIXth European Platelet Meeting, Bad Brückenau, Germany, October 14th-16th, 2004. *Platelets* 16 (3/4): 229-248, 2005.

3. **D. Pandey**, P. Goyal, J. R. Bamburg, and W. Siess**.** Regulation of LIMK-1 and cofilin in thrombin-stimulated platelets. International Conference on Mechanism of Thrombus Formation, Fraueninsel, Munich, Germany, Sep 24th-29th, 2005. *Poster presentation.*

4. **D. Pandey**, P. Goyal, J. R. Bamburg, and W. Siess. Rho-kinase activation stimulates LIM-kinase-1 and increases F-actin, but not cofilin phosphorylation in thrombin-stimulated platelets. XXth European Platelet Meeting, Ede, The Netherlands, Oct 13th-15th, 2005. *Platelets* 17(2): 108, 2006.

5. **D. Pandey**, P. Goyal, J. R. Bamburg, and W. Siess. Two-step regulation of cofilin phospho-cycle in lysophosphatidic acid-stimulated platelets. XXIst European Platelet Meeting, Lutherstadt Wittenberg, Germany, Oct 12th-14th, 2006.

Poster Presentations

1. P. Goyal, **D. Pandey**, and W. Siess. Regulation of LIM-Kinases in endothelial cells. 4th Symposium on the Biology of Endothelial cells, Munich, Germany, July 18th-20th, 2003. *Angiogenesis* 5(4):281-338, Abstract P33, 2002.

2. **D. Pandey**, P. Goyal, J.R. Bamburg, and W. Siess. Analysis of the Rho-kinase /LIM-kinase/cofilin signaling pathway in activated platelets. XIX Congress and 49th Annual SSC meeting of The International Society on Thrombosis and Haemostasis (ISTH), 12-18 July 2003, Birmingham, UK. *Journal of Thrombosis and Haemostasis* Volume 1, Supplement 1: Abstract P0229, 2003.

3. O. Bikou, **D. Pandey**, and W. Siess. Synergism of LPA and collagen in inducing platelet aggregation. XIXth European Platelet Meeting, Bad Brückenau, Germany, Oct 14th-16th, 2004. *Platelets* 16 (3/4): 229-248, 2005.

4. **D. Pandey**, P. Goyal, and W. Siess. Integrin $\alpha_{IIb}\beta_3$ independent regulation of LIMK1 activation and cofilin phosphorylation in activated platelets. Adhesion Meeting, Munich, Germany, April 28th-30th, 2005.

5. P. Goyal, **D. Pandey**, and W. Siess. Regulation of LIM-kinases and cofilin in activated endothelial cells. Adhesion Meeting, Munich, Germany, April 28th-30th, 2005.

6. **D. Pandey**, P. Goyal, J. R. Bamburg, and W. Siess. Regulation of LIMK1 and cofilin in thrombin-stimulated Platelets. 3rd Symposium on Cell Dynamics, Munich, Germany, Oct 5th-7th, 2005.

7. P. Goyal, **<u>D. Pandey</u>**, and W. Siess. LIM-kinases regulate actin dynamics in thrombin-stimulated endothelial cells. 3rd Symposium on Cell Dynamics, Munich, Germany, Oct 5th-7th, 2005.

8. **<u>D. Pandey</u>**, P. Goyal*, and W. Siess. Lysophosphatidic acid induces F-actin increase via Rho-kinase/ LIMK-1 activation without stimulation of cofilin phosphorylation in platelets. Gesellschaft für Mikrozirkulation und Vaskuläre Biologie Annual Meeting, Oct 12th-14th, 2006, German Heart Center, Munich, Germany (* presented the poster).

Curriculum vitae

Personal Data

Name   Dharmendra Pandey

Date of birth   5th September 1978

Place of birth   Ahmednagar, India

Nationality   Indian

Marital Status   Unmarried

Academic Qualification

1995-1998:   B.Sc Chemistry, University of Pune, Pune, India.

1999-2001:   M.Sc Biotechnology, Indian Institute of Tech-Bombay, Mumbai, India.

Scientific background

2002-present   Graduate student at the Institut für Prophylaxe und Epidemiologie der Kreislaufkrankheiten, Universität München, Germany.

July- Dec 2001   Junior research fellow (JRF) at Indian Institute of Technology Bombay, India.

Achievements

Qualified Graduate Aptitude Test for Engineers (Life Science)-2001 (GATE-2001) with percentile score of 97.05.

Awarded fellowship by Dept. of Biotechnology, Govt. of India for a duration of two years (1999-2001).